The Swiss Glaciers

2019/20 and 2020/21

Glaciological Report (Glacier) No. 141/142

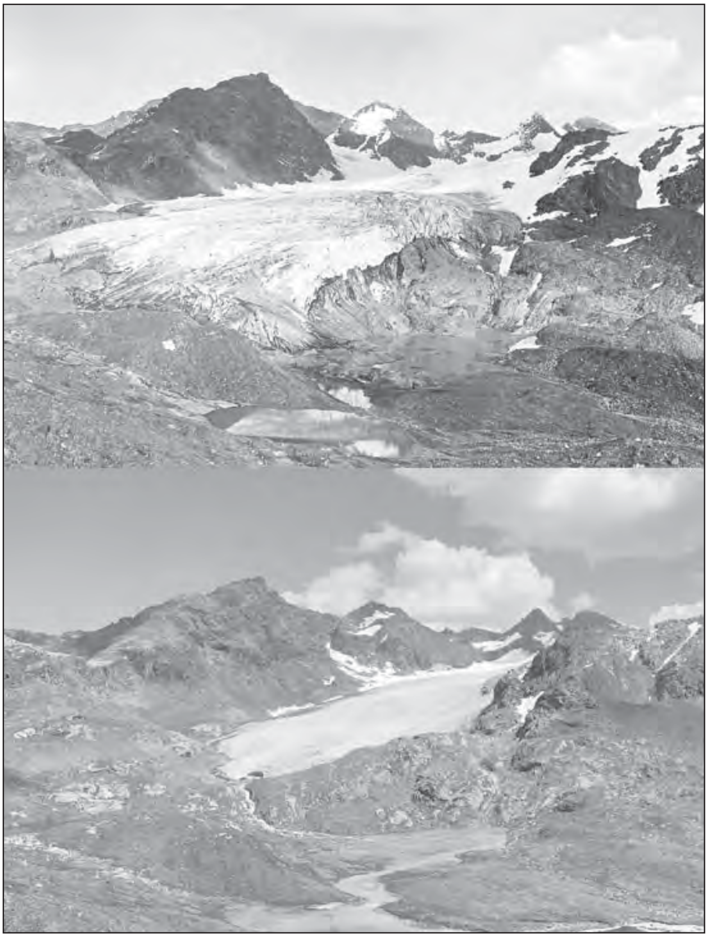

2022

The Swiss Glaciers

2019/20 and 2020/21

Glaciological Report No. 141/142

Edited by

Andreas Bauder[1,2], Matthias Huss[1,2,3], Andreas Linsbauer[4,3]

[1] Laboratory of Hydraulics, Hydrology and Glaciology (VAW), ETH Zurich

[2] Swiss Federal Institute for Forest, Snow and Landscape Research (WSL)

[3] Department of Geosciences, University of Fribourg

[4] Department of Geography, University of Zurich

GLAMOS
Glacier Monitoring Switzerland

2022

Publication of the Cryospheric Commission (EKK) of the Swiss Academy of Sciences (SCNAT)

c/o Laboratory of Hydraulics, Hydrology and Glaciology (VAW)
at the Swiss Federal Institute of Technology Zurich (ETH Zurich)
Hönggerbergring 26, CH-8093 Zürich, Switzerland
http://www.glamos.ch

DOI: http://doi.org/10.18752/glrep_141-142

ISSN 1424-2222

Imprint of author contributions:

Andreas Bauder	:	Chapt. 1, 2, 3, 4, 5, 7, 8, App. A, B, C
Elias Hodel	:	Chapt. 3, 4, 5, App. A
Martin Hoelzle	:	Chapt. 6
Matthias Huss	:	Chapt. 1, 2, 4, 7, 8
Giovanni Kappenberger	:	Chapt. 4
Andreas Linsbauer	:	Chapt. 4, 8
Urs Steinegger	:	Chapt. 4

Citation:
GLAMOS (2022). The Swiss Glaciers 2019/20 and 2020/21. Bauder, A., Huss, M., Linsbauer, A. (eds), Glaciological Report No. 141/142 of the Cryospheric Commission of the Swiss Academy of Sciences (SCNAT), 173p, doi:10.18752/glrep_141-142.

Printed by:
Staffel Medien AG, CH-8045 Zürich, Switzerland

Cover Page:
Silvrettagletscher 30.09.1967 (top, H. Siegenthaler) and 09.08.2021 (bottom, A. Bauder)

Summary

During the 141st and 142nd year under review by the Cryospheric Commission (EKK), Swiss glaciers continued to lose both in terms of length and mass. Although the two periods were characterized by somewhat less extreme summer air temperatures and thus melt rates than during the previous years, combined with mostly average winter snow accumulation, this resulted in considerable glacier mass loss. Despite of the global pandemic, all relevant observations could be performed without a break in the long-term series.

For late summer 2020, a change in glacier length was determined for 82 of the 115 glaciers currently under active observation, while for autumn 2021 77 glaciers were measured. In the two observation periods, 2019/20 and 2020/21, Swiss glaciers thus experienced further losses in length. Most of the measurement values are between 0 and -30 m in both periods. Several glaciers displayed remarkably high retreat rates in a single year. These can be attributed to the detachment of a mass of dead ice from the glacier snout, or to the melting of sections of the glacier that had been thinning constantly for many years.

Mass balance observations at seasonal to annual resolution were acquired on more than 20 glaciers using direct glaciological measurements, among others, Allalin, Basòdino, Clariden, Findelen, Giétro, Gries, Grosser Aletsch, Pers, Plaine Morte, Rhone, Silvretta and Tsanfleuron. In the first period (2019/20) under consideration, glaciers in all regions of Switzerland showed substantial mass loss, however being less extreme than during the previous three years. In the second period under observation (2020/21), abundant snowfall in winter and spring and a late onset of the melting period, combined with an often rainy summer season resulted reduced mass losses, especially in Central Switzerland. Nevertheless, not a single positive mass balance was registered and Swiss glaciers continued their decline.

Measurements of surface ice velocity were performed at eight glaciers throughout the Swiss Alps. The trend continued toward diminishing velocities reflecting the reduction in ice thickness due to the ongoing negative mass balances.

A new Swiss Glacier Inventory centred around the year 2016 (SGI2016) was published indicating a glacier area of $961 \pm 22\,\mathrm{km}^2$, whereof 11% ($104\,\mathrm{km}^2$) are debris-covered. By combining extensive ice thickness surveys by helicopter-borne ground-penetrating radar with modelling, a total ice volume of $52.9 \pm 2.7\ \mathrm{km}^3$ was inferred for the year 2020.

Measurements of borehole firn temperature at Colle Gnifetti, Valais, showed a further warming of englacial temperature over the last pentade indicating a regime shift with melting occurring even at very high elevations in the Alps during summer.

Published Reports

Annual reports of the Swiss glaciers started in the year of 1880 by F.A. Forel (1841-1912). While the first two reports appeared in "Echo des Alps", reports 3 to 90 were published in the yearbooks of the Swiss Alpine Club (SAC). Starting from report 91, they appeared as separate publication of the the Swiss Academy of Sciences (SCNAT) and only a summary was published in the magazine of the Swiss Alpine Club (SAC).

Authors of the annual reports:	No.	Year
F.A. Forel	1 - 15	1880 - 1894
F.A. Forel et L. Du Pasquier	16 - 17	1895 - 1896
F.A. Forel, M. Lugeon et E. Muret	18 - 27	1897 - 1906
F.A. Forel, E. Muret, P.L. Mercanton et E. Argand	28	1907
F.A. Forel, E. Muret et P.L. Mercanton	29 - 32	1908 - 1911
E. Muret et P.L. Mercanton	33 - 34	1912 - 1913
P.L. Mercanton	35 - 70	1914 - 1949
P.L. Mercanton et A. Renaud	71 - 75	1950 - 1954
A. Renaud	76 - 83	1955 - 1961/62
P. Kasser	84 - 91	1962/63 - 1969/70
P. Kasser und M. Aellen	92	1970/71

Authors and editors of the glaciological two year reports:		
P. Kasser und M. Aellen	93/94	1971/72 - 1972/73
P. Kasser, M. Aellen und H. Siegenthaler	95/96 - 99/100	1973/74 - 1978/79
M. Aellen	101/102	1979/80 - 1980/81
M. Aellen und E. Herren	103/104 - 111/112	1981/82 - 1990/91
E. Herren und M. Hoelzle	113/114	1991/92 - 1992/93
E. Herren, M. Hoelzle and M. Maisch	115/116 - 119/120	1993/94 - 1998/99
E. Herren, A. Bauder, M. Hoelzle and M. Maisch	121/122	1999/00 - 2000/01
E. Herren and A. Bauder	123/124	2001/02 - 2002/03
A. Bauder and R. Rüegg	125/126	2003/04 - 2004/05
A. Bauder and C. Ryser	127/128	2005/06 - 2006/07
A. Bauder, S. Steffen and S. Usselmann	129/130	2007/08 - 2008/09
A. Bauder	131/132 - 137/138	2009/10 - 2016/17
A. Bauder, M. Huss and A. Linsbauer	139/140 - 141/142	2017/18 - 2020/21

Contents

1 Introduction

Systematic and long-term records of glacier changes in Switzerland started in 1880 with annual length change measurements of selected glaciers. At that time, these measurements were motivated by the interest to gain insights into past and future ice ages. In the meantime, the goals of worldwide glacier monitoring have evolved and multiplied. Glacier change data are necessary for investigations of the glacier-climate interaction, but the data are also important for the assessment of water resources, sea-level rise and natural hazards. Finally, the broad public manifests an increasing interest in glacier retreat as an element of the Alpine environment excellently illustrating climate change.

The main focus of the Swiss glacier monitoring network is to collect the following data: (1) length variation, (2) mass balance, (3) volume change, (4) ice surface flow velocity, (5) glacier inventories, and (6) englacial temperature. The programme for GLAcier MOnitoring in Switzerland (GLAMOS) has been adopted by the Cryospheric Commission in March 2007 and receives long-term funding and support by the Federal Office for Environment (BAFU), MeteoSwiss within the Global Climate Observing System (GCOS) Switzerland, the Swiss Academy of Sciences (SCNAT), and the Federal Office of Topography (swisstopo) since 1.1.2016. A detailed description of the aims, the current status and perspectives of the monitoring programme was presented in Chapter 1.1 of "The Swiss Glaciers" Volume 125/126.

As part of GLAMOS ongoing effort to improve the monitoring programme the strategy for the evaluation of length variation has recently revised (GLAMOS, 2020b). An evaluation of the available dataset acquired in past offered crucial deficiencies. In order to ensure optimal data quality and the use of available resources and measurement techniques an adaptation of the monitoring strategy was needed. Details are introduced in the corresponding chapter 3.

The results of Swiss glacier monitoring contribute to the international efforts to document glacier fluctuations worldwide as part of global environmental monitoring initiatives of the Global Terrestrial Network for Glaciers (GTN-G) within the Global Terrestrial and Climate Observing System (GTOS/GCOS). All results are annually reported to the World Glacier Monitoring Service (WGMS).

This report is the new volume No. 141/142 in the series "The Swiss Glaciers" and presents the results of the two observational periods 2019/20 and 2020/21. It carries on the long tradition of yearbooks documenting monitored fluctuations of Swiss glaciers since 1880 (see page iv). Data and digital versions of the present and earlier volumes are available at www.glamos.ch. Thanks to the continuous efforts of many people, public and private organisations in Switzerland, long time-

series of data related to glacier changes have been acquired and are highly valuable for scientific research, applied questions and outreach.
The present data-report expands the short overview of general outcomes published annually in German, French and Italian in the magazine "Die Alpen - Les Alpes - Le Alpi" of the Swiss Alpine Club with detailed facts and figures.

2 Weather and Climate

In this section the weather and climate conditions for the two periods 2019/20 and 2020/21 are described. We focus on the variables that are most relevant for glacier mass balance – temperature and precipitation. In general, glacier mass balance is largely determined by the amount of winter snow fall and air temperature during summer. High temperatures in April, May or June can reduce the winter snow pack rapidly and expose the much darker ice surface already in July. During July and August solar radiation receipts are high and melting of the unprotected ice is enhanced. When these two factors are combined, very negative mass balances as during the heat waves of summer 2003, 2015 and 2018 are expected. On the other hand, summer snow down to the glacier termini protects the ice surface from melting and will lead to less negative mass balances.
We have selected the four high-elevation meteorological stations at Grand St-Bernard (2472 m a.s.l.), Jungfraujoch (3580 m a.s.l.), Säntis (2502 m a.s.l.) and Weissfluhjoch (2690 m a.s.l.) to illustrate the monthly anomalies in air temperature (Figure 2.1), and 14 stations (Airolo, Chateau-d'Oex, Disentis, Engelberg, Elm, Grand St-Bernard, Grimsel Hospiz, Montana, Lauterbrunnen, Säntis, Scuol, Sils-Maria, Weissfluhjoch, Zermatt) throughout all regions of the Swiss Alps to document monthly anomalies in precipitation (Figure 2.2) for the two reporting periods. For annual precipitation and mean summer temperature (May-September), the long-term record since 1880 is shown in Figures 2.3 and 2.4 as a mean of 12 homogenized stations (Begert et al., 2005; Begert and Frei, 2018). The description of the weather conditions in the two reporting periods refer to the annual and monthly reports of the meteorological conditions by MeteoSwiss. Data are provided by the observational networks maintained by MeteoSwiss.

2.1 Weather and Climate in 2019/20

With heavy snowfall at the beginning of November 2019, the onset of the snowy period in the Swiss Alps took place about two weeks earlier than usual. On the southern slope of the Alps, some new November maxima of fresh snow were recorded at snow monitoring stations. The air temperature during the winter months of December to February was record high with a plus of over 3°C compared to normal conditions (1961-1990, Figure 2.1). Spring was also clearly too warm and characterized by abundant sunshine. Thus, below 1000 m a.s.l., the precipitation fell mostly as rain during the entire winter half-year. For the first time, no fresh snow at all could be registered at some low-lying central Swiss stations (beginning of measurements in 1883). Above 2000 m a.s.l., i.e. at the elevation of glaciers, however, the snow depths were average, in northern

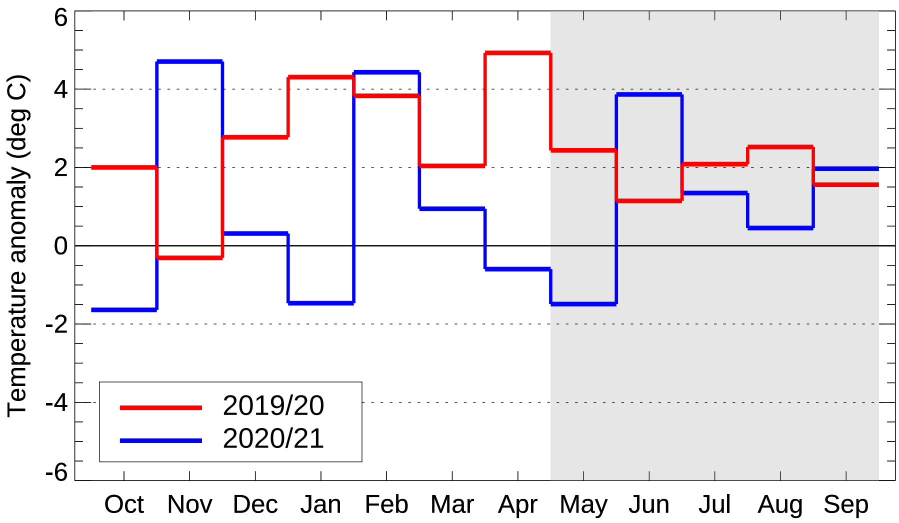

Figure 2.1: Mean monthly anomaly of temperature from the long-term climatic mean (period 1961-1990) for four selected stations at high elevation of the MeteoSwiss network. Anomalies in the two reporting periods 2019/20 and 2020/21 are shown. The grey shaded area indicates the months that are relevant for glacier mass loss.

Ticino and southern Valais even partly above average. This can be attributed to the generally high precipitation totals except for January and April (Figure 2.2) that fell as snow at this elevation even though the temperatures were much higher than usual.

Although snow depletion was already advanced also at the high elevations of the Alps in June, some snowfall events delayed the final disappearance of the snow cover. The months of July to

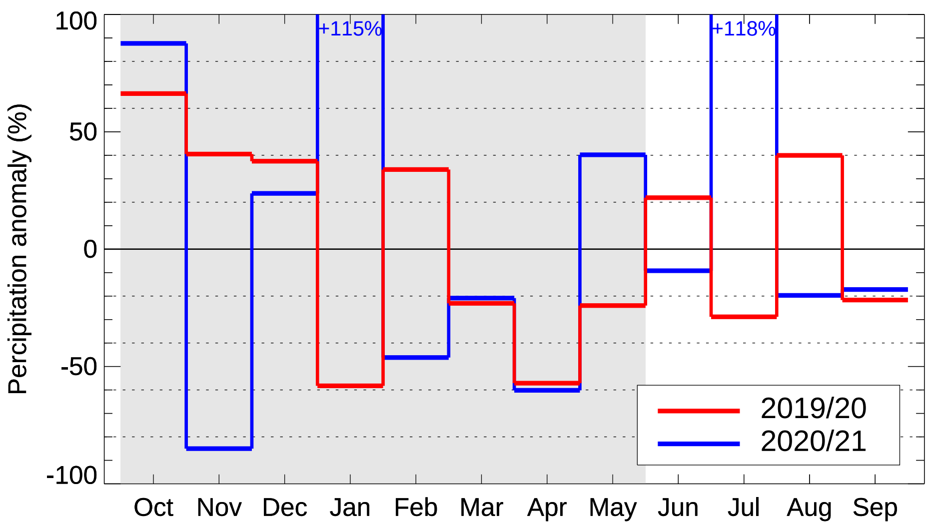

Figure 2.2: Mean monthly anomaly of precipitation from the long-term climatic mean (period 1961-1990) for 14 selected stations of the MeteoSwiss network. Anomalies in the two reporting periods 2019/20 and 2020/21 are shown. The grey shaded area indicates the months that are relevant for winter snow accumulation.

September were once again characterized by above-average temperatures but average precipitation totals (Figure 2.1, Figure 2.2). In contrast to the last years, however, two events with fresh snow down to 2000 m a.s.l. occurred in August. At the end of September, there was snow to partly below 1000 m a.s.l. on the northern side of the Alps, which is exceptional for this time of year, and abruptly ended the ablation season for most glaciers.
Compared to the reference period 1961-1990, summer air temperatures (May-September) were 2.1°C higher than the long-term mean evaluated for homogenized measurement series throughout Switzerland (Figure 2.3). This value ranks eight after the summers of 2003 (+3.5°C). Precipitation amounts were close to the average both in winter (October to April, +7.7%), as well as throughout the entire summer season (May to September, −2.1%, Figure 2.4). In summary, the weather conditions during the period 2019/20 resulted in mostly average conditions for the glaciers at the end of winter, but again strong and continuous melting throughout the summer season, although being less extreme than in the previous two reporting periods.

2.2 Weather and Climate in 2020/21

During a relatively cool month of October 2020 with abundant precipitation, especially on the southern side of the Alps, snow accumulation on glaciers started comparably early and was not hampered by the extraordinarily warm, sunny and dry November. In December and especially during January repeated major snowfall events massively increased snow coverage on glaciers and also resulted in a considerable snowpack at low elevation. The air temperatures from November to April were close to the long-term average, while the total precipitation of the winter months was above-average on both sides of the Alps, especially in October and January (Figure 2.2). March and April were characterized by lower precipitation than normal. At the elevation of glaciers, the snow accumulation season continued throughout the rather cool months of April and May and melting thus started several weeks later than usual.
According to MeteoSwiss, the summer months of 2021 north of the Alps are among the wettest in the more than 100-year-old records. The temperatures were close to the average of the last three decades, although June was significantly too warm (Figure 2.1). Overall, however, this still results in a temperature surplus of 1-2°C compared to the climatic normal period 1961-1990. The impact of climate change is clearly reflected in summer fresh snow, which was surprisingly limited despite the high precipitation totals: At Weissfluhjoch (Eastern Switzerland, 2540 m a.s.l.) a fresh snow sum of 155 cm was recorded during the wet summer of 1987 – in 2021 it was just 20 cm. The very warm and sunny September only twice brought small snowfalls on the glaciers and melting continued until early October.
Summer air temperatures (May to September) were 1.3°C higher than the 1961-1990 mean (Figure 2.3). Annual precipitation was above the long-term average (10.1%, Figure 2.4). Whereas abundant snowfall during the winter season, and especially the cool conditions and additional accumulation in April and May were favourable for the glaciers, the summer season was too warm again despite of the unsettled weather, thus resulting in continued glacier mas losses.

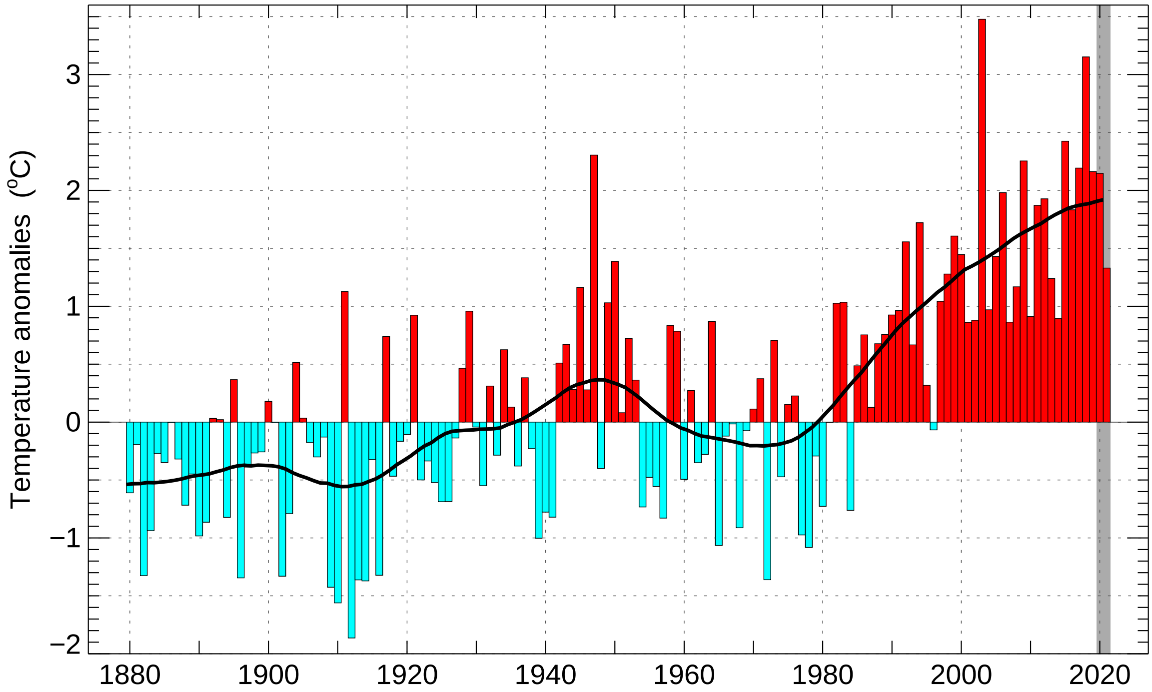

Figure 2.3: Anomalies of mean summer air temperature (May-September) from the mean value 1961-1990 in degrees Celsius for the period 1864-2021 based on 12 homogenized long-term stations of MeteoSwiss. The gray shaded area highlights the years of the current report.

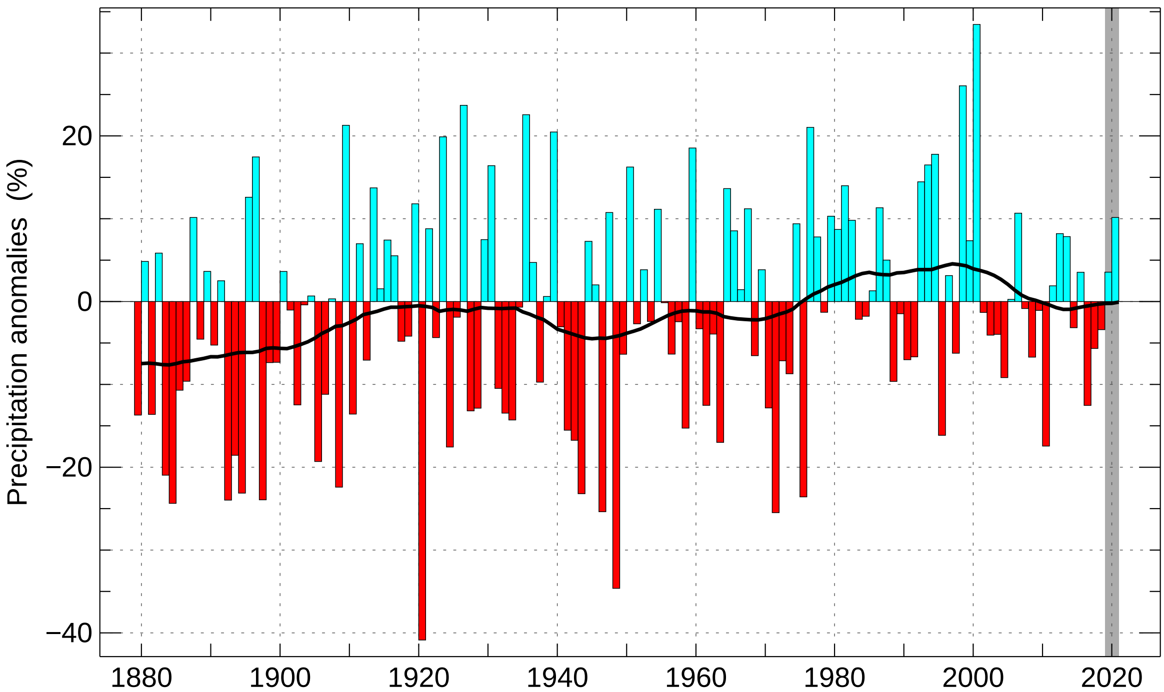

Figure 2.4: Anomalies of annual precipitation (hydrological year) from the mean value 1961-1990 in percentage for the period 1864-2021 based on 12 homogenized long-term stations of MeteoSwiss. The gray shaded area highlights the years of the current report.

3 Length Variation

3.1 Introduction

Systematic observations of length variations started in 1880. Due to ongoing and coordinated efforts long and continuous time-series documenting glacier length variations for a large number of glaciers have been collected. Since the beginning the annual surveys have been carried out by a collaborative network of people on different types of glaciers covering all regions of the Swiss Alps. Measurements based on simple techniques carried out by collaborators without any spacial training and hardware resources available turned out to be a key factor for the success of the extensive monitoring.

An evaluation of the existing dataset of length variations identified two major deficiencies: (1) Only the change in length has been evaluated and reported so far but the location of the underlying measurement is often not precisely known. (2) The summation of incremental differences, hence may show large systematic errors and biases when compared to actual distances of dated glacier extent as derived from aerial imagery or features in the terrain. In addition, several of the long-term series are affected by data gaps of some yeas up to several decades. A revision of the strategy was proposed to achieve the following goals: (1) continuation of existing long-term series, (2) a consistent and reproducible evaluation methodology, (3) improved data quality of only geo-localized measurements. The goals are accompanied by the requirement of the optimal use of available resources and integration of new measurement techniques. A considerable potential to higher data quality is attributed to the products of the Federal Office of Topography swisstopo due to more frequent periodical aerial surveys and operational photogrammetrical processing. A conceptual change of the observation principle with a reduction from annual to multi-annual observations is expected to make data acquisition more efficient, while providing geo-localized data with high quality and reduced costs.

In 2020 GLAMOS adopted a revised monitoring strategy for length variations (GLAMOS, 2020b). The major update to the previous concept is a multi-level data acquisition with a combination of four different observation types:

(1) FIELD: Annual field observations, periodically complemented with glacier outlines ensure continuity and high accuracy

(2) AIR: High spatial coverage at annual resolution with accurate and homogeneous data

(3) MIX: Combination of bi-annual field measurements and outlines from the swisstopo's operational products, large coverage, homogeneous data and still high temporal resolution

(4) TLM: Homogeneous data with strongly reduced effort and costs at 3-year intervals

Based on the various needs and requirements such as the quality of existing time-series, well balanced distribution over all regions and glacier types (size or shape), expected further evolution and accessibility, and also individual needs of local collaborators, the 121 glaciers with available length variation time-series and recent observations have been assigned to the four new observation types. This resulted in a selection of 43 glaciers (16%) to be continued with annual field observations (FIELD). 19 (16%) glaciers were selected for the AIR observation type, while another 22 (18%) glaciers were allocated to the MIX observation type. The 37 (30%) remaining glaciers eventually are evaluated based on the operational swisstopo products (3/6-year intervals).
The modifications in the observation strategy have been implemented gradually starting in 2020. In order to ensure continuous data acquisition avoiding any gaps, the data acquisition interval was taken into account for a change in the measurement technique as well as the needs of local collaborators are included. Complete implementation of the proposed modifications in the observation strategy are expected to be achieved after a transition phase of a few years. Due to the ongoing rapid changes expected during the next decade the classification may need to be refined to cope with the evolving conditions and to maximize the effect.

In the two periods covered by this report, 113 of 156 glaciers with documented length fluctuations have been actively observed (Figures 3.1, 3.2 and Table 3.1). The other glaciers have melted back drastically or are heavily debris-covered, with the result of only being observed at irregular intervals. As a result of the modified observation strategy, evaluated length change information for glaciers observed periodically based the operational swisstopo products is often not available at the time of the annual reporting.

During the two years under review, 2019/20 and 2020/21, Swiss glaciers suffered further losses in length. As in previous periods, most of the measurements were within the range of 0 to −30 metres. This overall trend was once again overshadowed in both years by a few very high retreat values, which could be traced to local influences, and in some cases also pertain to a period of several years. They are usually the result of a process extending over a longer period of time and thus are not unexpected.

3.2 Length Variations in 2019/20

In general, optimal measurement conditions were present for the survey in autumn 2020 after a summer with good weather conditions and intense melt. Changes in the terminus position as compared to the previous years were determined at 82 glaciers (Figure 3.1). Of these, 79 were found to be in recession, for one no change was observed, and another two glaciers showed a positive value. With the exception of ten glaciers, the values ranged from a retreat of −61 meters at Sankt Annafirn to a slight advance of +6 meters at Sardonagletscher. Nearly three-quarters of the measurements lay between −1 and −30 metres.

The ten exceptions refer to the larger recession observed at the snout and cover mostly a multy-year period. The large retreat values are a result of the evolution of the glaciers over the last decade and were therefore expected. Due to the continued absence of ice flow from the accumulation area or the increasingly thicker debris cover, the tongues of these glaciers were thinned out or were melting irregularly without any major reduction in length over the previous years.

The few positive values are the result of local changes at the terminus and do not stem from abundant ice flow from the accumulation area. Ice margins that are difficult to detect due to a thick and continuous coverage of debris may further cause erroneous interpretations. However, the cumulative length change is not affected by such uncertain individual results as they will cancel out in successive measurements.

3.3 Length Variations in 2020/21

In autumn 2021 the implementation of revised monitoring strategy for length variations (GLAMOS, 2020b) was initiated. This may result in a smaller number of glaciers with a length variation determined in the respective year but time-series of additional glacier will be continued in successive years. Results of length variations are available for 77 glaciers in autumn 2021 (Figure 3.2). Of these, 66 became shorter, five did not change their position, and six were slightly in advance. With the exception of three glaciers, the values ranged from a recession of −57 meters at Vadret da Morteratsch to an advance of +7 meters at Kehlengletscher. Again almost two-thirds of the measurement values lay between −1 and −30 meters. The relatively high number of measurements may be the result of some abundant snow accumulation left at the end of the summer season after a summ with variable weather conditions.

Glacier de Ferpècle, Langgletscher, Turtmangletscher and Findelengletscher were the exceptions featuring a very large reduction in length. As in the previous period, the high retreat values of several hundred meters for each is linked to a process that has been underway for many years. The tongue of the three glaciers Ferpècle, Findelen and Lang succesively thinned out over last years due to high melt rates and the absence of ice supply from the accumulation area. Eventually a larger part lost connection at a narrow gully in case of Ferpècle or the remaining thin flat tongue disintegrated into individual ice masses and the dynamic terminus shifted back abruptly.
At Turtmangletscher a major ice break occured in a steep section in the terrain on 6th August 2020. A large part of the tongue was disconnected and resulted in a large variation of the terminus position. In all three cases, the timing was rather arbitrary and only poorly reflects the continuous change of the glaciers in last decades.

3.4 Length Variations in 2019/20 and in 2020/21, Summary

No. [a]	Glacier	Ct. [b]	Length variation [c] (m) 2019/20	2020/21	Altitude [d] (m a.s.l.) 2021	Date of measurements (Day, Month) 2019	2020	2021
Catchment area of the river Rhone (II)								
1 [e,f]	Rhone	VS	−29.3	−14.5	2210.9 [16]	25.08.	13.09.	20.08.
2 [f]	Mutt	VS	−25.3 [2a]	−51.6	2696.5	n	08.08.	28.08.
3 [e,f]	Gries	VS	−30.0	−20.4	2430.4 [16]	25.08.	09.09.	24.09.
4 [f]	Fiescher	VS	−159 [3a]	n	1682 [15]	n	04.09.	n
5 [e,f]	Grosser Aletsch	VS	−51.6	−51.6	1602.0 [16]	04.09.	14.09.	29.07.
106	Mittelaletsch	VS	−188.7 [3a]	n	2360 [20]	n	04.09.	n
6 [f]	Oberaletsch	VS	x	n	2142 [03]	n	21.10.	n
7 [e,f]	Kaltwasser	VS	−0.6	x	2660 [12]	08.10.	02.09.	14.09.
173 [e]	Seewjinen	VS	+0.1	n	2735.5 [16]	21.09.	04.09.	n
10 [e,f]	Schwarzberg	VS	−14.2	n	2663.2 [16]	21.09.	27.08.	n
11 [e,f]	Allalin	VS	−4.9	n	2676.7 [16]	21.09.	27.08.	n
174 [e]	Hohlaub	VS	−1.7	n	2841.0 [16]	21.09.	27.08.	n
12 [e]	Chessjen	VS	x	n	2866.3 [16]	21.09.	27.08.	n
13 [f]	Fee	VS	x	n	2170 [19]	11.10.	07.08.	n
14 [e,f]	Gorner	VS	−79.8 [2a]	−38.9	2211 [15]	n	21.08.	14.08.
15 [f]	Zmutt	VS	−134 [3a]	n	2238.4 [10]	n	21.08.	n
16 [e,f]	Findelen	VS	−118.3	−132.0	2555.8 [16]	03.09.	21.08.	14.08.
17 [e]	Ried	VS	−10.7	n	2400 [20]	13.10.	18.10.	n
18 [e,f]	Lang	VS	n	−566 [4a]	2045 [17]	n	n	03.09.
19 [e,f]	Turtmann	VS	n	−474 [2a]	2270 [10]	04.10.	n	08.09.
20	Brunegg (Turtmann)	VS	n	−11.1 [2a]	2500 [10]	01.10.	n	08.09.
22 [e,f]	Zinal	VS	−12.6 [2a]	n	2130 [18]	n	03.09.	n
23 [f]	Moming	VS	−42.9 [3a]	n	2580 [13]	n	07.08.	n
24 [f]	Moiry	VS	−24.6 [2a]	−27.4	2410	n	03.09.	01.09.
25 [e,f]	Ferpècle	VS	x	−660 [2a]	2205 [14]	14.10.	13.11.	01.10.
26	Mont Miné	VS	−12.0 [4a]	n	2090 [12]	n	21.08.	n
27 [f]	Arolla (Mont Collon)	VS	−16.9	−49.7	2230	27.09.	16.09.	17.09.
28 [e,f]	Tsidjiore Nouve	VS	−13.0	−13.9	2290	27.09.	16.09.	17.09.
29 [f]	Cheillon	VS	−11.0	−12.5	2685	13.09.	22.09.	23.09.
30 [f]	En Darrey	VS	−13.7	n	2710 [17]	13.09.	22.09.	n
31 [f]	Grand Désert	VS	−17.3	−37.9	2810 [17]	12.09.	17.09.	16.09.
32 [e,f]	Mont Fort (Tortin)	VS	−10.8	−9.2	2785 [18]	13.09.	18.09.	27.08.
33 [e,f]	Tsanfleuron	VS	−6.5	−15.3	2520	20.09.	11.09.	14.09.
34	Otemma	VS	−192.9 [3a]	n	2480 [18]	n	15.08.	n
35	Mont Durand	VS	−9.6 [4a]	n	2380 [19]	n	15.08.	n

No. [a]	Glacier	Ct. [b]	Length variation [c] (m) 2019/20	2020/21	Altitude [d] (m a.s.l.) 2021	Date of measurements (Day, Month) 2019	2020	2021
36	Breney	VS	−98.7 [3a]	n	2575 [19]	n	15.08.	n
37	Giétro	VS	−80.2 [3a]	n	2718.6 [16]	n	21.08.	n
38	Corbassière	VS	−118.3 [3a]	n	2309.5 [16]	n	21.08.	n
39 [f]	Valsorey	VS	−33.4	−13.1	2490	20.09.	06.09.	30.09.
40 [e]	Tseudet	VS	−5.5	−35	2640	20.09.	06.09.	30.09.
41	Boveyre	VS	−1.9	n	2705 [20]	04.10.	10.09.	n
42 [e,f]	Saleina	VS	−14.5	+3.4	1920	16.10.	04.09.	24.09.
43 [e,f]	Trient	VS	−25	−40	2198	12.10.	18.10.	25.09.
44 [e,f]	Paneyrosse	VD	−7	−9.8		20.09.	09.09.	20.10.
45 [e,f]	Grand Plan Névé	VD	n	−3.6 [2a]		27.09.	n	20.10.
47 [e,f]	Sex Rouge	VD	−3.1	n	2747 [20]	15.09.	14.09.	n
48 [e]	Prapio	VD	x	n	2555 [19]	n	07.08.	n
Catchment area of the river Aare (Ia)								
50 [f]	Oberaar	BE	−126.7 [3a]	−15.1	2306.9 [09]	n	09.09.	23.09.
51 [f]	Unteraar	BE	−106.5 [3a]	−21.0	1930.3 [09]	n	04.09.	26.08.
52	Gauli	BE	n	−33.5 [2a]	2140	28.09.	n	25.09.
53 [e,f]	Stein	BE	−80	−12.5	2260	26.08.	13.09.	05.05.
54	Steinlimi	BE	n	x	2530 [19]	n	n	12.08.
55 [e,f]	Trift (Gadmen)	BE	−1.8	+0.3	2111.5 [16]	25.08.	13.09.	20.08.
57 [e,f]	Oberer Grindelwald	BE	−18.6	−0.8	2178.6 [16]	25.08.	13.09.	20.08.
58 [e,f]	Unterer Grindelwald	BE	−35.9	−8.7	1587.1 [16]	25.08.	13.09.	20.08.
59 [e]	Eiger	BE	−9.7	−22.9	2413.3 [20]	27.09.	03.09.	23.09.
60 [e]	Tschingel	BE	n	−5.3 [2a]	2310	14.10.	n	31.08.
61 [e,f]	Gamchi	BE	−29	+4	2135	18.10.	01.10.	14.10.
109 [e]	Alpetli (Kanderfirn)	BE	−49	−25	2410	20.09.	21.09.	01.10.
63 [e]	Lämmern	VS	n	−50 [2a]	2690	20.09.	n	01.10.
64 [e,f]	Blüemlisalp	BE	n	−160.7 [7a]	2394 [18]	n	n	23.09.
65 [e,f]	Rätzli	BE	−12.0	−4.1	2467.6 [16]	03.09.	13.09.	21.08.
111 [e]	Ammerten	BE	−3.6	−0.3	2350	21.09.	19.09.	12.09.
112	Dungel	BE	n	−8.5 [3a]	2620	n	n	30.09.
113	Gelten	BE	n	−15.2 [4a]	2595	n	n	30.09.
Catchment area of the river Reuss (Ib)								
66 [e,f]	Tiefen	UR	−34	−2.5	2655	19.09.	04.09.	02.09.
67 [e,f]	Sankt Anna	UR	−61	−22.5	2625	20.09.	04.09.	24.09.
68 [e,f]	Kehlen	UR	−12	+7.3	2400	11.10.	22.10.	25.08.
69	Rotfirn (Nord)	UR	n	−252.2 [4a]	2070 [17]	n	n	12.08.
70 [e,f]	Damma	UR	x	−61 [2a]	2500	11.10.	22.10.	25.08.

No. [a]	Glacier	Ct. [b]	Length variation [c] (m) 2019/20	2020/21	Altitude [d] (m a.s.l.) 2021	Date of measurements (Day, Month) 2019	2020	2021
71 [e,f]	Wallenbur	UR	−42.5	−9.6	2300	01.10.	14.09.	19.10.
72 [e,f]	Brunni	UR	−5.8	−9.6	2570	20.09.	28.08.	24.09.
73 [f]	Hüfi	UR	n	−259.4 [5a]	1920	n	n	01.10.
74 [e,f]	Griess	UR	−19.3	−8.3	2232	20.09.	15.09.	01.10.
75 [f]	Firnalpeli (Ost)	OW	n	x	2210 [19]	n	n	01.10.
76 [f]	Griessen	OW	n	x	2530 [19]	n	n	01.10.
Catchment area of the river Linth / Limmat (Ic)								
77 [e,f]	Biferten	GL	−15.3	−1.7	1964.0	14.09.	05.09.	25.09.
78 [e]	Limmern	GL	−3.3	n	2290 [20]	16.10.	11.09.	n
114 [e]	Plattalva	GL	−8.0	n	2629 [20]	16.10.	12.09.	n
79 [e,f]	Sulz	GL	−19.9	−1.9	1810 [19]	24.09.	01.10.	30.09.
80 [e,f]	Glärnisch	GL	−23.3	−11.7	2364.6	31.08.	12.09.	30.09.
81 [e,f]	Pizol	SG	−6.5	−3.6	2605	19.09.	17.09.	11.10.
Catchment area of the river Rhine / Lake Constance (Id)								
82 [e,f]	Lavaz	GR	−16.5	+0.1	2417	27.08.	28.08.	31.08.
83 [e,f]	Punteglias	GR	x	n	2370 [18]	n	20.08.	n
84 [e,f]	Lenta	GR	n	x	2760 [18]	n	n	26.08.
85 [e,f]	Vorab	GR	−23	−1.7	2618	15.09.	28.08.	25.08.
86 [e,f]	Paradies	GR	−2.5	−8.9	2722	20.09.	10.09.	10.09.
87 [e]	Suretta	GR	n	+3.1 [2a]	2591	27.08.	n	14.09.
88 [e,f]	Porchabella	GR	−15.8	−10.3	2709	13.09.	15.09.	10.09.
115 [e]	Scaletta	GR	−6	n	2721 [20]	20.09.	09.09.	n
89 [e,f]	Verstankla	GR	n	−43.5 [2a]	2438 [19]	22.08.	n	22.09.
90 [e]	Silvretta	GR	−18.5	−8.7	2471.8 [16]	29.09.	13.09.	01.09.
91 [e,f]	Sardona	SG	6.1	+1.9	2480	11.09.	14.09.	03.10.
Catchment area of the river Inn (V)								
92 [f]	Roseg	GR	n	n	2160 [09]	n	n	n
93	Tschierva	GR	−39.5	n	2318 [20]	13.09.	26.10.	n
94 [e,f]	Morteratsch	GR	−19	−56.6	2117	10.09.	16.09.	16.09.
95 [e]	Calderas	GR	n	−19.4 [2a]	2798	01.10.	n	27.08.
96 [e,f]	Tiatscha	GR	−3.6	−4.3	2671.5 [17]	29.09.	13.09.	01.09.
97 [e]	Sesvenna	GR	−4.3	−7	2815	29.08.	16.09.	24.08.
98 [e,f]	Lischana	GR	x	+2.2	2817	n	15.09.	01.09.
Catchment area of the river Adda (IV)								
99 [e]	Cambrena	GR	−5.4	−50.7	2620 [20]	27.09.	01.10.	01.10.
100 [e,f]	Palü	GR	+1.8	−8.9	2590	20.09.	25.08.	18.08.
101 [e]	Paradisino (Campo)	GR	sn	−15.7 [2a]	2865	13.09.	19.10.	22.09.
102 [f]	Forno	GR	−23.9	−27.1	2229	03.09.	03.09.	07.09.
116 [e]	Albigna	GR	−19	−10.5	2184	05.09.	09.09.	09.09.

No. [a]	Glacier	Ct. [b]	Length variation [c] (m) 2019/20	2020/21	Altitude [d] (m a.s.l.) 2021	Date of measurements (Day, Month) 2019	2020	2021
Catchment area of the river Ticino (III)								
103 [e,f]	Bresciana	TI	−11	−2	2991	03.10.	29.09.	03.09.
352	Croslina	TI	n	n	2728.7 [19]	10.10.	n	n
118	Val Torta	TI	n	0 [10a]	2525 [12]	n	n	24.09.
117 [e]	Valleggia	TI	−15	−7.2	2473	18.09.	30.09.	08.09.
119 [e]	Cavagnoli	TI	−16.8	−16	2672	18.09.	29.09.	13.09.
104 [e,f]	Basòdino	TI	−1.5	−10.7 [2a]	2663	17.09.	21.09.	07.09.
120 [e]	Corno	TI	−6	−5.3 [2a]	2670	26.09.	28.09.	13.09.
105 [f]	Rossboden	VS	−13.2 [3a]	n	2660 [20]	n	08.08.	n

Legend

+	advancing	x	value not determined
st	stationary, ±1 m	n	not observed
−	retreating	sn	snow covered

a Identification number of the glacier in the observational network (see Figures 3.1 and 3.2).

b If a specific glacier is situated in more than one canton, the canton indicated in the table is the one where the observed glacier tongue lies.

c If the value given relates to more than one year, the number of years is indicated as follows: −26 [5a] = Decrease of 26 meters within 5 years.

d If the altitude of the glacier tongue is not measured in 2021, the year of the last measurement is indicated: 2210.9 [16] = 2210.9 m a.s.l., measured in the year 2016.

e Compare Appendix B: Remarks on individual glaciers.

f Glacier with nearly complete data series since the beginning of the measurements at the end of the 19th century and one of the 73 glaciers selected in Figure 3.4.

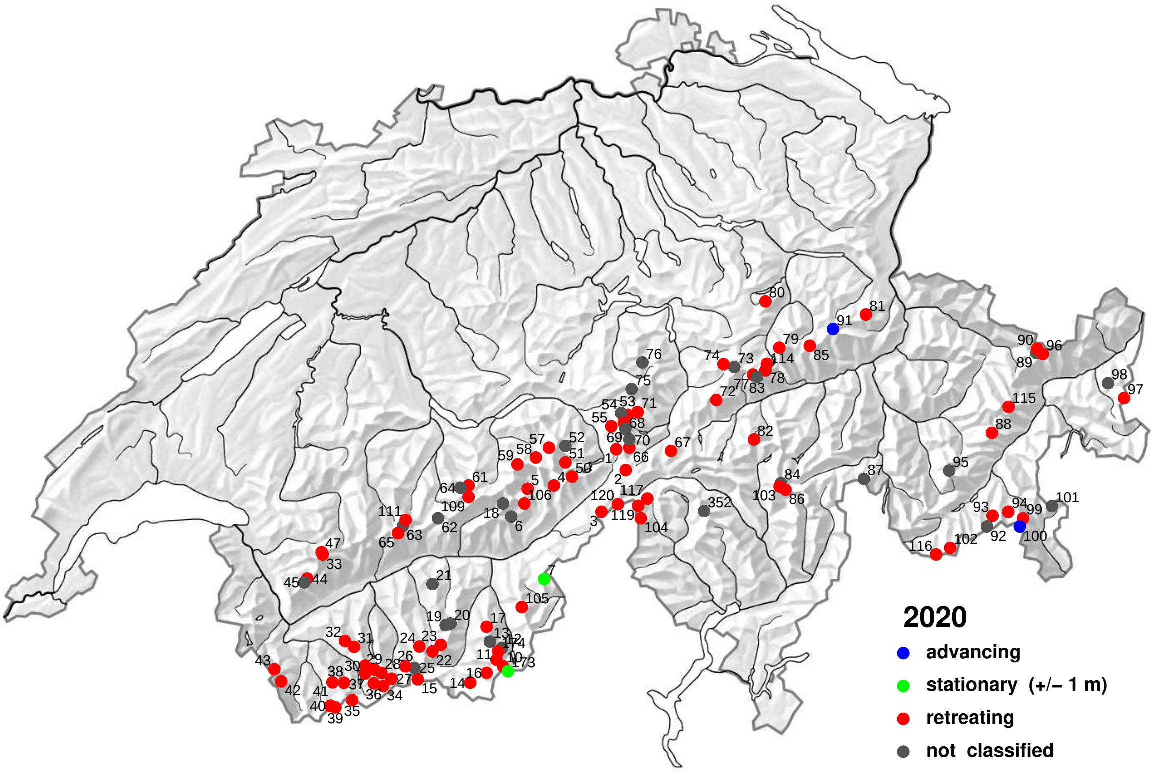

Figure 3.1: Observed glaciers in fall 2020.

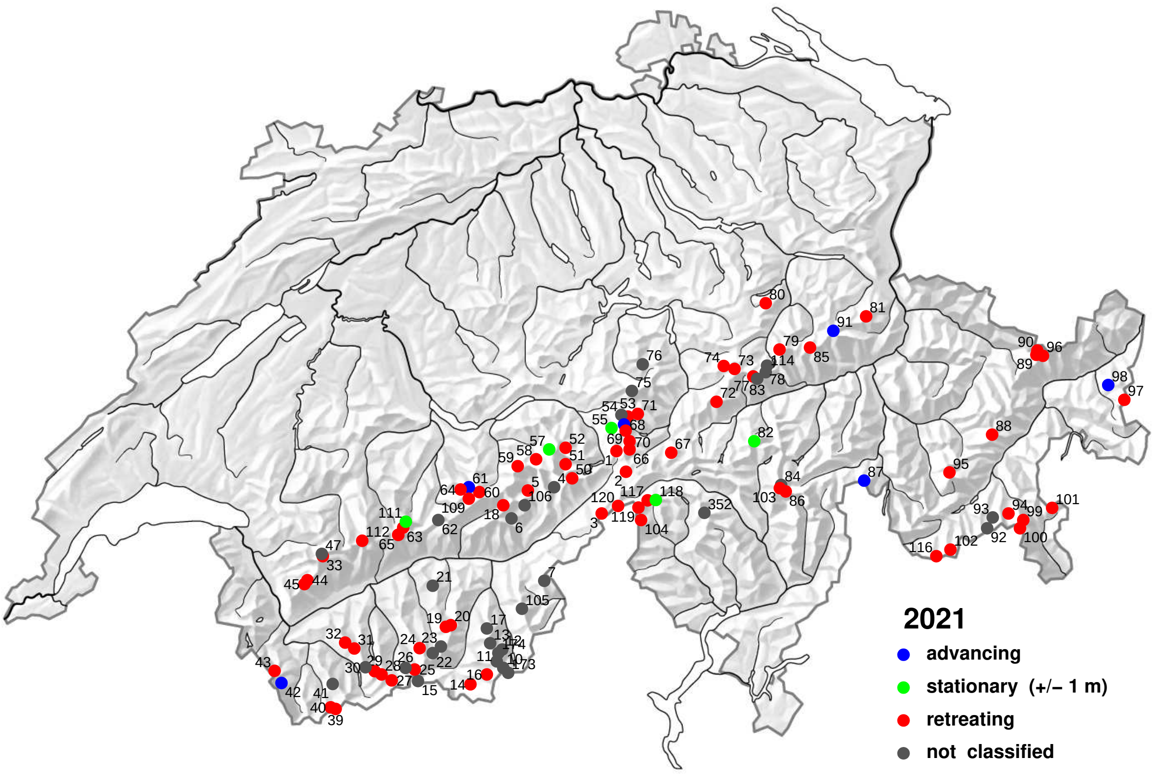

Figure 3.2: Observed glaciers in fall 2021.

3.5 Length Variations - Statistics for 1880-2021

The long-term development of glaciers in Switzerland is illustrated by using a selected sample of 73 glaciers (Figures 3.3 and 3.4), and the cumulative glacier length variations which have been classified according to length (Figures 3.5 - 3.8).
The dynamic response to climatic forcing of glaciers with variable geometry involves striking differences in the recorded cumulative length changes (Figures 3.4 and 3.5 - 3.8) (Hoelzle et al., 2003). Such differences reflect the considerable effects of size and slope-dependent reaction of the delayed response of the glacier terminus with respect to the undelayed input (mass balance) signal (Zekollari et al., 2020).
In order to avoid a glacier sample whose scope changes annually, not all glaciers were considered for the analysis of the long-term evolution. Only continuous and long series are included. From the entire dataset, 73 glaciers were selected as a sample with nearly complete series since the beginning of the measurements at the end of the 19th century. In Chapter 3.4, these 73 glaciers are indicated by a footnote f. Figure 3.3 presents absolute numbers of yearly measurements available in the database as well as for the selected glaciers. While in 2020 for 64 glaciers out of the reference sample a length variation was determined, in the following year only 55 glaciers were measured. In 2020, 61 of the reference glaciers and in 2021, 41 glaciers were retreating, two and five glaciers, respectively, were advancing and in both years one glacier showed no change.

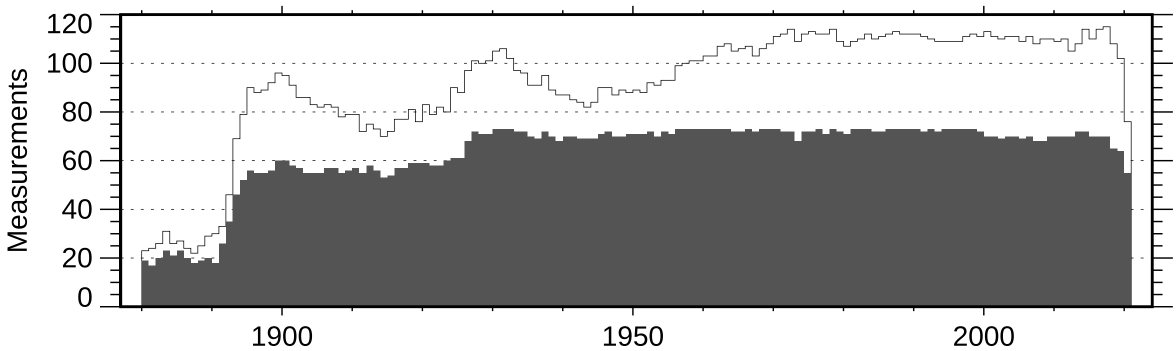

Figure 3.3: Annual number observed length variations in total (line) and number out of the set of the 73 reference glaciers (grey area) classified in the data base.

The sample is dominated by medium-sized glaciers (length between 1 to 5 km) with a typical response time in the order of decades. The periods of advance, such as those in the 1910s to 1920s and the 1970s to 1980s, can be seen clearly. Figure 3.4 shows the annual and individual length change of all 73 selected glaciers sorted for length. For the purpose of intercomparison, values of cumulative length change are presented with respect to size categories chosen in a way to optimally reflect common characteristics of the response signal at the glacier terminus. It is well recognized that large glaciers, such as Grosser Aletschgletscher, show continuous retreat since 1880, in contrast to the smaller glaciers such as Pizolgletscher, that has highly variable behavior.

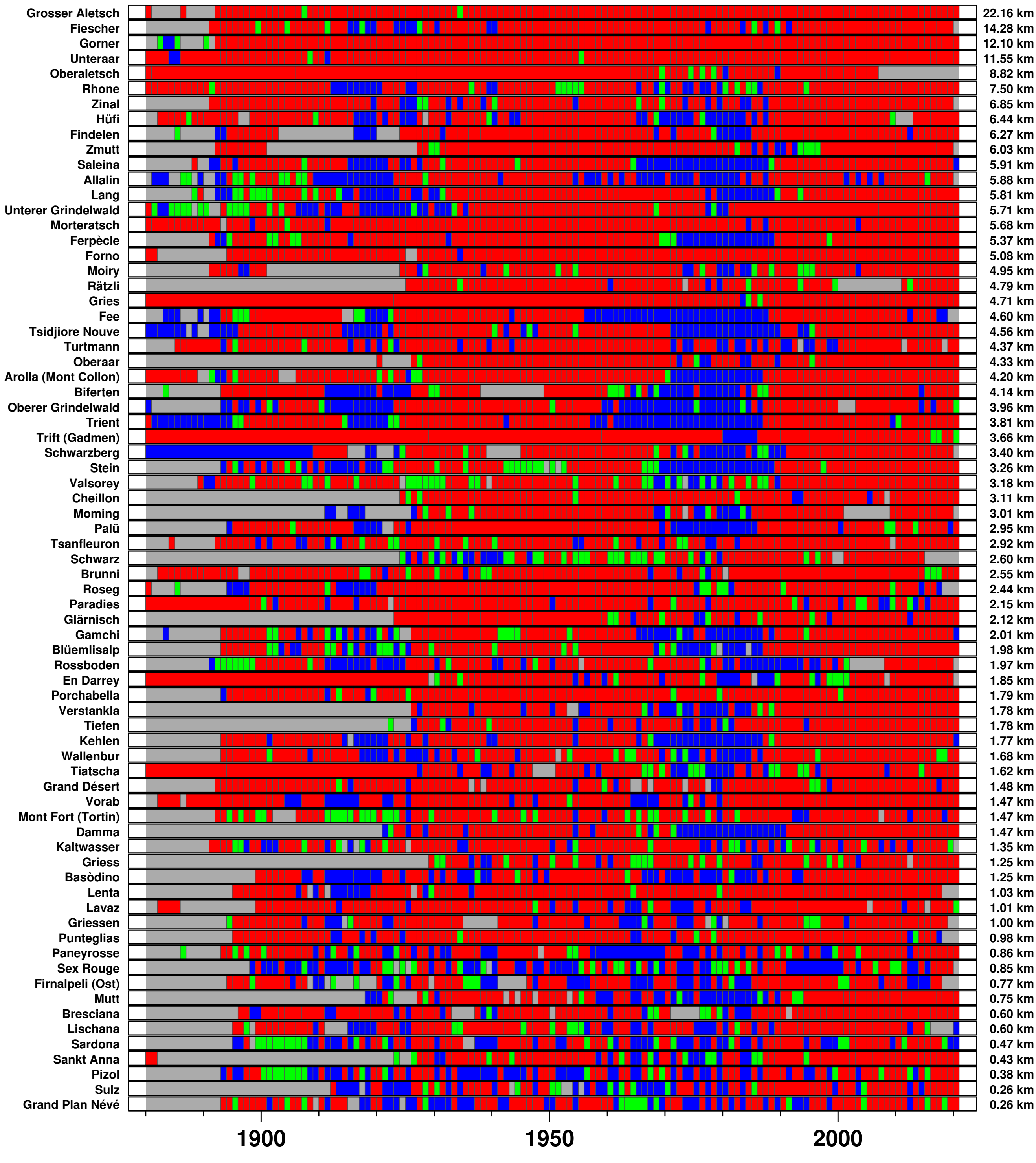

Figure 3.4: Individual pattern of advancing (blue), stationary (±1 m, green) and retreating (red) length variation of the same 73 selected glaciers (displayed in the descending order of current glacier length).

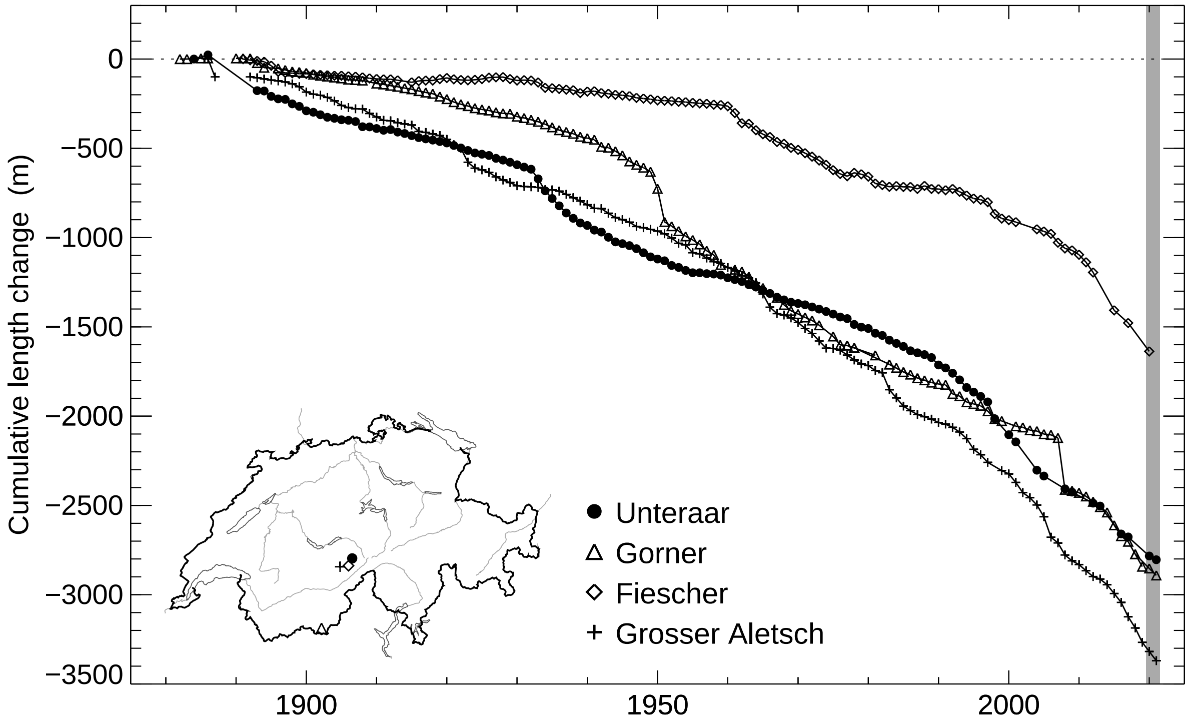

Figure 3.5: Large valley glaciers with a length of more than 10 km displaying a more or less continuous retreat over the entire time period. The gray shaded area highlights the years of the current report.

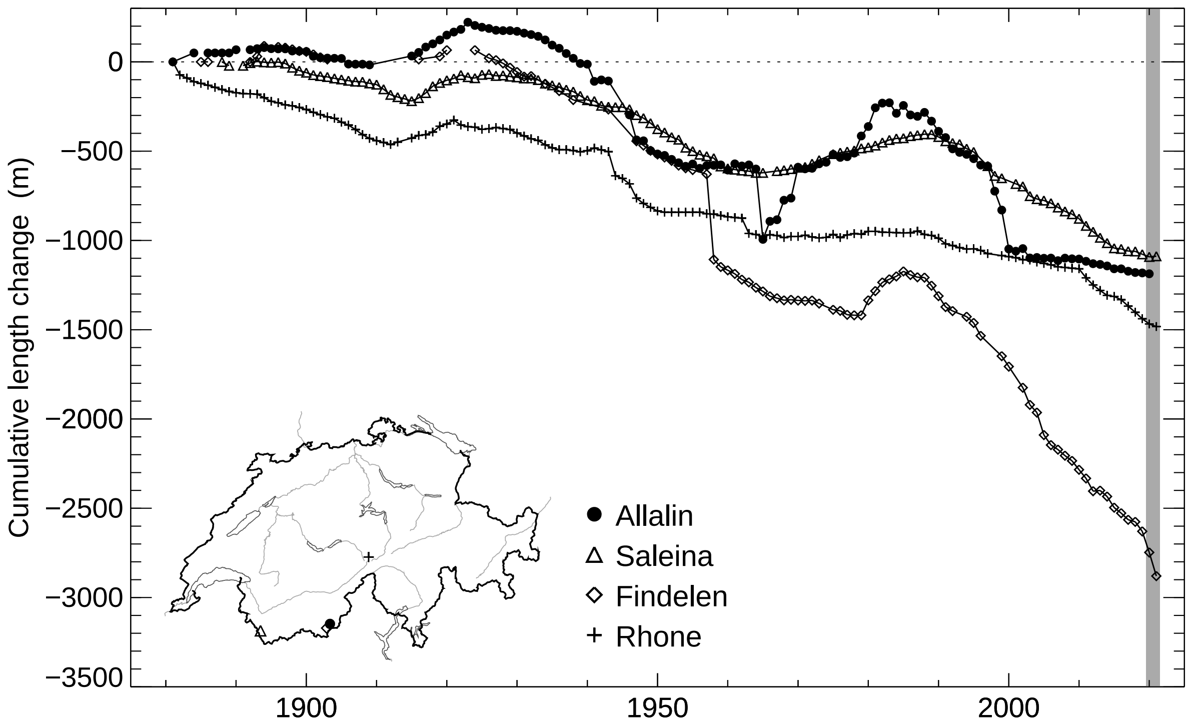

Figure 3.6: Mountain glaciers with a length of 5 to 10 km showing advance and retreat phases in two periods (around 1920 and 1970). The gray shaded area highlights the years of the current report.

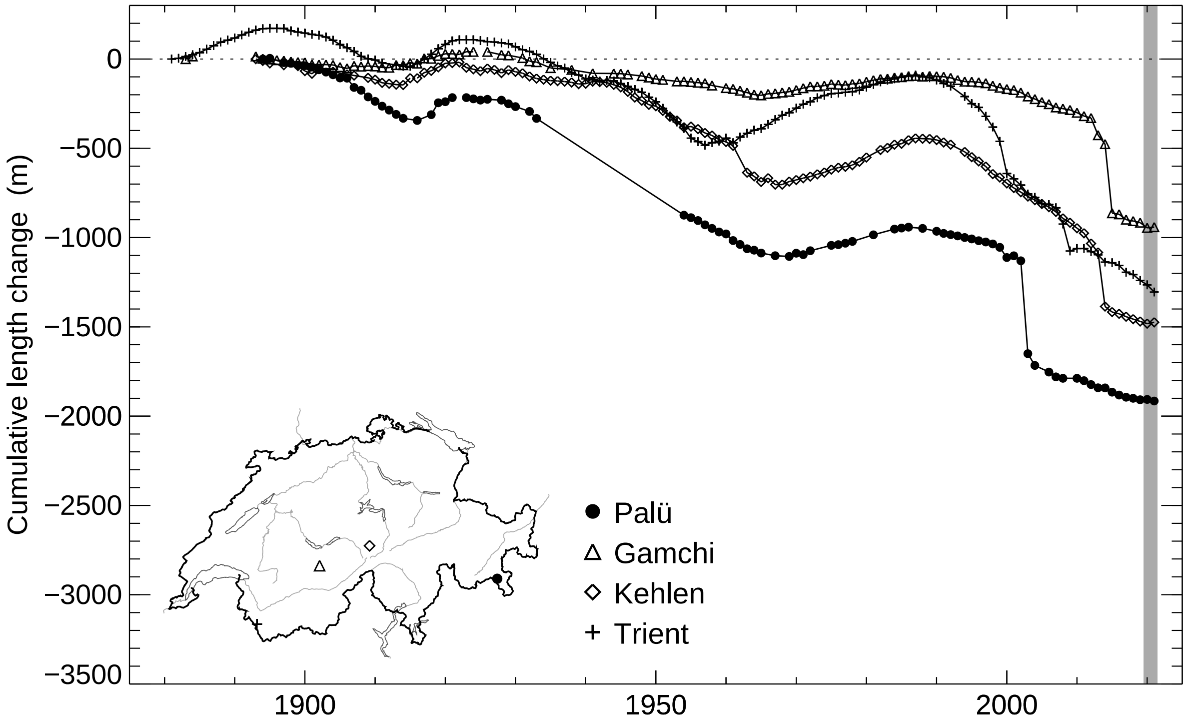

Figure 3.7: Medium-sized mountain glaciers with a length of 1 to 5 km showing two distinct advance and retreat phases. The gray shaded area highlights the years of the current report.

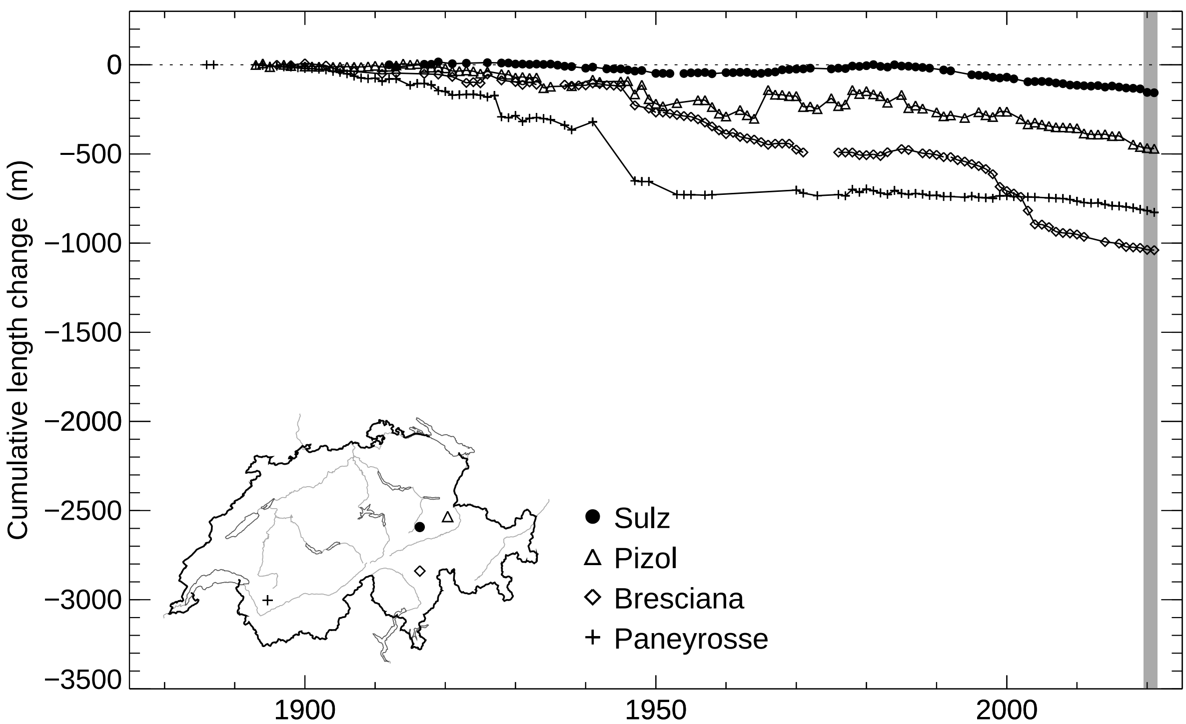

Figure 3.8: Very small cirque glaciers with a length of less than 1 km displaying generally small changes and a more irregular length change signal. The gray shaded area highlights the years of the current report.

Glaciers investigated for length variations that experienced a large retreat in the past decade: Glacier Mont Fort (Tortin) in August 2021 (top, Photo: DWFL/VS F. Bourban) and Glärnischfirn in September 2020 (bottom, Photo: N. Dobler)

Glaciers investigated for length variations that experienced a large retreat in the past decade: Lentagletscher in August 2021 (top, Photo: AWN/GR L. Brunner) and Ghiacciaio del Cavagnoli in September 2021 (bottom, Photo: SF/TI M. Soldati)

4 Mass Balance

4.1 Introduction, cumulative mean specific mass balances

Seasonal mass balance observations were collected using the glaciological method for Ghiacciaio del Basòdino, Claridenfirn, Findelengletscher, Griesgletscher, Grosser Aletschgletscher, Vadret dal Murtèl, Vadret Pers, Glacier de la Plaine Morte, Rhonegletscher, Sankt Annafirn, Silvrettagletscher and Glacier de Tsanfleuron as well as some additional smaller glaciers. Mass balance surveys at annual resolution at a network of mass balance stakes were conducted at Allalingletscher, Glacier de Corbassière, Glacier du Giétro, Hohlaubgletscher and Schwarzberggletscher. In Figure 4.1 the distribution of these monitoring sites throughout Switzerland is shown.

Figure 4.1: Investigated glaciers for mass balance with a focus on spatial distribution and analysis of seasonal mass balance components (dark blue), and investigated glaciers with lower spatial sampling density and/or only annual measurements (light blue).

The mass balance measurements at stakes, in snow pits, as well as extensive snow probing in spring were used to calculate the mean specific components of mass balance following the methods described in Huss et al. (2021). Extrapolation from individual measurement points to the entire glacier surface was performed using a distributed mass balance model constrained with all seasonal observations. It includes the most important processes governing spatial mass balance distribution. This approach is regarded as an advanced extrapolation tool to infer glacier-wide quantities from point measurements rather than a mass balance model in the conventional sense: the signal of seasonal and annual mass balance variability is purely given by the field measurements. The procedure is thus fully in line with more traditional techniques to extrapolate local observations of glacier mass balance, such as the profile or the contourline method (e.g. Østrem and Brugman, 1991) but takes into account more sophisticated methods to infer mass balance in unmeasured regions of the glacier. The procedure is divided into two steps:

(1) The model is tuned such that both the measurements of winter accumulation and summer ablation are matched optimally over the periods defined by the exact dates of the in-situ measurements which are reported for the years of the current report. This allows extrapolation of mass balance based on a physical representation of the spatial variability, as well as the calculation of mass balance over fixed-date periods (e.g. the hydrological year).

(2) A periodical, final reanalysis and homogenisation with independent ice volume changes derived from digital elevation models is performed in five to ten year intervals, and potential updates of the series are reported subsequently.

Field measurements were collected on 22 glaciers in total during the two reporting periods 2019/20 and 2020/21. Point mass balance was inferred by snow probings and snow density measurements during April/May, and at a network of mass balance stakes in September/October. Distributed measurements permitted inferring glacier-wide mass balance and the corresponding elevation distribution. As a result of accelerated atmospheric warming, several monitoring sites at small glaciers are on the verge of being lost, and some of the measurements will need to be discontinued soon, or active maintenance has already been abandoned (e.g. Pizolgletscher, Vadret dal Corvatsch, Schwarzbachfirn). To compensate for the loss of these series, mass balance monitoring programmes at the two large glaciers, Gross Aletschgletscher and Vadret Pers, were intensified during the reporting period with a suite of new measurements. These efforts have the aim to establish stable and strong long-term series far into the second half of the 21st century (see details in Chapter 4.11 and 4.14).

The mean specific winter and annual balances are presented in Table 4.1 for the periods defined by the individual measurement dates and in Table 4.2 for comparable fied-date periods corresponding to the hydrological year. The mass balance for Adlergletscher, a former tributary of Findelengletscher, has been evaluated separately but detailed figures are presented together with Findelengletscher. A similar situation exists at Glacier du Sex Rouge (close to Tsanfleuron), Vadret dal Corvatsch (close to Murtèl), and Schwarzbachfirn (close to Sankt Anna). Only glacier-wide

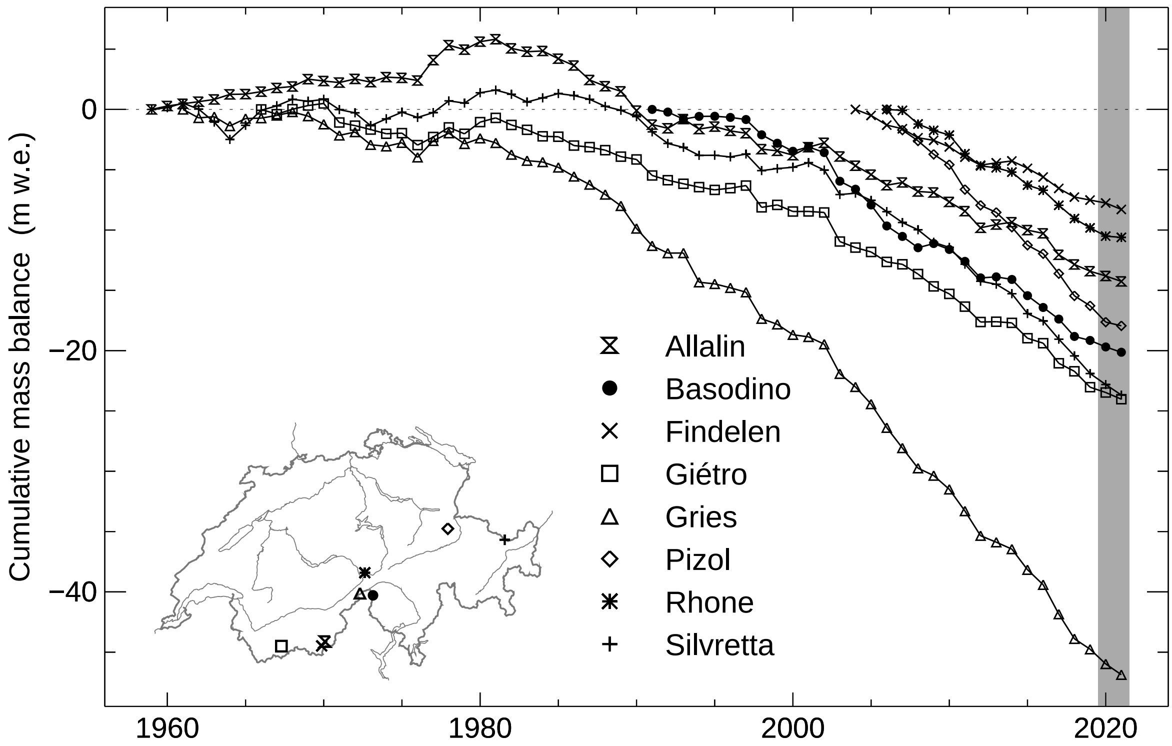

Figure 4.2: Cumulative mean specific mass balance over the whole observation period for the glaciers Allalin, Basòdino, Findelen, Giétro, Gries, Pizol, Rhone and Silvretta. The gray shaded area highlights the years of the current report.

specific values are presented in the summary Tables 4.1 and 4.2 for these glaciers but no detailed figures.

The long-term trends are clearly recognizable for Allalingletscher, Glacier du Giétro, Griesgletscher and Silvrettagletscher with very long and continuous time series (Figure 4.2). Notably, the accelerated mass loss since the mid-1980s is remarkable, as are the balanced mass budgets recorded in the 1960s and 70s. The point measurements of the mass balance are of particular significance with regard to answering questions related to climate change (Ohmura et al., 2007; Huss and Bauder, 2009; Gabbi et al., 2015; GLAMOS, 2020a). The four existing long-term time series (Claridenfirn, Grosser Aletschgletscher, Silvrettagletscher) start in the 1910s and cover almost the entire 20th century. Mass balance data of the present report has also been submitted to the World Glacier Monitoring Service (WGMS) as a contribution to the efforts of international glacier monitoring (WGMS, 2020). Allalingletscher, Glacier du Giétro, Griesgletscher and Silvrettagletscher have been selected by WGMS as their reference glaciers, a list of glaciers that stand out for the length of their data series and the completeness of mass balance observations.

4.2 Mass Balance in 2019/20

Over the past decade, glacier melt has been stronger than at any time since detailed mass balance observations began. The ice volume loss continued through the reporting period 2019/20, but thanks to somewhat less extreme summer temperatures, it was not as dramatic as for the three

Table 4.1: Summary table with area, mean specific winter ($B_{w,meas}$) and annual ($B_{a,meas}$) balance, equilibrium line altitude (ELA) and accumulation area ratio (AAR) for the measurement periods (defined by the exact dates of field surveys) in 2019/20 and 2020/21.

Glacier	Period	Area (km^2)	$B_{w,meas}$ (mm w.e.)	$B_{a,meas}$ (mm w.e.)	ELA (m a.s.l.)	AAR (%)
Allalin	2019/20	9.553	1114	−395	3365	49
	2020/21	9.553	822	−452	3385	47
Basòdino	2019/20	1.640	1904	−539	3055	10
	2020/21	1.640	1446	−439	3065	9
Clariden	2019/20	4.321	1762	−750	2905	37
	2020/21	4.321	2378	−408	2885	43
Findelen	2019/20	12.553	1551	−250	3285	58
	2020/21	12.511	1111	−531	3345	49
Adler	2019/20	1.979	1171	−491	3485	43
	2020/21	1.979	1014	−513	3505	40
Giétro	2019/20	5.280	1040	−439	3225	52
	2020/21	5.280	997	−556	3285	35
Gries	2019/20	4.186	1778	−1218	3075	16
	2020/21	4.102	1674	−892	3085	15
Grosser Aletsch	2019/20	78.532	738	−1165	3125	51
	2020/21	77.983	1480	−114	2965	61
Hohlaub	2019/20	2.128	1326	−174	3195	54
	2020/21	2.128	976	−183	3185	56
Murtèl	2019/20	0.272	933	−311	3202	43
	2020/21	0.269	1292	−371	3217	28
Pers	2019/20	6.661	1086	−591	3015	43
	2020/21	6.661	1652	−525	3025	42
Pizol	2019/20	0.020	1334	−1345	2722	5
	2020/21	0.019	1566	−311	2712	18
Plaine Morte	2019/20	6.981	1423	−1443	2805	0
	2020/21	6.889	1530	−982	2795	0
Rhone	2019/20	15.174	1771	−686	2915	57
	2020/21	15.174	1968	−102	2855	65
St. Anna	2019/20	0.144	1527	−766	2857	7
	2020/21	0.142	1622	−484	2842	11
Schwarzberg	2019/20	4.891	1478	−517	3125	40
	2020/21	4.891	1084	−698	3135	37
Silvretta	2019/20	2.485	1403	−915	2905	25
	2020/21	2.389	1513	−868	2925	20
Tsanfleuron	2019/20	2.451	1878	−2263	2975	0
	2020/21	2.324	2098	−607	2855	10
Sex Rouge	2019/20	0.256	1627	−1811	2882	0
	2020/21	0.257	1802	−479	2832	10

Table 4.2: Summary table with area, mean specific winter ($B_{w,fix}$) and annual ($B_{a,fix}$) balance, equilibrium line altitude (ELA) and accumulation area ratio (AAR) for fixed-date periods (1 October - 30 April - 30 September) in 2019/20 and 2020/21.

Glacier	Period	Area (km^2)	$B_{w,fix}$ (mm w.e.)	$B_{a,fix}$ (mm w.e.)	ELA (m a.s.l.)	AAR (%)
Allalin	2019/20	9.553	1108	−405	3415	44
	2020/21	9.553	790	−432	3435	42
Basòdino	2019/20	1.640	1951	−391	2975	31
	2020/21	1.640	1473	−693	3115	2
Clariden	2019/20	4.321	1553	−842	2905	36
	2020/21	4.321	2047	−293	2875	48
Findelen	2019/20	12.553	1354	−305	3275	58
	2020/21	12.511	1095	−386	3315	54
Adler	2019/20	1.979	1023	−554	3495	42
	2020/21	1.979	998	−358	3475	45
Giétro	2019/20	5.280	1046	−791	3305	25
	2020/21	5.280	938	−337	3235	50
Gries	2019/20	4.186	1796	−1079	3045	26
	2020/21	4.102	1684	−778	3075	16
Grosser Aletsch	2019/20	78.532	838	−1168	3125	52
	2020/21	77.983	1435	−183	2985	60
Hohlaub	2019/20	2.128	1318	−180	3205	51
	2020/21	2.128	945	−164	3195	54
Murtèl	2019/20	0.272	907	−530	3217	27
	2020/21	0.269	1263	−314	3207	39
Pers	2019/20	6.661	1061	−802	3055	39
	2020/21	6.661	1567	−629	3045	40
Pizol	2019/20	0.020	1310	−1249	2732	0
	2020/21	0.019	1499	−611	2727	2
Plaine Morte	2019/20	6.981	1380	−1929	2815	0
	2020/21	6.889	1441	−960	2795	0
Rhone	2019/20	15.174	1783	−627	2925	56
	2020/21	15.174	1865	−94	2845	67
St. Anna	2019/20	0.144	1442	−734	2857	7
	2020/21	0.142	1555	−633	2847	11
Schwarzberg	2019/20	4.891	1468	−501	3105	42
	2020/21	4.891	1038	−639	3125	38
Silvretta	2019/20	2.485	1211	−996	2935	19
	2020/21	2.389	1312	−888	2965	12
Tsanfleuron	2019/20	2.451	1928	−1888	2975	0
	2020/21	2.324	2018	−605	2875	5
Sex Rouge	2019/20	0.256	1671	−1497	2872	0
	2020/21	0.257	1721	−789	2852	4

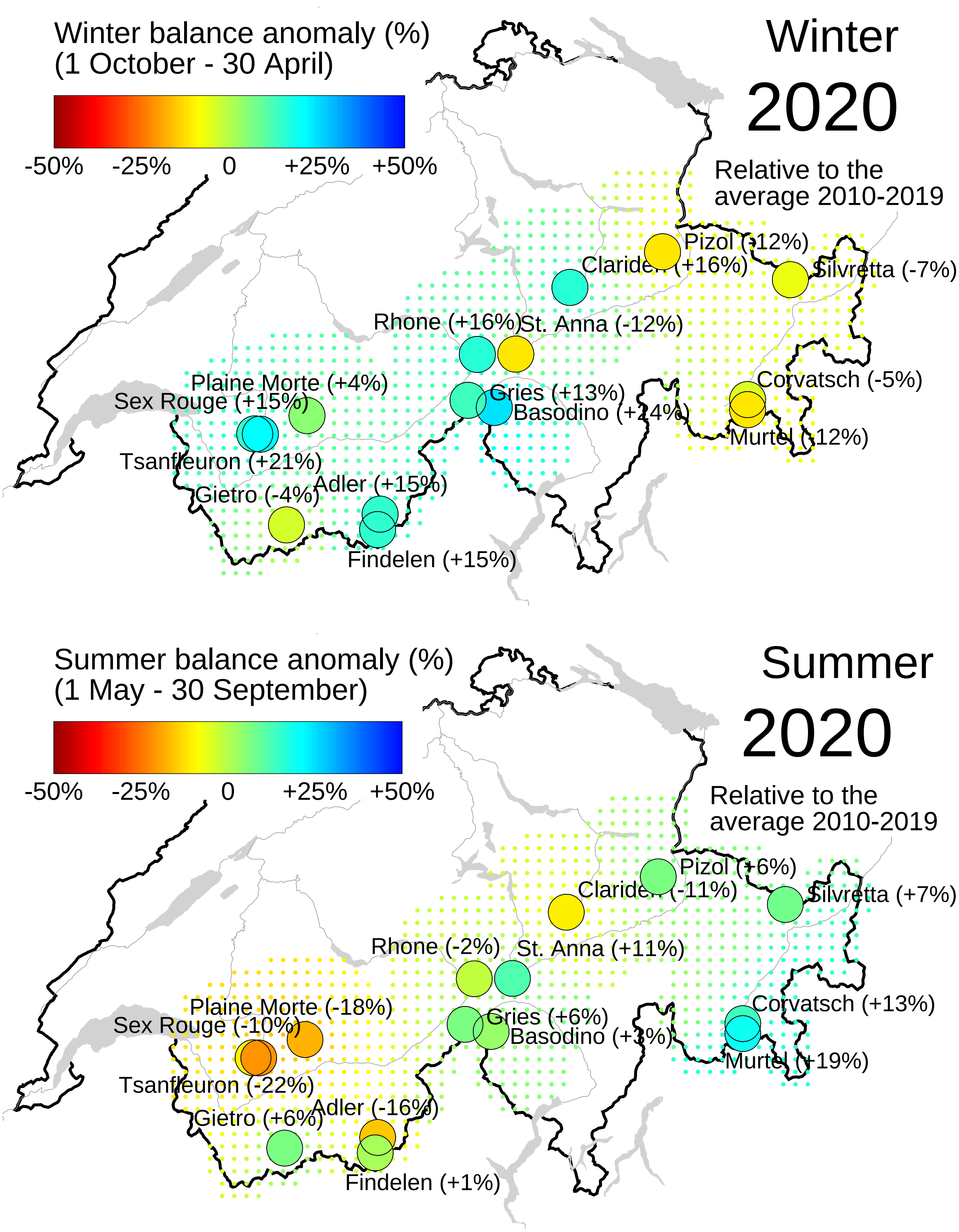

Figure 4.3: Anomaly of winter (top) and summer (bottom) mass balance in 2019/20 relative to the average 2009/10 to 2018/19 of all observed glaciers and extrapolated to the entire Swiss Alps.

previous years. At the end of April 2020, snow water equivalent on glaciers was around 10% higher than the average of the last 10 years except for eastern Switzerland where it was slightly below then mean (Figure 4.3). However, the melting of the glacier tongues began earlier than usual, and ablation totals near the termini even reached records values at some sites, whereas mass balance

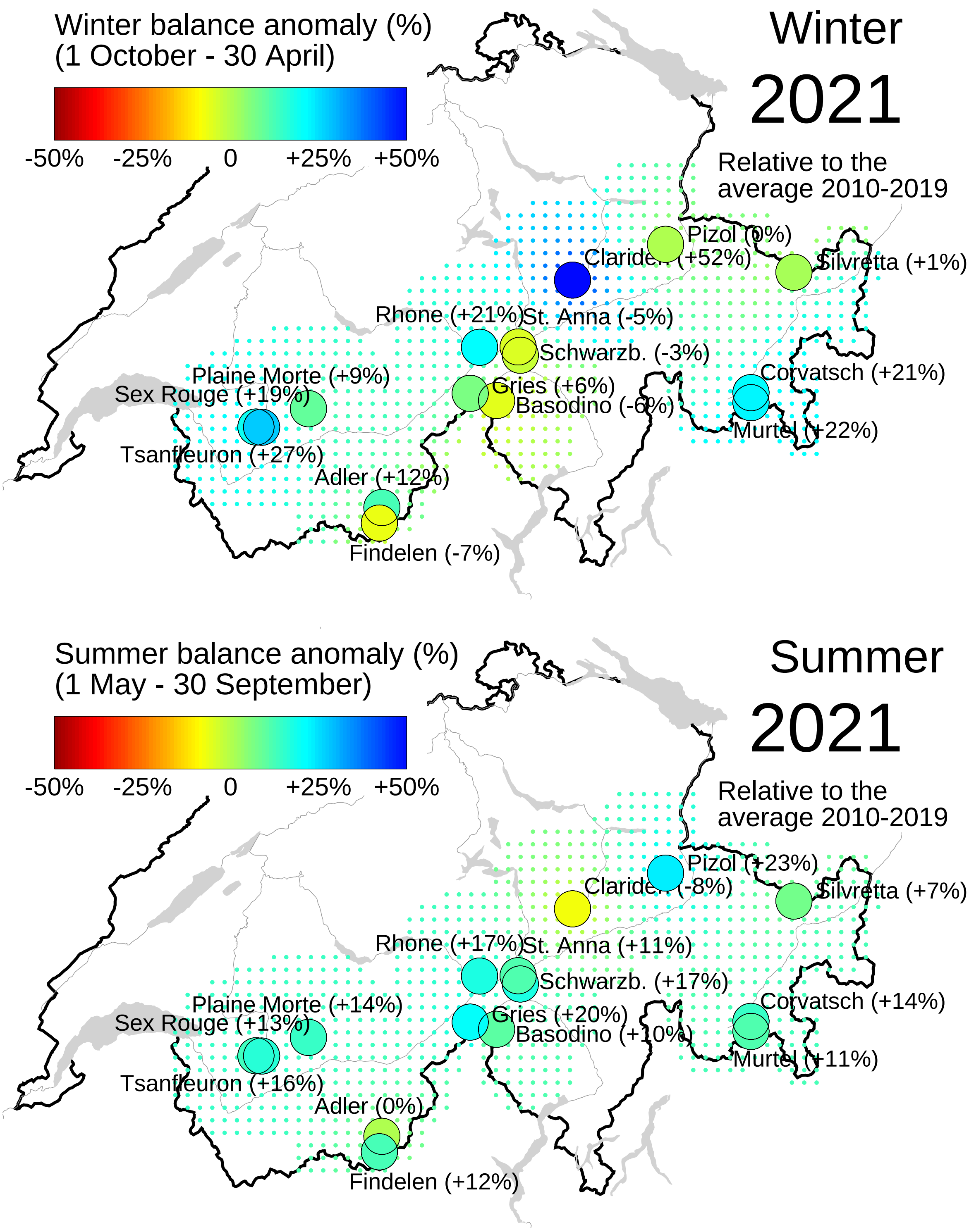

Figure 4.4: Anomaly of winter (top) and summer (bottom) mass balance in 2020/21 relative to the average 2009/10 to 2018/19 of all observed glaciers and extrapolated to the entire Swiss Alps.

at intermediate to high elevation was mostly only slightly below the average of the last decade. An exception is the site on Grosser Aletschgletscher near Jungfraujoch at an elevation of 3350 m a.s.l. where the lowest annual snow accumulation was measured since measurements began 100 years ago. 2.0% of the total glacier volume has been lost across Switzerland throughout the hydrological

year 2019/20 – the negative trend hence continues.
Mass balance was determined on 22 glaciers using the direct glaciological method. At most of them, the seasonal components were determined with dedicated surveys both at the end of winter and summer. The data indicate clear differences among the glaciers in relation to their specific geometry and the region, and thus the prevailing local meteorological conditions in the period under observation. While low-lying, flat glaciers (e.g. Glacier de Tsanfleuron, Glacier de la Plaine Morte) were subject to an average reduction in ice thickness of 2 metres, glaciers at higher elevation in the southern Valais, in Ticino and the Engadine (e.g. Findelgletscher, Ghiacciaio del Basòdino, Vadret dal Murtèl) lost only around 0.5 metres in thickness. For the latter group, this can be explained by a substantial amount of snow in early winter and the positive effect of summer snowfalls. Considering the difference in summer mass balance relative to typical losses at the scale of the surveyed glaciers, the year 2020 is close to the last decade's average with somewhat higher summer melting in the Bernese Alps and below-average losses in southeastern Switzerland (Figure 4.3).

4.3 Mass Balance in 2020/21

In terms of weather, the conditions in 2021 were right to give the glaciers a breather. Unfortunately, in times of climate change, even a "good" year is not good enough for glaciers: the loss continued – albeit at a slower pace – despite plenty of snow in winter and a comparatively cool and rainy summer. At the end of April snow water equivalent was slightly above-average, mostly on glaciers in the North and in the South-East, i.e. around 10-20% higher compared to the mean of the last decade. Glaciers influenced by the meteorological conditions of the southern side of the Alps, however, showed a small deficit relative to the decadal mean (Figure 4.4). The month of May brought a lot of additional snow in the high mountains. A snow depth of almost 7 meters was then observed at the upper measurement site on Claridenfirn (2890 m a.s.l.), the highest value since observations began in 1914. The glaciers were therefore relatively well protected by the winter snow until the rainy July. Nevertheless, over the entire summer season the melt was considerable and continued until the end of September. Around 400 million tons of ice were lost across Switzerland during the hydrological year 2020/21, about 0.8% of the remaining glacier volume.
Once again, the annual mass balance at all 22 glaciers surveyed with the direct glaciological method – encompassing glaciers of different size and characteristics in all regions of Switzerland – was negative, although the results are less alarming than in recent years. In the northern Valais (Rhonegletscher, Grosser Aletschgletscher), the decrease in mean ice thickness is moderate with just about 0.2 metres. In the southern Valais, the Ticino and in north-eastern Switzerland (e.g. Findelengletscher, Silvrettagletscher), on the other hand, the annual losses were hardly lower than the average of the last 10 years. Summer mass balance was between 10-20% less negative on most glaciers in comparison to the last decade's average (Figure 4.4). While snow accumulation was observed on large glaciers above around 3200 m a.s.l. in autumn, the snow coverage on low-lying glaciers was in some cases again completely depleted, and they are therefore doomed to disappear. Even though 2021 shows the lowest ice loss since 2013, there is no relief in sight for Swiss glaciers.

4.4 Allalingletscher

Introduction

Allalingletscher is a temperate large mountain glacier located in the Southern Valais Alps. It currently covers an area of 9.6 km^2 flowing in north-eastern direction from 4180 m a.s.l. down to 2680 m a.s.l. Mass balance measurements started in 1955 as a part of investigations for the construction of the Mattmark reservoir for hydro-power production (VAW, 1999; Antoni, 2005). Initially, the measurement network was set up to better cover the entire surface area. Following an ice avalanche on 30th August 1965 when the construction site of the Mattmark reservoir was destroyed and 88 people died in the accident, the observation network was re-arranged in 1967 with a main focus on ice flow investigations at the glacier tongue (see Chapter 5). However, also the readings of local annual mass balance were continued. Data of point mass balance and geodetic ice volume changes since the beginning of the measurements in 1955 were re-analyzed and homogenized (Huss et al., 2015). The results of the glacier-wide mean specific annual balance for

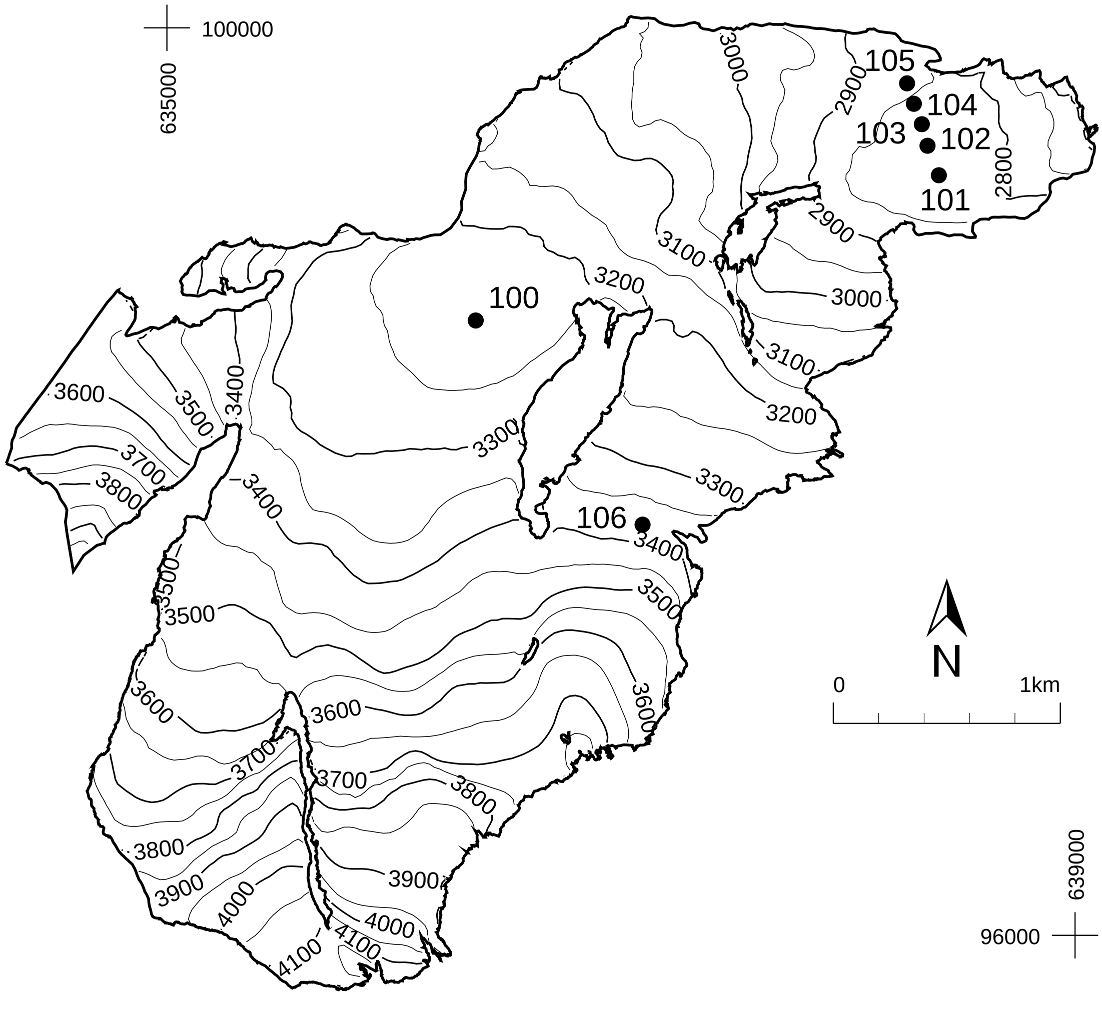

Figure 4.5: Surface topography and observational network of Allalingletscher.

comparable fixed-date periods were presented in Section 4.17 of Volume 135/136. Further details on long-term observations of ice flow velocities are shown in Section 5.2. Currently, only the annual mass balance is investigated and no survey for snow accumulation in spring is conducted.

Investigations in 2019/20

Annual observations of mass balance with maintenance of the stake network were carried out on 4th September 2020. All seven stakes were located and set back to the initial position. Negative local mass balances have been registered for all stakes except for the highest stake on 3370 m a.s.l. where a slightly positive value was found. Above about 3200 m a.s.l. the glacier was covered with remains of fresh snow accumulated in the days before the survey and it was difficult to determine the elevation of the end-of-summer snowline that was located slightly below the topmost stake.

Investigations in 2020/21

Annual observations of mass balance with maintenance of the stake network were carried out on 2nd September 2021. All stakes were located and set back to the initial position. As in the previous period negative local mass balances were measured for all but the highest stake where balanced conditions were registered. The transient snowline was found to reach an elevation of about 3300 m a.s.l.

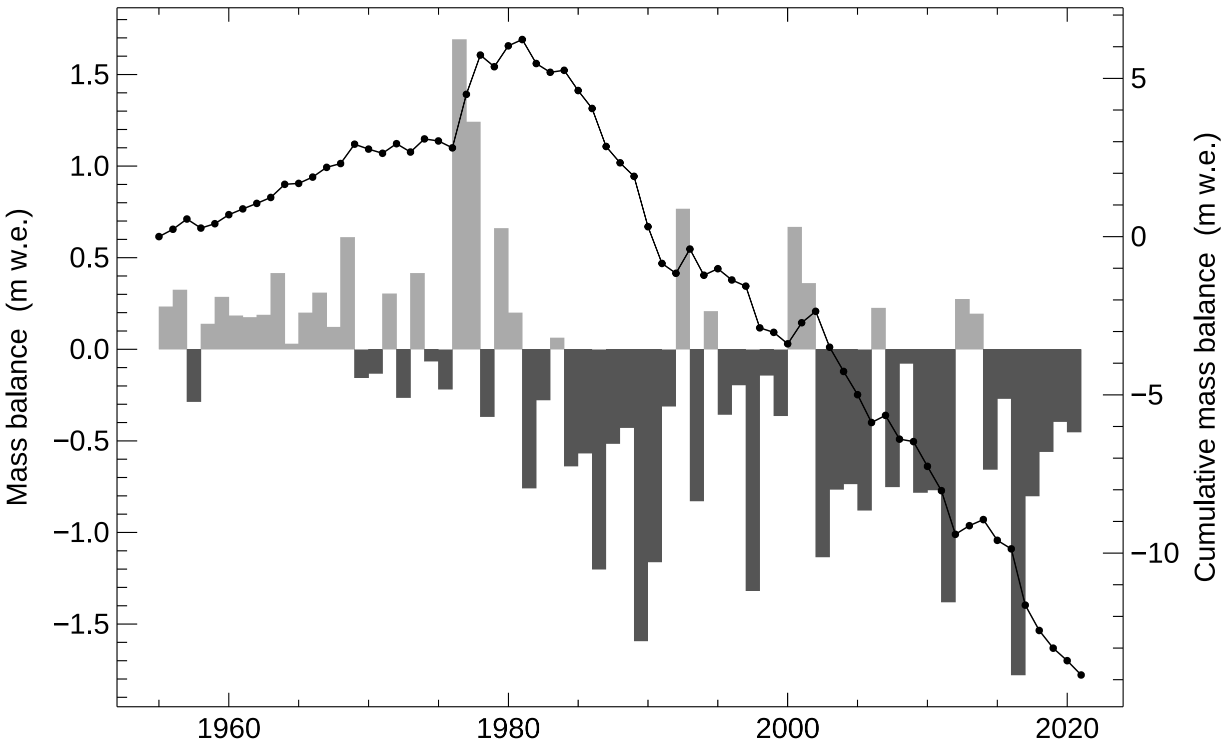

Figure 4.6: Allalingletscher - Mean specific annual balance (bars) and cumulative mass balance for the period 1955-2021. Values refer to the measurement period.

Table 4.3: Allalingletscher - Specific winter (b_w) and annual (b_a) balance according to elevation bands for the two periods 2019/20 and 2020/21. Results refer to the measurement period, defined by the dates of the field survey.

Altitude	2019/20			2020/21		
	Area	$\overline{b_w}$	$\overline{b_a}$	Area	$\overline{b_w}$	$\overline{b_a}$
(m a.s.l.)	(km^2)	(mm w.e.)	(mm w.e.)	(km^2)	(mm w.e.)	(mm w.e.)
2600 - 2700	0.001		−2507	0.001		−2179
2700 - 2800	0.134		−2862	0.134		−2634
2800 - 2900	0.528		−2476	0.528		−2472
2900 - 3000	0.463		−1679	0.463		−1874
3000 - 3100	0.713		−1356	0.713		−1443
3100 - 3200	0.739		−1193	0.739		−1085
3200 - 3300	1.592		−930	1.592		−808
3300 - 3400	1.005		−98	1.005		−142
3400 - 3500	1.063		230	1.063		94
3500 - 3600	0.949		434	0.949		284
3600 - 3700	0.838		537	0.838		390
3700 - 3800	0.517		645	0.517		482
3800 - 3900	0.449		656	0.449		490
3900 - 4000	0.291		699	0.291		528
4000 - 4100	0.181		692	0.181		538
4100 - 4200	0.091		612	0.091		493
2600 - 4200	9.553		−395	9.553		−452

Table 4.4: Allalingletscher - Individual stake measurements of winter and annual balance.

Stake	Period			Coordinates	Mass balance	
	Start	Spring	End		b_w	b_a
				(m / m / m a.s.l.)	(mm w.e.)	
100	30.08.2019		04.09.2020	636510 / 98797 / 3221		−1476
101	30.08.2019		04.09.2020	638400 / 99360 / 2819		−2664
102	30.08.2019		04.09.2020	638350 / 99480 / 2822		−2322
103	30.08.2019		04.09.2020	638325 / 99575 / 2820		−2763
104	30.08.2019		04.09.2020	638290 / 99665 / 2835		−2970
105	30.08.2019		04.09.2020	638260 / 99755 / 2852		−4545
106	30.08.2019		04.09.2020	637095 / 97796 / 3371		162
100	04.09.2020		02.09.2021	636513 / 98805 / 3219		−1197
101	04.09.2020		02.09.2021	638400 / 99360 / 2817		−2682
102	04.09.2020		02.09.2021	638350 / 99480 / 2820		−2070
103	04.09.2020		02.09.2021	638325 / 99575 / 2819		−2439
104	04.09.2020		02.09.2021	638290 / 99665 / 2833		−2565
105	04.09.2020		02.09.2021	638259 / 99755 / 2850		−3618
106	04.09.2020		02.09.2021	637097 / 97798 / 3370		65

4.5 Ghiacciaio del Basòdino

Introduction

Ghiacciaio del Basòdino is a small north-east facing temperate mountain glacier in the southern Swiss Alps. The small branch descending to the north below Kastelhorn with a separate tongue and no longer connected is not considered part of the glacier, and is not included in the mass balance evaluation. The main body of the glacier presently covers an area of 1.8 km^2 and extends from 2600 to 3186 m a.s.l. Detailed mass balance investigations have been carried out since 1991. Determination of volumetric changes in decadal resolution extend further back to 1929 (Bauder et al., 2007). Topographic maps or photogrammetrical surveys exist for 1929, 1949, 1971, 1985, 1991, 2002, 2008 and 2013. Huss et al. (2015) re-analyzed and homogenized the seasonal stake data and ice volume changes since the beginning of the measurements in 1991. The results of the mean specific winter and annual balance for comparable fixed-date periods were presented in Section 4.17 of Volume 135/136.

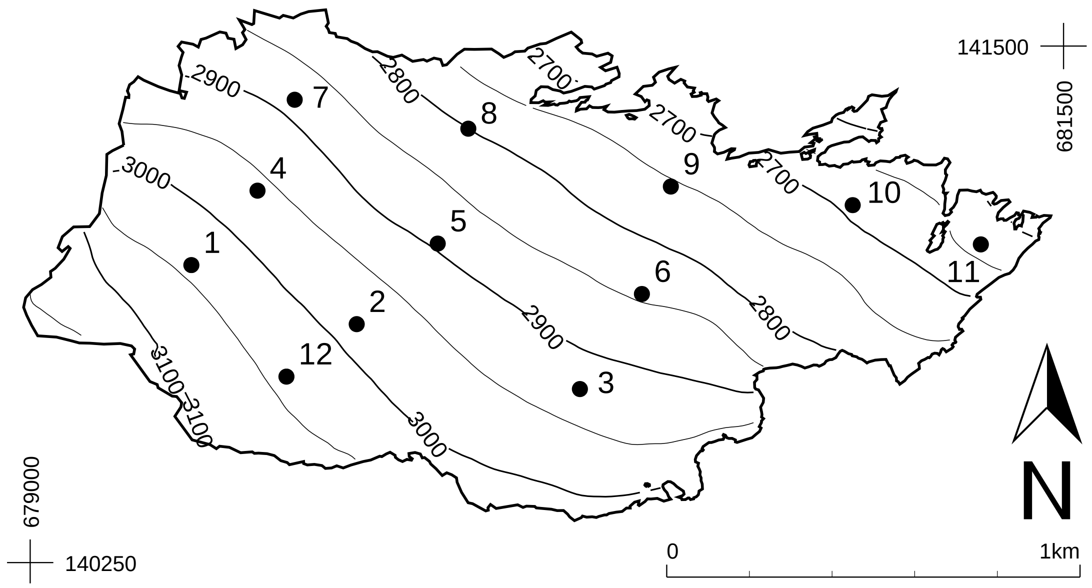

Figure 4.7: Surface topography and observational network of Ghiacciaio del Basòdino.

Investigations in 2019/20

The measurement period extended from 17th September 2019 to 21st September 2020 with a field visit in spring, on 23rd April 2020. The spring survey included snow depth probing at 123 locations and the determination of mean density of the snow pack using a core drill in the center of the glacier at stake 5. The annual mass balance was observed at 11 stakes. Additional field visits during the melting season were performed on 20th August and 11th September 2020.

Investigations in 2020/21

The measurement period was from 21st September 2020 to 10th September 2021. Winter balance was determined on 20th April 2021. Snow depth probing at 121 locations and measurement of the density using a core drill were carried out in spring at the two locations 5 and 9. An additional field visit during the melting season was conducted on 19th August 2021 and annual mass balance was determined at all 10 stakes.

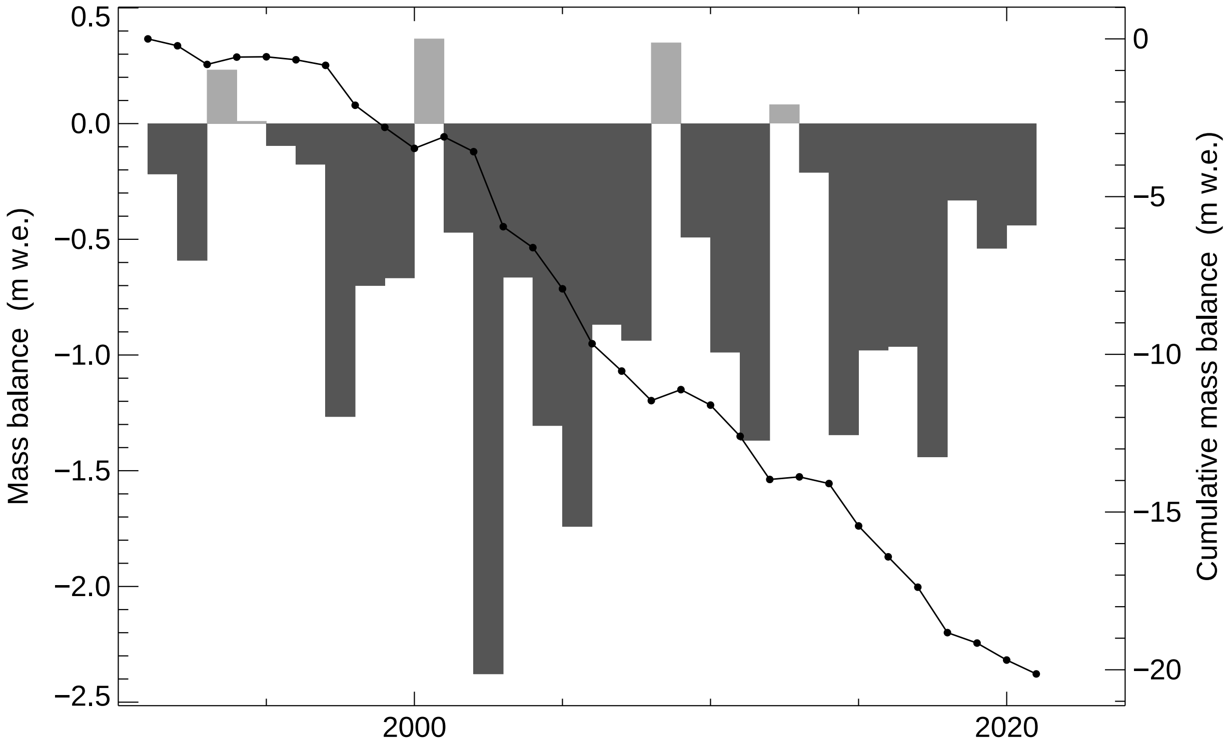

Figure 4.8: Ghiacciaio del Basòdino - Mean specific annual balance (bars) and cumulative mass balance for the period 1991-2021. Values refer to the measurement period.

Table 4.5: Ghiacciaio del Basòdino - Specific winter (b_w) and annual (b_a) balance according to elevation bands for the two periods 2019/20 and 2020/21. Results refer to the measurement period, defined by the dates of the field survey.

Altitude	2019/20			2020/21		
	Area	$\overline{b_w}$	$\overline{b_a}$	Area	$\overline{b_w}$	$\overline{b_a}$
(m a.s.l.)	(km^2)	(mm w.e.)	(mm w.e.)	(km^2)	(mm w.e.)	(mm w.e.)
2500 - 2600	0.001	1610	−1204	0.001	1230	−924
2600 - 2700	0.081	1601	−967	0.081	1229	−816
2700 - 2800	0.306	1721	−968	0.306	1301	−843
2800 - 2900	0.394	1893	−880	0.394	1402	−756
2900 - 3000	0.501	2073	−228	0.501	1552	−150
3000 - 3100	0.299	1966	−88	0.299	1535	−87
3100 - 3200	0.056	1599	−353	0.056	1447	74
2500 - 3200	1.640	1904	−539	1.640	1446	−439

Table 4.6: Ghiacciaio del Basòdino - Individual stake measurements of winter and annual balance.

Stake	Period			Coordinates	Mass balance	
	Start	Spring	End		b_w	b_a
				(m / m / m a.s.l.)	(mm w.e.)	
01	17.09.2019	23.04.2020	21.09.2020	679388 / 140962 / 3035	1684	−70
02	17.09.2019	23.04.2020	21.09.2020	679790 / 140825 / 2979	1992	−30
03	17.09.2019	23.04.2020	21.09.2020	680333 / 140668 / 2912	2102	270
04	17.09.2019	23.04.2020	21.09.2020	679545 / 141155 / 2960	1983	−310
05	17.09.2019	23.04.2020	21.09.2020	679981 / 141022 / 2886	1704	−820
06	17.09.2019	23.04.2020	21.09.2020	680476 / 140907 / 2836	1838	−680
07	17.09.2019	23.04.2020	21.09.2020	679634 / 141359 / 2882	1704	−1210
08	17.09.2019	23.04.2020	21.09.2020	680050 / 141300 / 2794	1247	−1330
09	17.09.2019	23.04.2020	21.09.2020	680553 / 141160 / 2748	1699	−1110
10	17.09.2019	23.04.2020	21.09.2020	680992 / 141127 / 2686	1235	−1520
12	17.09.2019	23.04.2020	21.09.2020	679621 / 140719 / 2631	2100	50
01	21.09.2020	20.04.2021	10.09.2021	679388 / 140962 / 3035	1443	−410
02	21.09.2020	20.04.2021	10.09.2021	679790 / 140825 / 2979	1754	0
03	21.09.2020	20.04.2021	10.09.2021	680333 / 140668 / 2912	1746	480
04	21.09.2020	20.04.2021	10.09.2021	679545 / 141155 / 2960	1685	−230
05	21.09.2020	20.04.2021	10.09.2021	679981 / 141022 / 2886	1271	−530
07	21.09.2020	20.04.2021	10.09.2021	679634 / 141359 / 2882	1328	−810
08	21.09.2020	20.04.2021	10.09.2021	680050 / 141300 / 2794	1328	−1130
09	21.09.2020	20.04.2021	10.09.2021	680553 / 141160 / 2748	1328	−930
10	21.09.2020	20.04.2021	10.09.2021	680992 / 141127 / 2686	1201	−1190
12	21.09.2020	20.04.2021	10.09.2021	679621 / 140719 / 2631	1595	200

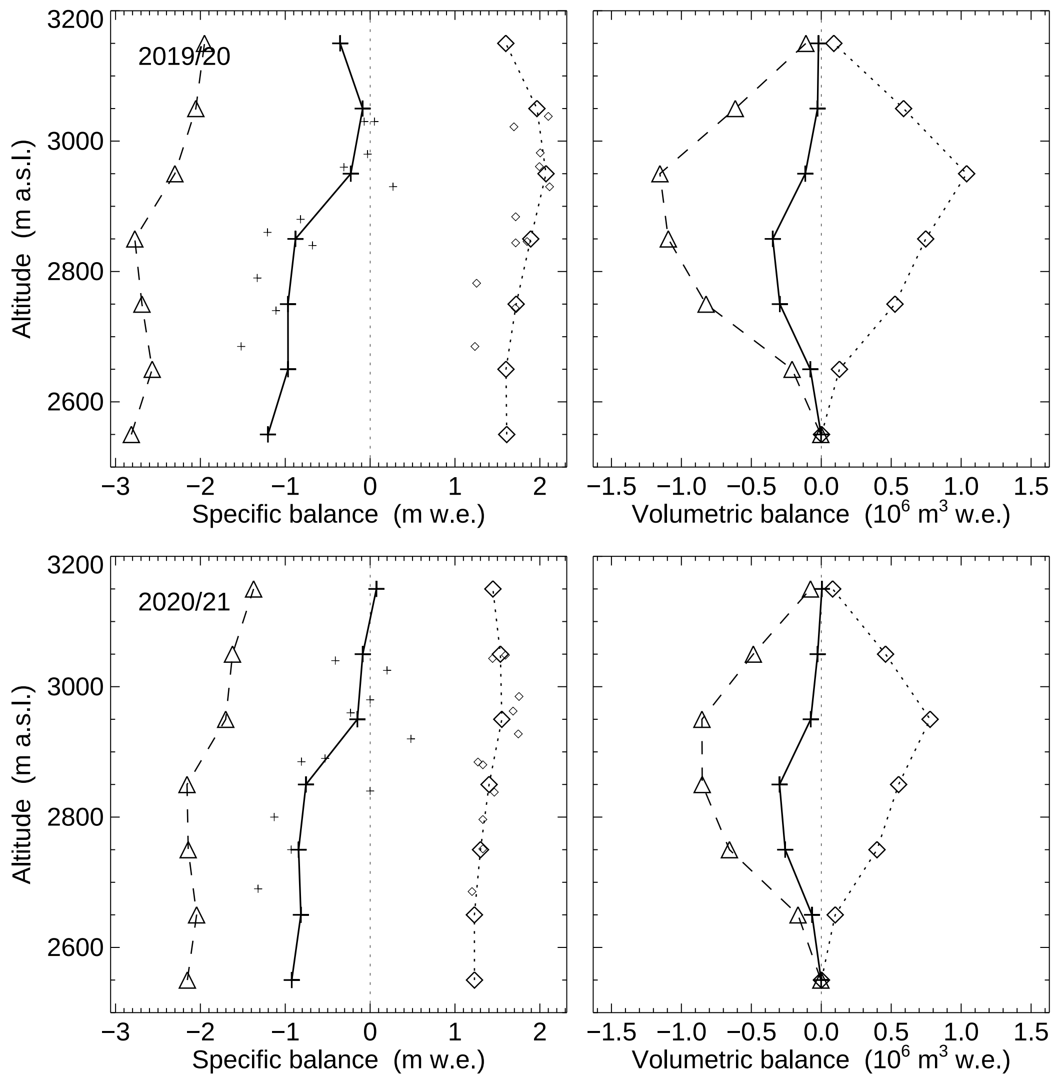

Figure 4.9: Specific (left) and volumetric (right) winter (dotted, ◇), summer (dashed, △) and annual (continuous line, +) balance in elevation bands for 2019/20 (top) and 2020/21 (bottom). Small symbols mark the individual measurements.

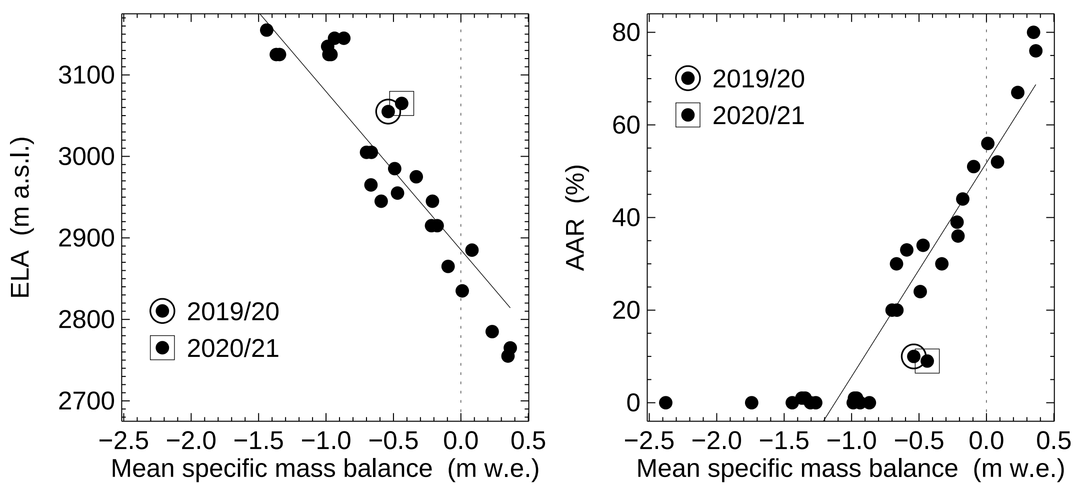

Figure 4.10: Equilibrium line altitude (ELA) and accumulation area ratio (AAR) versus mean specific balance including all previous observations.

4.6 Claridenfirn

Introduction

Claridenfirn is a plateau glacier in the hydrological drainage basin of the Linth with an area of currently 4.3 km^2. It consists of several accumulation basins and independent steep glacier fronts that are partly subject to frontal ice break-off. Measurements of accumulation and melt, as well as of total precipitation near the glacier margin, have been undertaken by various researchers continuously since 1914 using a consistent methodology. The series at the two point sites on Claridenfirn is thus by far the longest direct glacier mass balance record worldwide and is characterized by an excellent documentation (Müller and Kappenberger, 1991; Geibel et al., 2022). The traditional glaciological method was applied by digging a snow pit down to a horizon marking the previous end-of-summer surface, and by measuring the water equivalent of the accumulated snow layer. Annual point balance was determined every autumn since 1914 with very few data gaps and also regularly in spring, at two sites at elevations of about 2700 and 2900 m a.s.l. The reports focussing

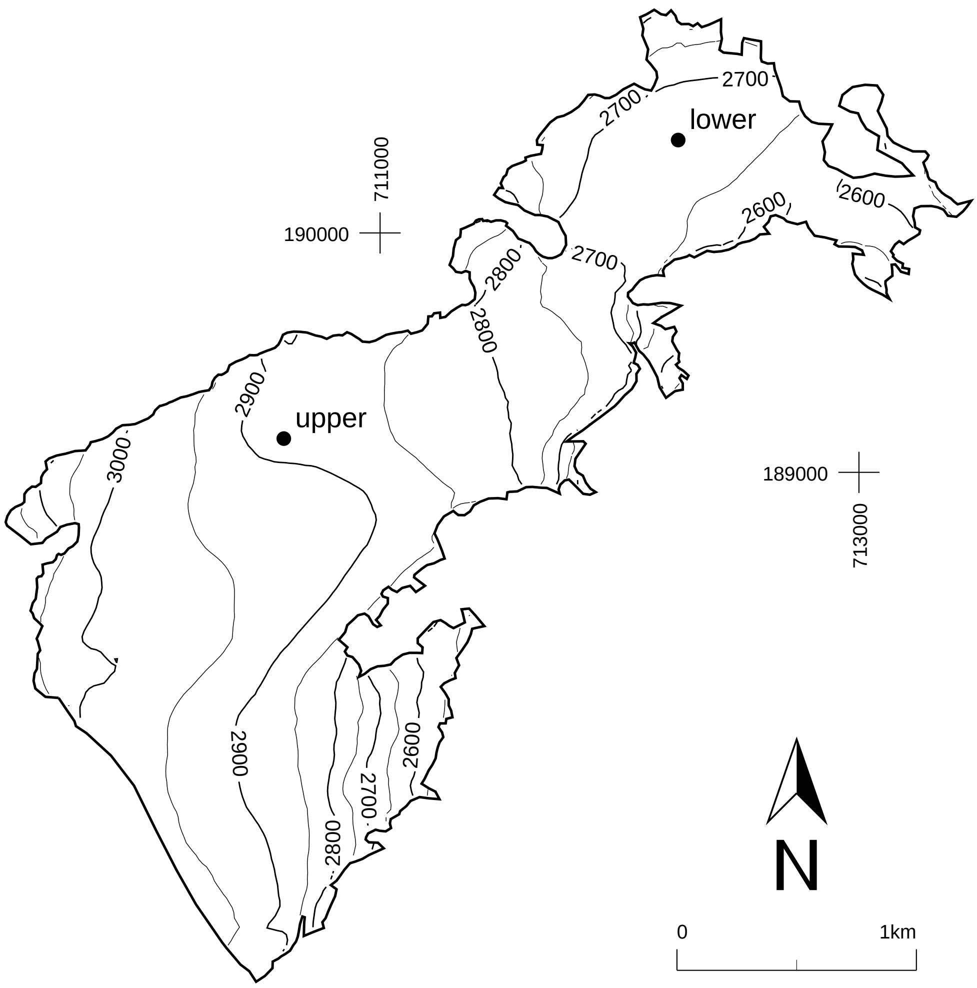

Figure 4.11: Surface topography and observational network of Claridenfirn.

on the years 1914 to 1978 are published in Kasser et al. (1986). Observational techniques and the results for the period 1914 to 1984 are published in Müller and Kappenberger (1991). A further update of the measurements until 2007 allowed Huss and Bauder (2009) to separate accumulation and melt and to interpret the entire time series in terms of climatic drivers (see Section 4.10 of Volume 127/128). Values of the entire homogenized time series of point mass balance 1914-2015 are compiled in Section 4.16 of Volume 135/136 (Figure 4.12). Based on this data, updated to 2020, Huss et al. (2021) calculated glacier-wide mass balance for the entire time series with a special consideration of the effect of mass losses by frontal ice avalanches. Even though spatial mass balance variability of the entire glacier is incompletely resolved by only two point measurements, a combination with decadal ice-volume changes from repeated digital elevation models allows constraining long-term glacier evolution. Investigations on the glacier are complemented by measurements of two precipitation storage gauges at Claridenhütte (2475 m a.s.l.) and Geissbützistock (2710 m a.s.l.) situated in the close vicinity of the glacier. Readings are taken both during spring and fall visits.

Table 4.7: Claridenfirn - Individual stake measurements of winter and annual balance.2 Note that the lowermost elevation band also includes estimated mass losses by frontal break-off of ice.

Stake	Period Start	Period Spring	Period End	Coordinates (m / m / m a.s.l.)	Mass balance b_w (mm w.e.)	Mass balance b_a (mm w.e.)
lower	29.09.2019	08.05.2020	18.09.2020	712261 / 190406 / 2660	1663	−990
upper	29.09.2019	08.05.2020	18.09.2020	710611 / 189126 / 2880	2403	421
lower	18.09.2020	28.05.2021	25.09.2021	712261 / 190406 / 2660	2409	−405
upper	18.09.2020	28.05.2021	25.09.2021	710611 / 189126 / 2880	3495	917

Investigations in 2019/20

Spring measurements were carried out on 8th May 2020. Only at the upper site the stake was visible. Density at both sites was obtained by coring to a marked horizon and supplemented by 10-20 snow depth probings in the vicinity of the stakes. Additional snow depth probings were carried out between the two stakes in a 200 m interval. At the upper site the density of 509 kg m^{-3} was measured while at the lower site a value of 467 kg m^{-3} was determined. Autumn measurements were carried out on 18th September 2020. At the lower site, snow accumulation during winter had melted completely with additional 1.1 m loss of ice. At the upper site a moderate mass gain of 77 cm of firn was found. In addition to the measurements of mass balance, surface lowering and horizontal displacement of the stakes was determined in autumn.

Investigations in 2020/21

The spring field survey was carried out on 28th May, and the late summer survey on 25th September 2021. The investigations included snow depth probing and density measurement using a core drill in spring at the two stakes. The observations were supplemented by additional snow depth probing between the two sites in a 200 m interval. A density of 528 $kg\,m^{-3}$ at the upper site and 479 $kg\,m^{-3}$ at the lower was found. At the end of September, a moderately negative mass balance was registered at the lower site while a positive mass balance was found at the upper site. A density of 525 $kg\,m^{-3}$ of the accumulated layer was measured in a pit. Lowering of the surface and displacement of the stakes were measured. Both stakes were redrilled at the original location.

Density measurement using a core drill at the upper site on Claridenfirn in spring 2021 (Photo: G. Kappenberger)

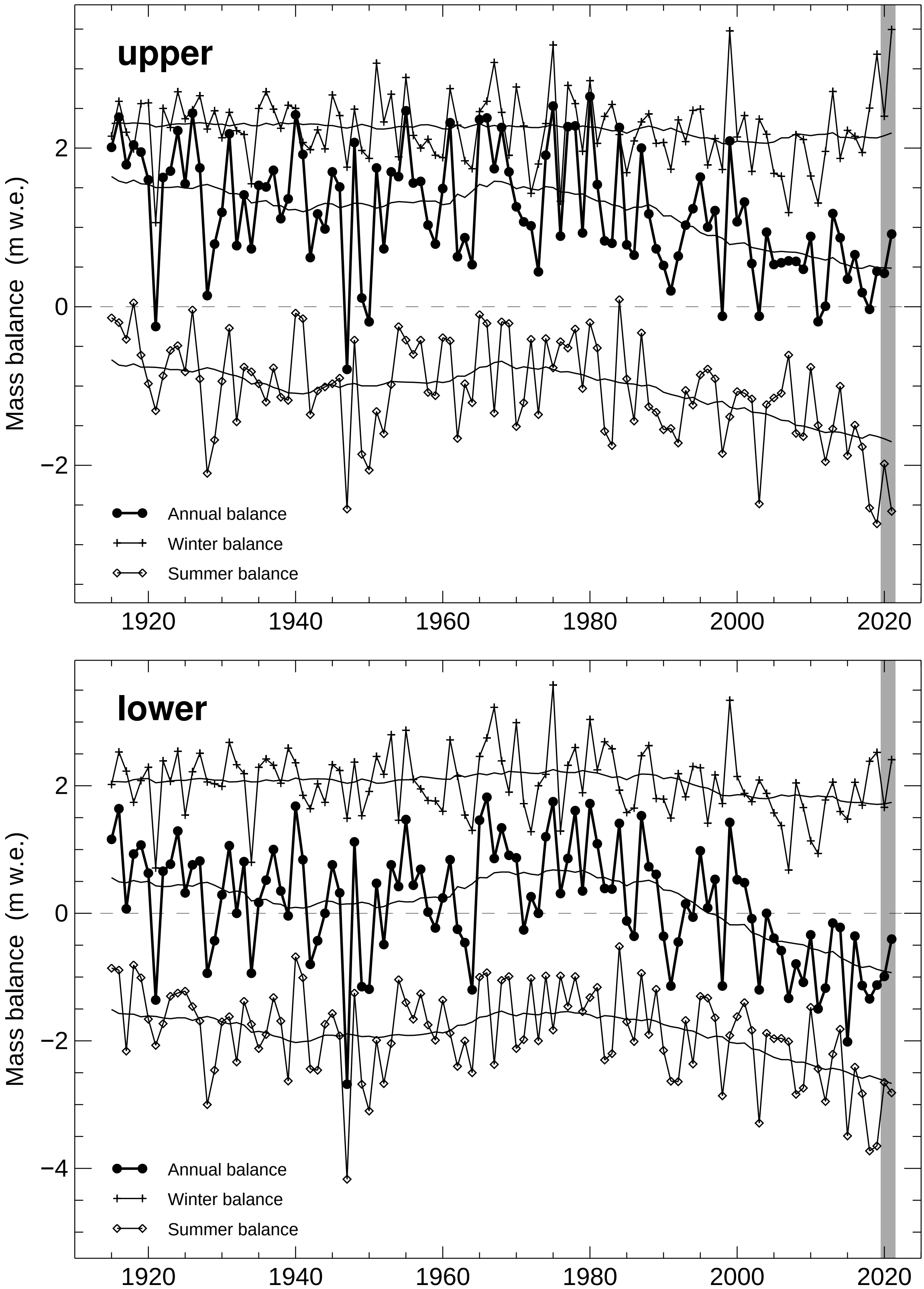

Figure 4.12: Mass balance of the upper (top) and lower (bottom) stake on Claridenfirn over the whole observation period. The gray shaded area highlights the years of the current report.

Table 4.8: Claridenfirn - Specific winter (b_w) and annual (b_a) balance according to elevation bands for the two periods 2019/20 and 2020/21. Results refer to the measurement period, defined by the dates of the field survey. Note that the lowermost elevation band also contains mass loss contributions from estimated ice break-off at the glacier snout.

Altitude (m a.s.l.)	2019/20 Area (km^2)	2019/20 $\overline{b_w}$ (mm w.e.)	2019/20 $\overline{b_a}$ (mm w.e.)	2020/21 Area (km^2)	2020/21 $\overline{b_w}$ (mm w.e.)	2020/21 $\overline{b_a}$ (mm w.e.)
2500 - 2600	0.058	1305	−2894	0.058	1899	−2424
2600 - 2700	0.723	1834	−1244	0.723	2539	−874
2700 - 2800	0.667	1699	−1089	0.667	2313	−887
2800 - 2900	1.332	1824	−653	1.332	2435	−284
2900 - 3000	1.363	1712	−456	1.363	2291	−90
3000 - 3100	0.152	1839	264	0.152	2465	581
3100 - 3200	0.026	1400	22	0.026	1894	366
2500 - 3200	4.321	1762	−750	4.321	2378	−408

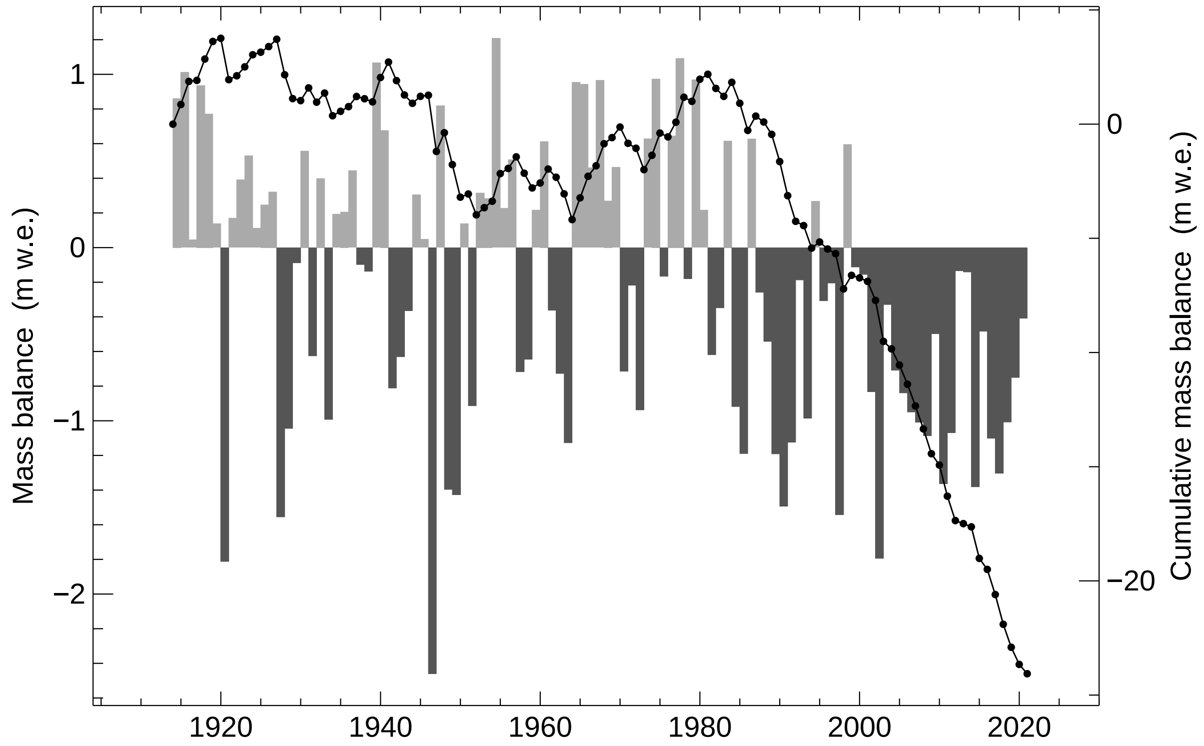

Figure 4.13: Claridenfirn - Mean specific annual balance (bars) and cumulative mass balance (line) for the period 1914-2021.

4.7 Glacier de Corbassière

Introduction

Since 1967, Glacier de Corbassière has been under observation by the Mauvoisin power company that exploits water from the catchment. Observations have been carried out on two profiles in the ablation area (Figure 4.14) where thickness change and ice flow was measured annually (see Chapter 5). Starting in 1996, stakes were maintained to measure annual quantities of ice flow velocity and local mass balance. Results of the glacier-wide mean specific annual balance for comparable fixed-date periods for 1996 to 2015 were presented in Section 4.17 of Volume 135/136. Here, we only present the results of annual point mass balance measurements. Glacier-wide mass balance estimates will be evaluated only periodically when new observations of geodetic ice volume

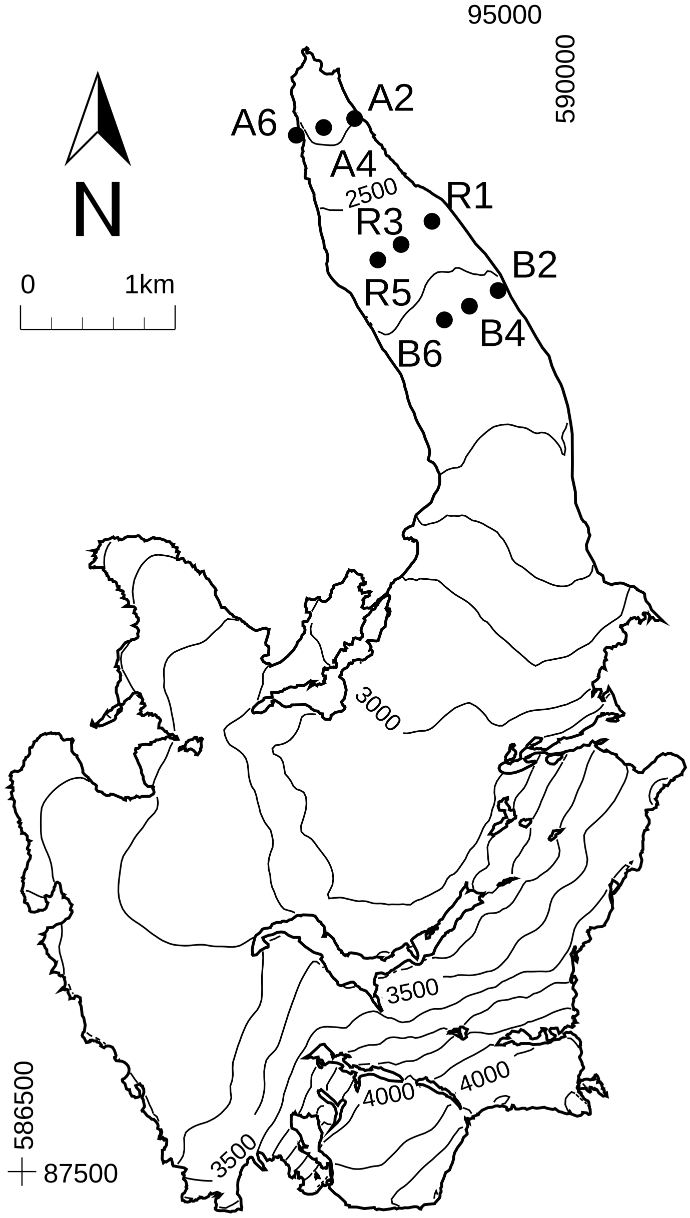

Figure 4.14: Surface topography and observational network of Glacier de Corbassière.

change is available. Further details on the long-term observations of ice flow velocities are given in Section 5.3.

Investigations in 2019/20

Annual observations of mass balance with maintenance of the stake network were carried out on 8th and 9th September 2020. Negative local mass balances resulted at all stakes. Due to rapid thinning at the lower profile (A2, A4, A6), complete wastage of the remaining ice is imminent and the measurements are no longer representative. The stake locations thus have been reorganized with a new profile (R1, R3, R5) and only stake A2 and A4 are maintained.

Investigations in 2020/21

The annual field survey took place on 14th and 15th September 2019. Seven stakes were located. At all stakes a negative local mass balance was determined. A local depression with enhanced winter snow accumulation formead over the past couple periods at stake A2 and resulted in non-representative measurements. Therefore the stake finally will be abandonned. Debris cover further increased at stake A2, but the site is still maintained.

Table 4.9: Glacier de Corbassière - Individual stake measurements of winter and annual balance.

Stake	Period Start	Spring	End	Coordinates (m / m / m a.s.l.)	Mass balance b_w (mm w.e.)	b_a
B2	27.09.2019		08.09.2020	589576 / 93202 / 2613		−4014
B4	27.09.2019		08.09.2020	589387 / 93100 / 2618		−3609
B6	27.09.2019		08.09.2020	589228 / 93009 / 2623		−3591
R1	27.09.2019		08.09.2020	589151 / 93649 / 2576		−5373
A2	28.09.2019		09.09.2020	588649 / 94310 / 2403		−5409
A4	28.09.2019		09.09.2020	588460 / 94258 / 2377		−2961
A6	28.09.2019		09.09.2020	588329 / 94194 / 2412		−3996
B2	08.09.2020		14.09.2021	589581 / 93204 / 2611		−3618
B4	08.09.2020		14.09.2021	589391 / 93098 / 2616		−3735
B6	08.09.2020		14.09.2021	589225 / 93010 / 2620		−3465
R1	08.09.2020		14.09.2021	589147 / 93647 / 2573		−4077
R3	08.09.2020		14.09.2021	588946 / 93512 / 2572		−3834
R5	08.09.2020		14.09.2021	588807 / 93401 / 2572		−3591
A2	09.09.2020		15.09.2021	588655 / 94312 / 2396		−5310
A4	09.09.2020		15.09.2021	588447 / 94251 / 2371		−2187

4.8 Findelengletscher

Introduction

Findelengletscher (12.5 km^2) and its former tributary Adlergletscher (2.0 km^2) are located in the southern Valais in the Zermatt area. The two glaciers cover an elevation range from 2580 m a.s.l. to 4120 m a.s.l. Findelengletscher is west-facing and is characterized by gently sloping high-elevation accumulation basins and a comparatively narrow glacier tongue. The region is relatively dry with equilibrium line altitudes among the highest in the Alps. Mass balance measurements on Findelengletscher were initiated in fall 2004 and the observational network was extended to Adlergletscher one year later.

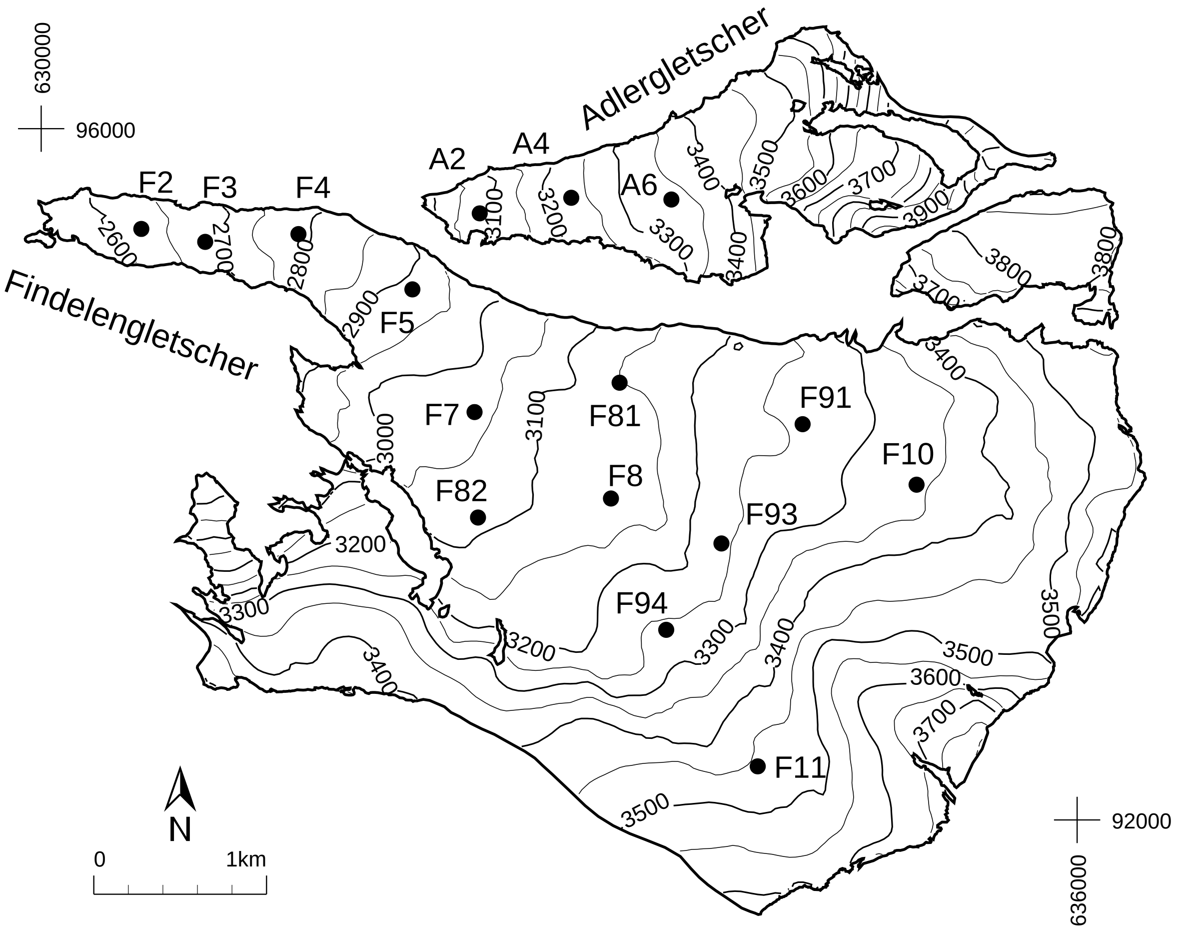

Figure 4.15: Surface topography and observational network on Findelengletscher and the former tributary Adlergletscher. Note that mass balance of Findelen- and Adlergletscher is evaluated over a homogenized perimeter that excludes some areas with very thick debris-coverage and unconnected tributaries below Stockhorn.

Investigations in 2019/20

Winter mass balance of Findelen- and Adlergletscher was determined on 7th May 2020 with a smaller team than usual due to the pandemic. Snow probings were acquired at 222 locations and snow density was measured by coring at four sites distributed over the glacier's entire elevation range. Relatively high snow densities of between 420 and 490 $kg\,m^{-3}$ were measured. Two autonomous stations to continuously measure ice ablation via a webcam observing a stake were installed on 16th June 2020 related to a project for real-time monitoring of glacier mass loss (see Landmann et al., 2021). All mass balance stakes were visited and re-installed on 15th September 2020. The annual mass balance was determined for 13 locations on Findelen-, and three on Adlergletscher. Due to technical problems, no firn density measurements could be performed at the uppermost two stakes that showed some accumulation. A station to continuously measure snow depth and snow water equivalent along with meteorological variables close to the glacier's long-term equilibrium line altitude was maintained (Gugerli et al., 2021). For the first time, the lower online camera was installed in a way that permits the continuous observation of winter snow accumulation.

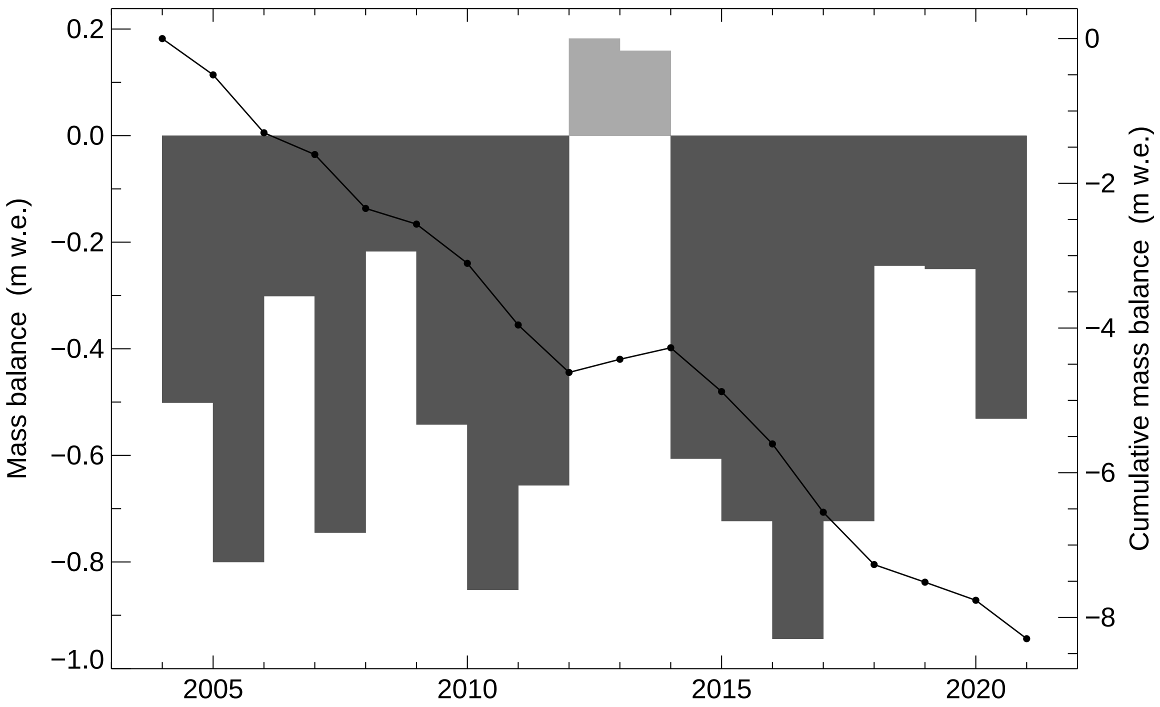

Figure 4.16: Findelengletscher - Mean specific annual balance (bars) and cumulative mass balance for the period 2004-2021.

Investigations in 2020/21

The winter survey was performed on 8th April 2021. In total, 312 snow probings distributed over the entire surface of Findelen- and Adlergletscher were obtained, and snow density was measured by coring at four sites. Snow densities ranged between 340 kg m^{-3} (lowest site) and 450 kg m^{-3} (at equilibrium line). On 30th July 2021 the lower autonomous camera needed to be rescued because of the rapid extension of a lateral moraine related to collapse of a massive subglacial void at the glacier snout. In consequence, the lowermost long-term measurement site had to be abandoned. On 22nd September 2021, the entire mass balance stake network was visited. Mass balance was determined at 13 stakes on Findelen- and at three on Adlergletscher. Firn density was measured at the topmost stake in the accumulation area while all other sites showed ablation. After the formation of an incised supraglacial channel beneath the meteorological station for snow water equivalent monitoring, the structure became instable and was thus dismantled in October 2021.

Portal of Findelengletscher in September 2021 (Photo: M. Huss)

Table 4.10: Findelengletscher and Adlergletscher - Individual stake measurements of winter and annual balance.

Stake	Period Start	Period Spring	Period End	Coordinates (m / m / m a.s.l.)	Mass balance b_w (mm w.e.)	Mass balance b_a (mm w.e.)
F2	17.09.2019	07.05.2020	15.09.2020	630638 / 95394 / 2598	435	−6156
F3	17.09.2019	07.05.2020	15.09.2020	630985 / 95377 / 2670	473	−6444
F4	17.09.2019	07.05.2020	15.09.2020	632136 / 95052 / 2788	1273	−5094
F5	17.09.2019	07.05.2020	15.09.2020	632164 / 95017 / 2922	1273	−2322
F7	17.09.2019	07.05.2020	15.09.2020	632527 / 94347 / 3038	1282	−1998
F8	17.09.2019	07.05.2020	15.09.2020	633276 / 93879 / 3121	1325	−1098
F81	17.09.2019	07.05.2020	15.09.2020	633280 / 94558 / 3142	1021	−2007
F82	17.09.2019	07.05.2020	15.09.2020	632533 / 93778 / 3088	1112	−1656
F91	17.09.2019	07.05.2020	15.09.2020	634373 / 94301 / 3253	1693	0
F93	17.09.2019	07.05.2020	15.09.2020	633942 / 93595 / 3239	1854	270
F94	17.09.2019	07.05.2020	15.09.2020	633628 / 93107 / 3262	1328	−369
F10	17.09.2019	07.05.2020	15.09.2020	635069 / 93942 / 3345	1605	420
F11	17.09.2019	07.05.2020	15.09.2020	634363 / 92294 / 3477	2199	1322
A2	17.09.2019	07.05.2020	15.09.2020	632538 / 95509 / 3075	1067	−2664
A4	17.09.2019	07.05.2020	15.09.2020	633069 / 95600 / 3238	1199	−2448
A6	17.09.2019	07.05.2020	15.09.2020	633645 / 95581 / 3338	1610	−819
F2	15.09.2020	08.04.2021	22.09.2021	630766 / 95400 / 2640	151	−6291
F3	15.09.2020	08.04.2021	22.09.2021	631002 / 95380 / 2664	332	−5832
F4	15.09.2020	08.04.2021	22.09.2021	631491 / 95390 / 2780	514	−4302
F5	15.09.2020	08.04.2021	22.09.2021	632169 / 95009 / 2879	576	−2844
F7	15.09.2020	08.04.2021	22.09.2021	632501 / 94371 / 3028	834	−2583
F8	15.09.2020	08.04.2021	22.09.2021	633276 / 93879 / 3121	1064	−1404
F81	15.09.2020	08.04.2021	22.09.2021	633321 / 94557 / 3144	963	−1917
F82	15.09.2020	08.04.2021	22.09.2021	632522 / 93769 / 3093	815	−1872
F91	15.09.2020	08.04.2021	22.09.2021	634447 / 94286 / 3264	1245	−450
F93	15.09.2020	08.04.2021	22.09.2021	633933 / 93597 / 3236	1491	−504
F94	15.09.2020	08.04.2021	22.09.2021	633623 / 93108 / 3258	931	−1179
F10	15.09.2020	08.04.2021	22.09.2021	635068 / 93938 / 3349	1036	50
F11	15.09.2020	08.04.2021	22.09.2021	634349 / 92293 / 3504	1526	1156
A2	15.09.2020	08.04.2021	22.09.2021	632547 / 95506 / 3079	709	−2682
A4	15.09.2020	08.04.2021	22.09.2021	633056 / 95609 / 3209	1043	−1953
A6	15.09.2020	08.04.2021	22.09.2021	633635 / 95577 / 3338	1060	−819

Table 4.11: Findelengletscher - Specific winter (b_w) and annual (b_a) balance according to elevation bands for the two periods 2019/20 and 2020/21. Results refer to the measurement period, defined by the dates of the field survey.

Altitude	2019/20			2020/21		
	Area	$\overline{b_w}$	$\overline{b_a}$	Area	$\overline{b_w}$	$\overline{b_a}$
(m a.s.l.)	(km^2)	(mm w.e.)	(mm w.e.)	(km^2)	(mm w.e.)	(mm w.e.)
2500 - 2600	0.019	-8	−7402	0.033	103	−6619
2600 - 2700	0.133	65	−6449	0.104	209	−5917
2700 - 2800	0.171	313	−5409	0.165	382	−4863
2800 - 2900	0.282	759	−3720	0.286	554	−3452
2900 - 3000	0.538	1036	−2389	0.551	704	−2808
3000 - 3100	0.979	1198	−1833	1.042	787	−2488
3100 - 3200	1.677	1320	−1144	1.634	1078	−1278
3200 - 3300	1.827	1577	−224	1.803	1166	−553
3300 - 3400	1.957	1746	397	1.942	1204	141
3400 - 3500	2.357	1901	832	2.353	1311	512
3500 - 3600	1.607	1831	989	1.601	1361	755
3600 - 3700	0.439	1476	739	0.445	1203	706
3700 - 3800	0.301	1442	841	0.290	835	313
3800 - 3900	0.252	1712	1274	0.253	811	391
3900 - 4000	0.011	1362	981	0.011	652	293
2500 - 4000	12.553	1551	−250	12.511	1111	−531

Table 4.12: Adlergletscher - Specific winter (b_w) and annual (b_a) balance according to elevation bands for the two periods 2019/20 and 2020/21. Results refer to the measurement period, defined by the dates of the field survey.

Altitude	2019/20			2020/21		
	Area	$\overline{b_w}$	$\overline{b_a}$	Area	$\overline{b_w}$	$\overline{b_a}$
(m a.s.l.)	(km^2)	(mm w.e.)	(mm w.e.)	(km^2)	(mm w.e.)	(mm w.e.)
2900 - 3000	0.006	1004	−3421	0.006	788	−3031
3000 - 3100	0.086	1095	−2863	0.086	841	−2680
3100 - 3200	0.123	1211	−2303	0.123	936	−2210
3200 - 3300	0.253	1148	−1915	0.253	981	−1721
3300 - 3400	0.399	1108	−971	0.399	920	−1092
3400 - 3500	0.315	1196	−229	0.315	1011	−421
3500 - 3600	0.246	1238	311	0.246	1135	281
3600 - 3700	0.208	1188	551	0.208	1124	581
3700 - 3800	0.177	1199	852	0.177	1111	874
3800 - 3900	0.103	1134	943	0.103	1030	921
3900 - 4000	0.046	1259	1197	0.046	1060	1045
4000 - 4100	0.014	1312	1367	0.014	962	970
4100 - 4200	0.004	1033	1070	0.004	826	808
2900 - 4200	1.979	1171	−491	1.979	1014	−513

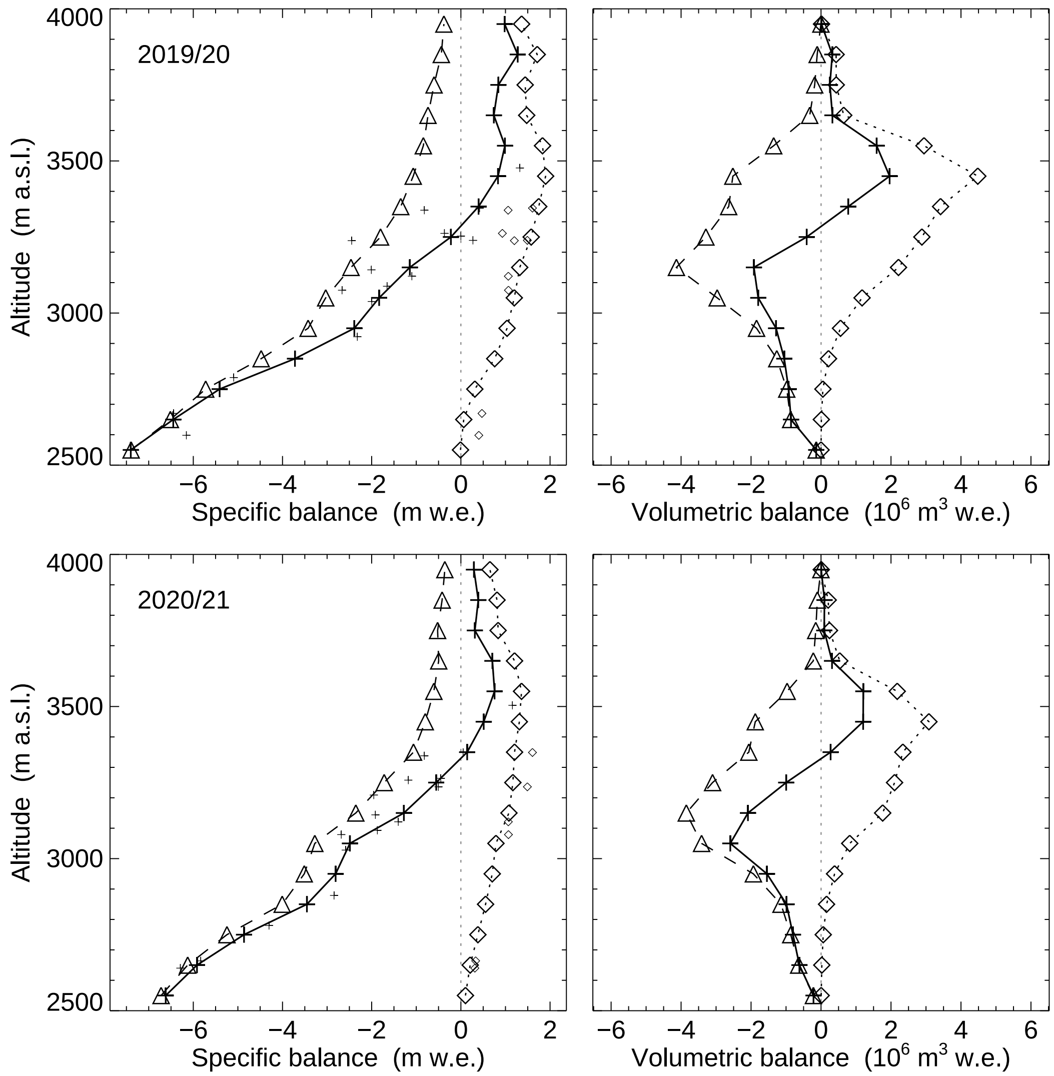

Figure 4.17: Findelengletscher - Specific (left) and volumetric (right) winter (dotted, $\diamond$), summer (dashed, $\triangle$) and annual (continuous line, $+$) balance in elevation bands for 2019/20 (top) and 2020/21 (bottom). Small symbols mark the individual measurements.

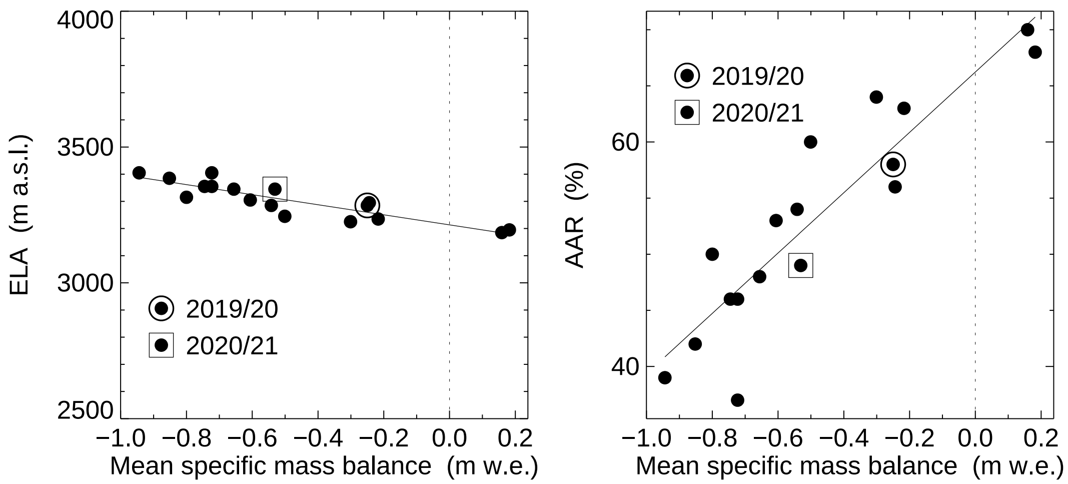

Figure 4.18: Equilibrium line altitude (ELA) and accumulation area ratio (AAR) versus mean specific balance including all previous observations.

4.9 Glacier du Giétro

Introduction

Glacier du Giétro is a temperate mountain glacier in the Southern Valais Alps (Val de Bagnes). The glacier has been under observations for early recognition of glacier break-off, which can endanger the reservoir operated by the Forces Motrices de Mauvoisin SA located in the outreach of ice avalanches. The measurements carried out since the mid-1960s include glacier evolution, ice flow, as well as mass balance. The observations of more than half a century document periods of glacier growth and recession (VAW, 1997, 1998; Bauder et al., 2002; Raymond et al., 2003). Annual mass balance is measured at stakes and glacier-wide mean specific annual balance is determined (Figure 4.20). No survey in spring to evaluate the winter snow accumulation is conducted. Data of point mass balance and volume changes since 1966 was re-analyzed and homogenized (Huss et al., 2015). The results of the glacier-wide mean specific annual balance for comparable fixed-date periods were presented in Section 4.17 of Volume 135/136. Further details on long-term observation of ice flow velocities are given in Section 5.4.

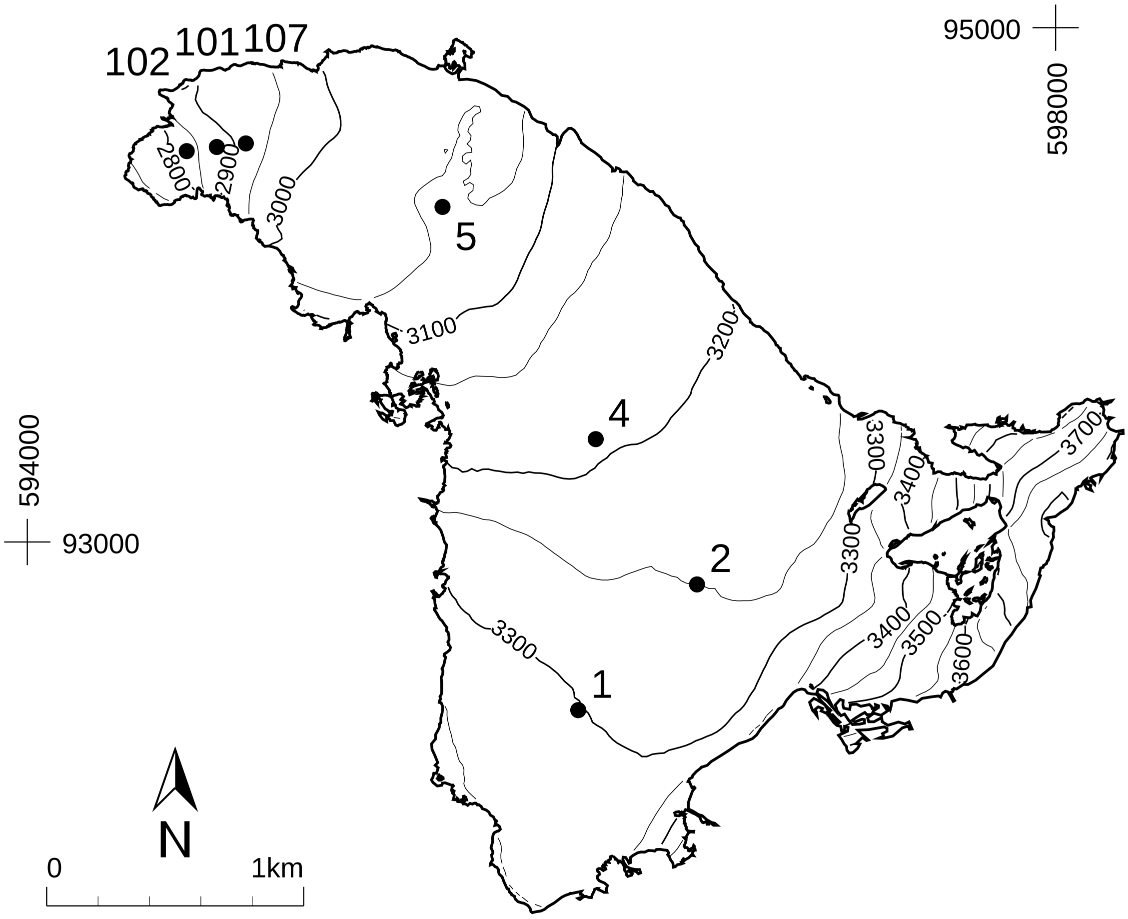

Figure 4.19: Surface topography and observational network of Glacier du Giétro.

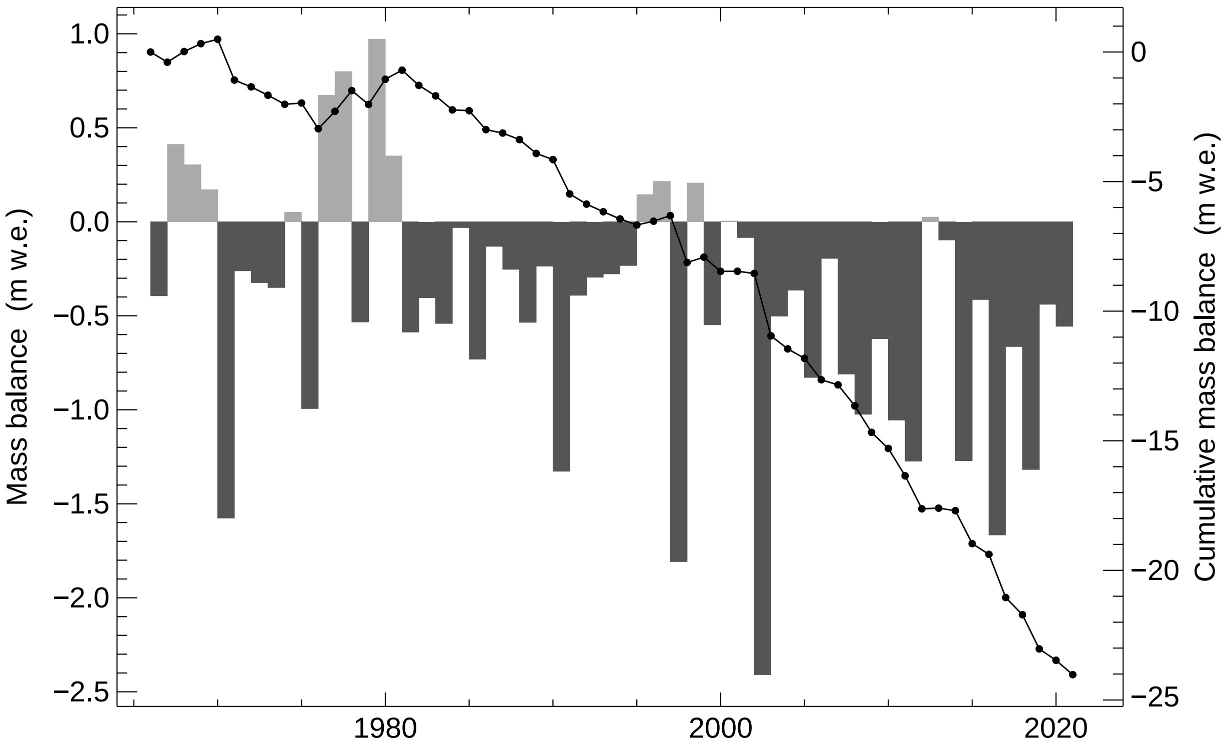

Figure 4.20: Glacier du Giétro - Mean specific annual balance (bars) and cumulative mass balance for the period 1966-2021. Values refer to the measurement period.

Investigations in 2019/20

Annual observations of mass balance with maintenance of the stake network were carried out on 8th September 2020. Negative local mass balances resulted at six stakes while the site 02 showed slightly positive balance. Due to the minimal amount of accumulation, no density measurement was performed.

Investigations in 2020/21

The annual field survey took place on 14th September 2021. At all stakes a negative local mass balance was determined. As there was no firn accumulation, no density measurement was performed.

Table 4.13: Glacier du Giétro - Specific winter (b_w) and annual (b_a) balance according to elevation bands for the two periods 2019/20 and 2020/21. Results refer to the measurement period, defined by the dates of the field survey.

Altitude	2019/20			2020/21		
	Area	$\overline{b_w}$	$\overline{b_a}$	Area	$\overline{b_w}$	$\overline{b_a}$
(m a.s.l.)	(km^2)	(mm w.e.)	(mm w.e.)	(km^2)	(mm w.e.)	(mm w.e.)
2700 - 2800	0.027		−4819	0.027		−5305
2800 - 2900	0.066		−3477	0.066		−4116
2900 - 3000	0.221		−2690	0.221		−2794
3000 - 3100	0.881		−1802	0.881		−1846
3100 - 3200	0.993		−638	0.993		−799
3200 - 3300	1.641		99	1.641		−102
3300 - 3400	0.916		387	0.916		299
3400 - 3500	0.172		595	0.172		649
3500 - 3600	0.117		638	0.117		761
3600 - 3700	0.121		633	0.121		807
3700 - 3800	0.116		662	0.116		878
3800 - 3900	0.009		674	0.009		917
2700 - 3900	5.280		−439	5.280		−556

Table 4.14: Glacier du Giétro - Individual stake measurements of winter and annual balance.

Stake	Period			Coordinates	Mass balance	
	Start	Spring	End		b_w	b_a
				(m / m / m a.s.l.)	(mm w.e.)	
01	27.09.2019		08.09.2020	596149 / 92350 / 3296		−50
02	27.09.2019		08.09.2020	596601 / 92850 / 3245		214
04	27.09.2019		08.09.2020	596210 / 93400 / 3182		−126
05	27.09.2019		08.09.2020	595628 / 94165 / 3049		−2007
101	27.09.2019		08.09.2020	594740 / 94533 / 2864		−1548
102	27.09.2019		08.09.2020	594603 / 94507 / 2797		−4635
107	27.09.2019		08.09.2020	594859 / 94560 / 2913		−4248
01	08.09.2020		14.09.2021	596152 / 92353 / 3294		−48
02	08.09.2020		14.09.2021	596603 / 92843 / 3244		−64
04	08.09.2020		14.09.2021	596200 / 93418 / 3180		−675
05	08.09.2020		14.09.2021	595613 / 94173 / 3045		−1800
101	08.09.2020		14.09.2021	594717 / 94529 / 2856		−954
102	08.09.2020		14.09.2021	594613 / 94499 / 2791		−4608
107	08.09.2020		14.09.2021	594835 / 94555 / 2898		−3168
107	17.09.2018		27.09.2019	594860 / 94557 / 2917		−4122

4.10 Griesgletscher (Aegina)

Introduction

Griesgletscher is a temperate valley glacier located in the central Swiss Alps. The glacier currently covers an area of 4.1 km^2 flowing in north-eastern direction from 3320 m a.s.l. down to 2440 m a.s.l. Mass balance measurements started in 1961 in connection with the construction of a reservoir for hydro-power production. Determination of volumetric changes in decadal resolution extend further back to 1884 (Bauder et al., 2007). Topographic maps or photogrammetrical surveys exist for 1884, 1923, 1961, 1967, 1979, 1986, 1991, 1998, 2003, 2007 and annually since 2012. Huss et al. (2009) re-analyzed and homogenized the seasonal stake data and ice volume changes for the period 1961-2007. The results of the mean specific winter and annual balance for comparable fixed-date periods including a periodic update until 2015 (Huss et al., 2015) were presented in Section 4.17 of Volume 135/136.

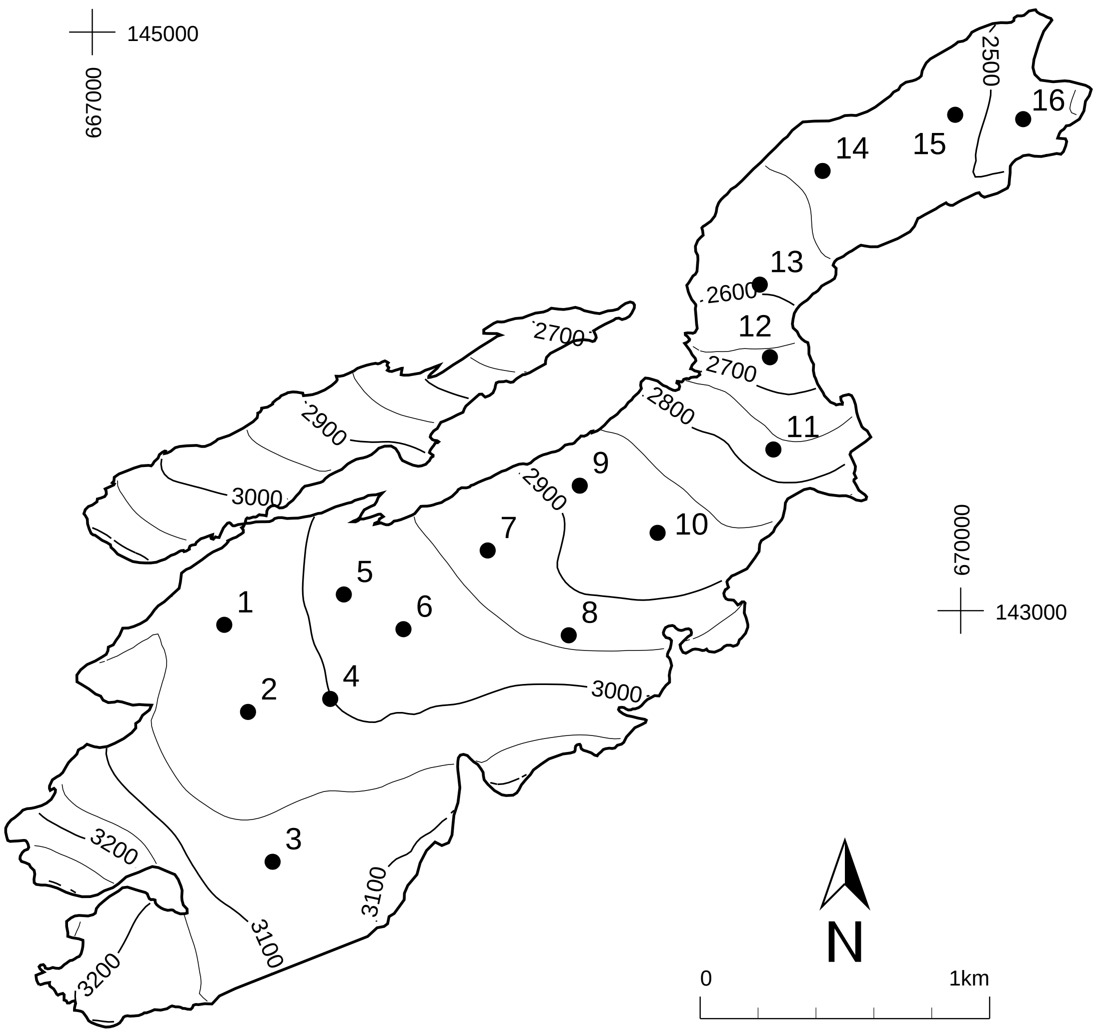

Figure 4.21: Surface topography and observational network of Griesgletscher.

Investigations in 2019/20

Winter snow depth probings were collected at 114 locations distributed across the glacier surface, and including all stake locations on 23rd April 2020. Snow density was measured by coring at two sites – in the former accumulation area, and on the tongue indicating values of 510 and 430 kg m^{-3}, respectively. On 12th August 2020, ground control points on prominent rocks around the entire glacier were re-painted and geolocated with differential GNSS, and all stakes were visited for an intermediate reading. The period for the determination of annual mass balance extended from 9th September 2019 to 14th September 2020. A negative mass balance was determined at all 18 stakes. While two sites showed an almost balanced mass budget, local ablation at the glacier snout reached the highest value ever observed since the beginning of the monitoring (-5.9 m w.e.). Even in the former accumulation area, firn coverage is completely depleted.

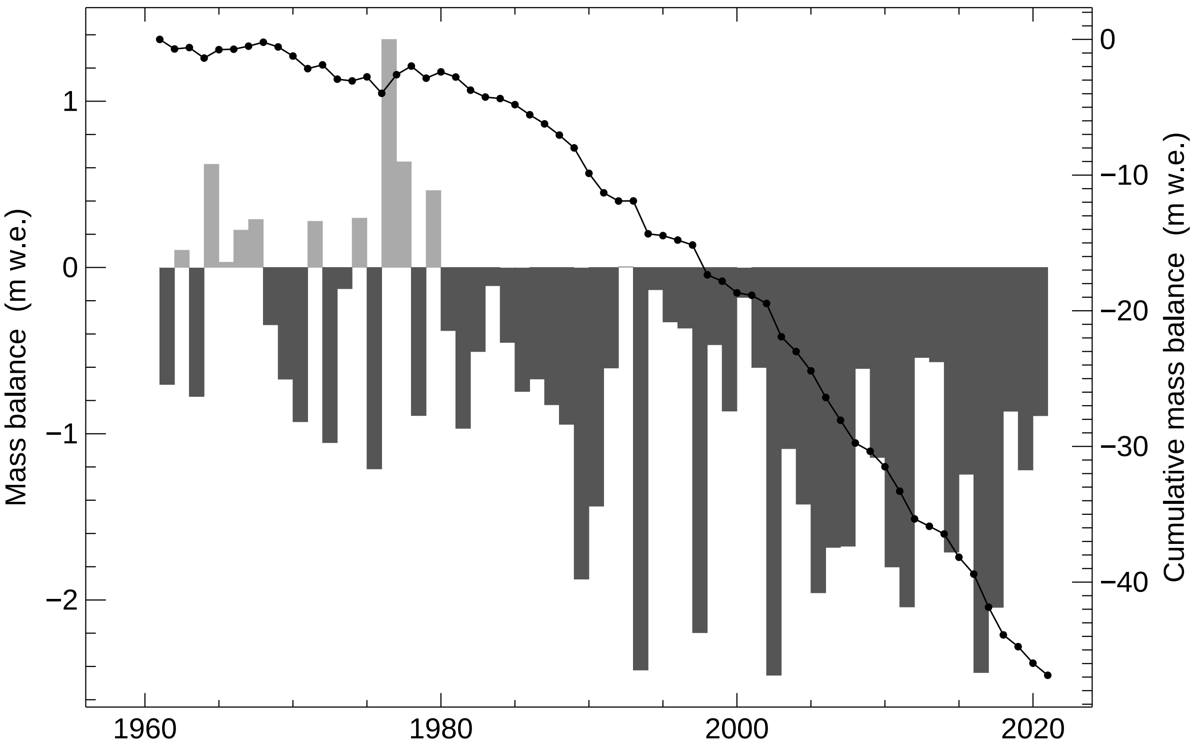

Figure 4.22: Griesgletscher - Mean specific annual balance (bars) and cumulative mass balance for the period 1961-2021.

Investigations in 2020/21

The winter mass balance was monitored on 20th April 2021. Snow soundings were performed at 148 locations over the glacier's entire elevation range. Snow density was measured by coring at two locations indicating values of 460 and 440 kg m^{-3}, respectively. On 18th September 2021, the mass balance was determined at all 16 sites with optimal conditions. While ablation on the glacier tongue was less extreme than during the previous period due to more winter snow in that part of Griesgletscher, ablation in the upper reaches was considerable and the entire glacier was again almost completely snow-free at the time of late-summer survey. Due to fast retreat of the terminus, the lowermost long-term measurement site had to be abandoned.

Table 4.15: Griesgletscher - Specific winter (b_w) and annual (b_a) balance according to elevation bands for the two periods 2019/20 and 2020/21. Results refer to the measurement period, defined by the dates of the field survey.

Altitude (m a.s.l.)	2019/20 Area (km^2)	$\overline{b_w}$ (mm w.e.)	$\overline{b_a}$ (mm w.e.)	2020/21 Area (km^2)	$\overline{b_w}$ (mm w.e.)	$\overline{b_a}$ (mm w.e.)
2400 - 2500	0.128	572	−5550	0.103	1033	−3449
2500 - 2600	0.494	644	−4600	0.482	1223	−2972
2600 - 2700	0.131	989	−3126	0.125	1522	−2369
2700 - 2800	0.241	1412	−1733	0.233	1628	−1434
2800 - 2900	0.536	1740	−1237	0.528	1680	−1142
2900 - 3000	0.931	1980	−686	0.920	1764	−606
3000 - 3100	1.329	2174	−162	1.320	1806	−159
3100 - 3200	0.279	2283	427	0.275	1794	200
3200 - 3300	0.115	2393	871	0.113	1869	602
3300 - 3400	0.002	2294	1553	0.003	1778	1283
2300 - 3400	4.186	1778	−1218	4.102	1674	−892

The snout of Alpetligletscher – the tongue of Kanderfirn – in October 2021 (Photo: U. Burgener)

Table 4.16: Griesgletscher - Individual stake measurements of winter and annual balance.

Stake	Period Start	Spring	End	Coordinates (m / m / m a.s.l.)	Mass balance b_w (mm w.e.)	b_a
1	09.09.2019		14.09.2020	667456 / 142951 / 3032		−621
2	09.09.2019	23.04.2020	14.09.2020	667538 / 142650 / 3021	1762	−657
3	09.09.2019	23.04.2020	14.09.2020	667623 / 142132 / 3071	1660	−18
4	09.09.2019		14.09.2020	667822 / 142695 / 3002		−360
5	09.09.2019	23.04.2020	14.09.2020	667869 / 143056 / 2986	1788	−972
6	09.09.2019	23.04.2020	14.09.2020	668075 / 142936 / 2981	1762	−747
7	09.09.2019	23.04.2020	14.09.2020	668366 / 143208 / 2935	1558	−1215
7	09.09.2019	23.04.2020	14.09.2020	668408 / 143144 / 2932	1778	−1080
8	09.09.2019	23.04.2020	14.09.2020	668646 / 142915 / 2935	2069	−36
9	09.09.2019	23.04.2020	14.09.2020	668684 / 143432 / 2885	1548	−1917
10	09.09.2019	23.04.2020	14.09.2020	668953 / 143269 / 2870	1660	−1332
11	09.09.2019	23.04.2020	14.09.2020	669353 / 143557 / 2768	1433	−1188
12	09.09.2019	23.04.2020	14.09.2020	669341 / 143876 / 2660	963	−2997
13	09.09.2019	23.04.2020	14.09.2020	669306 / 144127 / 2601	1219	−4329
14	09.09.2019	23.04.2020	14.09.2020	669523 / 144520 / 2544	868	−4293
15	09.09.2019	23.04.2020	14.09.2020	669981 / 144714 / 2508	890	−4959
16	09.09.2019	23.04.2020	14.09.2020	670281 / 144737 / 2466	783	−5922
1	14.09.2020	20.04.2021	18.09.2021	667454 / 142951 / 3032	1944	−495
2	14.09.2020	20.04.2021	18.09.2021	667538 / 142653 / 3022	1759	−387
3	14.09.2020	20.04.2021	18.09.2021	667623 / 142140 / 3069	1588	60
4	14.09.2020	20.04.2021	18.09.2021	667826 / 142699 / 3002	1828	−324
5	14.09.2020	20.04.2021	18.09.2021	667869 / 143056 / 2986	1759	−621
6	14.09.2020	20.04.2021	18.09.2021	668082 / 142942 / 2980	1643	−711
7	14.09.2020	20.04.2021	18.09.2021	668367 / 143203 / 2931	1472	−1368
8	14.09.2020	20.04.2021	18.09.2021	668650 / 142920 / 2937	1921	−60
9	14.09.2020	20.04.2021	18.09.2021	668686 / 143424 / 2889	1449	−2151
10	14.09.2020	20.04.2021	18.09.2021	668955 / 143272 / 2867	1527	−819
11	14.09.2020	20.04.2021	18.09.2021	669353 / 143560 / 2764	1794	−909
12	14.09.2020	20.04.2021	18.09.2021	669344 / 143871 / 2664	1484	−2331
12	14.09.2020	20.04.2021	18.09.2021	669309 / 144131 / 2598	1196	−3645
14	14.09.2020	20.04.2021	18.09.2021	669510 / 144499 / 2540	1439	−2484
15	14.09.2020	20.04.2021	18.09.2021	669970 / 144714 / 2507	1395	−3267
16	14.09.2020	20.04.2021	18.09.2021	670216 / 144699 / 2479	1218	−3582

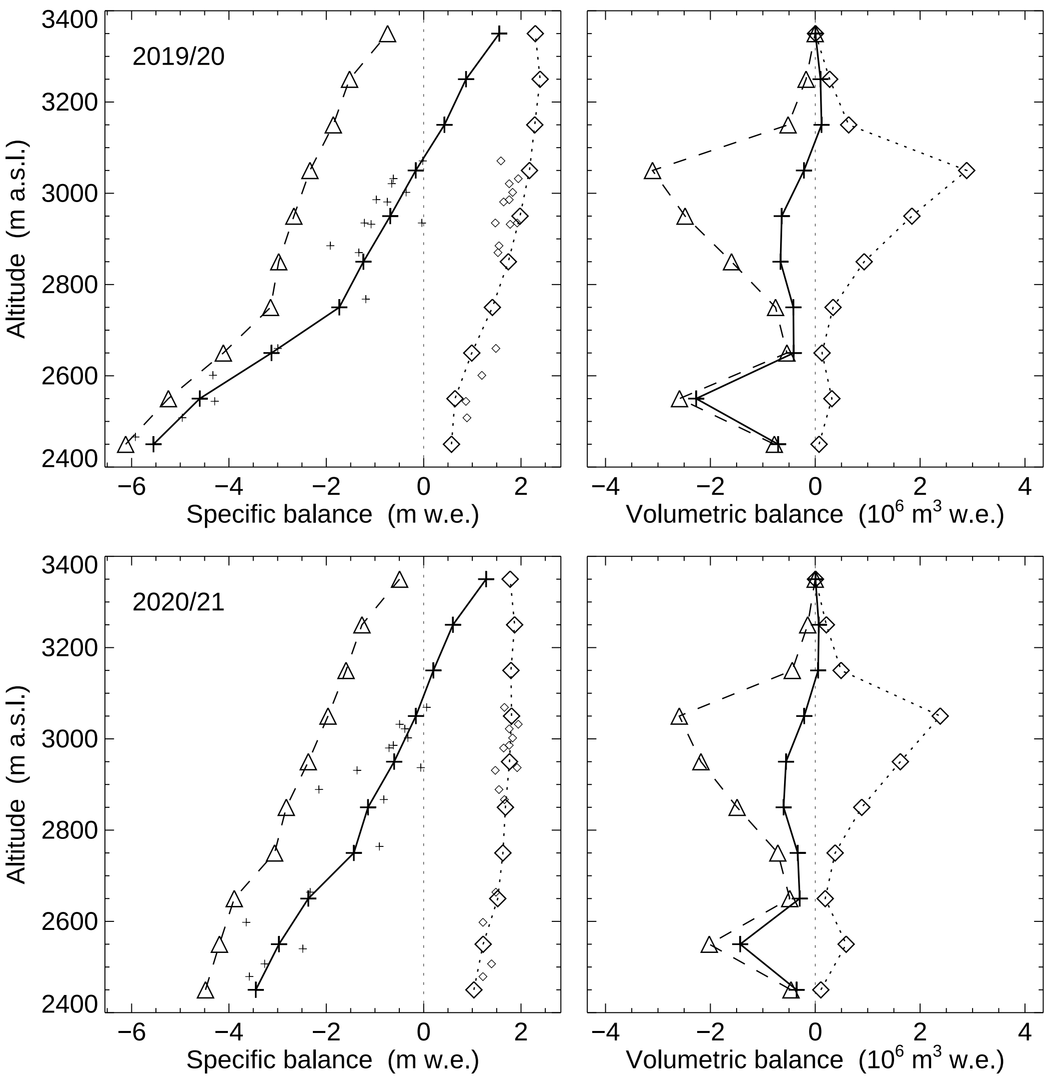

Figure 4.23: Specific (left) and volumetric (right) winter (dotted, ⋄), summer (dashed, △) and annual (continuous line, +) balance in elevation bands for 2019/20 (top) and 2020/21 (bottom). Small symbols mark the individual measurements.

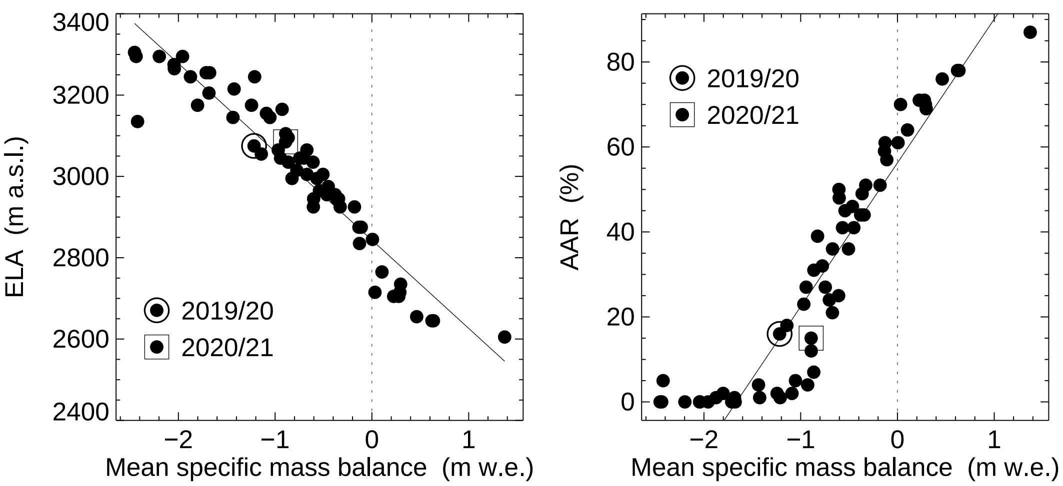

Figure 4.24: Equilibrium line altitude (ELA) and accumulation area ratio (AAR) versus mean specific balance including all previous observations.

4.11 Grosser Aletschgletscher

Introduction

Grosser Aletschgletscher is the largest ice mass in the European Alps and borders the major northern Alpine crest. By 2017 it covered an area of 78.5 km^2 and had a volume of 11.6 km3, thus accounting for a fifth of the total ice mass of Switzerland (Linsbauer et al., 2021; Grab et al., 2021). The three main tributaries converge at the Konkordiaplatz and form the common tongue which extends southwards for about 13 km. Starting in 1918, the first stake was installed at 3350 m a.s.l. on Jungfraufirn and snow accumulation and annual mass balance was measured almost continuously until today at site 3 (Figure 4.25). Huss and Bauder (2009) compiled and homogenized all existing measurements to provide a continuous time series of seasonal resolution

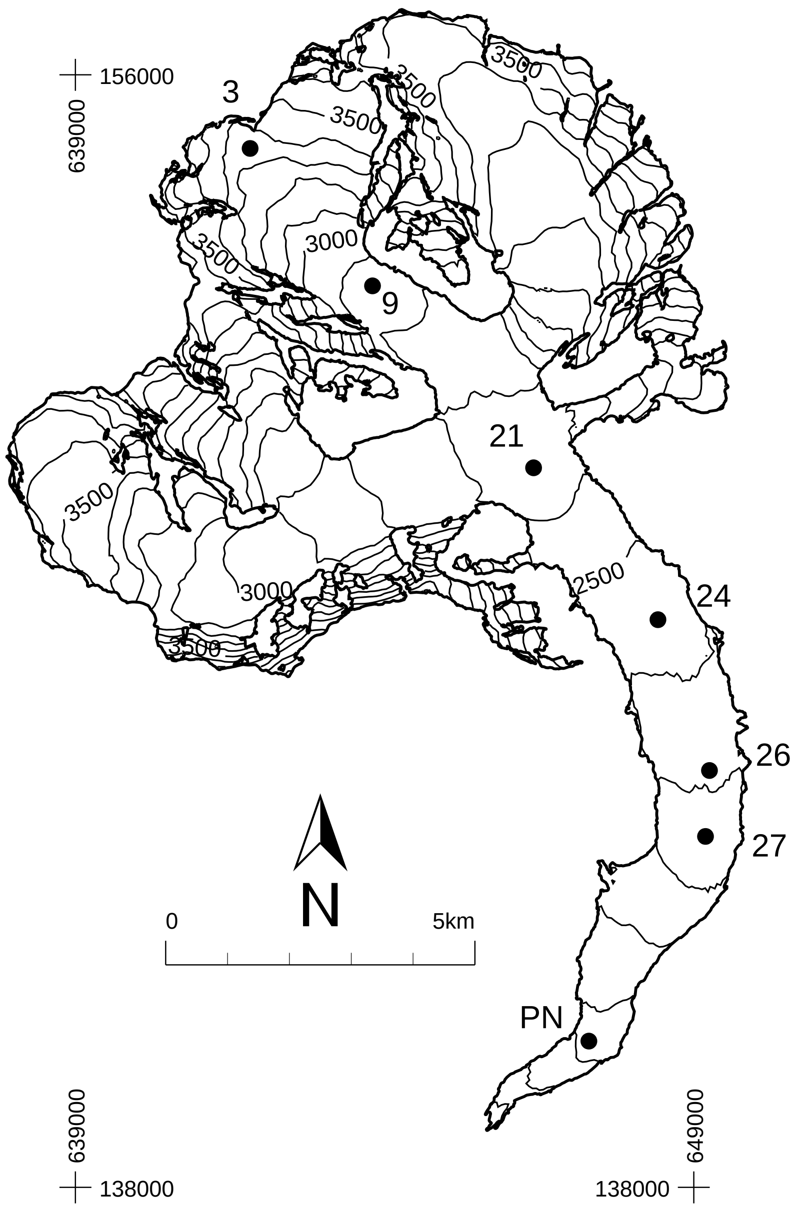

Figure 4.25: Surface topography and observational network of Grosser Aletschgletscher.

(see Section 4.10 in Volume 127/128). Between the 1940s and 1990s a network of stakes on a longitudinal and several cross profiles was maintained with a focus on both mass balance and ice flow velocity (Zoller, 2010; Geibel et al., 2022). As part of the educational activities of ProNatura, mass balance is measured at site PN on the glacier tongue. Starting in 1992, weekly readings have been carried out during the summer season, and since the year 1995/96 the annual balance has been determined as well. Since 2020, a parsimonious network of four additional stakes along the central longitudinal transect between Jungfraujoch and Märjelensee is maintained and observed both in April and September to provide a stronger basis for assessing the seasonal mass change of the entire glacier system. Results from additional investigations of ice flow velocities are given in Section 5.5.

Investigations in 2019/20

The investigations at site 3 consisted of snow depth measurements and density profiling using a core drill in spring and fall. The surface was marked at the time of the survey in the previous fall and could be located in the firn cores retrieved for density determination. This monitoring program was supplemented by stake readings approximately twice a month. The measurements were taken in spring on 29th May 2020 and in fall on 18th September 2020. In spring, mean density of the layer accumulated during winter was found to be 466 ± 15 kg m^{-3}, and in fall a density of 516 ± 20 kg m^{-3} was found for the annual layer. At site PN an ablation stake is maintained and usually re-drilled twice during summer because of the high melt rate at this site. A first reading in spring was taken on 22th June 2020 and a last one in fall on 8th October 2020. Results of seasonal mass balance measurements were reported by ProNatura. On 19th June 2020, two additional mass balance stakes were installed on the glacier tongue between Konkordiaplatz and

Table 4.17: Grosser Aletschgletscher - Individual stake measurements of winter and annual balance.

Stake	Period Start	Period Spring	Period End	Coordinates (m / m / m a.s.l.)	Mass balance b_w (mm w.e.)	Mass balance b_a (mm w.e.)
3	03.10.2019	29.05.2020	18.09.2020	641825 / 154810 / 3337	1179	490
24	03.10.2019		18.09.2020	648420 / 147185 / 2426		−5499
26	03.10.2019		18.09.2020	649253 / 144745 / 2297		−5850
27	03.10.2019		18.09.2020	649520 / 143636 / 2231		−7407
PN	11.10.2019	22.06.2020	08.10.2020	647366 / 140595 / 1956	−3411	−11178
3	18.09.2020	26.05.2021	30.09.2021	641825 / 154810 / 3336	2861	2313
9	18.09.2020	19.04.2021	24.09.2021	643804 / 152586 / 2861	1226	−819
21	18.09.2020	19.04.2021	24.09.2021	646409 / 149642 / 2639	783	−2439
24	18.09.2020	19.04.2021	24.09.2021	648420 / 147185 / 2426	944	−3708
27	18.09.2020	19.04.2021	24.09.2021	649189 / 143678 / 2206	490	−5652
PN	08.10.2020	14.06.2021	13.10.2021	647465 / 140845 / 2002	−1422	−9612

Märjelensee, and were equipped with autonomous cameras for monitoring glacier melt at real time (see Landmann et al., 2021). Another two additional stakes were installed on 18th September 2020 close to the equilibrium line on Jungfraufirn and at Konkordiaplatz, respectively, and all stakes along the central longtudinal transect were maintained. The installation of the autonomous camera at Märjelensee changed in order to be able to continuously monitor winter snow depth.

Investigations in 2020/21

The same set of measurements was conducted as in the previous period. At site 3, the spring field survey was carried out on 26th May 2021 and the fall survey on 30th September 2021. Snow depth measurements and firn coring in May showed a homogeneous layer of winter accumulation. Corresponding measurements from stake readings, firn drilling, and snow depth sounding delivered similar results. Mean density of the layer accumulated in winter was found to be 537 $\mathrm{kg\,m^{-3}}$ in spring, and a density of 598 ± 5 $\mathrm{kg\,m^{-3}}$ in fall was found for the annual layer. Mass balance investigations at site PN were undertaken by ProNatura with measurement in spring on 14th June 2021 and on 13th September 2021 with the determination of summer and annual balance. On 19th April 2021, a complete winter mass balance survey along the central longitudinal transect of Grosser Aletschgletscher was performed. Snow probings were acquired every few hundred meters and snow density was measured at two sites. The camera for automated ice ablation readings was maintained on 13thJuly and 25th August 2021, and stakes around Konkordiaplatz and on the lower glacier tongue were visited and maintained on 2nd and 24th September 2021, respectively. Two additional stakes were installed along the central transect to decrease the distance between the sites.

4.12 Hohlaubgletscher

Introduction

Hohlaubgletscher is a temperate mountain glacier located in the Mattmark area in the Southern Valais Alps. It currently covers an area of 2.1 km^2 flowing in east direction from 4020 m a.s.l. down to 2850 m a.s.l. Mass balance measurements started in 1955 as a part of investigations for the construction of the Mattmark reservoir for hydro-power production (VAW, 1999; Antoni, 2005). Initially a network of three stakes in the ablation area was maintained for mass balance and ice flow measurements (see Chapter 5). After 1967 measurements were continued at only one stake until 2019 when a second stake was installed. Only the annual mass balance is investigated and no survey in spring for winter snow accumulation is conducted. Data of point mass balance and geodetic ice volume changes since 1955 has been re-analyzed and homogenized (Huss et al., 2015). Here we only present the results of annual point mass balance measurements. Glacier-wide mass balance estimates are presented periodically in a complete form after a calibration with geodetic mass balance based on repeated digital elevation models has been performed. Further details on long-term observations of ice flow velocities are presented in Section 5.6.

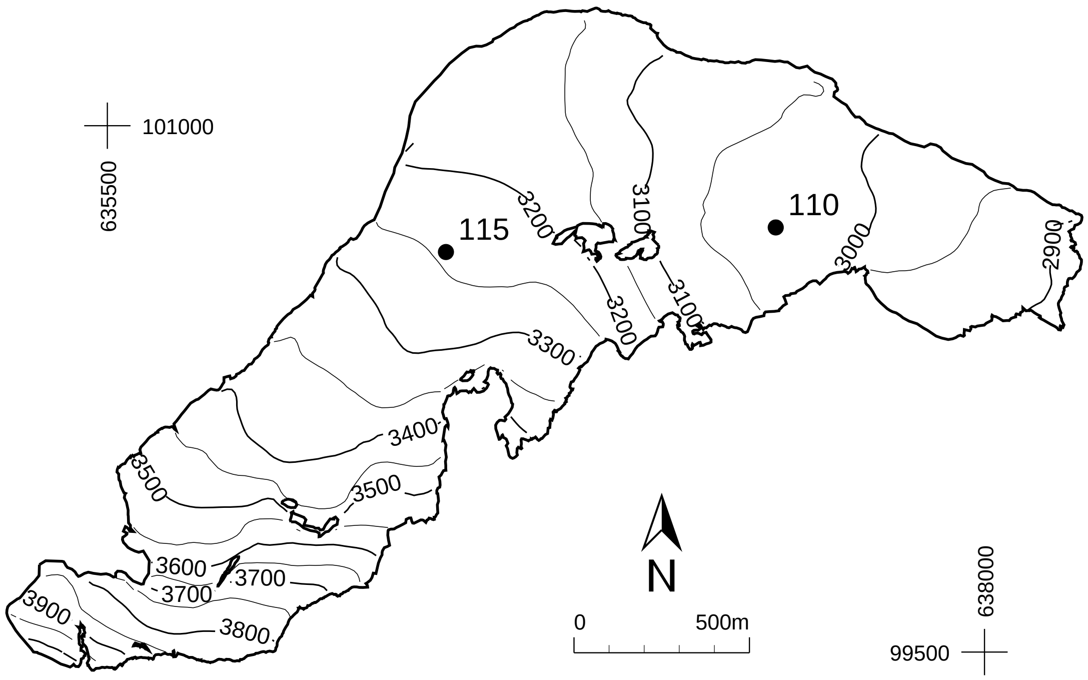

Figure 4.26: Surface topography and observational network of Hohlaubgletscher.

Investigations in 2019/20 and 2020/21

Annual observation of local mass balance at two stakes were carried out on 4th September 2020. A negative local mass balance has been registered at the lower site while some very limited accumulation resulted at the new site.

In the second observation period under review, the annual field measurements were carried out on 2nd September 2021. Again, a negative local mass balance resulted at stake 110 and a slightly positive balance at stake 115.

Table 4.18: Hohlaubgletscher - Individual stake measurements of winter and annual balance.

Stake	Period			Coordinates	Mass balance	
	Start	Spring	End		b_w	b_a
				(m / m / m a.s.l.)	(mm w.e.)	
110	30.08.2019		04.09.2020	637414 / 100707 / 3024		−1224
115	30.08.2019		04.09.2020	636467 / 100638 / 3241		103
110	04.09.2020		02.09.2021	637415 / 100707 / 3023		−1377
115	04.09.2020		02.09.2021	636484 / 100666 / 3233		174

Blüemlisalpgletscher in October 2021 (Photo: U. Burgener)

4.13 Vadret dal Murtèl

Introduction

Vadret dal Murtèl is situated in the inner-alpine Upper Engadine of south-eastern Switzerland. The east-facing cirque glacier next to Piz Corvatsch (3451 m a.s.l.) covers 0.3 km^2 and still shows some crevassing in its steeper middle part. Exhibiting only very little debris cover along the foot of steep headwalls confining the glacier to the north and west, Vadret dal Murtèl is a typical clean-ice glacier. Mass balance investigations were started in 2013, and are also performed on the southern lobe of nearby Vadret dal Corvatsch (0.2 km^2).

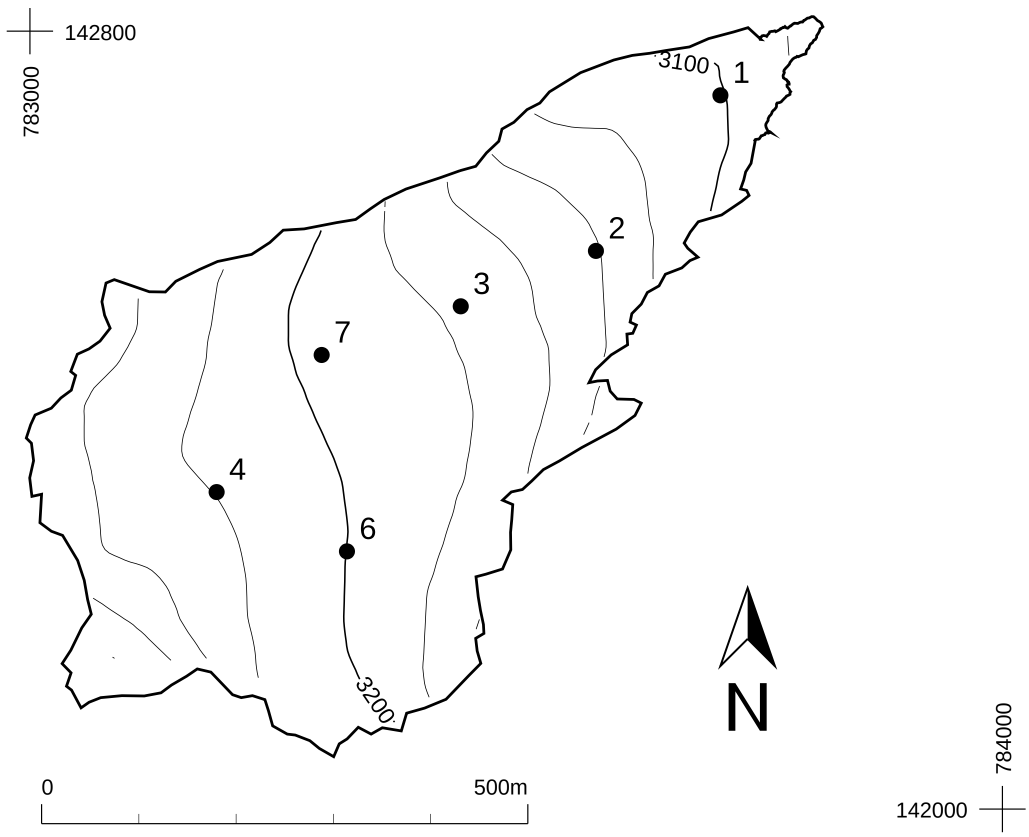

Figure 4.27: Surface topography and observational network of Vadret dal Murtèl.

Investigations in 2019/20

Winter balance was measured on 26th April 2020. Due to the pandemic, field access was not supported by the cablecar to Piz Corvatsch and, hence, no snow density measurements could be performed. Snow depth was determined based on 101 probings on Vadret dal Murtèl and 26 on Vadret dal Corvatsch. Unfortunately, artificial relocation of snow related to the preparation of ski

Table 4.19: Vadret dal Murtèl - Specific winter (b_w) and annual (b_a) balance according to elevation bands for the two periods 2019/20 and 2020/21. Results refer to the measurement period, defined by the dates of the field survey.

Altitude	2019/20			2020/21		
	Area	$\overline{b_w}$	$\overline{b_a}$	Area	$\overline{b_w}$	$\overline{b_a}$
(m a.s.l.)	(km^2)	(mm w.e.)	(mm w.e.)	(km^2)	(mm w.e.)	(mm w.e.)
3050 - 3100	0.006	650	−2573	0.004	963	−2508
3100 - 3150	0.046	691	−1277	0.045	1029	−1273
3150 - 3200	0.105	831	−445	0.105	1109	−671
3200 - 3250	0.101	1112	247	0.101	1523	199
3250 - 3300	0.013	1348	856	0.013	1998	1392
3300 - 3350	0.000	1286	1108	0.000	1903	1719
3050 - 3350	0.272	933	−311	0.269	1292	−371

runs have increased, thus impacting measurement values on this glacier. The late summer field survey was performed on 7th September 2020 during strong snowfall. Measured point mass balance on Vadret dal Murtèl was negative at the lower three stakes, but close to balanced conditions above 3150 m a.s.l.. On nearby Vadret dal Corvatsch, a negative mass balance was measured at the remaining four stakes. Due to the limited size of the glacier and the effects of activities related to the ski resort, no further maintenance of the stake network was performed and the stakes will only be measured until they have melted out.

Table 4.20: Vadret dal Murtèl - Individual stake measurements of winter and annual balance.

Stake	Period			Coordinates	Mass balance	
	Start	Spring	End		b_w	b_a
				(m / m / m a.s.l.)	(mm w.e.)	
1	21.09.2019	26.04.2020	07.09.2020	783709 / 142733 / 3058	640	−2610
2	21.09.2019	26.04.2020	07.09.2020	783586 / 142572 / 3091	908	−945
3	21.09.2019	26.04.2020	07.09.2020	783447 / 142519 / 3149	840	−657
4	21.09.2019	26.04.2020	07.09.2020	783191 / 142325 / 3179	1000	81
6	21.09.2019	26.04.2020	07.09.2020	783327 / 142264 / 3164	972	−279
7	21.09.2019	26.04.2020	07.09.2020	783293 / 142468 / 3159	960	−36
1	07.09.2020	02.04.2021	06.09.2021	783707 / 142738 / 3052	931	−2259
2	07.09.2020	02.04.2021	06.09.2021	783586 / 142572 / 3091	817	−1296
3	07.09.2020	02.04.2021	06.09.2021	783450 / 142524 / 3139	893	−711
4	07.09.2020	02.04.2021	06.09.2021	783191 / 142325 / 3179	1299	120
6	07.09.2020	02.04.2021	06.09.2021	783334 / 142268 / 3165	1169	−603
7	07.09.2020	02.04.2021	06.09.2021	783293 / 142468 / 3159	1255	−200

Investigations in 2020/21

Winter balance was determined on 2nd April 2021. Snow probings at 126 and 38 locations on Vadret dal Murtèl and Vadret dal Corvatsch were performed, respectively. Snow density was measured in two snow pits close to the terminus of Vadret dal Murtèl and in the accumulation area, indicating densities of 380 and 430 kg m^{-3}, respectively. The late summer field survey was performed on 6th September 2021. Five of the six stakes on Vadret dal Murtèl showed a negative local mass balance, while about half a meter of firn accumulation was found at the uppermost site with a measured density of 460 kg m^{-3}. On Vadret dal Corvatsch, mass balance was negative at three stakes, while balanced conditions were found at one site on the meanwhile detached lobe (250 m×100 m) northeast of Piz Murtèl that collects significantly higher amounts of snow accumulation than the rest of the glacier.

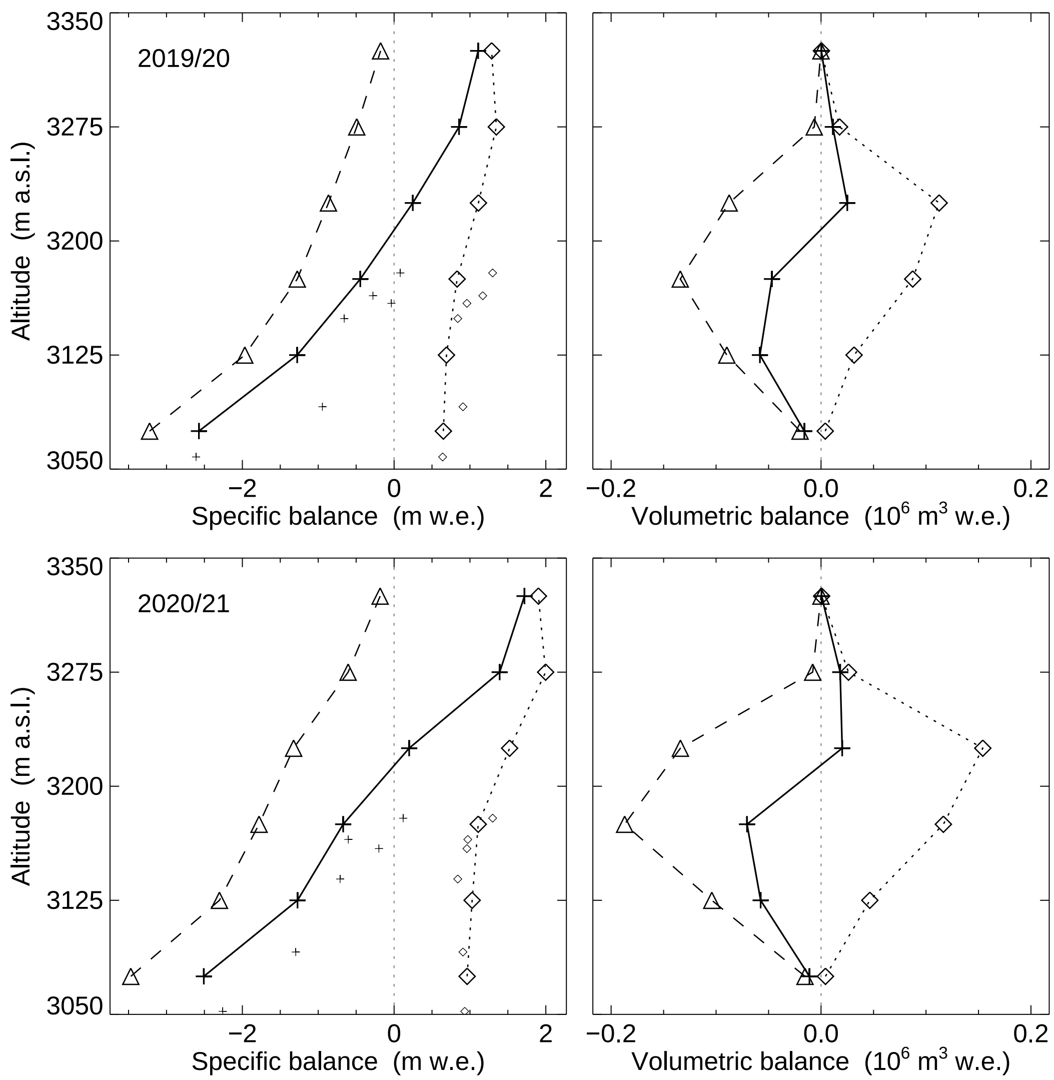

Figure 4.28: Specific (left) and volumetric (right) winter (dotted, ◇), summer (dashed, △) and annual (continuous line, +) balance in elevation bands for 2019/20 (top) and 2020/21 (bottom). Small symbols mark the individual measurements.

4.14 Vadret Pers

Introduction

Vadret Pers was a major tributary glacier to Vadret dal Morteratsch, the largest valley glacier in eastern Switzerland but separated in about 2017, and can thus be considered as an individual glacier. Vadret Pers currently has an area of 6.7 km^2. It is characterized by a glacier tongue with moderate crevassing that is increasingly constricted towards the snout, a wide and gently-sloping section at intermediate elevation and a very steep accumulation area shaped by seracs and ice avalanches. In 2019, Vadret Pers was chosen by GLAMOS as a representative site for long-term mass balance monitoring in south-eastern Switzerland because of previous local annual ablation measurements since 2002 performed by Belgian glaciologists (see Zekollari and Huybrechts, 2018), the high resilience to climate change due to an altitudinal extent up to almost 3900 m a.s.l. The monitoring is jointly performed by the Vrije Universiteit Brussel (VUB) that is conducting annual mass balance surveys at a stake network in some parts of the ablation area (Van Tricht et al., 2021). The contribution of GLAMOS adds measurements in the accumulation area and more

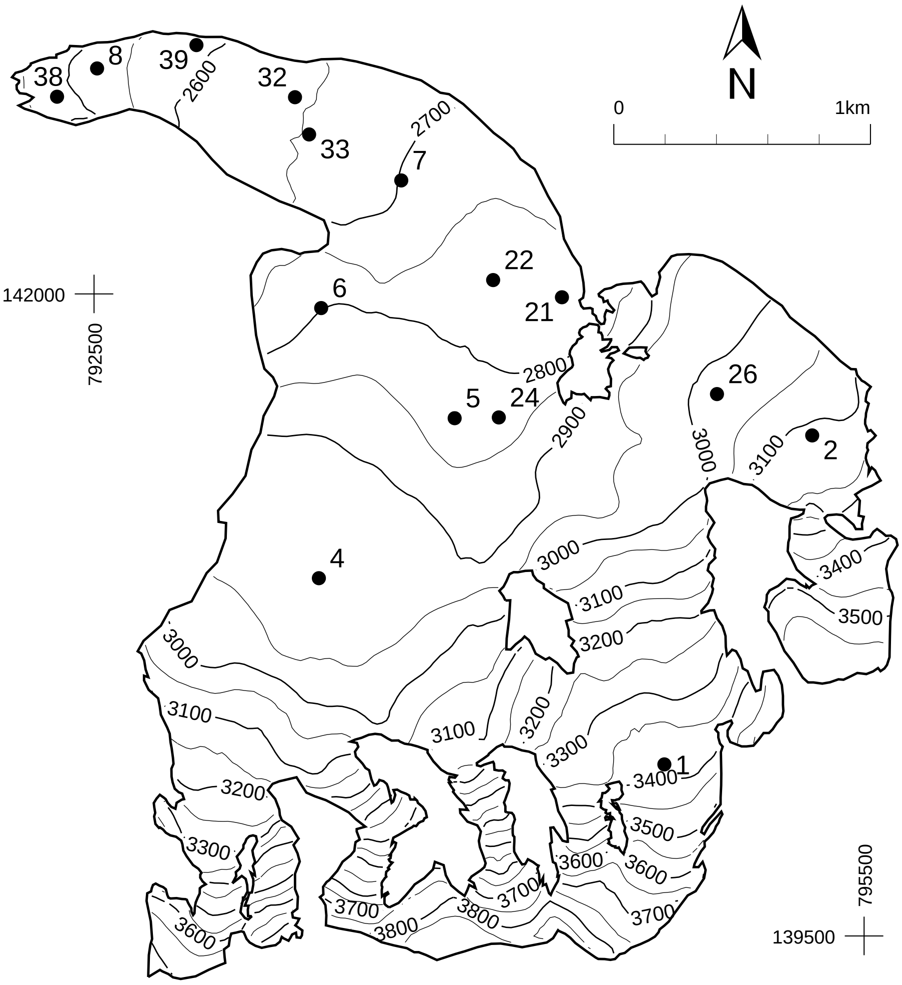

Figure 4.29: Surface topography and observational network of the Vadreat Pers.

remote parts of the ablation area, as well as winter snow accumulation.

Table 4.21: Vadret Pers - Individual stake measurements of winter and annual balance.

Stake	Period			Coordinates	Mass balance	
	Start	Spring	End		b_w	b_a
				(m / m / m a.s.l.)	(mm w.e.)	
1	28.09.2019		08.09.2020	794722 / 140168 / 3394		1800
4	28.09.2019		08.09.2020	793376 / 140893 / 2935		−828
5	28.09.2019		08.09.2020	793905 / 141516 / 2824		−1773
7	28.09.2019		08.09.2020	793697 / 142442 / 2694		−3672
21	28.09.2019		08.09.2020	794323 / 141987 / 2764		−2340
22	28.09.2019		08.09.2020	794055 / 142054 / 2766		−2277
24	28.09.2019		08.09.2020	794077 / 141519 / 2830		−1188
26	28.09.2019		08.09.2020	794927 / 141610 / 3061		−180
32	28.09.2019		08.09.2020	793283 / 142766 / 2624		−3537
33	28.09.2019		08.09.2020	793338 / 142621 / 2647		−3348
38	28.09.2019		08.09.2020	792356 / 142768 / 2484		−5634
39	28.09.2019		08.09.2020	792899 / 142969 / 2575		−4536
1	08.09.2020	16.04.202	06.09.2021	794673 / 140210 / 3386	2390	1953
2	08.09.2020	16.04.2021	06.09.2021	795298 / 141449 / 3114	1727	660
4	08.09.2020	16.04.2021	06.09.2021	793376 / 140893 / 2935	1156	−1278
5	08.09.2020	16.04.2021	06.09.2021	793907 / 141516 / 2820	1052	−2043
6	08.09.2020	16.04.2021	06.09.2021	793385 / 141945 / 2791	904	−2484
7	08.09.2020	16.04.2021	06.09.2021	793701 / 142443 / 2684	748	−3618
8	08.09.2020	16.04.2021	06.09.2021	792512 / 142878 / 2508	475	−4518
21	08.09.2020		06.09.2021	794325 / 141992 / 2760		−2574
22	08.09.2020	16.04.2021	06.09.2021	794050 / 142087 / 2767	928	−2475
24	08.09.2020	16.04.2021	06.09.2021	794082 / 141588 / 2814	1000	−1854
26	08.09.2020	16.04.2021	06.09.2021	794920 / 141615 / 3010	1489	−450
32	08.09.2020	16.04.2021	06.09.2021	793268 / 142777 / 2622	816	−2862
33	08.09.2020	16.04.2021	06.09.2021	793314 / 142630 / 2641	848	−3231
38	08.09.2020	16.04.2021	06.09.2021	792350 / 142768 / 2457	683	−4536
39	08.09.2020	16.04.2021	06.09.2021	793029 / 142944 / 2589	383	−4167

Investigations in 2019/20

On 8th August 2019 the VUB network consisting of eight stakes on Vadret Pers was extended with four additional stakes in underrepresented regions of the glacier. One stake was placed at "Schnapsboden", the only flat section of the accumulation area at an elevation of 3400 m a.s.l. Even though a seasonal monitoring was intended from 2020 onwards, we postponed the first winter survey on Vadret Pers to 2021 due to the pandemic situation. The GLAMOS fall survey was conducted on 8th September 2020. All stakes of the network were visited and maintained, and three additional stakes were supplemented to improve knowledge on mass balance distribution.

Unfortunately, the topmost stake could not be located, either because of too high accumulation, or too fast ice flow into a crevassed zone, and a new stake was placed. VUB stakes were visited and maintained between 22nd and 24th September 2020. Over the annual period a negative mass balance was determined at 11 sites, whereas partly substantial snow accumulation likely occurred above about 3100 m a.s.l.

Table 4.22: Vadret Pers - Specific winter (b_w) and annual (b_a) balance according to elevation bands for the two periods 2019/20 and 2020/21. Results refer to the measurement period, defined by the dates of the field survey.

Altitude	2019/20			2020/21		
	Area	$\overline{b_w}$	$\overline{b_a}$	Area	$\overline{b_w}$	$\overline{b_a}$
(m a.s.l.)	(km^2)	(mm w.e.)	(mm w.e.)	(km^2)	(mm w.e.)	(mm w.e.)
2400 - 2500	0.053	750	−5403	0.053	677	−4341
2500 - 2600	0.152	819	−4660	0.152	701	−4526
2600 - 2700	0.491	902	−3663	0.491	1064	−3218
2700 - 2800	0.768	1012	−2245	0.768	1215	−2495
2800 - 2900	0.722	1103	−1219	0.722	1419	−1598
2900 - 3000	1.431	1184	−461	1.431	1628	−751
3000 - 3100	0.780	1266	266	0.780	1861	263
3100 - 3200	0.485	1300	652	0.485	2048	855
3200 - 3300	0.364	1185	764	0.364	2218	1209
3300 - 3400	0.361	1179	978	0.361	2419	1650
3400 - 3500	0.307	1064	1039	0.307	2201	1646
3500 - 3600	0.274	895	955	0.274	1869	1398
3600 - 3700	0.203	886	1123	0.203	1591	1244
3700 - 3800	0.166	683	873	0.166	1599	1353
3800 - 3900	0.104	190	77	0.104	1448	1168
2400 - 3900	6.661	1086	−591	6.661	1652	−525

Investigations in 2020/21

On 16th April 2021, the first winter snow survey on the glacier was performed. At the uppermost measurement site, more than 5 metres of snow were measured. In total, 159 snow probings covering the entire glacier surface except for most parts of the steep and crevassed accumulation area were obtained. Snow density was measured by coring at three sites ranging from 3400 to 2500 m a.s.l., and densities of between 430 and 300 kg m^{-3} were found. The late-summer field survey was conducted on 6th September 2021 and all stakes were visited. Unfortunately, the uppermost stake again could not be located and was not re-installed. We thus shifted to estimating accumulated snow/firn depth based on layer stratigraphy in crevasses, a method that is simple and efficient but sometimes ambiguous. The density of the accumulated layer (500 kg m^{-3}) was determined by coring. The VUB survey was conducted during the last week of September.

4.15 Pizolgletscher

Introduction

Pizolgletscher is a steep cirque glacier in the north-eastern Swiss Alps. With a surface area of about 0.02 km^2 Pizolgletscher represents the size class of very small glaciers that include almost 80% of the total number of glaciers in Switzerland (Fischer et al., 2014). Pizolgletscher is north-exposed and located at relatively low elevation (2650-2730 m a.s.l.) indicating that it depends on high quantities of winter accumulation. Seasonal mass balance measurements were started in 2006 (Huss, 2010). Active maintenance of the stake network was abandoned in 2019 after the glacier had disintegrated due to continued mass losses and now only consists of several small dead-ice bodies strongly covered by debris. Mass balance observations are continued however until all stakes have melted out.

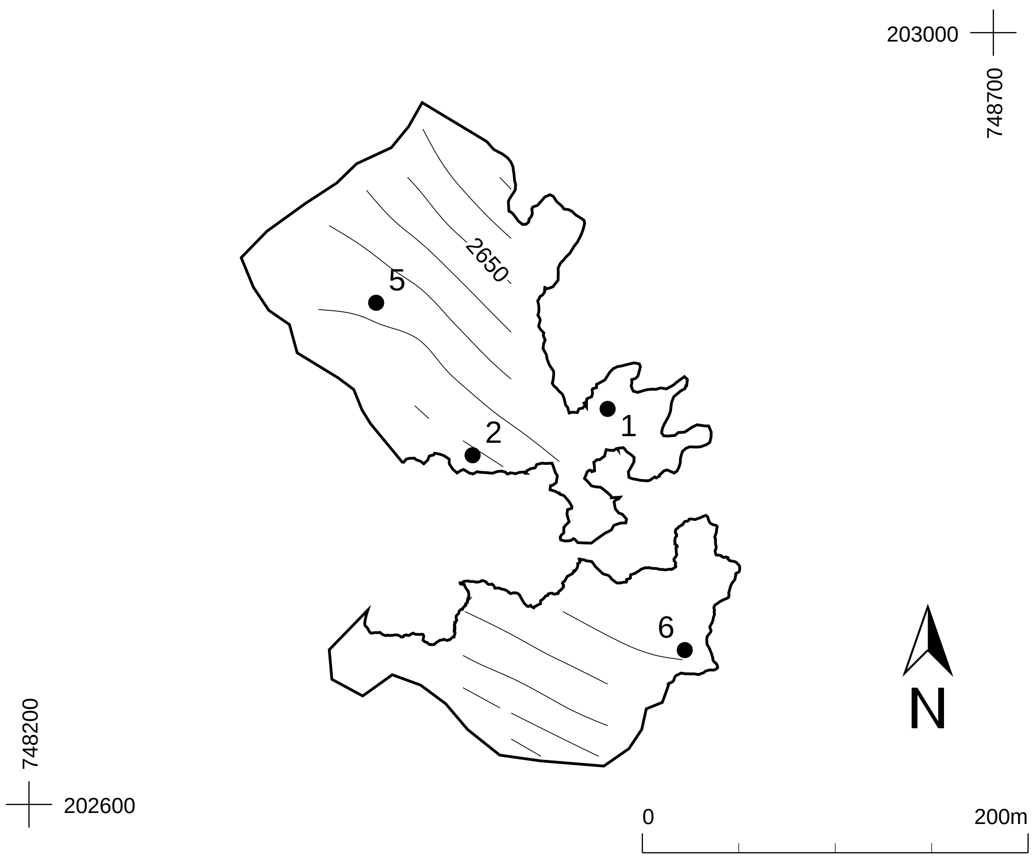

Figure 4.30: Surface topography and observational network of Pizolgletscher.

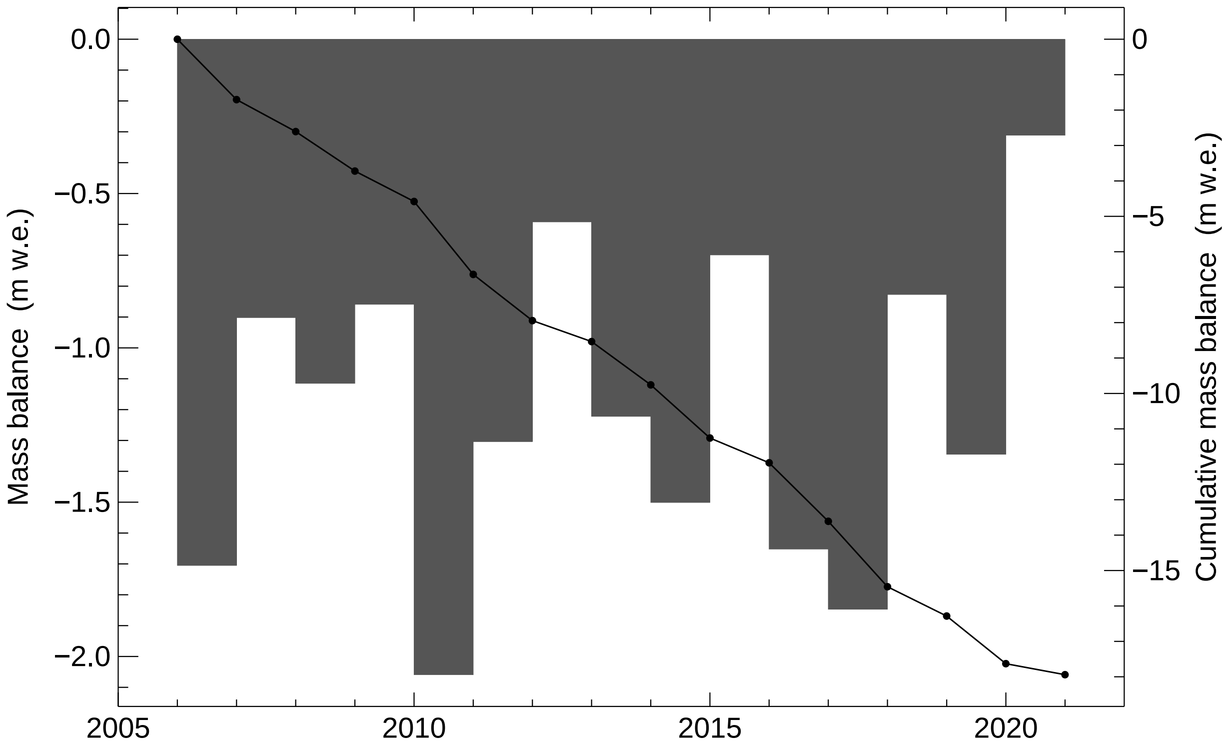

Figure 4.31: Pizolgletscher - Mean specific annual balance (bars) and cumulative mass balance for the period 2006-2021.

Investigations in 2019/20

Due to the pandemic, winter balance was determined later than usual (22nd April 2020) and without support of the cablecar. Snow probings at 76 locations were performed but no snow density measurements were performed. All stakes were visited on 27th July and 23rd September 2020 and a strongly negative mass balance over the annual period was observed at all four remaining measurement sites. Almost all material from the mass balance monitoring programme could be collected and be carried out. Rapid disintegration of the glacier has continued, and ice is only present at some spots with strong topographic shading, enhanced protection with much wind-transported snow, or beneath thick rockfall debris originating from the steep slopes exposed by glacier retreat.

Investigations in 2020/21

A winter field survey was conducted on 26th March 2021. Snow probings at 50 locations were realized but we abstained from measuring snow density. On 7th September 2021 the last two remaining stakes were visited. Whereas the western site in a steep ice flank subject to considerable rockfall hazard showed substantial ablation, and was finally removed, the eastern site exhibited a positive mass balance. Almost ironically, since the beginning of the mass balance surveys in 2006, this observation represents the very first local mass gain anywhere on Pizolgletscher in the last year of the series. The subsidence of the ice surface probably has contributed to more favourable conditions in terms of snow accumulation and shading for this site, and the positive balance was supported by the unsettled weather during the summer. Throughout the entire year 2021 repeated major rockfall events were observed. The deposits covered some remaining dead ice and the former lower part of Pizolgletscher by partly several meters of rock debris.

Table 4.23: Pizolgletscher - Specific winter (b_w) and annual (b_a) balance according to elevation bands for the two periods 2019/20 and 2020/21. Results refer to the measurement period, defined by the dates of the field survey.

Altitude (m a.s.l.)	2019/20 Area (km^2)	$\overline{b_w}$ (mm w.e.)	$\overline{b_a}$ (mm w.e.)	2020/21 Area (km^2)	$\overline{b_w}$ (mm w.e.)	$\overline{b_a}$ (mm w.e.)
2600 - 2650	0.000	1080	−2207	0.000	1526	−560
2650 - 2700	0.014	1291	−1616	0.013	1543	−443
2700 - 2750	0.006	1440	−699	0.006	1619	−19
2600 - 2750	0.020	1334	−1345	0.019	1566	−311

Table 4.24: Pizolgletscher - Individual stake measurements of winter and annual balance.

Stake	Period Start	Period Spring	Period End	Coordinates (m / m / m a.s.l.)	Mass balance b_w (mm w.e.)	Mass balance b_a (mm w.e.)
1	22.09.2019	22.04.2020	23.09.2020	748497 / 202803 / 2645	1404	−1386
2	22.09.2019	22.04.2020	23.09.2020	748428 / 202782 / 2667	1300	−1962
5	22.09.2019	22.04.2020	23.09.2020	748371 / 202853 / 2675	1400	−1980
6	22.09.2019	22.04.2020	23.09.2020	748531 / 202685 / 2697	1488	−846
5	23.09.2020	26.03.2021	07.09.2021	748371 / 202853 / 2675	1609	−1008
6	23.09.2020	26.03.2021	07.09.2021	748531 / 202685 / 2697	1776	112

4.16 Glacier de la Plaine Morte

Introduction

Glacier de la Plaine Morte (6.9 km^2) is the largest plateau glacier in the European Alps and thus represents a particularly interesting site for studying accelerating effects of climate change on Alpine glaciers. Plaine Morte is situated at the main Alpine divide between the cantons Berne and Valais. 90% of the glacier surface lie in a narrow altitudinal band of between 2650 and 2800 m a.s.l.. From the 5 km wide plateau with an average slope of less than four degrees, a small outlet glacier (Rezligletscher) flows northwards. Large circular depressions of the glacier surface, probably related to cryo-karst, are common features and are stable over several decades. Lac des Faverges, an ice marginal lake with a water volume of more than 2 million m^3 is subject to annual drainage events (Ogier et al., 2021). The seasonal mass balance of Glacier de la Plaine Morte is determined since 2009 using the direct glaciological method (Huss et al., 2013). The spatial variability in melt is mainly driven by differences in ice surface albedo (Naegeli et al., 2015).

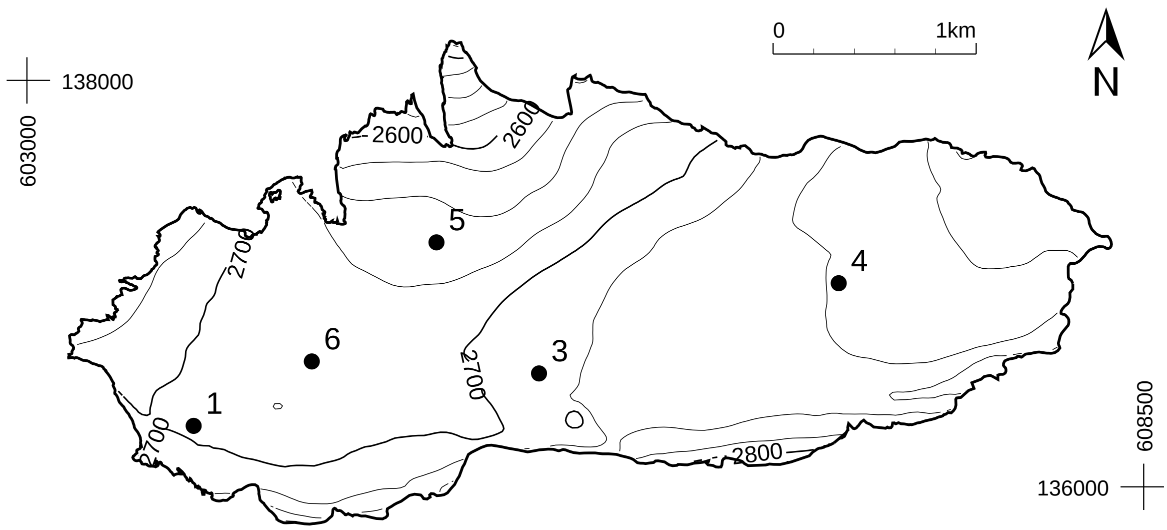

Figure 4.32: Surface topography and observational network of Glacier de la Plaine Morte.

Investigations in 2019/20

Due to the lock-down in April 2020 related to the global pandemic, field accessibility of Glacier de la Plaine Morte for regular winter mass balance surveys was not given. Therefore, no in situ measurement could be performed. As the spatial mass balance variability is small over the entire glacier, and patterns are well constrained from previous field campaigns, we fully relied on automatic measurements of snow depth and density at the site of the meteorological station in the central part of Plaine Morte. Snow water equivalent is continuously monitored at this location using a cosmic ray sensor deployed at the snow-ice interface (Gugerli et al., 2019). On 30th June 2020, an autonomous station to continuously measure ice ablation was installed (Landmann et al., 2021),

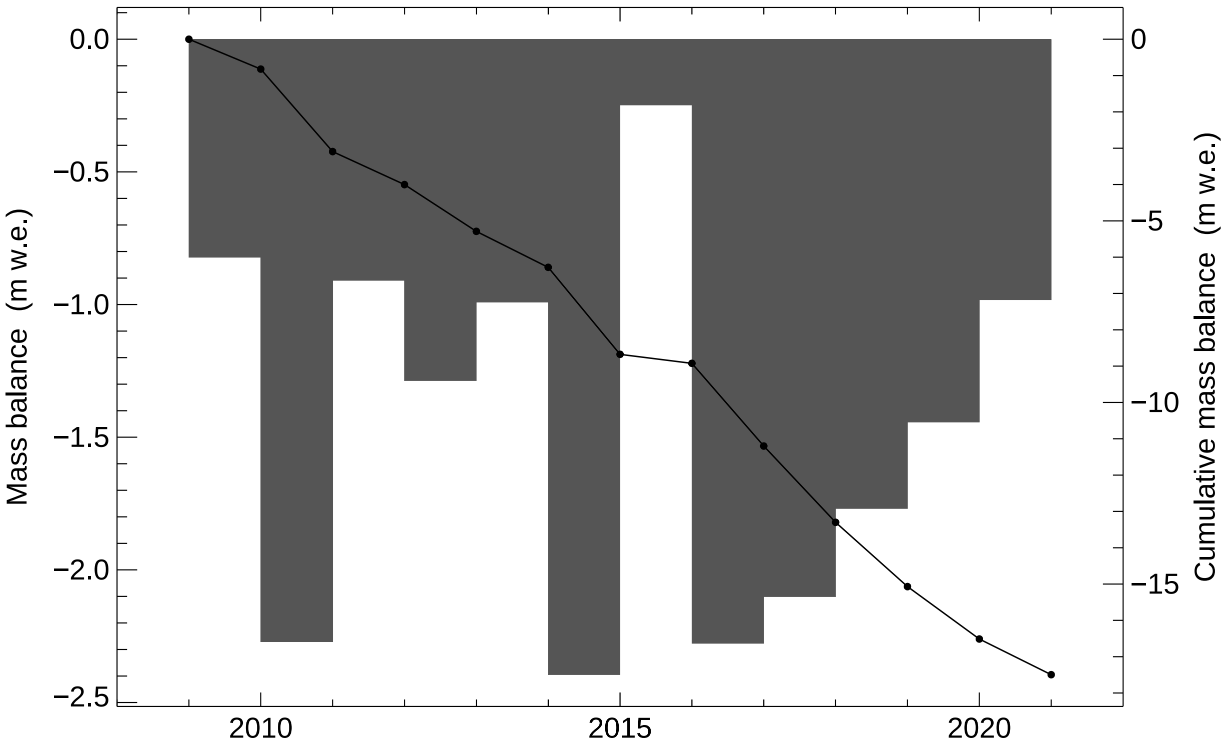

Figure 4.33: Glacier de la Plaine Morte - Mean specific annual balance (bars) and cumulative mass balance for the period 2006-2021.

summer snow density was measured and the condition at Lac des Faverges was inspected. The stake network was maintained on 4th September 2020. All five stakes showed substantial ablation and winter snow was depleted on the entire glacier surface. The artificial supraglacial channel to limit the water volume in Lac des Faverges remained filled with winter snow far into the summer. The ice-dammed lake thus grew up to a substantial volume. Some artificial surface excavation of the snow activated water flow through the channel and the lake started draining subglacially on 5th August 2020, but outflow rates remained limited so that the lake only completely emptied by 17th August.

Investigations in 2020/21

During the winter field survey on 30th March 2021 snow probings at 104 locations distributed over the entire glacier were acquired and a snow density of 390 kg m^{-3} was measured in a snow pit. A second snow survey was performed on 20th May 2021, with a snow density measurement at the meteorological station and some snow depth soundings, indicating a considerable increase in snow water equivalent on the glacier since late March 2021. On 1st September 2021 all five stakes were visited and maintained, and the camera to continuously monitor ice ablation was taken down for the winter. Again, the entire glacier was snow-free but ablation rates were somewhat smaller than in previous years with around 1 metre ice loss since early September 2020. Substantial ablation likely also occurred after the field visit however. Lac des Faverges filled up to an intermediate volume also in this year but drained through the artificial channel as well as subglacially after 26th

July 2021 without causing impacts in the Simme valley.

Table 4.25: Glacier de la Plaine Morte - Specific winter (b_w) and annual (b_a) balance according to elevation bands for the two periods 2019/20 and 2020/21. Results refer to the measurement period, defined by the dates of the field survey.

Altitude	2019/20			2020/21		
	Area	$\overline{b_w}$	$\overline{b_a}$	Area	$\overline{b_w}$	$\overline{b_a}$
(m a.s.l.)	(km^2)	(mm w.e.)	(mm w.e.)	(km^2)	(mm w.e.)	(mm w.e.)
2400 - 2500	0.006	1330	−1953	0.005	1607	−1126
2500 - 2600	0.164	1376	−1900	0.152	1535	−1333
2600 - 2700	2.729	1440	−1627	2.709	1536	−1151
2700 - 2800	4.072	1415	−1305	4.014	1526	−858
2800 - 2900	0.011	1471	37	0.008	1590	301
2400 - 2900	6.981	1423	−1443	6.889	1530	−982

Table 4.26: Glacier de la Plaine Morte - Individual stake measurements of winter and annual balance.

Stake	Period			Coordinates	Mass balance	
	Start	Spring	End		b_w	b_a
				(m / m / m a.s.l.)	(mm w.e.)	
1	30.09.2019		04.09.2020	603821 / 136300 / 2691		−1521
3	30.09.2019		04.09.2020	605522 / 136558 / 2717		−1260
4	30.09.2019		04.09.2020	606998 / 137002 / 2751		−1044
5	30.09.2019		04.09.2020	605017 / 137203 / 2664		−1683
6	30.09.2019	26.04.2020	04.09.2020	604403 / 136617 / 2680	1447	−1629
1	04.09.2020	30.03.2021	01.09.2021	603821 / 136300 / 2691	1478	−1107
3	04.09.2020	30.03.2021	01.09.2021	605522 / 136558 / 2717	1594	−738
4	04.09.2020	30.03.2021	01.09.2021	606998 / 137002 / 2751	1478	−810
5	04.09.2020	30.03.2021	01.09.2021	605017 / 137203 / 2664	1575	−1035
6	04.09.2020	30.03.2021	01.09.2021	604403 / 136617 / 2680	1478	−1359

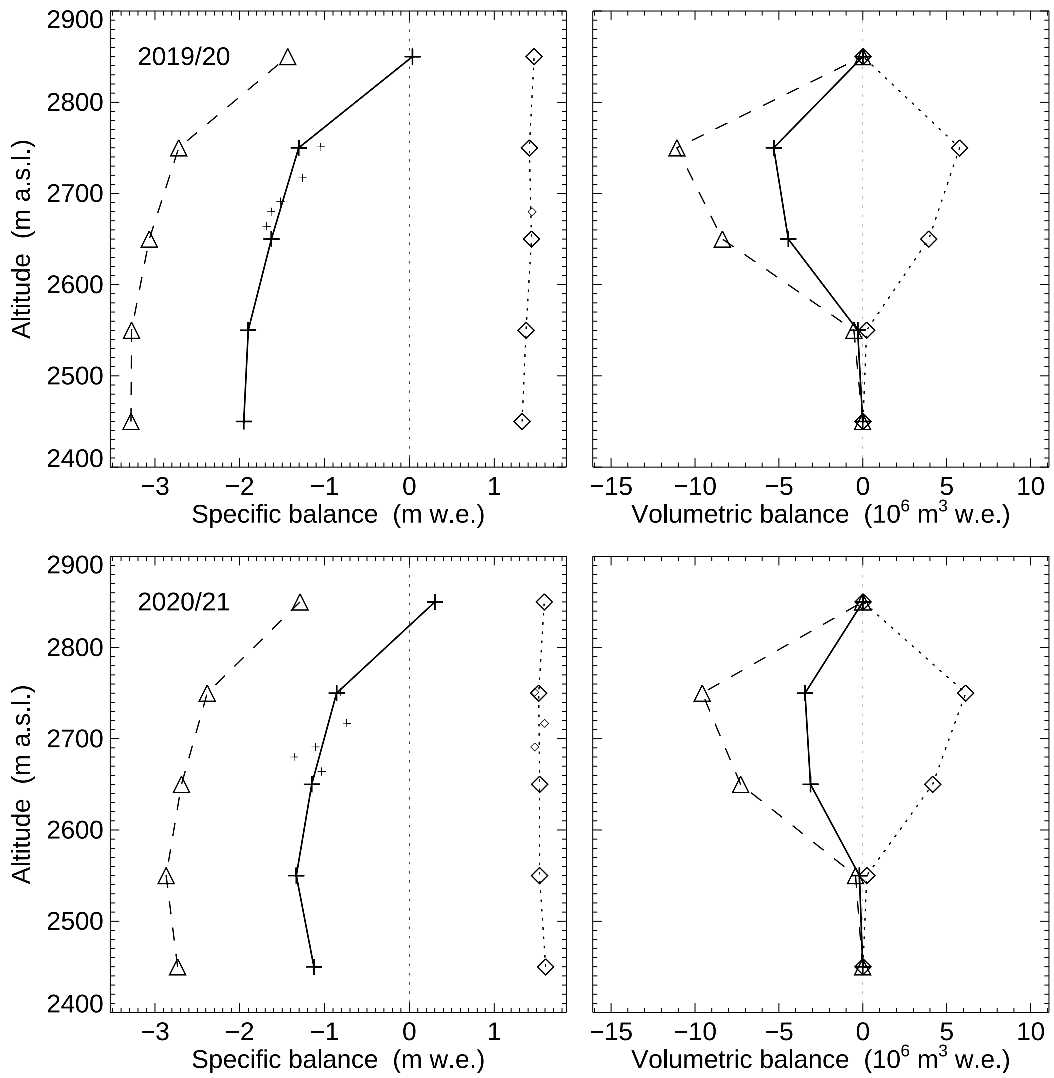

Figure 4.34: Specific (left) and volumetric (right) winter (dotted, ◇), summer (dashed, △) and annual (continuous line, +) balance in elevation bands for 2019/20 (top) and 2020/21 (bottom). Small symbols mark the individual measurements.

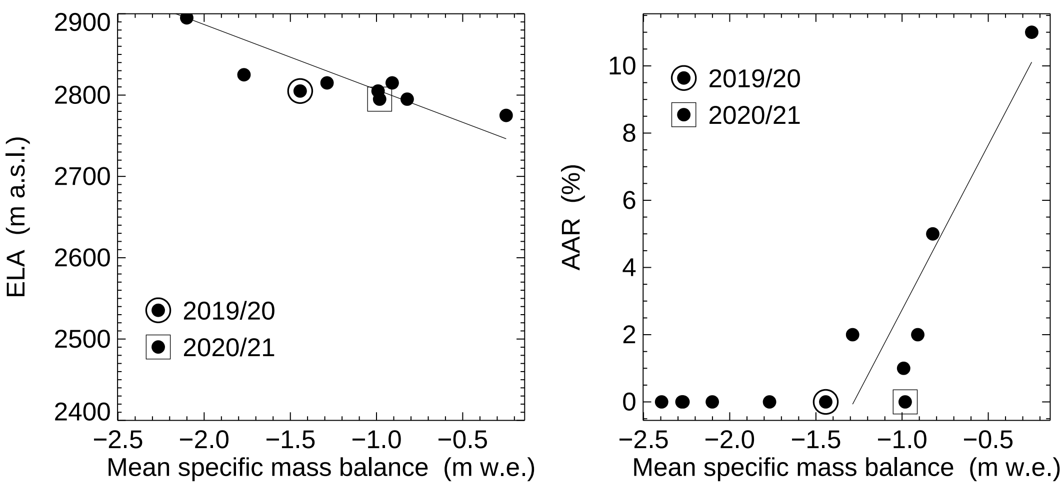

Figure 4.35: Equilibrium line altitude (ELA) and accumulation area ratio (AAR) versus mean specific balance including all previous observations.

4.17 Rhonegletscher

Introduction

Rhonegletscher is a temperate valley glacier located in the central Swiss Alps, and is the source of the Rhone river. The glacier is easily accessible and therefore has been under observation since the 19th century. The total surface area of the glacier is 15.2 km^2 flowing in a southern direction from 3600 m a.s.l. down to 2200 m a.s.l. The first mass balance measurements were carried out in 1884 and are the first such observations worldwide. After two periods of measurements between 1884-1910, and 1980-1982, the mass balance monitoring was resumed in 2006. Determination of volumetric changes in decadal resolution extends even further back to 1874 (Bauder et al., 2007).

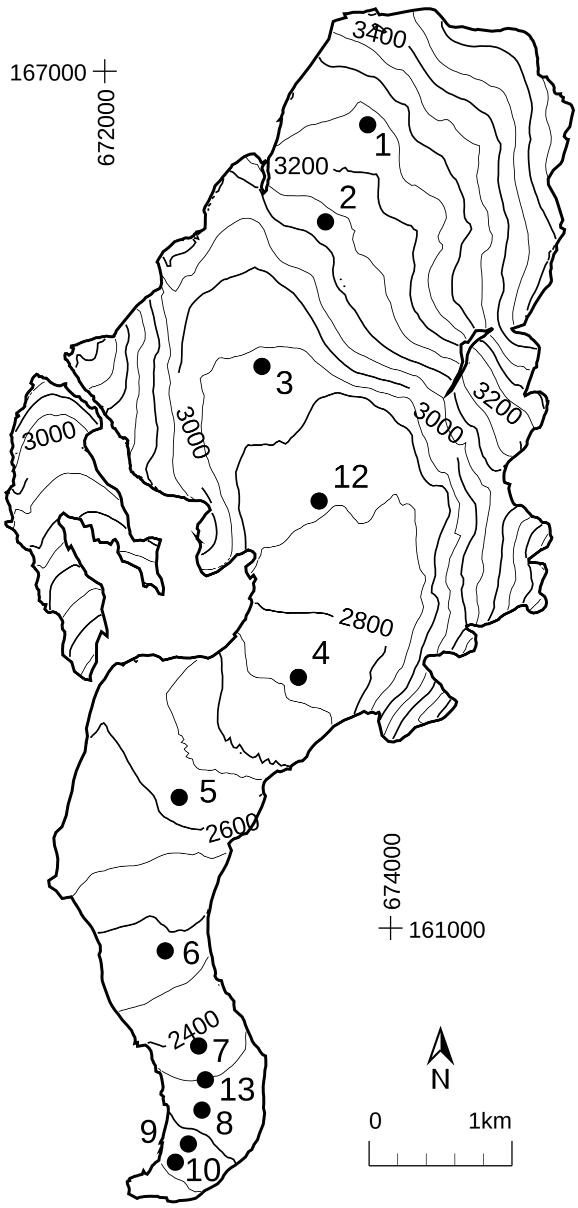

Figure 4.36: Surface topography and observational network of Rhonegletscher.

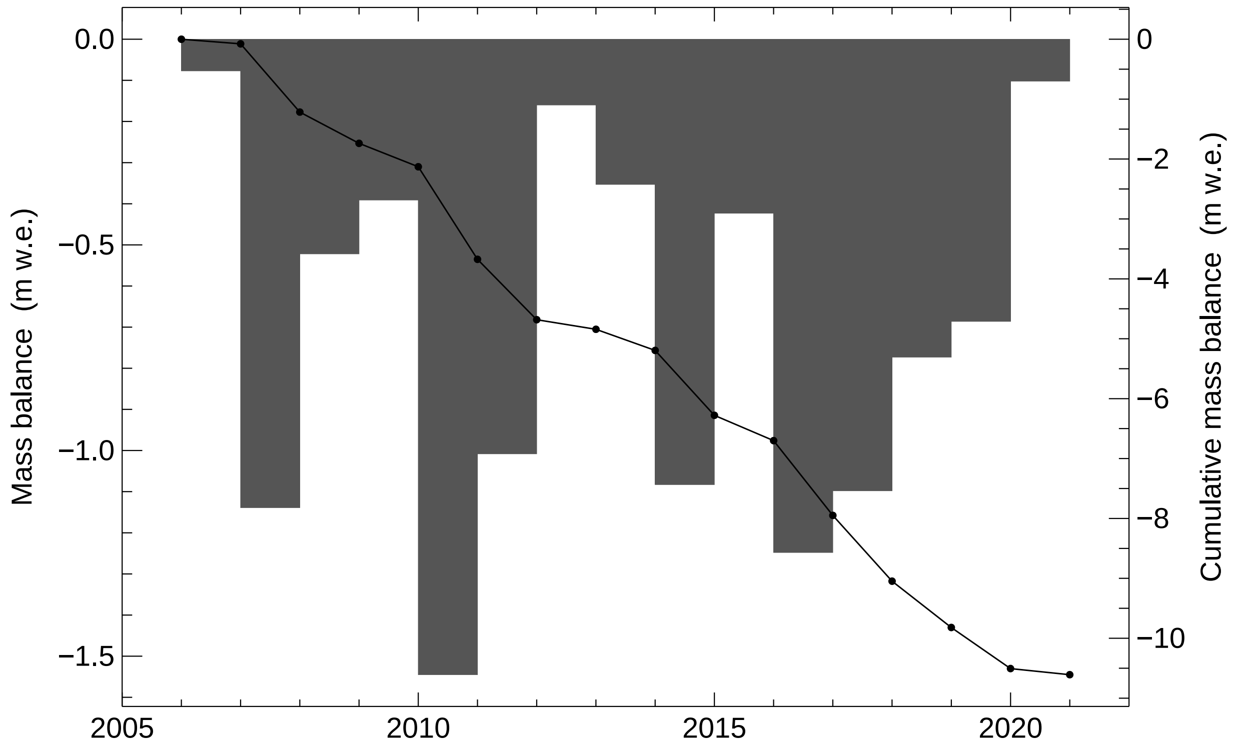

Figure 4.37: Rhonegletscher - Mean specific annual balance (bars) and cumulative mass balance (line) for the period 2006-2021.

Topographic maps or photogrammetrical surveys exist for 1874, 1929, 1959, 1980, 1991, 2000, and 2007 and annually for the glacier tongue below 2700 m a.s.l. since 2012. Further details on observations of ice flow velocities are presented in Section 5.7.

Investigations in 2019/20

The spring survey for the determination of winter mass balance was performed on 24th April 2020. Due to the lock-down related to the global pandemic, a reduced survey was carried out. A total of 273 snow probings distributed over the entire area of Rhonegletscher were obtained. The density was measured at the three sites 1, 3 and 13 based on coring resulting values of 540 ± 2 kg m^{-3}, 510 ± 18 kg m^{-3} and 470 ± 20 kg m^{-3}, respectively. The ablation area was repeatedly visited in July and August for additional intermediate stake readings during the melting season. On 11th September 2020 all measurement sites were visited for the determination of the annual mass balance. Density was measured using a core drill at sites 1, 2 and 3 and revealed 580 ± 5 kg m^{-3}, 515 ± 10 kg m^{-3} and 535 ± 10 kg m^{-3}. Net accumulation was found only above 2900 m a.s.l. but with many exposed bumps that show complete melt-out even above.

Investigations in 2020/21

The winter mass balance was determined on 21st April 2021. Snow depth soundings were performed at 330 locations including all measurement sites. A snow density of 502 ± 8 kg m^{-3} an

Table 4.27: Rhonegletscher - Individual stake measurements of winter and annual balance.

Stake	Period Start	Spring	End	Coordinates (m / m / m a.s.l.)	Mass balance b_w (mm w.e.)	b_a
01	12.09.2019	24.04.2020	11.09.2020	673815 / 166615 / 3230	2559	1015
02	12.09.2019	24.04.2020	11.09.2020	673499 / 165900 / 3106	1902	355
03	12.09.2019	24.04.2020	11.09.2020	673099 / 164928 / 2924	1978	214
04	12.09.2019	24.04.2020	11.09.2020	673345 / 162774 / 2739	1515	−1746
05	12.09.2019	24.04.2020	11.09.2020	672521 / 161919 / 2594	498	−4833
06	12.09.2019	24.04.2020	11.09.2020	672421 / 160843 / 2454	488	−6066
07	12.09.2019	24.04.2020	11.09.2020	672659 / 160175 / 2341	479	−7056
08	12.09.2019	24.04.2020	11.09.2020	672680 / 159723 / 2274	742	−5949
09	12.09.2019	24.04.2020	11.09.2020	672608 / 159501 / 2222	761	−6822
12	12.09.2019	24.04.2020	11.09.2020	673511 / 163951 / 2834	1846	−1206
13	12.09.2019	24.04.2020	11.09.2020	672701 / 159939 / 2301	582	−6237
01	11.09.2020	21.04.2021	08.09.2021	673815 / 166615 / 3233	2570	2040
02	11.09.2020	21.04.2021	08.09.2021	673490 / 165892 / 3102	2329	1056
03	11.09.2020	21.04.2021	08.09.2021	673103 / 164914 / 2921	2204	892
04	11.09.2020	21.04.2021	08.09.2021	673348 / 162772 / 2737	1702	−954
05	11.09.2020	21.04.2021	08.09.2021	672518 / 161923 / 2592	943	−3465
06	11.09.2020	21.04.2021	08.09.2021	672417 / 160844 / 2450	684	−4356
07	11.09.2020	21.04.2021	08.09.2021	672657 / 160174 / 2335	667	−5130
08	11.09.2020	21.04.2021	08.09.2021	672676 / 159724 / 2267	1084	−4617
09	11.09.2020	21.04.2021	08.09.2021	672625 / 159568 / 2227	1448	−4860
12	11.09.2020	21.04.2021	08.09.2021	673496 / 163987 / 2836	2053	−260
13	11.09.2020	21.04.2021	08.09.2021	672705 / 159937 / 2294	737	−5193

439 ± 7 kg m^{-3} was measured by coring at the two sites 3 and 13. In addition, a ground penetrating radar was operated on a longitudinal transect for a continuous snow depth survey between stakes 1 and 13. Measurements at 11 stakes for annual mass balance were carried out on 8th September 2021. Density measurements were performed at the topmost three sites and yielded a value of 595 ± 5 kg m^{-3}, 551 ± 10 kg m^{-3} and 563 ± 10 kg m^{-3}, repectively. Summer melt out reached about 2850 m a.s.l. to site 12, but the snowline was significantly higher locally in more wind-exposed regions. Additional intermediate stake readings were obtained during the melting season as well as after the fall campaign in mid of October 2021.

Table 4.28: Rhonegletscher - Specific winter (b_w) and annual (b_a) balance according to elevation bands for the two periods 2019/20 and 2020/21. Results refer to the measurement period, defined by the dates of the field survey.

Altitude	2019/20			2020/21		
	Area	$\overline{b_w}$	$\overline{b_a}$	Area	$\overline{b_w}$	$\overline{b_a}$
(m a.s.l.)	(km^2)	(mm w.e.)	(mm w.e.)	(km^2)	(mm w.e.)	(mm w.e.)
2200 - 2300	0.340	-22	−7778	0.340	649	−4863
2300 - 2400	0.329	50	−6090	0.329	514	−4977
2400 - 2500	0.617	380	−4673	0.617	955	−3837
2500 - 2600	1.031	459	−4447	1.031	1044	−3294
2600 - 2700	0.712	740	−3696	0.712	1247	−2652
2700 - 2800	1.068	1508	−1742	1.068	1786	−1168
2800 - 2900	2.255	2035	−354	2.255	2178	−18
2900 - 3000	1.874	2180	317	1.874	2309	798
3000 - 3100	1.817	2188	543	1.817	2273	1017
3100 - 3200	1.535	2245	740	1.535	2352	1173
3200 - 3300	1.468	2327	1128	1.468	2379	1473
3300 - 3400	0.968	2243	1244	0.968	2287	1627
3400 - 3500	0.781	2173	1362	0.781	2125	1644
3500 - 3600	0.376	1690	927	0.376	1781	1357
3600 - 3700	0.003	1126	383	0.003	1408	1127
2200 - 3700	15.174	1771	−686	15.174	1968	−102

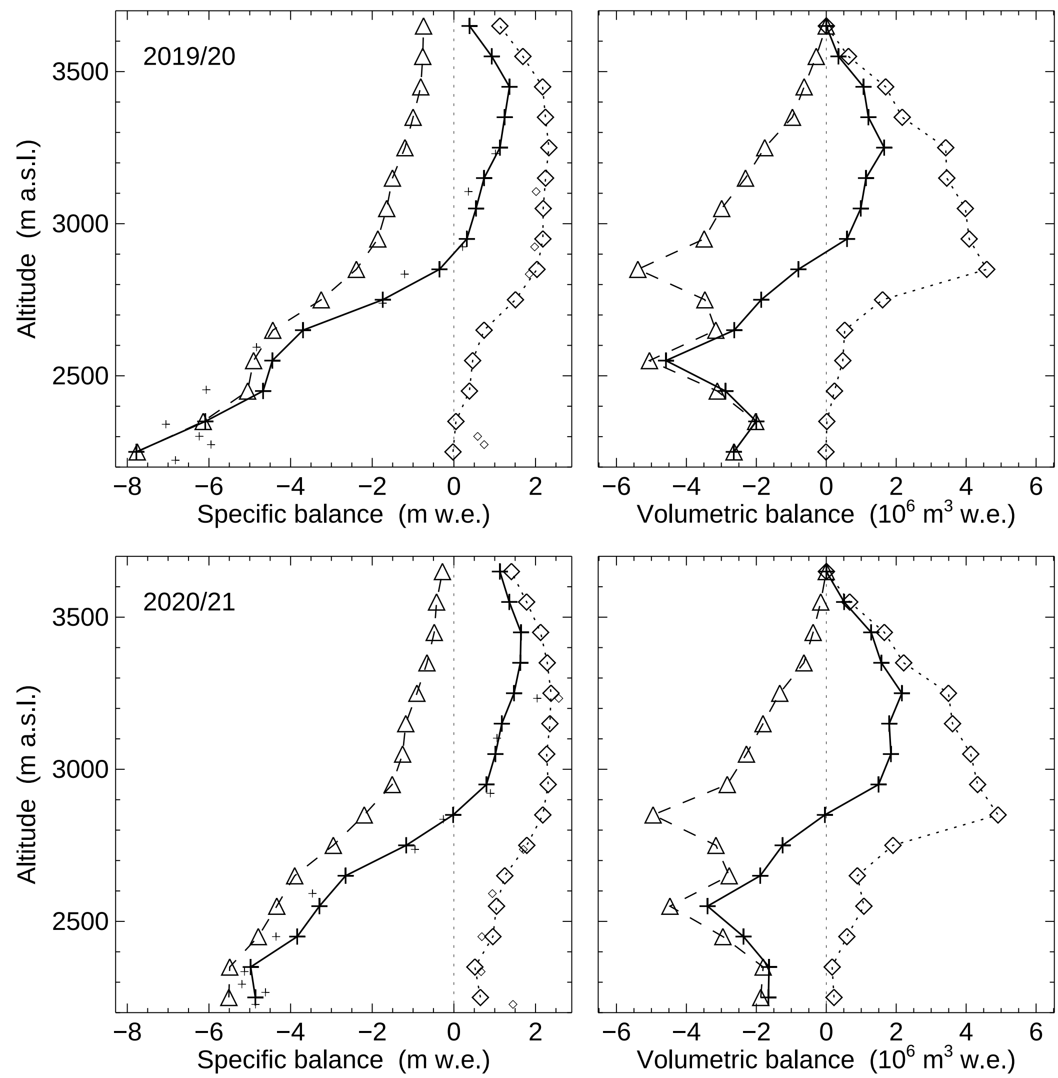

Figure 4.38: Specific (left) and volumetric (right) winter (dotted, ◇), summer (dashed, △) and annual (continuous line, +) balance in elevation bands for 2019/20 (top) and 2020/21 (bottom). Small symbols mark the individual measurements.

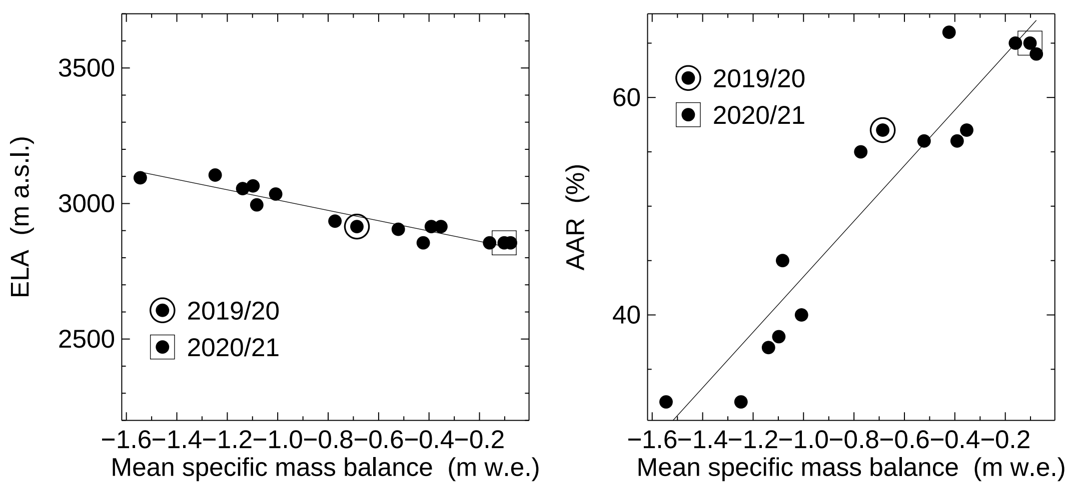

Figure 4.39: Equilibrium line altitude (ELA) and accumulation area ratio (AAR) versus mean specific balance including all previous observations.

4.18 Sankt Annafirn

Introduction

Sankt Annafirn is a north-facing cirque glacier in the central Swiss Alps protected by steep rock-walls connecting Sankt Annahorn (2937 m a.s.l.) with Chastelhorn (2973 m a.s.l.). The glacier covers an area of currently 0.14 km^2. Investigations of the glacier mass balance were started in 2012. Since 2013, measurements are also performed on nearby Schwarzbachfirn (0.02 km^2). Both glaciers represent the size class of glacierets and deliver direct observations of seasonal glacier mass change in the hydrological catchment of the Reuss. Because of rapid disintegration, the network on Schwarzbachfirn is no longer actively maintained, and observations on Sankt Annafirn are increasingly impacted by operations related to the skiing area, as well as effects of fast retreat and rockfall events, and likely will need to be discontinued in the next years.

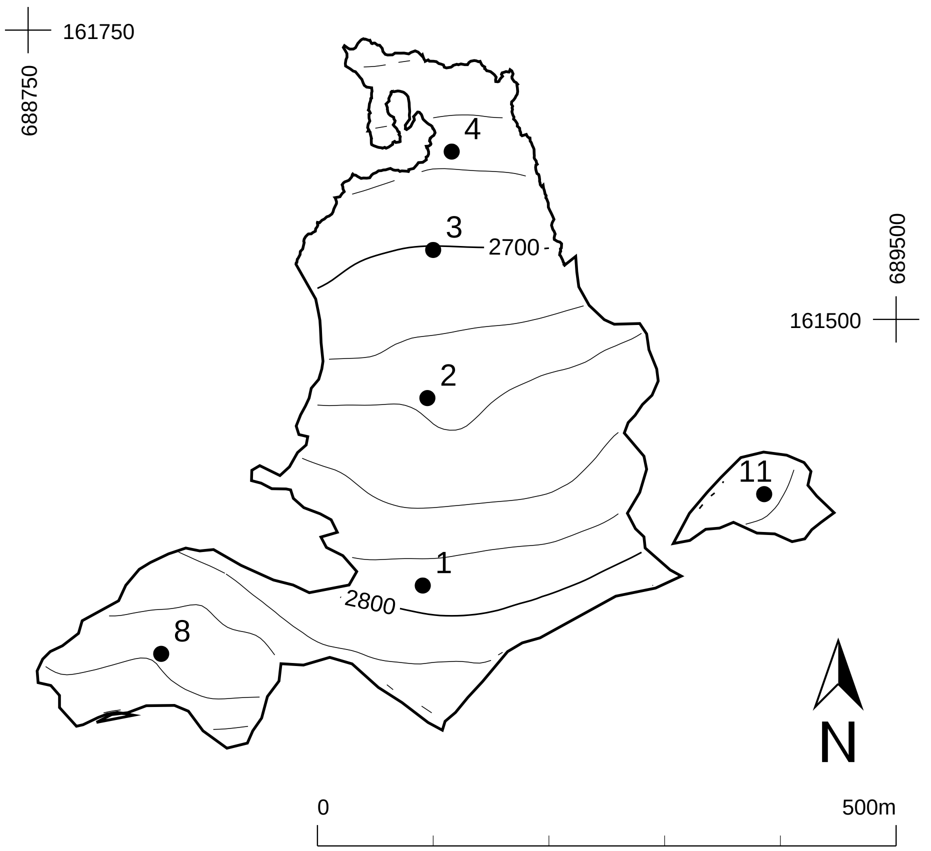

Figure 4.40: Surface topography and observational network of Sankt Annafirn.

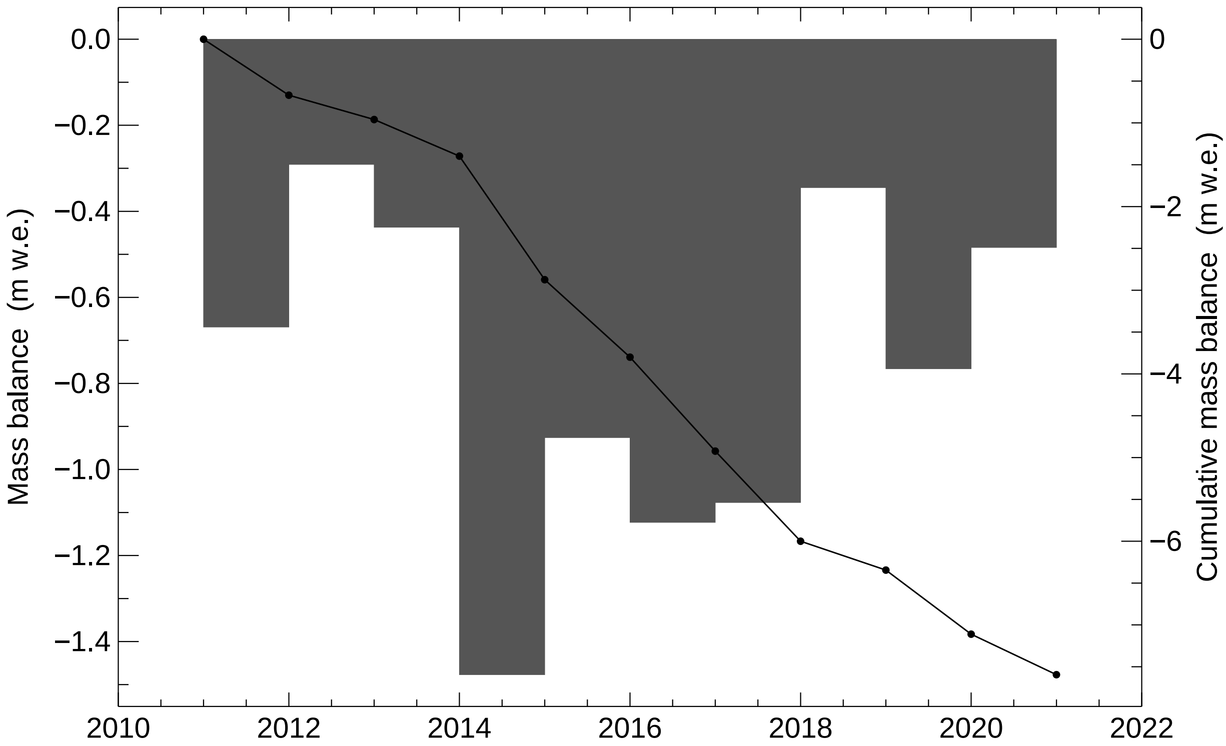

Figure 4.41: Sankt Annafirn - Mean specific annual balance (bars) and cumulative mass balance for the period 2012-2021.

Investigations in 2019/20

Due to the pandemic situation in spring 2020 and shut-down of the cablecar operation no survey of winter snow accumulation was possible on Schwarzbachfirn. On 6th May 2020, however, measurements on Sankt Annafirn were performed. A density of 480 kg m^{-3} was measured based on snow coring at one location. Snow depth was determined using probing at 69 locations. On 17th September 2020, a negative mass balance was measured at all stakes on Sankt Annafirn, and at two stakes on Schwarzbachfirn, and the stake network was maintained.

Table 4.29: Sankt Annafirn - Specific winter (b_w) and annual (b_a) balance according to elevation bands for the two periods 2019/20 and 2020/21. Results refer to the measurement period, defined by the dates of the field survey.

Altitude	2019/20			2020/21		
	Area	$\overline{b_w}$	$\overline{b_a}$	Area	$\overline{b_w}$	$\overline{b_a}$
(m a.s.l.)	(km^2)	(mm w.e.)	(mm w.e.)	(km^2)	(mm w.e.)	(mm w.e.)
2650 - 2700	0.015	1385	−1807	0.014	1303	−1407
2700 - 2750	0.043	1686	−882	0.042	1541	−717
2750 - 2800	0.039	1475	−726	0.039	1755	−346
2800 - 2850	0.034	1383	−487	0.034	1722	−90
2850 - 2900	0.012	1728	12	0.012	1567	−168
2650 - 2900	0.144	1527	−766	0.142	1622	−484

Table 4.30: Sankt Annafirn - Individual stake measurements of winter and annual balance.

Stake	Period Start	Spring	End	Coordinates (m / m / m a.s.l.)	Mass balance b_w (mm w.e.)	b_a
1	19.09.2019	06.05.2020	17.09.2020	689053 / 161221 / 2764	2232	−2160
2	19.09.2019	06.05.2020	17.09.2020	689095 / 161432 / 2707	1560	−909
3	19.09.2019	06.05.2020	17.09.2020	689107 / 161558 / 2663	1872	−1359
4	19.09.2019	06.05.2020	17.09.2020	689115 / 161643 / 2635	1176	−2529
8	19.09.2019	06.05.2020	17.09.2020	688865 / 161221 / 2824	1392	−549
11	19.09.2019		17.09.2020	689386 / 161349 / 2810		−459
1	17.09.2020		14.09.2021	689053 / 161221 / 2764		−702
2	17.09.2020	29.03.2021	14.09.2021	689093 / 161432 / 2702	1580	−774
3	17.09.2020	29.03.2021	14.09.2021	689101 / 161550 / 2666	1680	−936
4	17.09.2020	29.03.2021	14.09.2021	689147 / 161620 / 2635	1080	−2106
8	17.09.2020	29.03.2021	14.09.2021	688847 / 161238 / 2808	1140	−315
11	17.09.2020	29.03.2021	14.09.2021	689386 / 161349 / 2810	1860	50

Glacier du Ferpècle in November 2020 after the tongue disconnected in a steep section and separated the debris covered former snout from the glacier in summer 2020 (Photo: F. Fellay)

Investigations in 2020/21

End-of-winter snow depth was measured at 76 locations on Sankt Annafirn, and at 21 locations on Schwarzbachfirn on 29th March 2021 but no snow density measurements were performed. The late summer field survey was conducted on 14th September 2021. As melt rates were relatively limited in comparison to previous years, no maintenance of the stake network was necessary. Nevertheless, both stakes on Schwarzbachfirn, and five of the six stakes on Sankt Annafirn showed a negative mass balance, whereas one stake had a balanced mass budget. Due to rapid retreat of the glacier terminus into a steep and shallow zone, the lowermost ablation stake had to be abandoned.

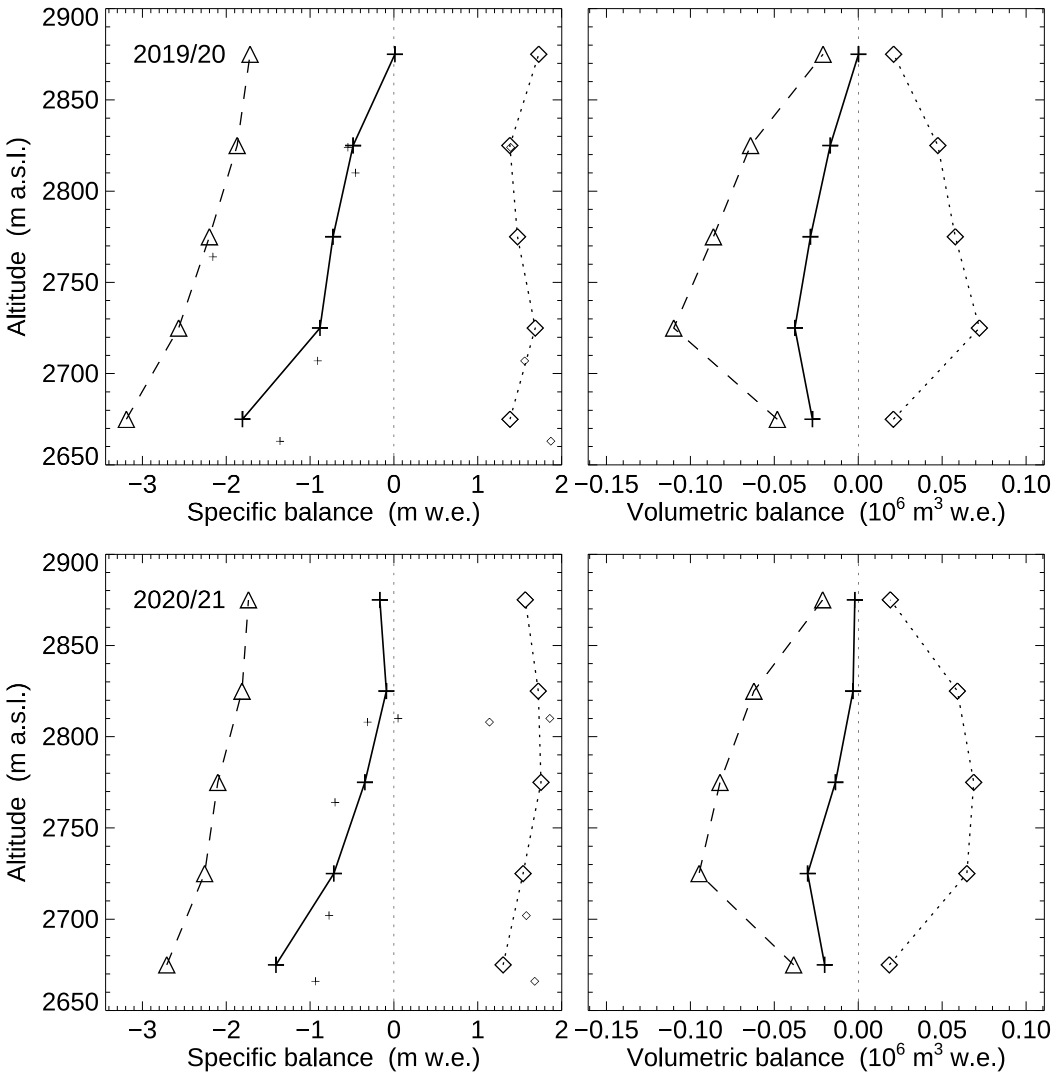

Figure 4.42: Specific (left) and volumetric (right) winter (dotted, ⋄), summer (dashed, △) and annual (continuous line, +) balance in elevation bands for 2019/20 (top) and 2020/21 (bottom). Small symbols mark the individual measurements.

4.19 Schwarzberggletscher

Introduction

Schwarzberggletscher is a temperate mid-sized mountain glacier located in the Mattmark area in the Southern Valais Alps. It currently covers an area of 4.9 km^2 flowing in north direction from 3570 m a.s.l. down to 2690 m a.s.l. Mass balance measurements started in 1955 as a part of investigations for the construction of the Mattmark reservoir for hydro-power production (VAW, 1999; Antoni, 2005). Initially a network of seven stakes distributed over the entire area was maintained for mass balance and ice flow measurements (see Chapter 5). After 1967 measurements were continued at only four sites. Presently, annual observations at three sites are maintained. Collected data of point mass balance and geodetic ice volume changes since 1955 have been re-analyzed and homogenized (Huss et al., 2015). The results of the glacier-wide mean specific annual balance for comparable fixed-date periods were presented in Section 4.17 of Volume 135/136. Further details on long-term observations of ice flow velocities are in Section 5.8.

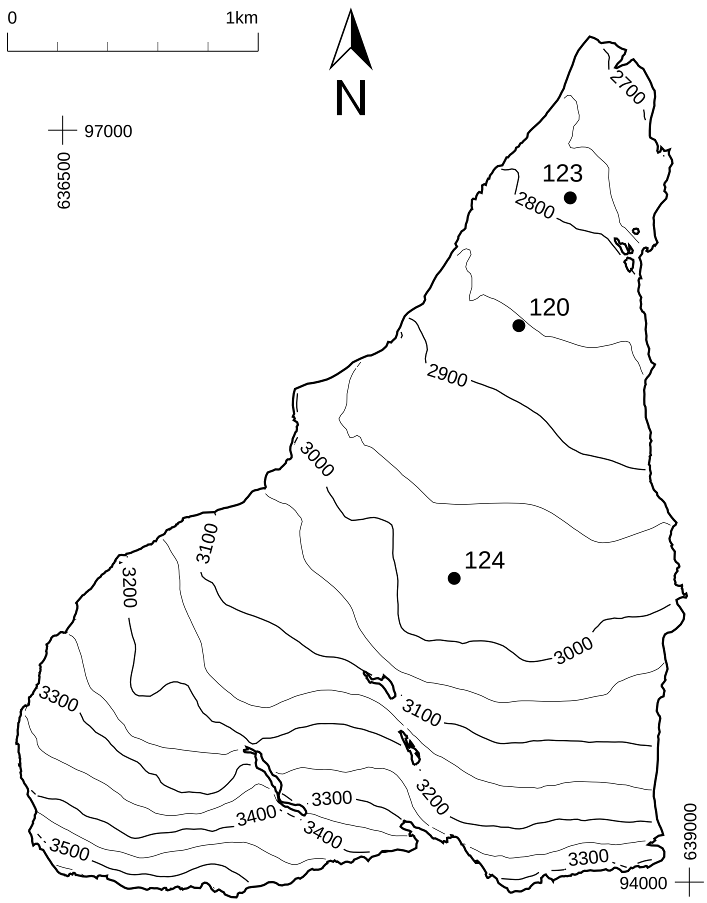

Figure 4.43: Surface topography and observational network of Schwarzberggletscher.

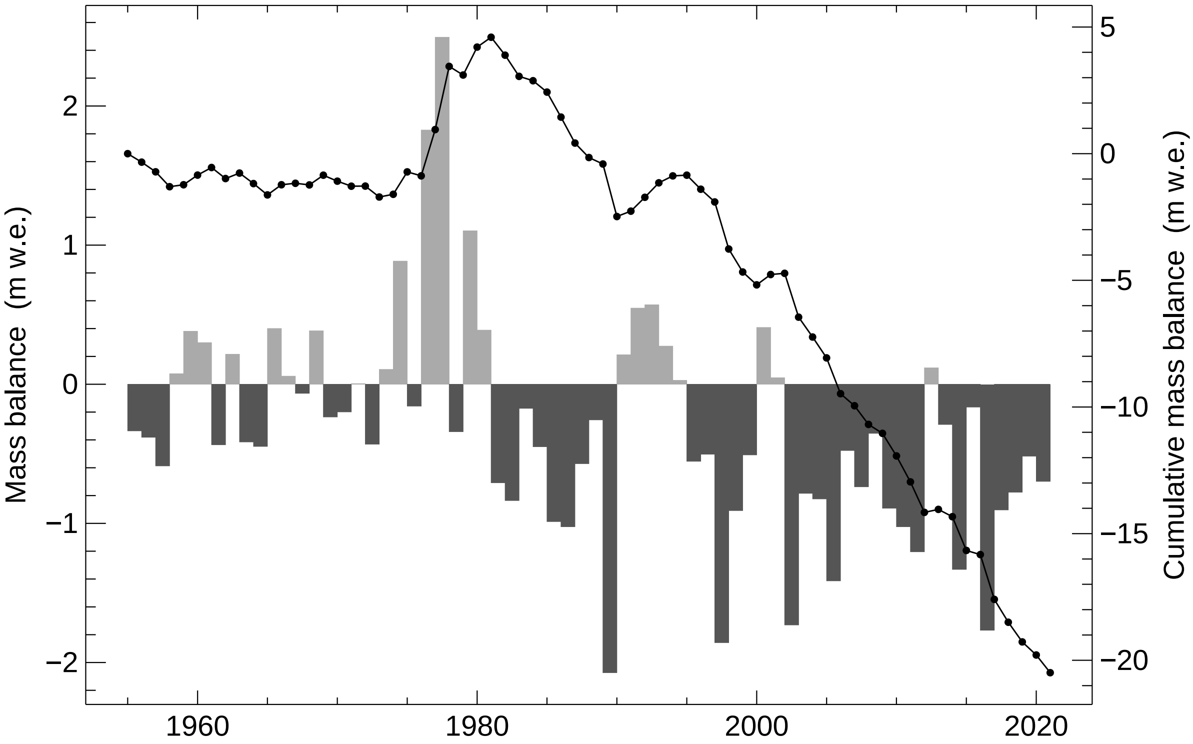

Figure 4.44: Schwarzberggletscher - Mean specific annual balance (bars) and cumulative mass balance for the period 1955-2021. Values refer to the measurement period.

Investigations in 2019/20 and 2020/21

Annual observations of mass balance with maintenance of the stake network were carried out on 4th September 2020. All three stakes were located and set back to the initial position. Negative local mass balances were measured for all stakes. As the glacier was covered with some fresh snow from the previous week, the end-of-summer snowline could not be determined during the field visit. In the second observation period under review, the annual field measurements were carried out on 2nd September 2021. Again, negative local mass balances resulted at all stakes. The transient snowline was located at about 3150 m a.s.l.

Table 4.31: Schwarzberggletscher - Specific winter (b_w) and annual (b_a) balance according to elevation bands for the two periods 2019/20 and 2020/21. Results refer to the measurement period, defined by the dates of the field survey.

Altitude (m a.s.l.)	2019/20 Area (km^2)	$\overline{b_w}$ (mm w.e.)	$\overline{b_a}$ (mm w.e.)	2020/21 Area (km^2)	$\overline{b_w}$ (mm w.e.)	$\overline{b_a}$ (mm w.e.)
2600 - 2700	0.001		−4143	0.001		−3787
2700 - 2800	0.228		−3470	0.228		−3259
2800 - 2900	0.627		−2229	0.627		−2218
2900 - 3000	1.107		−1258	1.107		−1559
3000 - 3100	0.838		−416	0.838		−710
3100 - 3200	0.788		177	0.788		72
3200 - 3300	0.648		703	0.648		541
3300 - 3400	0.367		1110	0.367		872
3400 - 3500	0.229		1404	0.229		1098
3500 - 3600	0.058		1321	0.058		1035
2600 - 3600	4.891		−517	4.891		−698

Table 4.32: Schwarzberggletscher - Individual stake measurements of winter and annual balance.

Stake	Period Start	Spring	End	Coordinates (m / m / m a.s.l.)	Mass balance b_w (mm w.e.)	b_a (mm w.e.)
120	30.08.2019		04.09.2020	638319 / 96219 / 2842		−2223
123	30.08.2019		04.09.2020	638525 / 96726 / 2759		−3141
124	30.08.2019		04.09.2020	638061 / 95211 / 2978		−1179
120	04.09.2020		02.09.2021	638319 / 96220 / 2840		−2214
123	04.09.2020		02.09.2021	638525 / 96728 / 2756		−2988
124	04.09.2020		02.09.2021	638062 / 95211 / 2978		−1557

4.20 Silvrettagletscher

Introduction

Silvrettagletscher is a small temperate mountain glacier located in the north-eastern part of Switzerland in the Silvretta massif at the border to Austria. The present surface area is 2.5 km^2, extending from 3080 m a.s.l. down to 2470 m a.s.l. First mass balance measurements date back to the 1910s (Firnberichte, 1914–1978). Seasonal observations at two stakes were conducted until 1959, when the stake network was increased to about 40 stakes. Huss and Bauder (2009) compiled and homogenized all existing measurements of stake 5 to obtain a continuous time series of seasonal point mass balance for the period 1914 to 2007 (see Section 4.10 in Volume 127/128). Determination of volumetric changes in decadal resolution extends even further back to 1892 (Bauder et al., 2007). Topographic maps and photogrammetrical surveys exist for 1892, 1938, 1959, 1973, 1986, 1994, 2003, 2007, 2012 and every year since then. Huss et al. (2009) reanalyzed and homogenized the seasonal point mass balance data and geodetic ice volume changes for the period 1959 to 2007 to derive glacier wide mass balances. An update for the period 1918 to 2015 with corresponding values of the mean specific winter and annual balance for comparable fixed-date periods was presented in Section 4.17 of Volume 135/136. Further details on observations of ice flow velocities are presented in Section 5.9.

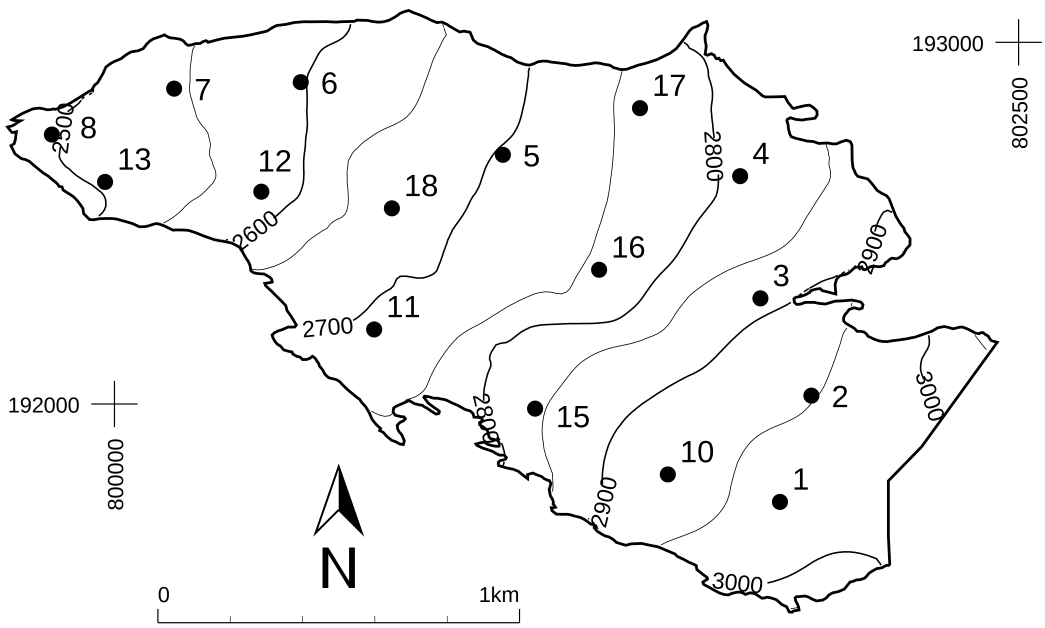

Figure 4.45: Surface topography and observational network of Silvrettagletscher.

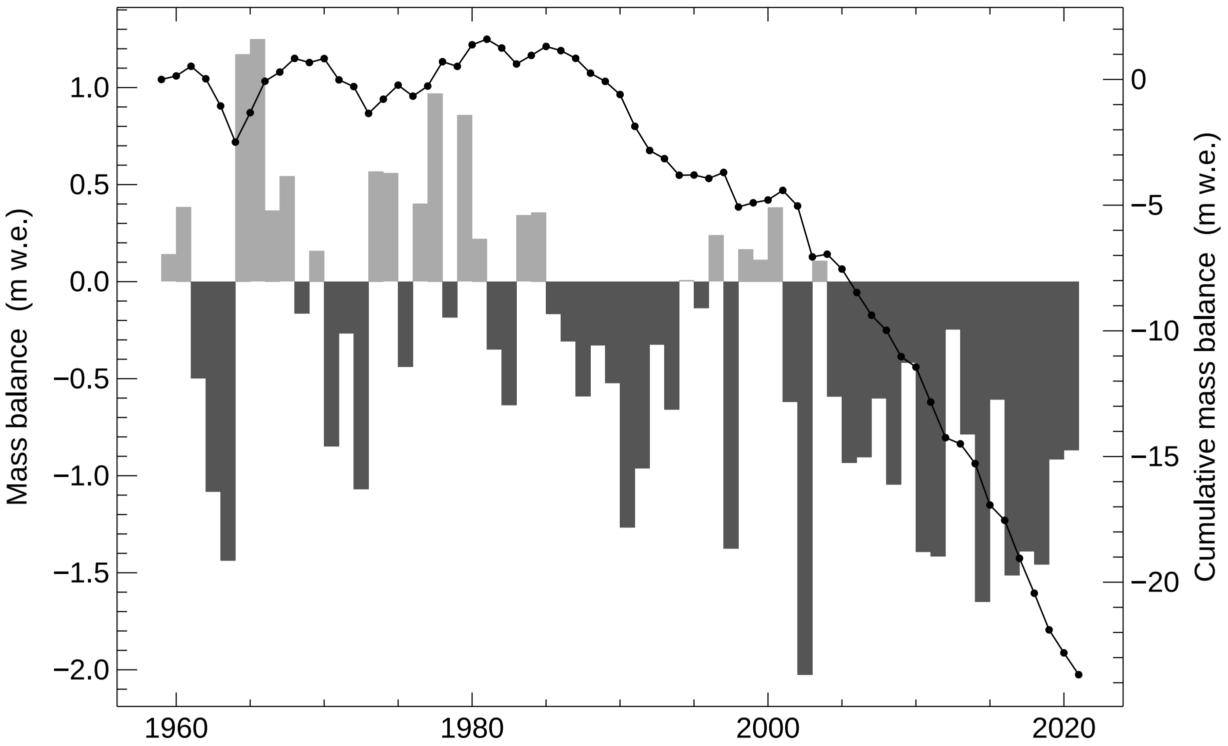

Figure 4.46: Silvrettagletscher - Mean specific annual balance (bars) and cumulative mass balance (line) for the period 1959-2021.

Investigations in 2019/20

Field measurements of winter mass balance were conducted on 4th May 2020. Snow depth probings were taken at 174 locations including all sites in the observational network. Density profiles using a core drill method were acquired at the sites 2, 4 and 7 ranging between 416 and 437 kg m^{-3}. The glacier remained completely snow-covered until mid-June 2020. During the melting season intermediate readings of the stakes were taken in mid-July, beginning and end of August. Observations of mass balance in the fall with maintenance of the stake network were carried out on 13th and 14th September 2020. Depletion of the winter snow extended to almost the entire area and only a marginal accumulation at highest or sheltered areas and in depressions was left. No measurement of firn density was possible. At all but four stakes a negative balance was registered while two stakes showed balanced conditions and at another two stakes minor accumulation was found. Measurements at 16 stakes were available for the determination of the annual mass balance. An additional melt of 200 mm to 450 mm w.e. occured after the fall campaign until melt was shut off by the formation of the winter snow cover after 25th September 2020. Daily pictures from a time lapse camera taken from end of June until early November document progressive melt-out and snowfall events during and after the summer season.

Table 4.33: Silvrettagletscher - Specific winter (b_w) and annual (b_a) balance according to elevation bands for the two periods 2019/20 and 2020/21. Results refer to the measurement period, defined by the dates of the field survey.

Altitude	2019/20			2020/21		
	Area	$\overline{b_w}$	$\overline{b_a}$	Area	$\overline{b_w}$	$\overline{b_a}$
(m a.s.l.)	(km^2)	(mm w.e.)	(mm w.e.)	(km^2)	(mm w.e.)	(mm w.e.)
2400 - 2500	0.030	936	−3524	0.024	1118	−3054
2500 - 2600	0.324	1121	−2823	0.319	1292	−2310
2600 - 2700	0.409	1337	−1542	0.407	1397	−1588
2700 - 2800	0.583	1453	−886	0.578	1493	−879
2800 - 2900	0.501	1532	−328	0.480	1641	−276
2900 - 3000	0.554	1493	103	0.522	1673	39
3000 - 3100	0.084	1279	−8	0.058	1422	62
2400 - 3100	2.485	1403	−915	2.389	1513	−868

Investigations in 2020/21

The spring survey to evaluate the winter mass balance was performed on 4th May 2021. Snow depth probings were collected at 198 locations distributed over the entire glacier surface. An mean snow depth of 333 cm was found. Snow density was determined at the same two locations as in the previous period using a core drill. A density of 417 kg m^{-3} at 2550 m a.s.l., 422 kg m^{-3} at 2830 and 462 kg m^{-3} at 2950 m a.s.l. was determined, respectively. First bare-ice patches on the glacier were only observed in the first half of July. Three visits during the melt season were carried out in June, July and August for intermediate readings of stakes on the glacier tongue. The late-summer field survey took place on 17th and 18th September 2021. A larger than unusual area with accumulation of winter snow was observed. A density of 553 ± 1 kg m^{-3} was measured at stake 2. At three stakes a postive annual mass balance was found while a negative mass balance was determined for 13 stakes. After a snow fall event on 6th October 2021 the glacier remained snow-covered. Additional stake readings three days earlier revealed an additional melt between 350 mm w.e. at the lowest site and 30 mm w.e. at 2800 m a.s.l. The investigations are again supplemented by the operation of a time lapse camera between the end of June and early November 2021.

Table 4.34: Silvrettagletscher - Individual stake measurements of winter and annual balance.

Stake	Start	Period Spring	End	Coordinates (m / m / m a.s.l.)	Mass balance b_w (mm w.e.)	b_a
01	21.09.2019	04.05.2020	13.09.2020	801840 / 191729 / 2972	1303	−8
02	21.09.2019	04.05.2020	13.09.2020	801927 / 192023 / 2947	1460	280
03	21.09.2019	04.05.2020	13.09.2020	801786 / 192292 / 2885	1739	440
04	20.09.2019	04.05.2020	13.09.2020	801724 / 192634 / 2809	1348	−720
05	20.09.2019	04.05.2020	13.09.2020	801071 / 192691 / 2704	1361	−1161
06	20.09.2019	04.05.2020	13.09.2020	800515 / 192892 / 2600	1116	−2394
07	20.09.2019	04.05.2020	13.09.2020	800165 / 192872 / 2547	1183	−2529
08	20.09.2019	04.05.2020	13.09.2020	799827 / 192745 / 2498	1013	−3069
10	21.09.2019	04.05.2020	13.09.2020	801530 / 191805 / 2927	1402	8
11	20.09.2019	04.05.2020	14.09.2020	800718 / 192207 / 2708	1224	−1215
12	20.09.2019	04.05.2020	14.09.2020	800406 / 192587 / 2574	1309	−2259
13	20.09.2019	04.05.2020	14.09.2020	799975 / 192614 / 2513	748	−4131
15	20.09.2019	04.05.2020	14.09.2020	801160 / 191988 / 2843	1108	−1287
16	20.09.2019	04.05.2020	14.09.2020	801336 / 192374 / 2756	1431	−728
17	20.09.2019	04.05.2020	14.09.2020	801457 / 192822 / 2765	1386	−1143
18	20.09.2019	04.05.2020	14.09.2020	800761 / 192539 / 2675	1245	−1548
01	13.09.2020	04.05.2021	18.09.2021	801838 / 191730 / 2971	1667	50
02	13.09.2020	04.05.2021	18.09.2021	801920 / 192028 / 2946	1690	180
03	13.09.2020	04.05.2021	18.09.2021	801780 / 192299 / 2882	1963	210
04	13.09.2020	04.05.2021	17.09.2021	801727 / 192632 / 2808	1503	−504
05	13.09.2020	04.05.2021	17.09.2021	801072 / 192691 / 2702	1360	−1080
06	13.09.2020	04.05.2021	17.09.2021	800516 / 192889 / 2596	1251	−2430
07	13.09.2020	04.05.2021	17.09.2021	800166 / 192872 / 2542	1297	−2286
08	13.09.2020	04.05.2021	17.09.2021	799827 / 192745 / 2491	1318	−2529
10	13.09.2020	04.05.2021	18.09.2021	801526 / 191807 / 2926	1640	−190
11	14.09.2020	04.05.2021	17.09.2021	800719 / 192205 / 2706	1436	−1341
12	14.09.2020	04.05.2021	17.09.2021	800403 / 192589 / 2568	1432	−2088
13	14.09.2020	04.05.2021	17.09.2021	799979 / 192614 / 2506	1234	−3231
15	14.09.2020	04.05.2021	17.09.2021	801160 / 191989 / 2841	1281	−1197
16	14.09.2020	04.05.2021	17.09.2021	801335 / 192373 / 2755	1912	−180
17	14.09.2020	04.05.2021	17.09.2021	801452 / 192823 / 2763	1499	−855
18	14.09.2020	04.05.2021	17.09.2021	800762 / 192540 / 2671	1373	−1494

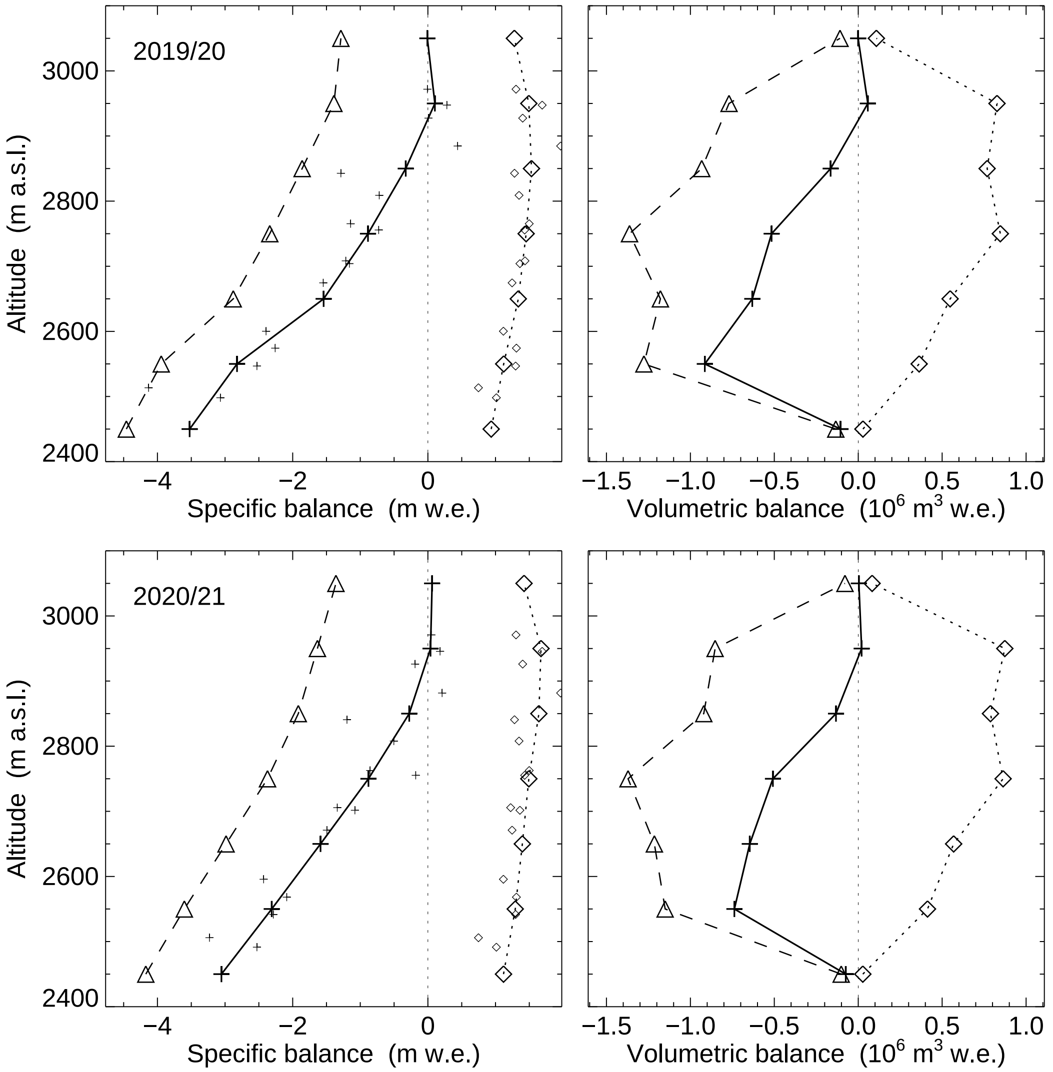

Figure 4.47: Specific (left) and volumetric (right) winter (dotted, ◇), summer (dashed, △) and annual (continuous line, +) balance in elevation bands for 2019/20 (top) and 2020/21 (bottom). Small symbols mark the individual measurements.

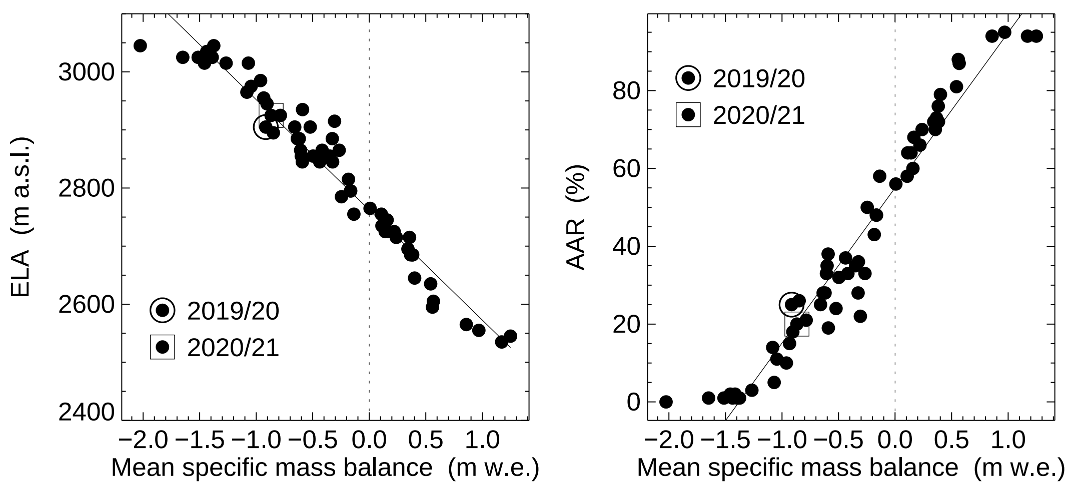

Figure 4.48: Equilibrium line altitude (ELA) and accumulation area ratio (AAR) versus mean specific balance including all previous observations.

4.21 Glacier de Tsanfleuron

Introduction

Glacier de Tsanfleuron is a well-accessible medium-sized glacier at the border between the cantons of Valais, Vaud and Berne. The glacier currently has an area of 2.3 km^2 and exhibits relatively small surface slopes. Glaciological investigations were started in 2009. In addition, measurements are also performed on the very small Glacier du Sex Rouge (0.3 km^2) connected to Tsanfleuron in its accumulation area. This permits comparing the mass balance response of neighbouring glaciers of different size and characteristics.

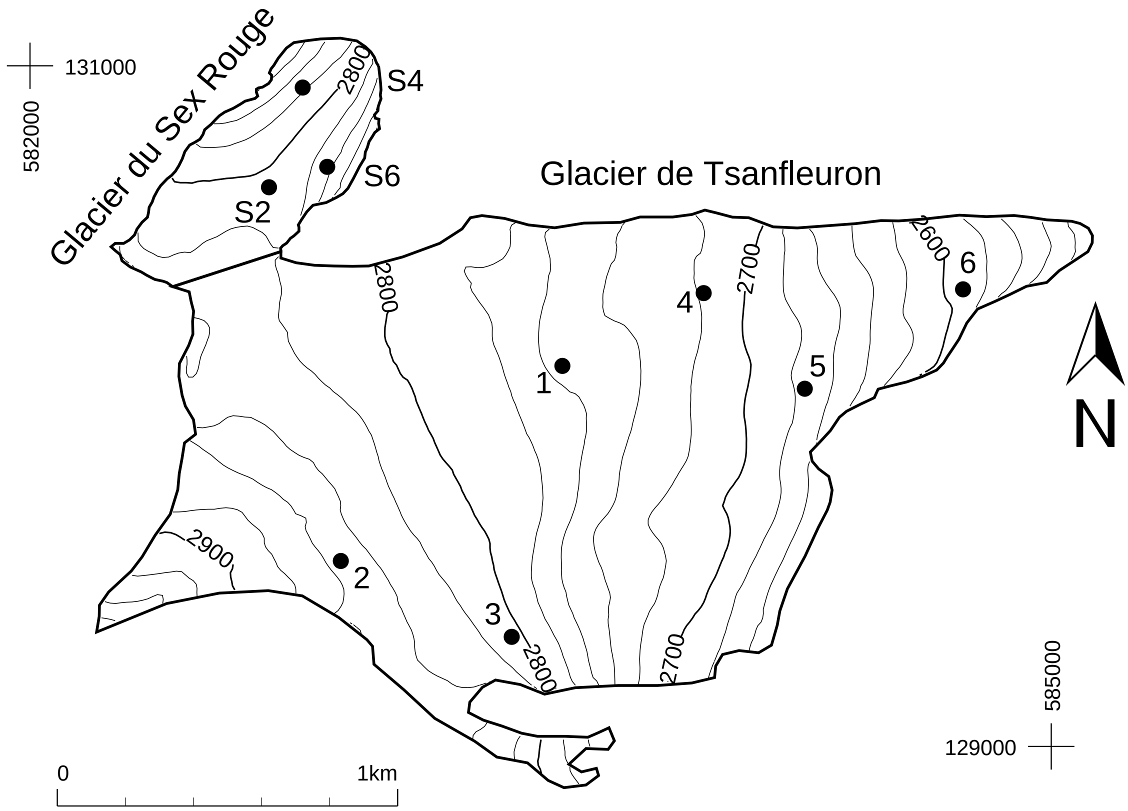

Figure 4.49: Surface topography and observational network of Glacier de Tsanfleuron and Glacier du Sex Rouge.

Investigations in 2019/20

The winter mass balance observations were conducted on 23rd April 2020. A snow density of 470 kg m^{-3} was determined in a snow pit. Snow depth was measured based on 81 snow probings on Glacier de Tsanfleuron and 20 probings on Glacier du Sex Rouge. Stakes were maintained during an intermediate survey on 20th August, as well as during the late summer survey on 19th September 2020. A strongly negative mass balance was measured at all six stakes on Tsanfleuron and three stakes on Sex Rouge.

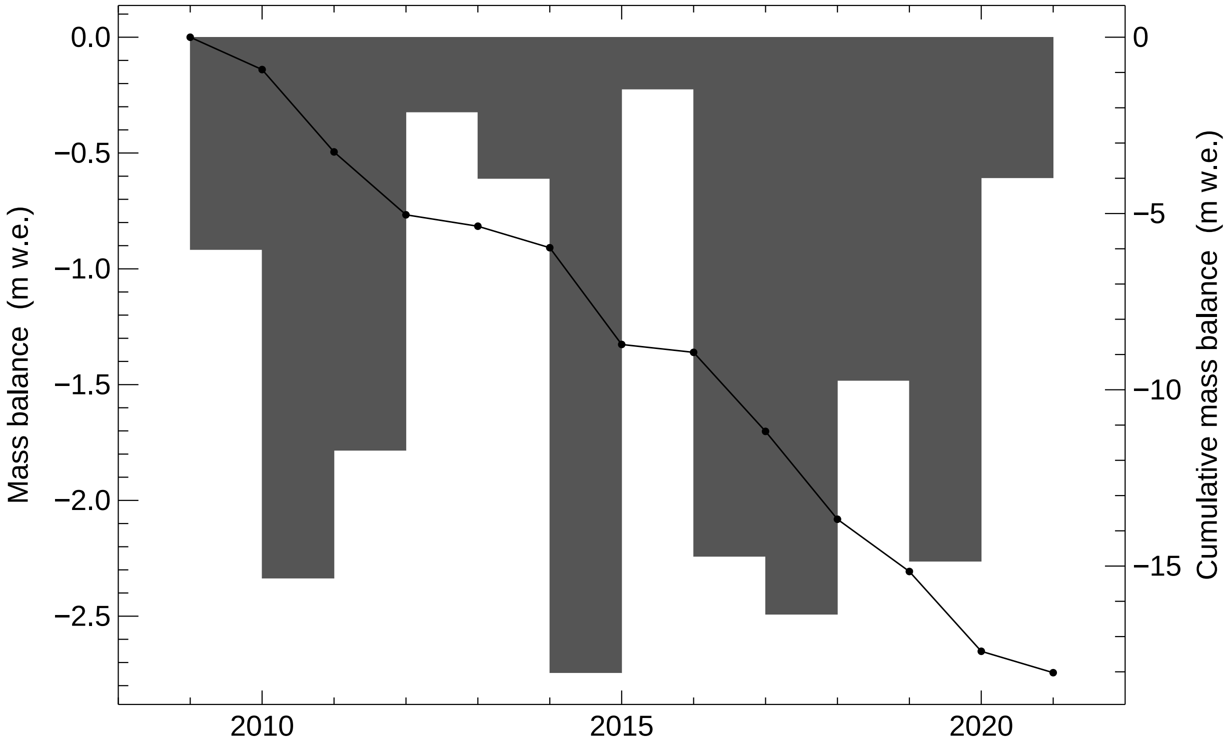

Figure 4.50: Glacier de Tsanfleuron - Mean specific annual balance (bars) and cumulative mass balance for the period 2009-2021.

Table 4.35: Glacier de Tsanfleuron - Specific winter (b_w) and annual (b_a) balance according to elevation bands for the two periods 2019/20 and 2020/21. Results refer to the measurement period, defined by the dates of the field survey.

Altitude	2019/20			2020/21		
	Area	$\overline{b_w}$	$\overline{b_a}$	Area	$\overline{b_w}$	$\overline{b_a}$
(m a.s.l.)	(km^2)	(mm w.e.)	(mm w.e.)	(km^2)	(mm w.e.)	(mm w.e.)
2500 - 2600	0.030	1387	−3619	0.029	1752	−2479
2600 - 2700	0.404	1669	−3327	0.338	1965	−1706
2700 - 2800	1.097	1979	−2210	1.081	2199	−561
2800 - 2900	0.863	1873	−1861	0.827	2044	−205
2900 - 3000	0.057	1772	−1115	0.049	1930	253
2500 - 3000	2.451	1878	−2263	2.324	2098	−607

Investigations in 2020/21

During the winter field survey on 24th April 2021, snow depth was measured based on 45 probings on Glacier du Tsanfleuron, and 26 on Glacier du Sex Rouge. A snow density of 470 $kg\,m^{-3}$ was determined in a snow pit. All stakes were maintained on 12th September, and visited again on 2nd October 2021 after a melt-intense fall. For the first time since 2016, a slightly positive mass balance could be determined at the uppermost site on both Tsanfleuron and Sex Rouge, whereas the other stakes indicated limited to moderate ablation. Related to the operations of the skiing area, geotextiles are placed at some locations on both glaciers to limit the melt rates and to maintain some ski runs. The affected areas are too small, however, to have a recognizable effect on overall glacier mass balance.

Table 4.36: Glacier de Tsanfleuron and Glacier du Sex Rouge - Individual stake measurements of winter and annual balance.

Stake	Period Start	Spring	End	Coordinates (m / m / m a.s.l.)	Mass balance b_w (mm w.e.)	b_a (mm w.e.)
1	15.09.2019	23.04.2020	19.09.2020	583545 / 130149 / 2748	2066	−1692
2	15.09.2019	23.04.2020	19.09.2020	582917 / 129550 / 2844	1948	−1062
3	15.09.2019	23.04.2020	19.09.2020	583422 / 129320 / 2789	2038	−1215
4	15.09.2019	23.04.2020	19.09.2020	583960 / 130341 / 2706	1986	−2358
5	15.09.2019	23.04.2020	19.09.2020	584233 / 130041 / 2662	1606	−3429
6	15.09.2019	23.04.2020	19.09.2020	584707 / 130366 / 2587	1526	−3492
S2	15.09.2019	23.04.2020	19.09.2020	582712 / 130672 / 2791	1659	−1665
S4	15.09.2019	23.04.2020	19.09.2020	582793 / 130937 / 2756	1398	−2007
S6	15.09.2019	23.04.2020	19.09.2020	582875 / 130711 / 2818	1720	−1692
1	19.09.2020	24.04.2021	02.10.2021	583545 / 130149 / 2748	2204	−117
2	19.09.2020	24.04.2021	02.10.2021	582917 / 129550 / 2844	2204	200
3	19.09.2020	24.04.2021	02.10.2021	583422 / 129320 / 2789	2204	−90
4	19.09.2020	24.04.2021	02.10.2021	583960 / 130341 / 2706	2227	−828
5	19.09.2020	24.04.2021	02.10.2021	584233 / 130041 / 2662	1969	−1674
6	19.09.2020	24.04.2021	02.10.2021	584707 / 130376 / 2587	1899	−2394
S2	19.09.2020	23.04.2021	12.09.2021	582712 / 130672 / 2791	1664	−738
S4	19.09.2020	23.04.2021	12.09.2021	582793 / 130937 / 2756	1758	−360
S6	19.09.2020	23.04.2021	12.09.2021	582875 / 130711 / 2818	1946	60

Table 4.37: Glacier du Sex Rouge - Specific winter (b_w) and annual (b_a) balance according to elevation bands for the two periods 2019/20 and 2020/21. Results refer to the measurement period, defined by the dates of the field survey.

Altitude	2019/20			2020/21		
	Area	$\overline{b_w}$	$\overline{b_a}$	Area	$\overline{b_w}$	$\overline{b_a}$
(m a.s.l.)	(km^2)	(mm w.e.)	(mm w.e.)	(km^2)	(mm w.e.)	(mm w.e.)
2700 - 2750	0.004	1447	−2274	0.005	1743	−775
2750 - 2800	0.080	1530	−1938	0.080	1767	−532
2800 - 2850	0.161	1668	−1800	0.161	1809	−507
2850 - 2900	0.011	1811	−894	0.011	1991	403
2700 - 2900	0.256	1627	−1811	0.257	1802	−479

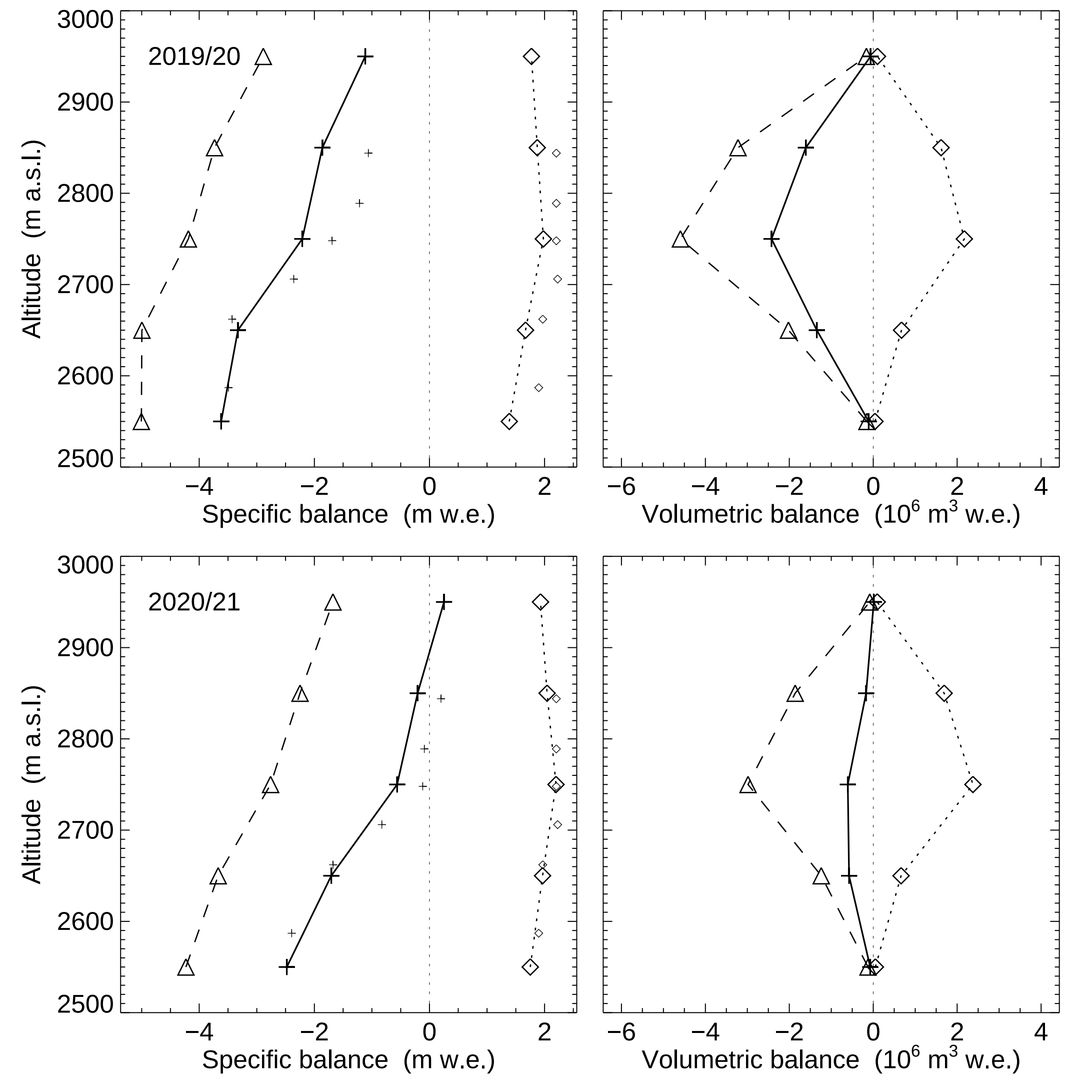

Figure 4.51: Specific (left) and volumetric (right) winter (dotted, ◇), summer (dashed, △) and annual (continuous line, +) balance in elevation bands for 2019/20 (top) and 2020/21 (bottom). Small symbols mark the individual measurements.

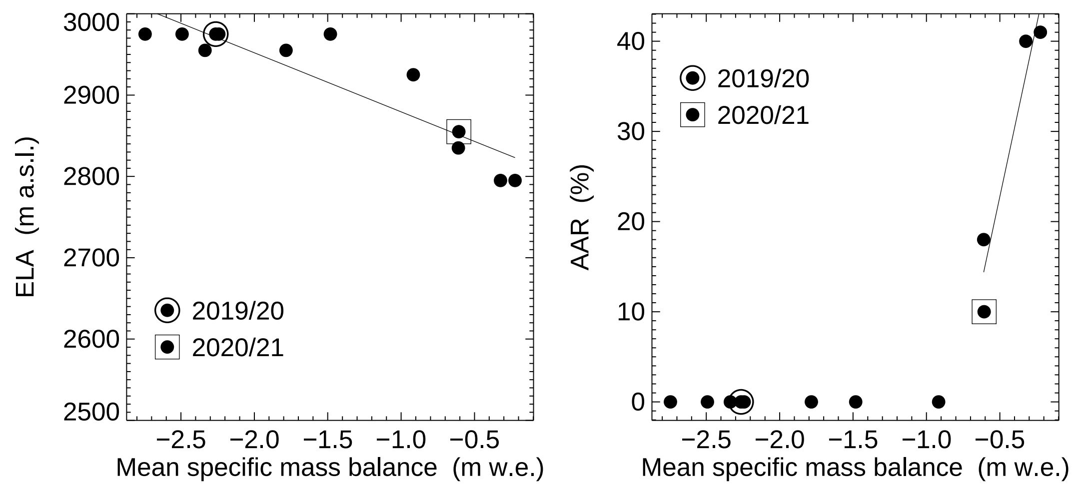

Figure 4.52: Equilibrium line altitude (ELA) and accumulation area ratio (AAR) versus mean specific balance including all previous observations.

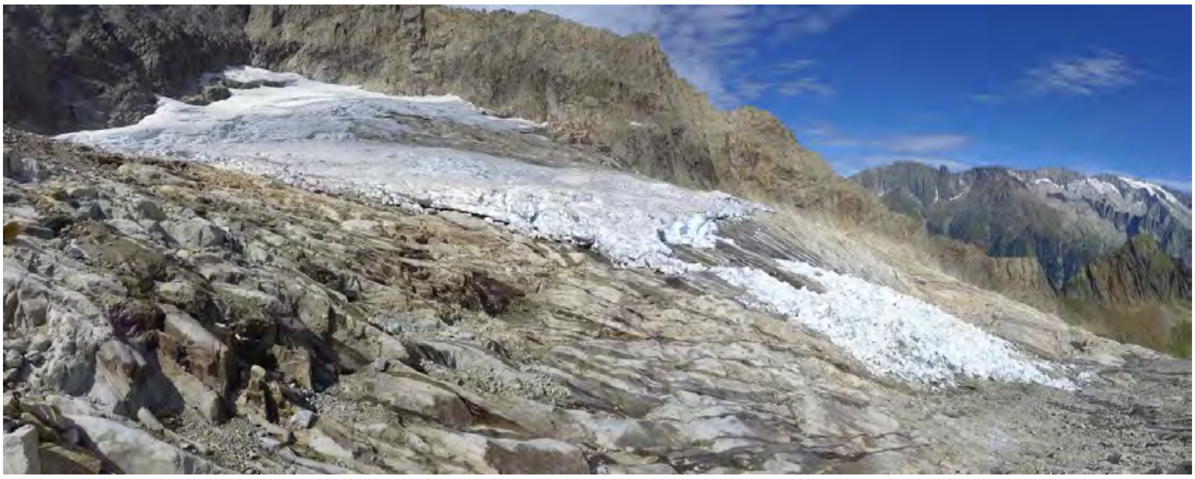

Illustrations for Chapter 7: Ärlengletscher before (top) and after (center) the slope failure in August 2020 (Photos: Kraftwerke Oberhasli); Deposits of a rock fall cover the snout of Steingletscher (bottom) and hamper the measurements for length variations. (Photo: D. Rohrer)

5 Flow Velocity

5.1 Introduction

On eight glaciers (Figure 5.1) long-term investigations for the measurement of local surface ice flow velocity are carried out. These observations are acquired at a network of one to 16 stakes per glacier. Presented numbers are annual velocities for a normalized period of 365 days to allow comparability, while corresponding thickness change is determined directly between successive surveys and is shown cumulatively. The VAW/ETHZ has been contracted by two hydro-electric power companies Kraftwerke Mattmark, and Forces Motrices de Mauvoisin SA to survey the glaciers in the operated catchments. The main objective of these investigations is to observe the ice flow dynamics of the glaciers, particularly with regard to their potential threat to the buildings and the operation of the power station in the valley. The observations are mainly focused on the two glaciers Corbassière and Giétro in the Mauvoisin area (Val de Bagnes), and the three glaciers

Figure 5.1: Investigated glaciers for surface velocity measurements.

Allalin, Hohlaub and Schwarzberg in the Mattmark area (Saastal). Further measurements are acquired related to long-term mass balance programmes (see Chapter 4) on Grosser Aletschgletscher, Rhonegletscher and Silvrettagletscher. Thanks to reduced efforts in surveying using global navigation satellite system (GNSS) technology, positions of stakes used for mass balance observations are available in necessary precision for evaluation of the surface flow velocity.

The debris covered tongue of Langgletscher disintegrated over large parts over the last decade that resulted in a large retreat of the active snout in September 2021 (Photo: H. Henzen)

5.2 Allalingletscher

Introduction

The first ice flow velocity measurements at Allalingletscher date back to 1955 (VAW, 1999). Initially, investigations were carried out at a network of nine stakes with the aim to determine glacier mass balance for planning and construction of the Mattmark reservoir for hydro-power production (VAW, 1999). In 1967 the observation network was re-arranged to the present configuration with a main focus for ice flow measurements. Measurements are currently being continued on seven selected stakes (Figure 4.5) as part of the investigations by VAW/ETHZ for the Mattmark hydro-power company (VAW, 2022). Figure 5.2 shows the horizontal surface flow velocities on Allalingletscher. In addition to ice flow velocity, annual mass balance is measured at the stakes (Table 4.4).

Investigations in 2019/20 and in 2020/21

The field surveys were carried out on 4th September 2018 and on 2nd September 2021. During both field campaigns all seven stakes were located, surveyed and set back to their initial position. The position of the stakes was surveyed using differential GNSS relative to a local reference station. Results for horizontal flow velocity and thickness change are given in Table 5.1.
The ice flow velocity decreased further during the two periods under review. The general long-term trend of decreasing speed accompanied by a lowering of the ice surface was maintained.

Table 5.1: Allalin - Individual measurements of surface flow velocity and thickness change

Stake	Period		Coordinates	Thickness change	Velocity
	Start	End	(m / m / m a.s.l.)	(m)	(m a^{-1})
100	30.08.2019	04.09.2020	636360 / 98710 / 3230	−1.57	32.96
100	04.09.2020	02.09.2021	636360 / 98710 / 3230	−0.55	29.77
101	30.08.2019	04.09.2020	638400 / 99360 / 2850	−1.78	9.98
101	04.09.2020	02.09.2021	638400 / 99360 / 2850	−1.76	8.98
102	30.08.2019	04.09.2020	638350 / 99480 / 2850	−1.76	10.69
102	04.09.2020	02.09.2021	638350 / 99480 / 2850	−1.46	9.76
103	30.08.2019	04.09.2020	638325 / 99575 / 2855	−1.45	11.42
103	04.09.2020	02.09.2021	638325 / 99575 / 2855	−1.73	10.72
104	30.08.2019	04.09.2020	638290 / 99665 / 2865	−1.94	12.00
104	04.09.2020	02.09.2021	638290 / 99665 / 2865	−1.81	10.71
105	30.08.2019	04.09.2020	638260 / 99755 / 2885	−1.67	13.30
105	04.09.2020	02.09.2021	638260 / 99755 / 2885	−1.77	12.10
106	30.08.2019	04.09.2020	637095 / 97810 / 3375	−0.03	2.82
106	04.09.2020	02.09.2021	637095 / 97810 / 3375	−0.34	3.00

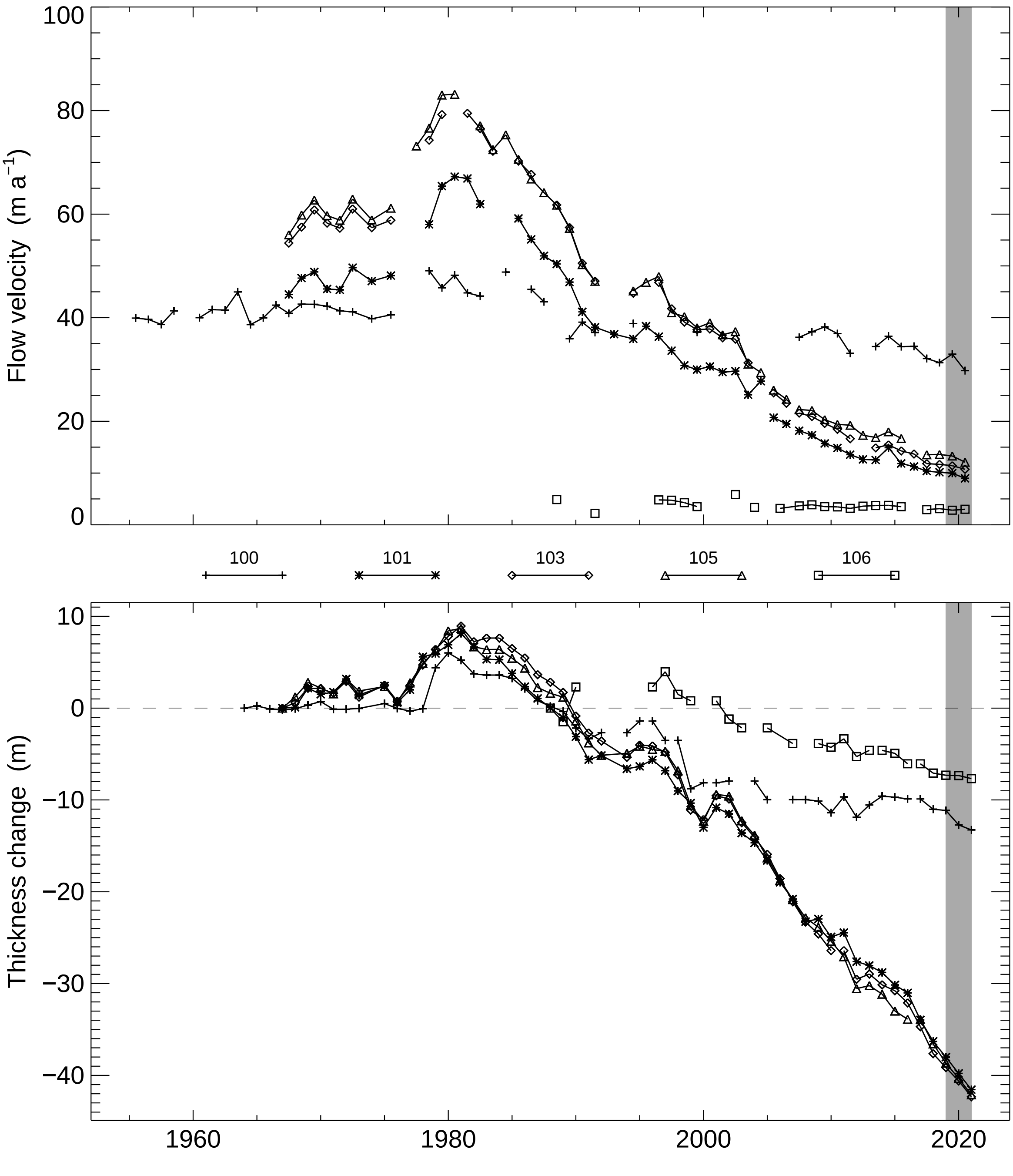

Figure 5.2: Surface flow velocities (top) and thickness change (below) of Allalingletscher at five stakes. The gray shaded area highlights the years of the current report.

5.3 Glacier de Corbassière

Introduction

Since 1967, Glacier de Corbassière (Figure 4.14) has been under observation regarding surface ice flow velocities. On two cross-profiles in the ablation area of the glacier flow markers were placed on the surface and annually moved back to the initial position. In 1996 the flow markers were replaced by ablation stakes. Annual surveying has been carried out to determine the ice flow velocities and local mass balance (Section 4.7, Table 4.9). Figure 5.3 shows the horizontal surface flow velocities for the two profiles since 1967.

Investigations in 2019/20 and in 2020/21

The field surveys were carried out on 8th/9th September 2020 and on 14th/15th September 2021. As in previous years, in both observation periods seven stakes were maintained and surveyed on the glacier tongue. In addition, the surface elevation has been measured along the two cross profiles at additional points with fixed position to determine ice thickness change. Due to the continuous reduction in ice thickness and glacier width in the lower profile in fall 2020 it was decided to finally give up the stakes and they were installed again for a last period an at the same time a new profile was installed complementing the existing stake R1 with two additional stakes R3 and R5 (Figure 4.14).

Table 5.2: Glacier de Corbassière - Individual measurements of surface flow velocity and thickness change

Stake	Period Start	End	Coordinates (m / m / m a.s.l.)	Thickness change (m)	Velocity (m a^{-1})
B2	27.09.2019	08.09.2020	589577 / 93202 / 2650	−2.75	7.33
B2	08.09.2020	14.09.2021	589577 / 93202 / 2650	−2.75	7.09
B4	27.09.2019	08.09.2020	589392 / 93101 / 2650	−2.28	12.85
B4	08.09.2020	14.09.2021	589392 / 93101 / 2650	−2.32	12.76
B6	27.09.2019	08.09.2020	589230 / 93012 / 2655	−2.44	13.47
B6	08.09.2020	14.09.2021	589230 / 93012 / 2655	−2.18	13.48
R1	08.09.2020	14.09.2021	589150 / 93650 / 2580	−2.99	7.37
R2	08.09.2020	14.09.2021	588950 / 93500 / 2580	−3.00	7.44
R3	08.09.2020	14.09.2021	588800 / 93400 / 2580		5.61
A2	27.09.2019	08.09.2020	588650 / 94315 / 2475	−6.93	3.22
A2	08.09.2020	14.09.2021	588650 / 94315 / 2475	−6.05	2.99
A4	27.09.2019	08.09.2020	588450 / 94257 / 2400	−7.12	3.46
A4	08.09.2020	14.09.2021	588450 / 94257 / 2400	−5.05	2.26
A6	27.09.2019	08.09.2020	588273 / 94207 / 2470	−8.30	2.10
A6	08.09.2020	14.09.2021	588273 / 94207 / 2470	−1.46	3.02

The ice flow velocity decreased further during the two periods under review. The general long-term trend of decreasing speed accompanied by a lowering of the ice surface was maintained. Due to repetedly shifting the position of A6 the evaluated flow velocity is less representative than for the other measurement sites.

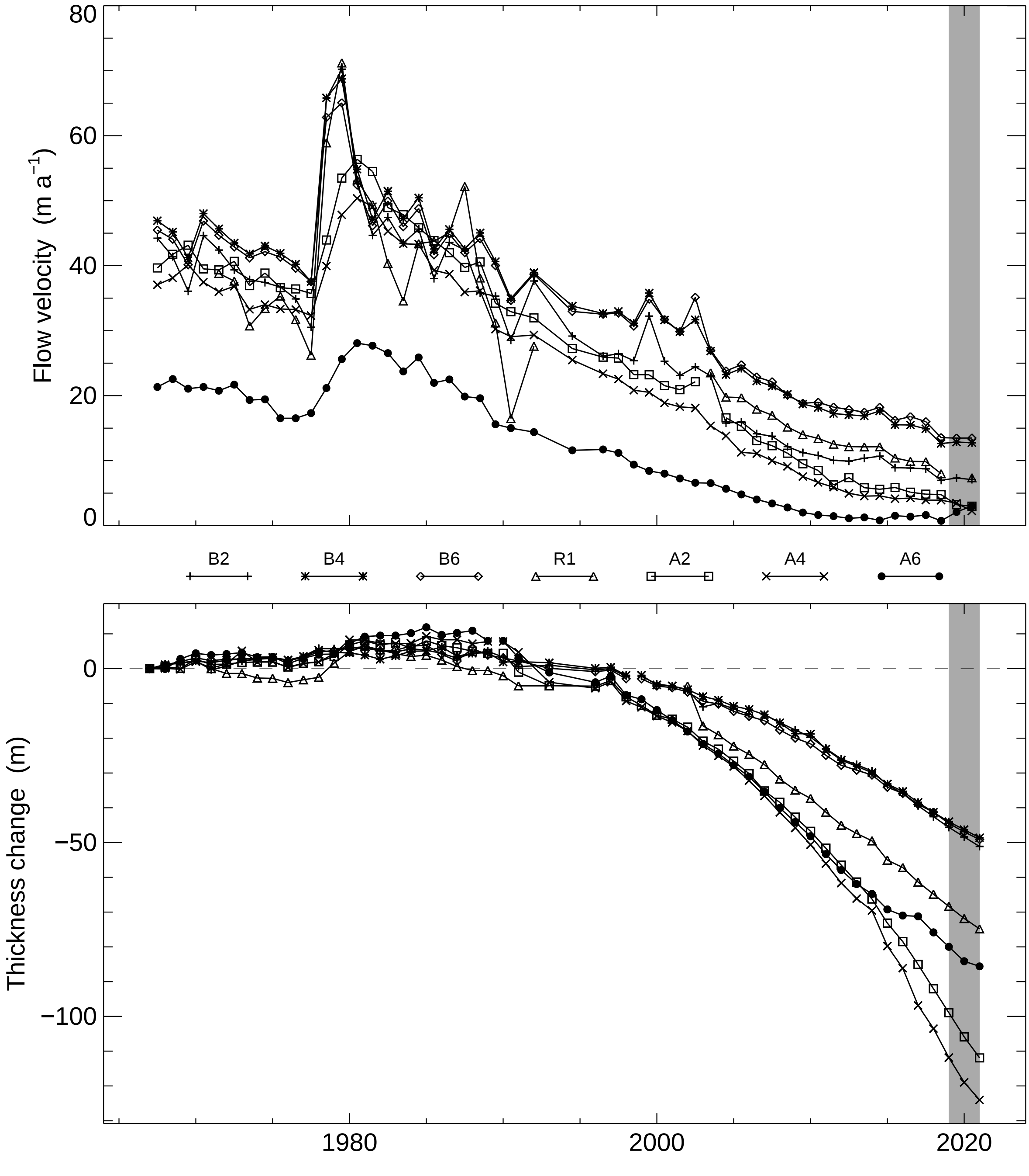

Figure 5.3: Surface flow velocities (top) and thickness change (bottom) of Glacier de Corbassière at two profiles with three stakes each and the additional stake in between. The gray shaded area highlights the years of the current report.

5.4 Glacier du Giétro

Introduction

For Glacier du Giétro (Figure 4.19) in the Val de Bagnes (Valais) a very long measurement series of ice flow velocity is being maintained by VAW/ETHZ under contract with Forces Motrices de Mauvoisin SA. The aim of these annual observations was the early recognition of glacier break-offs, which could endanger the dammed lake located in the outreach of ice avalanches. The glacier tongue shrank drastically in recent years reducing the hazard potential substantially. The measurements, which have been carried out for more than 55 years, include periods of glacier growth and recession (VAW, 1997, 1998; Bauder et al., 2002; Raymond et al., 2003). In addition to ice flow velocity, annual mass balance is measured at the stakes (Section 4.9, Table 4.14).

Figure 5.4 shows the horizontal surface flow velocity measurements at seven stakes along the central longitudinal profile of the glacier, acquired since 1966. There are three distinct periods: in the first period (1966 to 1976), the velocities in the accumulation area (stakes 1, 2 and 4) were approximately 5-20 m a^{-1}, in the central region of the glacier (stake 5) about 35 m a^{-1} and in the steep tongue area (stakes 102, 8 and 10) they were in the range of 50-90 m a^{-1}. The second period (1977 to 1982) is marked by a distinct acceleration, in which the speeds (for example at stake 102) increased from 90 m a^{-1} to 120 m a^{-1}. From the mid-1980s onward, the velocities decreased sharply, and in the last years reached the lowest values measured since 1966.

Table 5.3: Glacier du Giétro - Individual measurements of surface flow velocity and thickness change

Stake	Period Start	Period End	Coordinates (m / m / m a.s.l.)	Thickness change (m)	Velocity (m a^{-1})
1	27.09.2019	08.09.2020	596143 / 92346 / 3310	−0.35	2.60
1	08.09.2020	14.09.2021	596143 / 92346 / 3310	−0.36	2.32
2	27.09.2019	08.09.2020	596605 / 92835 / 3255	−0.51	7.73
2	08.09.2020	14.09.2021	596605 / 92835 / 3255	−0.26	7.74
4	27.09.2019	08.09.2020	596211 / 93400 / 3195	−0.77	9.98
4	08.09.2020	14.09.2021	596211 / 93400 / 3195	−0.68	10.89
5	27.09.2019	08.09.2020	595615 / 94303 / 3060	−1.71	13.91
5	08.09.2020	14.09.2021	595615 / 94303 / 3060	−0.69	14.04
101	27.09.2019	08.09.2020	594735 / 94540 / 2860	−1.31	23.56
101	08.09.2020	14.09.2021	594735 / 94540 / 2860	−1.38	20.47
102	27.09.2019	08.09.2020	594568 / 94497 / 2830	−4.74	14.58
102	08.09.2020	14.09.2021	594568 / 94497 / 2830	−3.45	11.94
107	27.09.2019	08.09.2020	594860 / 94560 / 2915	−1.89	23.68
107	08.09.2020	14.09.2021	594860 / 94560 / 2915	−1.12	20.88

Investigations in 2019/20 and in 2020/21

Measurements of surface flow velocity and local mass balance were performed at seven stakes. The field survey in fall 2020 was carried out on 8th September. All stakes have been located and moved back to the initial position. On 14th September 2021, the field measurements were carried out for the second period. Again, all stakes have been located and surveyed. Due to substantial ice loss and large crevasses at the tongue the initial postion at stakes 102 and 107 had to be slightly shifted within a radius of 30 m in the individual periods.
The decrease in ice flow velocity over the past years continued during the two periods covered by this report. Due to the glacier retreat with complete ice melt at the glacier snout, the two sites 8 and 10 had to be abandoned already in 2010 and are no longer under observation but kept in Figure 5.4 for comparison. The change observed at the lower sites still reflects to large extent the lowering of the surface but is also slightly hampered by local effects caused by the formation of large crevasses and shifts of the initial position.

The tongue of Turtmanngletscher in September 2021 after a spectacular break off of the ice masses in the steep connection of former snout that occurred in August 2020 (see Chapter 7) (Photo: A. Brigger)

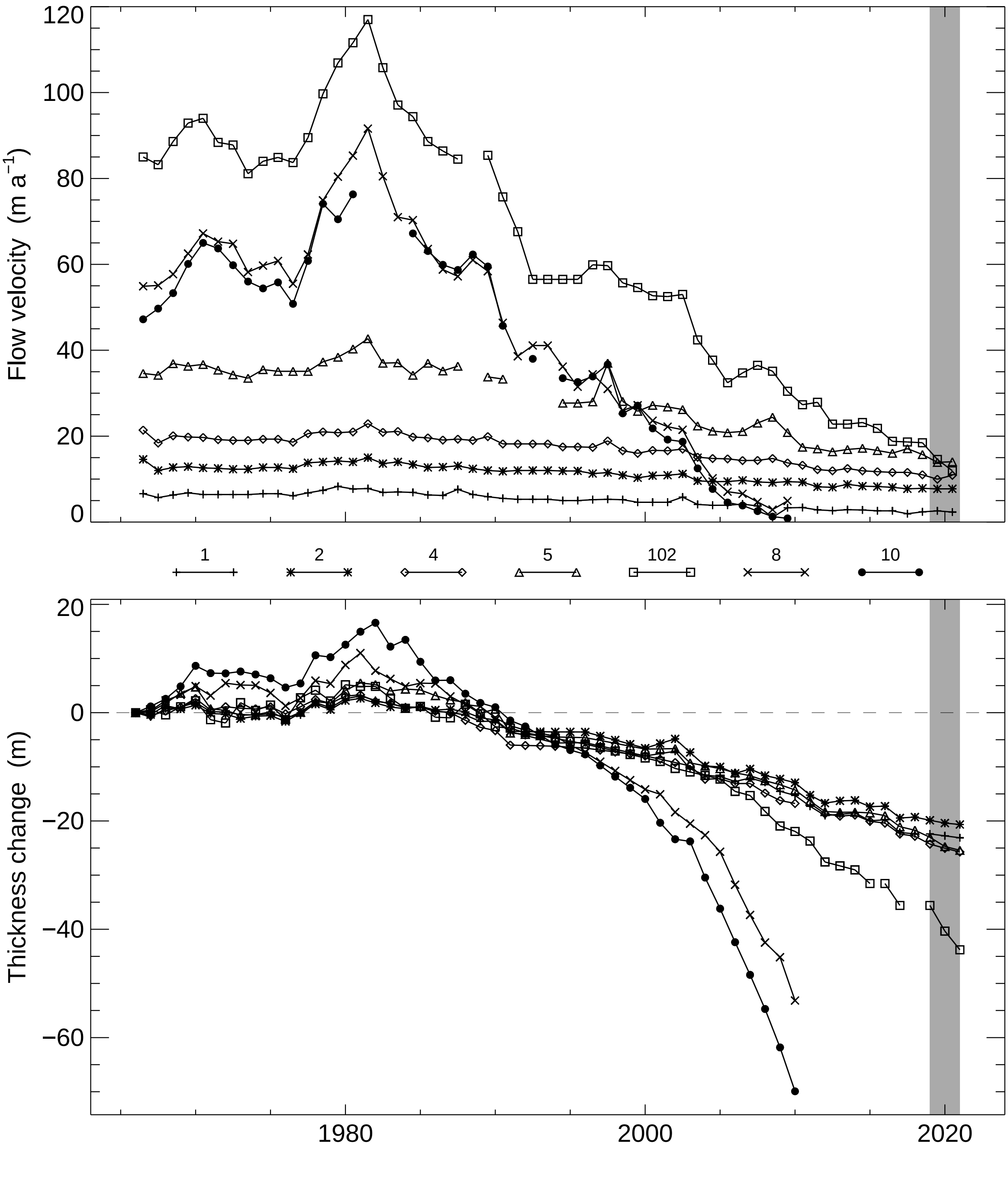

Figure 5.4: Surface flow velocities (top) and thickness change (bottom) of Glacier du Giétro at seven stakes. The gray shaded area highlights the years of the current report.

5.5 Grosser Aletschgletscher

Introduction

Grosser Aletschgletscher (Figure 4.25) has been under observation for surface ice flow velocities since several decades. Between 1940s and 1980s a network of stakes on a longitudinal and several cross profiles was maintained with a focus on both mass balance and ice flow velocity (Zoller, 2010). As a part of the ongoing mass balance investigations at stake 3 close to Jungfraujoch the position is surveyed systematically since 2004, thus allowing the determination of the surface flow velocity and thickness change. The results of the mass balance observations are presented in Section 4.11 and Table 4.17 of this report.

Investigations in 2019/20 and in 2020/21

Field surveys were carried out on a seasonal basis on 29th May and 18th September in 2020, and 26th May and 30th September in 2021, respectively. Using high-precision differential GNSS the position of stake 3 was surveyed. In fall, the stake was moved back to the initial position. The results of the annual horizontal surface flow velocity and the change in ice thickness during the two measurement periods of this report are presented in Table 5.4.

Table 5.4: Grosser Aletschgletscher - Individual measurements of surface flow velocity and thickness change

Stake	Period		Coordinates	Thickness change	Velocity
	Start	End	(m / m / m a.s.l.)	(m)	(m a^{-1})
3	03.10.2019	18.09.2020	641825 / 154810 / 3345	−1.27	32.06
3	18.09.2020	30.09.2021	641825 / 154810 / 3345	1.33	30.66

In period 2019/20 an annual horizontal velocity of 32.1 m a^{-1} was determined with slight variation between the winter and summer season of 5%. In the second measuring period, an annual flow velocity of 30.7 m a^{-1} was recorded with an 8% higher velocity in the summer season compared to the winter. The results of the annual horizontal surface flow velocity as well as the change in thickness since 2004 are shown in Figure 5.5. Only relatively small year-to-year fluctuations are evident. In an evaluation of historical measurements at site 3 between 1957 and 1966, Zoller (2010) determined annual surface flow velocities of 30 m a^{-1} to 40 m a^{-1} that were slightly higher than the observed values in the recent two decades. During the past 17 years with continuous observation, the ice thickness decreased by about 7 m at site 3. The inter-annual fluctuations are attributed to mass balance variations.

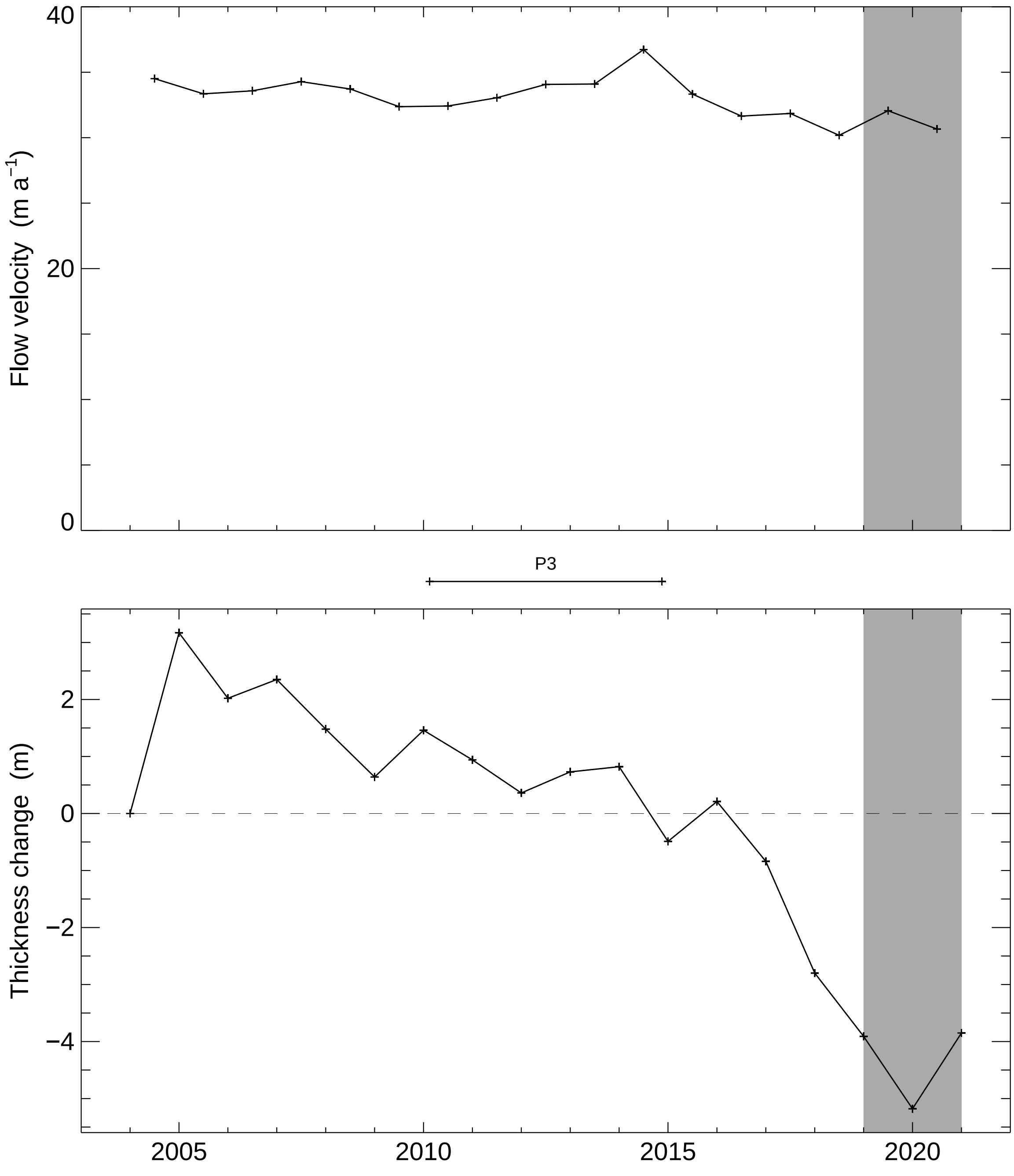

Figure 5.5: Surface flow velocities (top) and thickness change (bottom) at stake P3 on Grosser Aletschgletscher. The gray shaded area highlights the years of the current report.

5.6 Hohlaubgletscher

Introduction

The first ice flow velocity measurements on Hohlaubgletscher date back to 1955 (VAW, 1999). Initially, investigations were carried out at a network of three stakes with the aim to determine glacier mass balance for planning and construction of the Mattmark reservoir for hydro-power production (VAW, 1999). In 1967 the observation network the glacier was reduced. Measurements were continued at only one stake and extended by a second site in 2019 (Figure 4.26) as part of the investigations by VAW/ETHZ for the Mattmark hydro-power company (VAW, 2022). In addition to ice flow velocity, annual mass balance is measured at the two stakes (Table 4.18).

Investigations in 2019/20 and in 2020/21

The field surveys were carried out on 4th September 2020 and on 2nd September 2021. During both field campaigns all stakes were located, surveyed and set back to their initial position. The position of the stakes was surveyed using differential GNSS relative to a local reference station. Results for horizontal flow velocity and thickness change are given in Table 5.5.

Table 5.5: Hohlaub - Individual measurements of surface flow velocity and thickness change

Stake	Period		Coordinates	Thickness change	Velocity
	Start	End	(m / m / m a.s.l.)	(m)	(m a^{-1})
110	30.08.2019	04.09.2020	637405 / 100710 / 3050	−0.31	10.15
110	04.09.2020	02.09.2021	637405 / 100710 / 3050	−0.60	10.29
115	30.08.2019	04.09.2020	636465 / 100640 / 3240	−0.24	32.33
115	04.09.2020	02.09.2021	636465 / 100640 / 3240	−0.14	33.22

Only small fluctuations of ice flow velocity was observed during the two periods. Although a slight decrease in the ice thickness occured no influence of the ice velocity is registered yet.

5.7 Rhonegletscher

Introduction

Starting in 2006, as part of the mass balance investigations at Rhonegletscher (Figure 4.36), the positions of all stakes are also surveyed for the evaluation of surface flow velocity. The substantial glacier melt and the associated retreat over the past two decades required modification of the observational network. However, several continuous time series of surface flow velocity distributed along a longitudinal transect have been acquired. The corresponding results of the mass balance observations are presented in Section 4.17 and Table 4.27 of this report.

Investigations in 2019/20 and in 2020/21

Measurement of surface flow velocity and mass balance were performed at 11 stakes. The field survey in fall 2020 was carried out on 11th September. All 11 stakes have been located and moved back to the initial position. On 8th September 2021, the field measurements were carried out for the second period. Once again, all stakes have been maintained. High-precision differential GNSS

Table 5.6: Rhonegletscher - Individual measurements of surface flow velocity and thickness change

Stake	Period		Coordinates	Thickness change	Velocity
	Start	End	(m / m / m a.s.l.)	(m)	(m a^{-1})
01	12.09.2019	11.09.2020	673815 / 166615 / 3235	−0.42	20.42
01	11.09.2020	08.09.2021	673815 / 166615 / 3235	0.49	20.97
02	12.09.2019	11.09.2020	673552 / 165950 / 3125	−1.48	60.60
02	11.09.2020	08.09.2021	673552 / 165950 / 3125	1.37	61.30
03	12.09.2019	11.09.2020	673100 / 164930 / 2930	−1.77	47.50
03	11.09.2020	08.09.2021	673100 / 164930 / 2930	−0.66	45.83
04	12.09.2019	11.09.2020	673357 / 162758 / 2745	−1.75	58.64
04	11.09.2020	08.09.2021	673357 / 162758 / 2745	−0.28	56.98
05	12.09.2019	11.09.2020	672521 / 161919 / 2605	−2.47	58.24
05	11.09.2020	08.09.2021	672521 / 161919 / 2605	−1.00	56.54
06	12.09.2019	11.09.2020	672423 / 160843 / 2465	−4.35	29.54
06	11.09.2020	08.09.2021	672423 / 160843 / 2465	−2.36	28.17
07	12.09.2019	11.09.2020	672657 / 160173 / 2360	−5.91	26.16
07	11.09.2020	08.09.2021	672657 / 160173 / 2360	−3.29	22.40
08	12.09.2019	11.09.2020	672680 / 159724 / 2295	−7.48	11.54
08	11.09.2020	08.09.2021	672680 / 159724 / 2295	−5.03	9.09
09	12.09.2019	11.09.2020	672605 / 159500 / 2250	−7.51	6.14
09	11.09.2020	08.09.2021	672605 / 159500 / 2250	−3.90	5.21
12	12.09.2019	11.09.2020	673500 / 163990 / 2845	−1.46	41.63
12	11.09.2020	08.09.2021	673500 / 163990 / 2845	−0.52	39.24
13	12.09.2019	11.09.2020	672705 / 159937 / 2320	−7.23	14.02
13	11.09.2020	08.09.2021	672705 / 159937 / 2320	−4.79	11.97

was used for surveying the positions of the stakes in both periods. The results of annual horizontal surface flow velocity and change in ice thickness determined during the two measurement periods of this report are presented in Table 5.6.

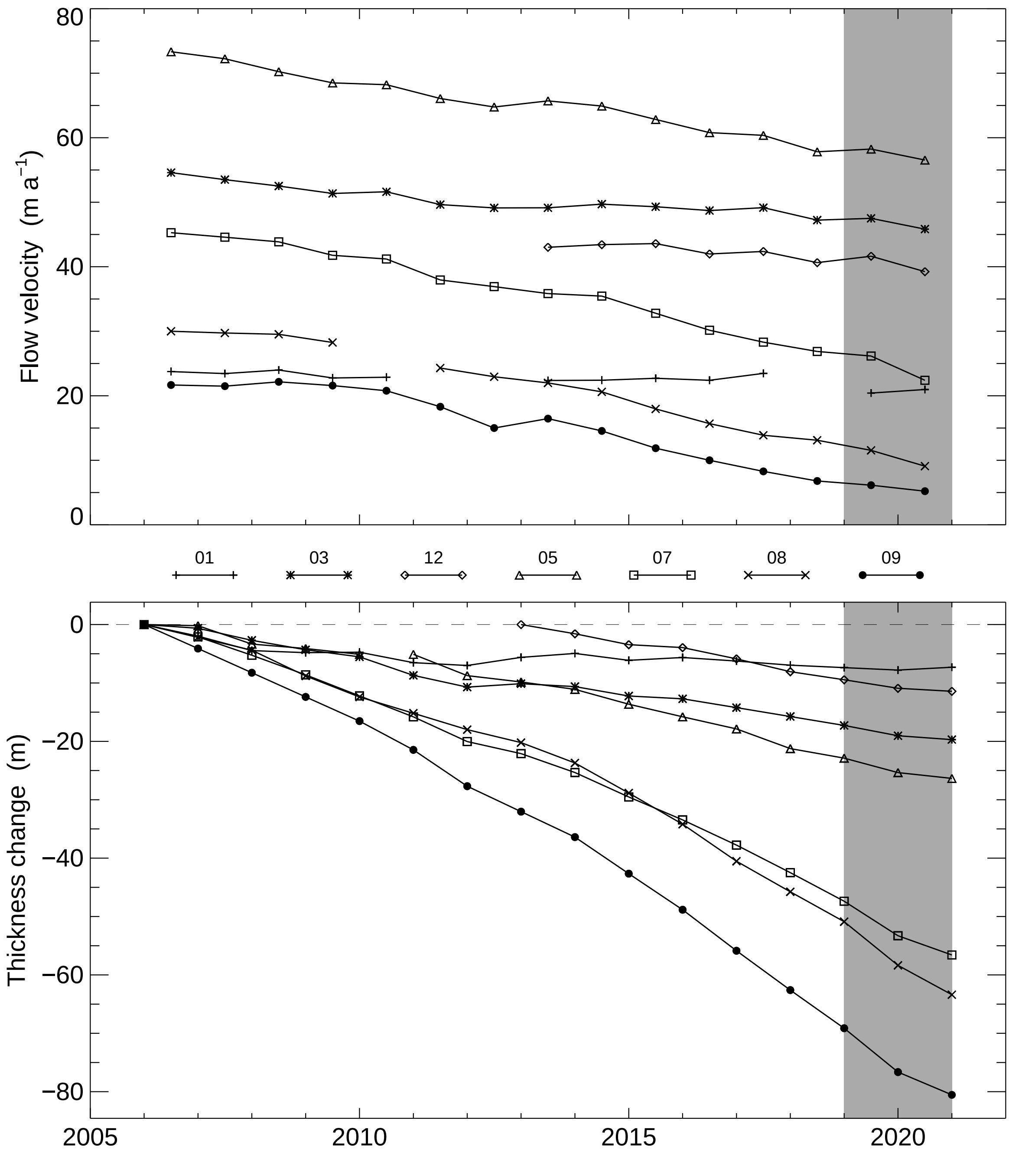

Figure 5.6: Surface flow velocities (top) and thickness change (bottom) of Rhonegletscher at selected stakes. The gray shaded area highlights the years of the current report.

Observed flow velocities in the two measurement periods range from about 5 $m\,a^{-1}$ at the lowermost stake on the glacier tongue to about 60 $m\,a^{-1}$ at three stakes at about 2600 m a.s.l., 2750 m a.s.l. and 3100 m a.s.l., respectively. With the exception of the uppermost two stakes, the flow velocities further decreased at all stakes in the two periods (Figure 5.6).

5.8 Schwarzberggletscher

Introduction

The first ice flow velocity measurements on Schwarzberggllletscher date back to 1955 (VAW, 1999). Initially, investigations were carried out at a network of seven stakes with the aim to determine glacier mass balance for planning and construction of the Mattmark reservoir for hydro-power production (VAW, 1999). In 1967 the observation network was reduced to two stakes. Measurements are currently being continued on three selected stakes (Figure 4.43) as part of the investigations by VAW/ETHZ for the Mattmark hydro-power company (VAW, 2022). In addition to ice flow velocity, annual mass balance is measured at the stakes (Table 4.32).

Investigations in 2019/20 and in 2020/21

The field surveys were carried out on 4th September 2020 and on 2nd September 2021. During both field campaigns all stakes were located, surveyed and set back to their initial position. The position of the stakes was surveyed using differential GNSS relative to a local reference station. Results for horizontal flow velocity and thickness change are given in Table 5.7.

Table 5.7: Schwarzberg - Individual measurements of surface flow velocity and thickness change

Stake	Period		Coordinates	Thickness change	Velocity
	Start	End	(m / m / m a.s.l.)	(m)	(m a^{-1})
120	30.08.2019	04.09.2020	638320 / 96220 / 2880	−1.66	5.37
120	04.09.2020	02.09.2021	638320 / 96220 / 2880	−1.73	5.13
123	30.08.2019	04.09.2020	638525 / 96730 / 2805	−2.99	3.48
123	04.09.2020	02.09.2021	638525 / 96730 / 2805	−2.98	2.97
124	30.08.2019	04.09.2020	638062 / 95212 / 2985	−0.21	7.03
124	04.09.2020	02.09.2021	638062 / 95212 / 2985	−1.33	6.93

Annual velocities in the two measurement periods varies between three and seven metres per year and reflect the limited ice thickness and the generelly gentle slope. The decrease in ice flow velocity over the past years continued during the two periods covered by this report. Hence, the general long-term trend of decreasing speed accompanied by a lowering of the ice surface was maintained.

5.9 Silvrettagletscher

Introduction

Starting in 2003, as part of the mass balance monitoring programme at Silvrettagletscher (Figure 4.45), the positions of the available stakes are also surveyed for the evaluation of surface flow velocity. Until 2008 the observational network consisted of 11 stakes that were annually surveyed. Afterwards the network was extended to 16 stakes. The corresponding results of the mass balance observations are presented in Section 4.20 and Table 4.34 of this report.

Investigations in 2019/20 and in 2020/21

In the two periods under review in this report, measurements of surface flow velocity were performed at 16 stakes. The field survey in fall 2020 was carried out on 13th/14th September. All stakes have been located and surveyed. On 17th/18st September 2021, the field measurements were taken for the second period. Positions have been surveyed using high-precision differential GNSS. Some stakes are moved back annually to their initial position while maintenance of others is only needed every second year. The results of annual horizontal surface flow velocity and change in ice thickness determined during the two measurement periods covered by this report are presented in Table 5.8.
Observed ice flow velocities on Silvrettagletscher are small due to limited ice thickness and generally gentle slopes. Annual velocities in the two measurement periods varies between less than one and several metres per year. A further decrease in flow speed was found. This decrease reflects the ongoing reduction of ice thickness registered over the past two decades at all sites. Figure 5.7 shows the results of the annual horizontal surface flow velocity as well as the cumulative change in thickness since 2003.

Table 5.8: Silvrettagletscher - Individual measurements of surface flow velocity and thickness change

Stake	Period Start	End	Coordinates (m / m / m a.s.l.)	Thickness change (m)	Velocity (m a^{-1})
01	21.09.2019	13.09.2020	801840 / 191729 / 2980	−0.54	0.87
01	13.09.2020	17.09.2021	801840 / 191729 / 2980	−0.08	0.99
02	21.09.2019	13.09.2020	801927 / 192023 / 2955	−0.22	4.16
02	13.09.2020	17.09.2021	801927 / 192023 / 2955	0.02	4.25
03	21.09.2019	13.09.2020	801783 / 192252 / 2900	−0.19	4.60
03	13.09.2020	17.09.2021	801783 / 192252 / 2900	−0.31	4.81
04	21.09.2019	13.09.2020	801730 / 192630 / 2820	−0.83	3.41
04	13.09.2020	17.09.2021	801730 / 192630 / 2820	−0.36	3.12
05	21.09.2019	13.09.2020	801074 / 192689 / 2720	−1.40	4.04
05	13.09.2020	17.09.2021	801074 / 192689 / 2720	−1.23	3.86
06	21.09.2019	13.09.2020	800515 / 192890 / 2625	−2.35	2.32
06	13.09.2020	17.09.2021	800515 / 192890 / 2625	−2.48	2.15
07	21.09.2019	13.09.2020	800165 / 192872 / 2580	−2.88	0.48
07	13.09.2020	17.09.2021	800165 / 192872 / 2580	−2.49	0.44
08	21.09.2019	13.09.2020	799827 / 192745 / 2535	−3.78	0.56
08	13.09.2020	17.09.2021	799827 / 192745 / 2535	−2.97	0.50
10	21.09.2019	13.09.2020	801530 / 191805 / 2940	−0.26	2.27
10	13.09.2020	17.09.2021	801530 / 191805 / 2940	−0.40	2.28
11	21.09.2019	13.09.2020	800718 / 192206 / 2725	−1.54	0.70
11	13.09.2020	17.09.2021	800718 / 192206 / 2725	−1.21	0.62
12	21.09.2019	13.09.2020	800406 / 192587 / 2600	−2.72	2.06
12	13.09.2020	17.09.2021	800406 / 192587 / 2600	−2.48	1.86
13	21.09.2019	13.09.2020	799949 / 192607 / 2545	−4.56	1.14
13	13.09.2020	17.09.2021	799949 / 192607 / 2545	−3.87	1.13
15	21.09.2019	13.09.2020	801163 / 191987 / 2855	−1.22	3.30
15	13.09.2020	17.09.2021	801163 / 191987 / 2855	−0.84	3.12
16	21.09.2019	13.09.2020	801340 / 192371 / 2765	−0.50	5.32
16	13.09.2020	17.09.2021	801340 / 192371 / 2765	0.18	5.18
17	21.09.2019	13.09.2020	801453 / 192818 / 2775	−0.90	2.44
17	13.09.2020	17.09.2021	801453 / 192818 / 2775	−0.85	2.43
18	21.09.2019	13.09.2020	800767 / 192541 / 2695	−1.81	3.90
18	13.09.2020	17.09.2021	800767 / 192541 / 2695	−1.55	3.61

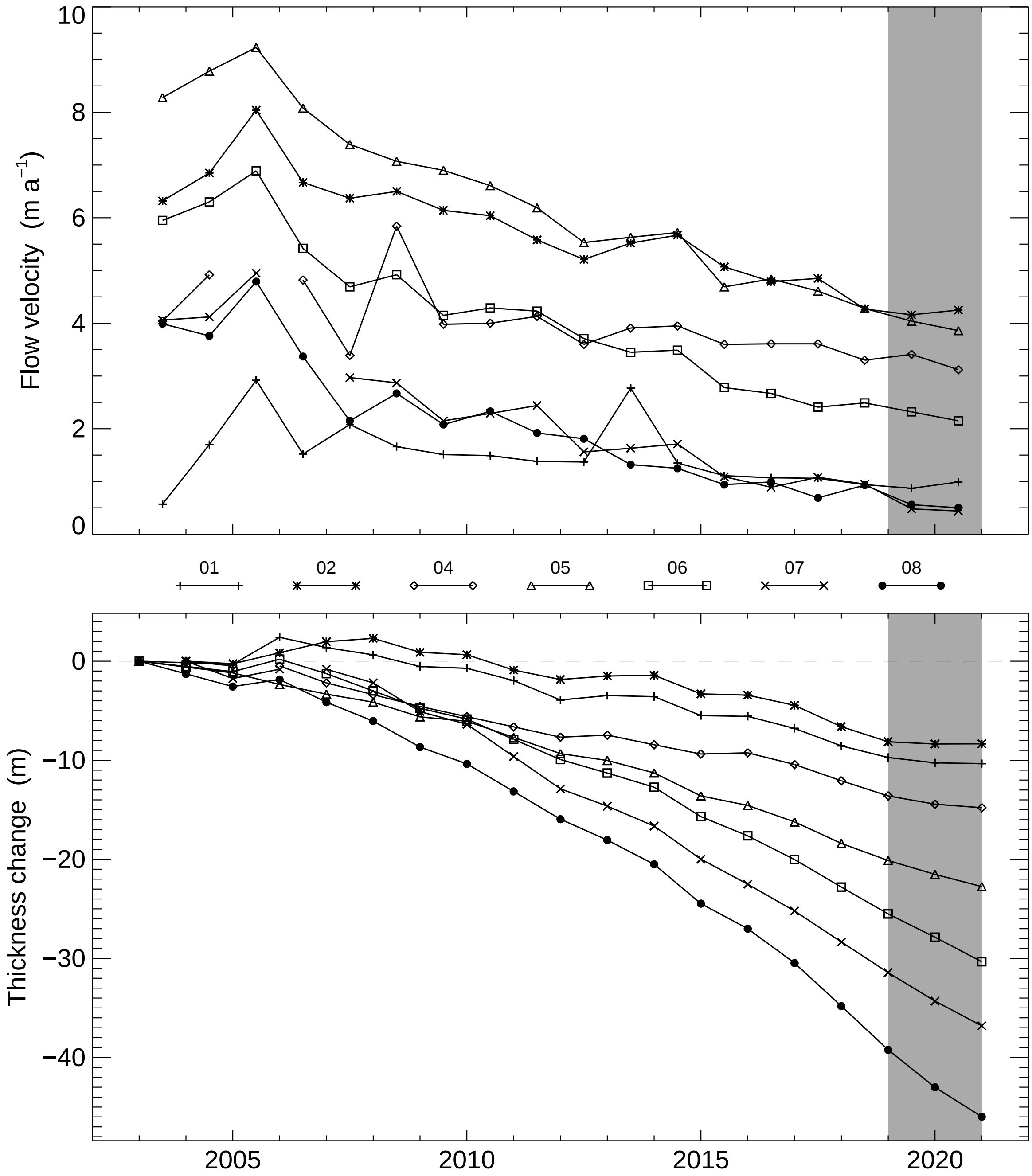

Figure 5.7: Surface flow velocities (top) and thickness change (bottom) of selected stakes at Silvrettagletscher. The gray shaded area highlights the years of the current report.

6 Englacial Temperature

6.1 Introduction

Besides glacier mass balance, firn and ice temperatures can be considered as a key parameter in detecting global warming trends at high elevation. These temperatures have a sort of a memory function as they register short- and mid-term evolution of the energy balance at the surface. By measuring firn and ice temperatures, it is possible to assess climate change in areas where no direct observations of common climatic parameters are available. Cold firn and ice in glaciers, ice caps and ice sheets occur when the firn and ice show permanently negative temperatures over the minimum time span of a year. If this is not the case, glaciers are temperate, thus their temperature is at the pressure melting point. Ice bodies that contain both cold and temperate parts are called polythermal (Blatter and Hutter, 1991; Cuffey and Paterson, 2010).
Englacial temperature measurements on the Colle Gnifetti site are part of GLAMOS monitoring

Figure 6.1: Investigated site for englacial temperatures.

programme. The Colle Gnifetti site was selected to perform regular measurements updating the surveys made in the years 1983, 1991, 1999, 2000, 2007, 2008, 2013, 2014, 2015, 2018 and 2019. The results of measurements taken in 2021 are presented in this report. The previous results of 2007 until 2019 have been reported in Volumes 129/130, 135/136 and 139/140.

6.2 Colle Gnifetti (Monte Rosa)

Introduction

Colle Gnifetti is a small and very wind-exposed firn saddle at 4450 m a.s.l. in the region of Monte Rosa, Valais Alps, Switzerland. The saddle is situated between Zumsteinspitze and Signalkuppe with the famous Margerita hut, and belongs to the accumulation area of Grenzgletscher, a tributary of Gornergletscher. Strong wind erosion causes extraordinarily low annual accumulation of snow. Alean et al. (1983) and Lüthi (2000) showed accumulation rates of 0.1 m w.e. a^{-1} at the northwest slope of Signalkuppe to 1.2 m w.e. a^{-1} at the sunny south slope of Zumsteinspitze. Thus, Colle Gnifetti represents a unique Alpine key site for collecting long-term ice core records.

Initially, it was considered to repeat the measurements every four to five years. However, a recent evaluation showed that more frequent measurements would be appropriate to account for shorter-term changes. Therefore, in summer 2018, a fixed thermistor chain was installed at the repeatedly investigated site CG18 (Table 6.1), for which measurements exist since 1982. This site is located close to the center of the Colle Gnifetti saddle. For this site, currently four surveys were conducted, one each in 2018 and 2019, and two in 2021.

Investigations in 2020 and in 2021

No measurements could be performed in 2020, because of the Corona pandemic. In 2021, a new borehole was drilled mechanically within the Ice Memory project, organized by the Institute of Polar Sciences of the Italian National Research Council, Ca'Foscari University of Venice, and the Paul Scherrer Institute. The University of Fribourg measured the temperature profile of the new borehole on 10th June 2021. The borehole is located exactly at the same place on Colle Gnifetti, where a deep borehole was drilled by the Paul Scherrer Institute in the year 2003 (CG03-1/03), which was remeasured in 2004. Therefore, three temperature profiles exist for this place down to a depth of around 80 m.

In Figure 6.2, measured temperature profiles at the position with the long-term boreholes of CG82-1/82, CG91-A/91, CG99-2/99, CG00-A/00, CG08-2/08, CG18-1/18, CG18-1/19, CG18-1/21a, CG18-1/21b) are shown. There appears to be a remarkable cooling between 2008 and 2018/19. This observation is in qualitative agreement with other measurements in the Mont Blanc area (Vincent et al., 2020). Nonetheless, the observed cooling is difficult to explain. It might be related to an enhanced formation of near-surface ice layers, blocking vertical percolation of meltwater to depth. This process would decrease the release of latent heat by refreezing (Reijmer et al., 2012).

However, the temperature profile in the new borehole since 2018 shows a clear warming of firn and ice down to a depth of 80 m. Figure 6.3 shows the temperature profile at the new deep borehole compared to the previous deep profiles (CG03-1/03 and CG03-1/04). At a depth of 20 m, a remarkable warming of the firn of around 0.7°C can be observed during the past 18 years.

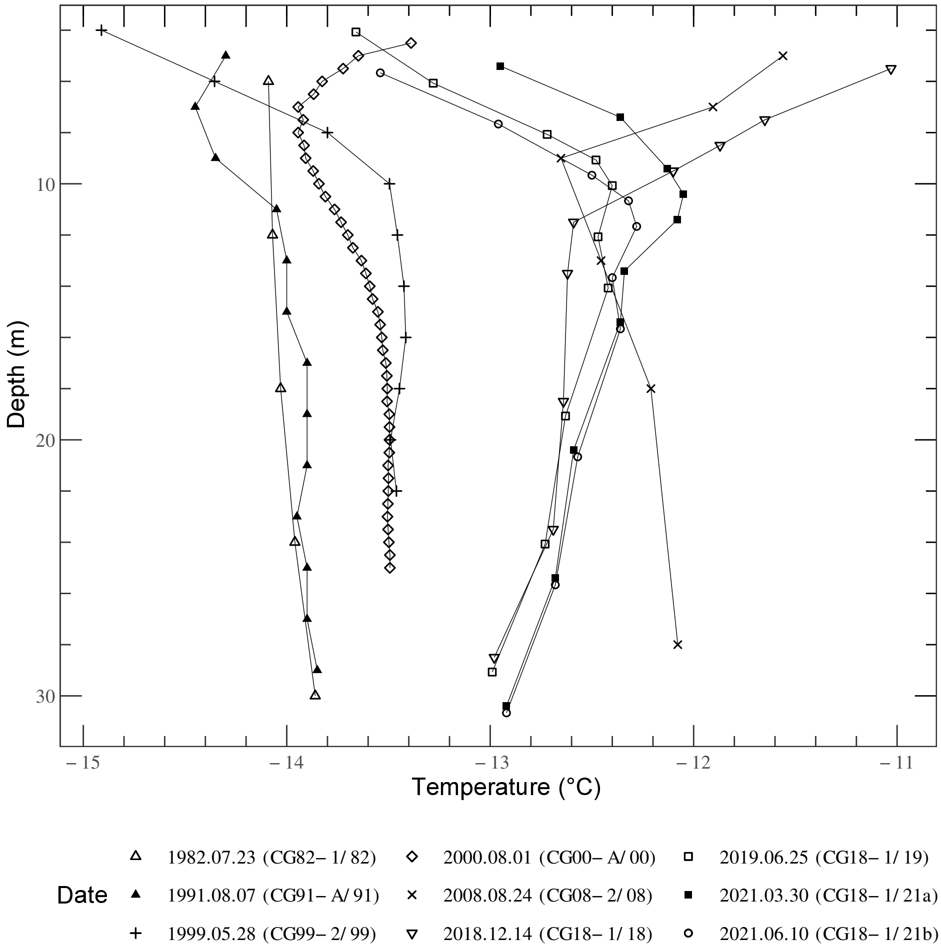

Figure 6.2: Firn temperature profiles at the Colle Gnifetti saddle, measured in 1982 (Haeberli and Funk, 1991), 1991 (Laternser, 1992; Suter et al., 2001), 1999 (Suter, 2002; Suter and Hoelzle, 2002), 2000 (Suter, 2002; Suter and Hoelzle, 2002), 2008 (Hoelzle et al., 2011), 2018/2019 (Mattea, 2020) and 2021. Boreholes CG82-1, CG08-1 and CG18-1 are loacatet at the same position.

Table 6.1: Borehole number, measurement date, total depth of the borehole, coordinates of the borehole location, and drilling technique.

number	date	depth	coordinates (m / m / m a.s.l.)	drill types
CG18-1/21	30.03.2021[a]	30.4	633798 / 86576 / 4455	steam
CG18-2/21	10.06.2021[a]	30.7	633798 / 86576 / 4455	steam
CG21-1/21	10.06.2021[b]	83	633846.5 / 86526.4 / 4460	mechanical

Type of thermistors: [a] YSI 44031; [b] YSI 4460031

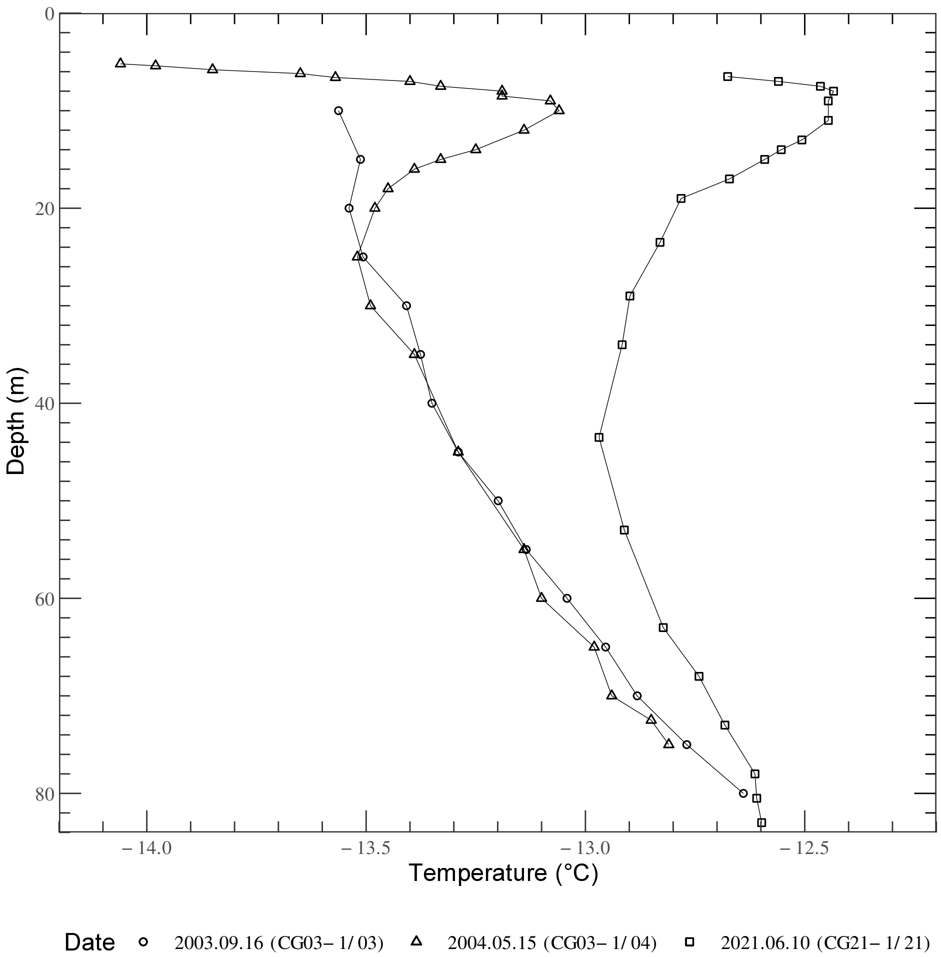

Figure 6.3: Firn temperature profiles at the Colle Gnifetti saddle, measured in 2003 (Hoelzle et al., 2011), 2004 (Hoelzle et al., 2011) and 2021. Boreholes CG03-1/03, CG03-1/04 and CG21-1/21 are loacatet at the same position.

Table 6.2: Colle Gnifetti - Englacial temperature measurements in 2021 in two different boreholes CG18-2/21b and CG21-1/21.

Borehole: CG18-1/21 / CG18-2/21

depth (m)	30.03.2021 temperature (°C)	10.06.2021 temperature (°C)
5.4	−12.95	
5.67		−13.54
7.4	−12.36	
7.67		−12.96
9.4	−12.13	
9.67		−12.50
10.4	−12.05	
10.67		−12.32
11.4	−12.08	
11.67		−12.28
13.4	−12.34	
13.67		−12.40
15.4	−12.36	
15.67		−12.36
20.4	−12.59	
20.67		−12.57
25.4	−12.68	
25.67		−12.68
30.4	−12.92	
30.67		−12.92

Borehole: CG21-1/21

depth (m)	10.06.2021 temperature (°C)
6.5	−12.68
7.0	−12.56
7.5	−12.46
8.0	−12.43
9.0	−12.45
11.0	−12.45
13.0	−12.51
14.0	−12.55
15.0	−12.59
17.0	−12.67
19.0	−12.78
23.5	−12.83
29.0	−12.90
34.0	−12.92
43.5	−12.97
53.0	−12.91
63.0	−12.82
68.0	−12.74
73.0	−12.68
78.0	−12.61
80.5	−12.61
83.0	−12.60

Impressive icebergs left after calving event in the proglacial lake at Chüebodengletscher in November 2020 (top, Photo: J. Vismara) and section of Glacier de Corbassière six month after a speed-up event of September 2020 (bottom, Photo: St. Harvey)

7 Hazardous Glaciers in Switzerland

7.1 Introduction

As an update to the inventory of hazardous glaciers (Raymond et al., 2003), ten recent events that occurred during the two periods under review of this report and six additional events from previous periods for completness are presented (Figure 7.1). The compilation includes events that are directly related to hazard potential originating from glaciers but also observations of special behavior and extraordinary processes. Available information may not be conclusive, as it is possible that some smaller events were not reported to us.

Figure 7.1: Glaciers with documented hazardous events in this report.

7.2 Events

Ärlengletscher

Starting in 2018, a surge-type speed-up of the entire relatively flat (inclination of about 15°) tongue resting on a rock bed occurred on the very small glacier (approx. 0.3 km^2). This resulted in glacier advance and a highly crevassed surface.

26 August 2020: Part of the glacier tongue of about 200'000 m^3 broke off. The ice was deposited just about 100 m below. As a consequence, an increase in ice flow was observed accompanied by additional ice fall events of small volumes.

Bisgletscher

Break-offs from a hanging glacier located at the east-face of Weisshorn repeatedly triggered ice or combined snow and ice avalanches. A teal-time monitoring system for early warning has been installed (Faillettaz et al., 2008; w/s/l, 2014).

20 January 2018: A combined snow and ice avalanche reached the main road and the railway line valley bottom and where road and train lines are. Volume unknown, no damages occurred.

18 December 2019: Two ice break-offs from the hanging glacier of about 50'000 m^2 occur-ed. No avalanche was triggered and deposits were found below on the flat section of the glacier at 3400 m a.s.l.

Chüebodengletscher

25-27 November 2020: A significant ice mass at the glacier snout in direct contact with the proglacial lake broke off due to buoyancy forces. Most of the ice was below the water line before the event. A large amount of icebergs was produced. Some of the them showed a spectacular size of several meters.

Glacier de Corbassière

5-11 September 2020: An active phase characterized by high surface velocity occurred on a part of the tributary Glacier de Grand Combin. The potential speed-up at an elevation range of between 3200 and 3400 m a.s.l is revealed by extensive crevassing at this section of the glacier. The area involved is estimated to about 50'000 m^2. It is speculated that the instability if was triggered by a reduction of support at the foot of the slope as a consequence of the ongoing thinning of the main branch of the glacier.

Fletschhorngletscher

1-20 August 2020: Several ice falls occurred from the tongue of Fletschhorngletscher. In total a volume of about 300'000 m^3 of ice broke off in the course of several events as has been revealed by aerial photographs and satellite imagery available in this period. No damages have been reported.

Im Griess

16 June 2019: Outflow of a proglacial lake at 2100 m a.s.l was blocked by snow masses at the onset of the snow melt. An abrupt outburst caused some flooding and river bank erosion downstreams in the area of Unerboden. An outburst volume of 266'000 m^3 of water was determined. Maximum discharge at Chlus, Urnerbode was estimted to 30-40 $m^3 s^{-1}$ (Amt für Forst und Jagd, 2019).

Glacier de la Plaine Morte

During the past decade, three glacier-dammed lakes formed around the Glacier de la Plaine Morte. These lakes, especially Lac de Faverges, represent a considerable hazard potential in the Simme Valley north of the glacier. The lake level has been monitored in real time since 2012 by GEO-PRAEVENT AG for early warning purposes. In 2018, the lake volume reached more than two million m^3 of water, and the resulting flood caused damage to the infrastructure downstream. Therefore, a supraglacial channel was dug in 2019 to artificially initiate an early surface lake drainage and to limit the lake water volume and the corresponding hazard (Ogier et al., 2021).

11 July 2019: After artificially lowering the lake level of Lac de Faverges the remaining water volume of approx. 0.7 million m^3 drained not causing any flooding downstreams nor any damage have been obsereved.

7 August 2020: Sudden drainage of Lac de Faverges (approx. 0.5 million m^3 of water) that occurred subglacially during several days. No damage reported.

29 Juli 2021: Drainage of Lac de Faverges (approx. 1 million m^3 of water). Lowering of the lake level started on 29th July and increased until 1st August. Drainage lasted until 12th August. Due to the artificial supraglacial channel still in existence the lake drainage occured slowely over several days with out any threat to any infrastructure downstreams.

Rhonegletscher

11-12 September 2021: A part of the glacier tongue of Rhonegletscher that was remaining subaquatic in the proglacial lake suddenly became a float but did not detach from the snout. Based on simple assessment of the visible ice mass, the volume of the relocated ice was estimated to be in the order of about 200'000 m^3.

Steingletscher

21 February 2020: A combined ice and rock fall occurred at a rock outcrop at about 2500 m a.s.l. The volume of this avalanche was tentatively estimated to about 100'000 m^3. The deposits covered the lower and flat part of the tongue to a large part.

Tödifirn

Tödifirn situated in the north-eastern slope of Glarner Tödi forms a step suspended ice front with frequent ice break-off events. Ice avalanches have been repeatedly observed to reach the Hinter Rötifirn located beneath a approx, 700 m high rock wall.

19 July 2020: An ice break-off triggered an ice avalanche that was closely observed by tourists sitting in front of the nearby Fridolinshütte. No damages are reported.

Triftgletscher (Weissmies)

In 2014 a portion of the glacierized north face of Weissmies became unstable and a teal-time monitoring system for early warning purpose has been installed (Section 6.2 of Volume 137/138).

2 July 2019: At the unstable hanging glacier an ice mass of about 100'000 m^3 broke off. Endangered are was relatively limited as the avalanche stopped at foot of the steep section of the north face. No damage occurred.

Triftgletscher (Zermatt)

24 July 2019: A sudden release of a water pocket of unknown origin in Triftgletscher caused a flood wave. In late afternoon overflow of the river channel with some damage on the settlement infrastructure occurred downstream in the Zermatt village. If a supraglacial lake visible on Sentinel satellite-images before and after the event was involved could not be verified. Only a supraglacial runoff could be excluded (Geoplan AG, 2020).

Turtmanngletscher

6 August 2020: The lower part of the tongue of Turtmanngletscher situated in a step section broke off. The subsequent ice avalanche was deposited on the dead-ice body in the glacier forefield. The ice mass that broke off was roughly estimated to about 100'000 m^3.

8 Area and volume of Swiss glaciers

8.1 Introduction

With increasing anthropogenic greenhouse gas emissions and corresponding global warming, glaciers in Switzerland are shrinking rapidly as in many mountain ranges on Earth. Detailed information on glacier coverage and thickness is not only needed to quantify glacier area and volume, but is also required for a wide range of glaciological and hydrological applications, with local impact e.g. on the energy sector, tourism industry and natural hazard management. Scientific application based on glacier area and volume estimates range from glacier-change assessments, mass balance and ice volume estimates, ice flow and estimates of past, present and future runoff, as well as projections of glacier mass loss to sea-level rise.

Repeated glacier inventories are therefore a key task to monitor overall glacier changes beyond a single glacier and provide detailed information on the glacier extent and additional important parameters such as area, elevation range, slope, aspect etc. for a given point or period in time. Based on the long-standing and intense cooperation between GLAMOS and swisstopo, sustainable synergies could be used to produce the latest Swiss Glacier Inventory for 2016 (SGI2016 Linsbauer et al., 2021) at a previously unachieved level of detail. The SGI2016 contains 1'400 glaciers covering an area of $961 \pm 22\,\mathrm{km}^2$ whereof 11%, or $104\,\mathrm{km}^2$, are debris-covered.

Within a large project at ETH Zurich (Grab et al., 2021), 251 glaciers – making up 81% of the glacierized area – have been covered by about 2'500 km of GPR surveys in order to directly measure the ice thickness. This large amount of data combined with two independent modelling algorithms for covering unmeasured areas resulted in glacier-wide ice thickness distribution and maps of glacier bed topography with an unprecedented accuracy. The total glacier volume in the Swiss Alps was thereby determined to be $58.7 \pm 2.5\,\mathrm{km}^3$ in the year 2016, over the extent given by the SGI2016. A projection of these results based on mass-balance data results in an estimated total ice volume of $52.9 \pm 2.7\,\mathrm{km}^3$ for the year 2020.

8.2 The New Swiss Glacier Inventory SGI2016

Previous glacier inventories and swisstopo baseline data

In Switzerland, topographical mapping has a long-standing tradition and swisstopo's topographical maps are famous for their precision, level of detail and temporal consistency. Starting from the

Dufour Map (1844-1864) to the Siegfried Map (1870-1926) and all the following releases of national topographic maps, swisstopo always sought to generate high precision topographical and geospatial information covering entire Switzerland, based on the latest technologies.

Based on the topographical maps and aerial images acquired by swisstopo, the Swiss Glacier Inventories (SGIs) SGI1850 (Maisch et al., 2000), SGI1973 (Müller et al., 1976) and SGI2010 (Fischer et al., 2014) were produced. The SGI2000 (Paul, 2003)(Paul, 2004) was fully based on satellite imagery and a semi-automated methodology that was also used for the inventories covering the entire European Alps for 2003 (Paul et al., 2011) and 2015 (Paul et al., 2020). All inventories are as accurate as possible, reflecting the possibilities and technologies available at the time of their establishment. In principle, the data sets can be divided into two classes: inventories based on (a) maps, aerial images and manual digitization of glacier outlines, and (b) satellite images and semiautomatic mapping. The two classes also differ in their spatial resolution, which is generally coarser for (b).

Even though most past inventories are derivatives from swisstopo data, they have so far not been co-produced by topographers (from swisstopo) and glaciologists. The compilation of Swiss Glacier Inventories was not an institutionalized task, and rather was based on research projects and individual initiatives. Since 2016, the task to regularly produce updated glacier inventories was assigned to GLAMOS, relying on swisstopo's accurate data products. Within defined time intervals (3 to 6 years), swisstopo acquires high-quality aerial images (0.1-0.25 m resolution) and digital elevation models (swissALTI3D, 2 m resolution) which are the base for the Topographic Landscape Model (swissTLM3D). The various objects are digitally recorded and stored with the aid of photogrammetric 3D evaluation, with an accuracy of about $\pm$ 1-3 m for landscape features. The swissTLM3D contains the mapping of all ground surface types, including "glaciers" and "debris" (also on glacier ice) and therefore serve as a perfect basis to compile repeated and high-resolution glacier inventories for Switzerland. The swissTLM3D is digitized by professional swisstopo topographers and serves primarily as a topographical land-cover data set, but requires further adaptations to meet the needs of a (glaciological) glacier inventory.

From a Topographical to a Glaciological Dataset

The swissTLM3D object class "glacier" is generally mapped on an extremely high level of detail. However, for a number of locations, entities were found that do not strictly belong to a glacier per definition (e.g. perennial snow patches and avalanche deposits at glacier margins, strongly debris-covered dead-ice bodies, permafrost features in very few cases). Based on previous SGIs, aerial photographs of the preceeding 5-10 years and glaciological knowledge, GLAMOS staff cross-checked all glacier boundaries. To create a glacier inventory fulfilling glaciological criteria, in some cases the outlines had to be simplified and some non-glacier features had to be removed. Thereafter a minimal glacier size threshold, defined as 0.01 km^2, was applied, the polylines were homogenized and generalized and the hydrologically-based unique SGI-IDs were assigned to the glacier entities. In order to get a layer of supraglacial debris cover, the glacier outlines were

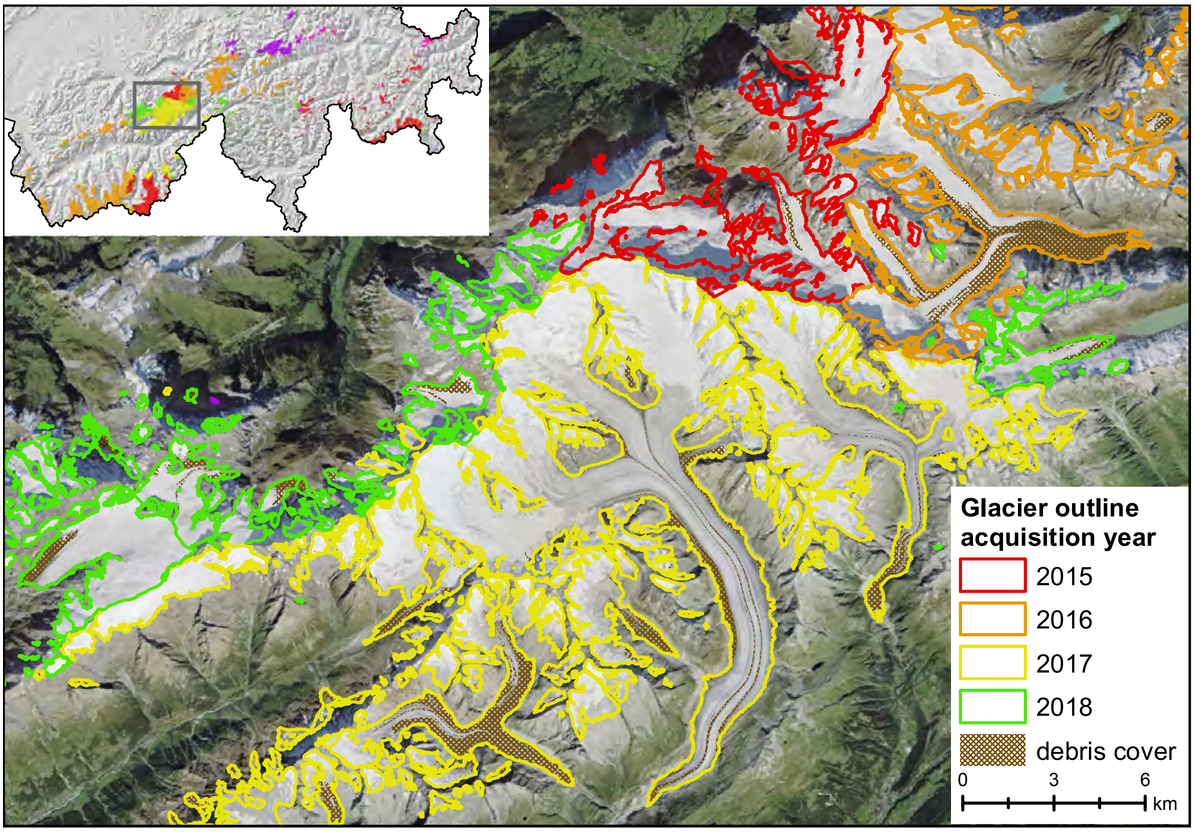

Figure 8.1: Glacier outlines colored according to the acquisition year of the aerial image used for digitizing. Overview map of entire Switzerland and selected area of the Bernese Alps with the debris cover indicated.

used to clip with the swissTLM3D object class "debris". Compiling the inventory parameter (e.g. area, elevation and slope variables) and preparing additional layers (e.g. debris cover, ice divides, center-lines) completes the data package. The Swiss Glacier Inventory 2016 (SGI2016) provides glacier outlines (areas), supraglacial debris cover, ice divides, center lines and location points of all glaciers in Switzerland referring to the years 2013-2018 and is openly available for download from the GLAMOS data portal (http://doi.glamos.ch/data/inventory/inventory_sgi2016_r2020.zip).

Key values on glacier area and debris cover for the SGI2016

The SGI2016 comprises 1,400 individual glacier entities (unique SGI-IDs) with a total surface area of $961 \pm 22\,\text{km}^2$. Most glacier entities are very small (82% of the glaciers are $<0.5\,\text{km}^2$), but the 46 glaciers with an area greater than $5\,\text{km}^2$ account for 52% of the total Swiss glacier area. The catchments of Rhine and Rhone show the highest glacierization (in terms of the number of glaciers with 46% and 41%, and in terms of area with 31% and 61%, respectively) (Table 1).

A new feature of the SGI2016 in comparison to typical glacier inventories is the separate debris-cover layer. Although large-scale data sets of supraglacial debris cover are available (Scherler et al., 2018; Herreid and Pellicciotti, 2020), the level of detail of the debris-cover product included in the SGI2016 paves the way for further process-based studies on feedback effects between debris cover and glacier evolution. Analyzing the dependencies between topographic parameters (mean slope, glacier length, median elevation) and debris-cover fraction reveals that short (<0.5 km) glaciers with a moderate mean slope (20-30 degrees) and a low median elevation (<2'600 m a.s.l.) tend to have high debris-cover fractions. In total, 11% (104.0 km^2) of the total Swiss glacier area were debris-covered in 2016. The share of debris-covered ice surfaces is similar in the Rhone, Rhine and Danube catchments (10-11%), but is higher (16%) in the Po catchment (Table 1).

Table 8.1: Area and ratio of debris-covered glacier surface per main hydrological catchment and for the entire inventory

	major river catchments				total
	Rhine (A)	Rhone (B)	Po (C)	Danube (E)	Switzerland
glacier count	639	570	84	107	1400
glacier area (km^2)	295.4	582.0	34.9	49.0	961.3
debris-cover (km^2)	33.4	60	5.4	5.2	104.0
ratio (%)	11.3	10.3	15.6	10.7	10.8

Area changes since 1973

Due to the fact that glaciers, separating into multiple entities over time, can be traced back to the parent glacier via unique SGI-IDs, a glacier-specific change assessment is possible. However, as all SGIs have been compiled based on different source data and somewhat differing methodologies, direct comparison requires caution. The area changes and time difference between SGI1973 and SGI2016 are sufficiently large that the effect of methodological differences is small in relation to the changes and a change assessment is possible.

The 2'732 mapped glacier entities in the SGI1973 cover an area of 1'311 km^2, and the 1'400 individual glaciers in the SGI2016 cover an area of 961 km^2. This corresponds to an overall area change of -350 km^2, -26.7% or $-0.6\%\,a^{-1}$ between 1973 and 2016. The strongest relative change in glacier area between 1973 and 2016 occurred in the Po catchment (-36.4%). Relative area change was least negative in the Rhone basin (-18.7%). These regional differences can be attributed to the glacier size distribution. Relative area changes are largest for small glaciers that are predominant in the Po catchment, whereas the Rhone basin includes the largest glaciers with smaller relative area changes (despite of large absolute area changes; e.g. the two largest glaciers: Grosser Aletschgletscher $-8.13\,km^2/-9.4\%$, Gornergletscher $-5.38\,km^2/-9.0\%$). A very clear dependence of relative area changes on classes of surface slope is evident: the steeper the glacier on average, the larger the relative area change. This finding corresponds to observations of glacier mass balances (e.g. Fischer et al., 2015; Brun et al., 2019). Small glaciers exhibit large relative area changes, and they are generally steeper than large glaciers. Furthermore, steep glaciers are thinner and will thus respond more quickly to a change in climate by adapting their length and thus area.

Glacier area change since the SGI2010

The total glacier area according to the last complete inventory, referring to the year 2010, SGI2010, amounts to $944 \pm 24\,\mathrm{km}^2$ (Fischer et al., 2014). In light of major glacier mass losses observed in the Alps between 2010 and 2016 (e.g. GLAMOS, 1881–2020; WGMS, 2020), this increase in glacier area is counter-intuitive, and is suspected to stem from methodological differences. Re-digitizing a sample of 100 selected glaciers from all size classes for the SGI2010 with the approaches and the definitions elaborated for the compilation of the SGI2016 results in generally larger glacier areas for 2010, particularly for highly debris-covered areas. By upscaling the results of the re-digitization experiment to all glaciers in the SGI2010 and area of 1,009 km2 was found. This indicates that an area change of −4.7% between SGI2010 and SGI2016 after correcting the observation-bias of the former.

Towards consistent, repeated glacier inventories

The production of the SGI2016 was only possible due to the close exchange between the topographers at swisstopo and the glaciologists at GLAMOS over the past years. It was self-evident to embed the production of the next Swiss glacier inventories into already existing products of swisstopo. The constraint to regularly produce an updated glacier inventory required both institutions to boost the cooperation and to start mutual learning. This process led to adapted and adjusted production guidelines on both sides. Meetings and workshops helped to understand the different professional backgrounds of topographers and glaciologists, to find common solutions for specific problems related to glacier mapping, and finally to derive a state-of-the-art glaciological data set. The SGI2016 influences the coming swissTLM3D releases and will streamline the production of future Swiss glacier inventories. The SGI2016 is the first step towards a consistent and accurate data product of repeated glacier inventories in six-year time intervals that promises a high comparability for individual glaciers and glacier samples, secured due to the integration into long-term projects on both sides.

8.3 Ice thickness distribution of all Swiss glaciers

Ice thickness measurements (GPR Data)

Since 2008 helicopter-based ground penetrating radar (GPR) systems have been used to efficiently acquire ice thickness data on glaciers in the Swiss Alps. Various systems have been deployed between 2008 and 2014 (Rutishauser et al., 2016). Further development resulted in the specially designed AIR-ETH helicopter-based GPR platform and data processing procedure (Langhammer et al., 2019) optimized for data acquisition on temperate mountain glaciers with complex geometry. Additional GPR measurements of 950 km profile length have been collected during 2016-2019 (Grab et al., 2021). GPR measurements are preferentially carried out in winter and spring when there is minimal melt water present that may cause scattering and hamper the

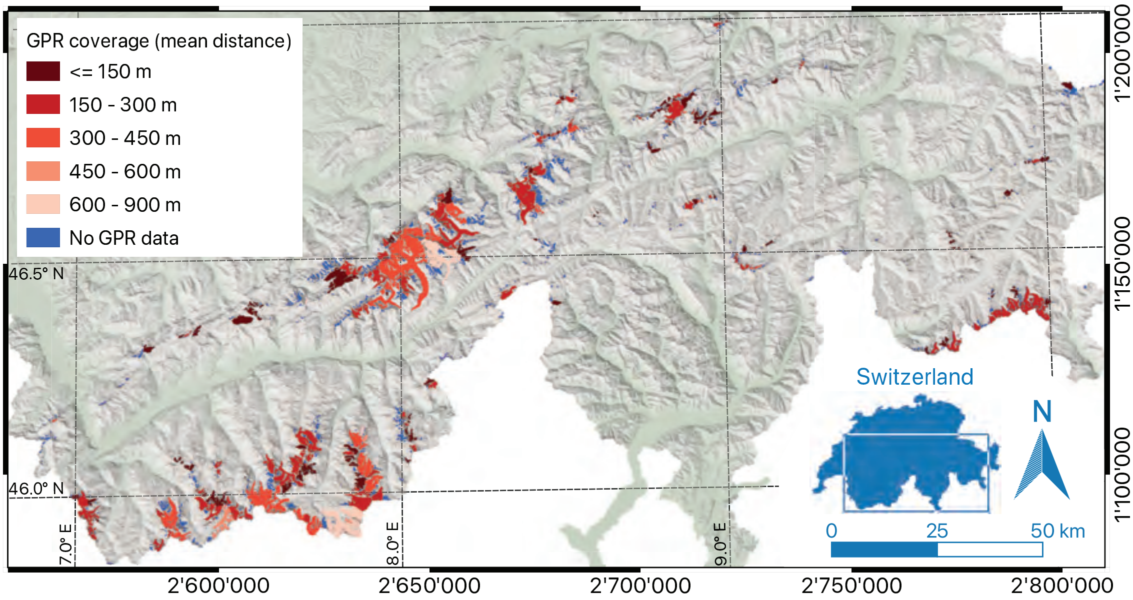

Figure 8.2: Overview of GPR coverage of all glaciers in the Swiss Alps. Available thickness measurements are color-coded indicating the mean of the distance of all grid points on a glacier to the closest thickness measurement. Glaciers with no direct thickness measurements are shown in blue.

penetration depth of the electromagnetic waves through temperate ice. In the first phase, selected and mainly large glaciers in the Western Swiss Alps have been surveyed. The focus in the more recent phase was to complement these sites by yet unsurveyed glaciers over the entire Swiss Alps. First ground-based GPR measurements on Swiss glaciers for determining the ice thickness date back to the 1980s. Many surveys were part of various projects and most data have not been published so far. In a special effort to recover historic, unpublished ice thickness measurements, an addition of 550 km profiles have been integrated from the archives of VAW.

Since these ice thickness measurements were acquired over various years and seasons, all measurements were standardized by subtracting the interpreted glacier bed elevation from the glacier surface elevation. In addition, the thickness has been corrected for the surface elevation change between the time of the measurement and the most recent digital elevation model (DEM) available. If no information on the surface elevation for the time of the measurement was documented or the datum used was not clear, the elevation model closest to the time of the measurement was consulted.

Figure 8.2 shows the achieved coverage of the data set over the Swiss Alps. As a measure of density in coverage, the mean distance of all measurements to a regular 10x10 m grid was calculated for each glacier. Ice thickness measurements exist for 251 glaciers and mean distances vary between 57 m at Glacier de la Plaine Morte with the best coverage and 810 m at Gornergletscher with the lowest measurement density, respectively. With a total area of 782 km^2, glaciers with GPR surveys correspond to 81% of the current total area of Swiss glaciers.

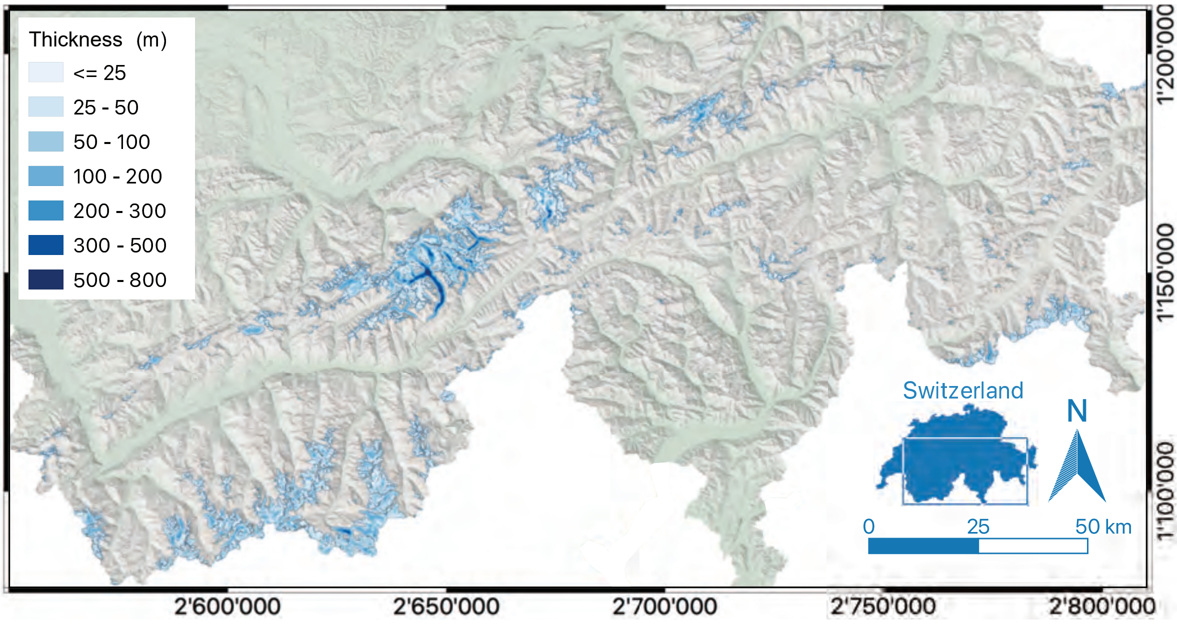

Figure 8.3: Ice thickness of glaciers in the Swiss Alps. Spatial distribution is shown for all glaciers of the SGI2016 extent.

Ice thickness distribution

A continuous area-wide spatial ice thickness distribution on a 10x10 m grid was derived from the ice thickness measurements acquired along profiles for all individual glaciers irrespective of the density of measurements. Two algorithms to infer ice thickness distribution from surface characteristics have been applied. Both approaches are based on the concept of mass conservation and ice flow mechanics and require a DEM of the glacier surface with a corresponding glacier outline as input (Grab et al., 2021). Available ice thickness measurements were directly integrated into the computed ice thickness distribution while the thickness in unmeasured regions was inferred by the locally optimized model. This approach also allows the calibrated models to optimally estimate the ice thickness distribution of glaciers without any direct measurements. The results of the two individual algorithms have been averaged to get a more robust final estimate of the ice thickness distribution. The glacier bed topography can be directly inferred by subtracting ice thickness distribution from surface topography.

The final ice thickness distribution of all glaciers in the Swiss Alps is shown in Figure 8.3. Larger ice masses are mainly found in Western Switzerland in the Valais and Bernese Alps. Grosser Aletschgletscher, the largest glacier in the Alps, reaches a maximum thickness of 790 m and an average thickness of 147 m was obtained. The data set is also available on Switzerland's web-map interface map.geo.admin.ch (topic Glacier thickness). The spatial ice thickness distribution as well as the location of the individual measurement profiles are visualized. Available meta-information on mean and maximum thickness, the year of survey and area of selected objects is provided.

Total glacier ice volume

The volume of the individual glaciers was determined by integration of the thickness over all individual grid cells. The volume refers to the survey years of glacier outline and the DEM of the surface topography. In order to provide a temporally consistent ice volume for the entire Swiss Alps, the results for the individual glaciers require a temporal homogenization to the center year 2016, also corresponding to the SGI2016. Therefore, the volume of each individual glacier was corrected to the center year using geodetic volume changes of 1980-2010 of each glacier (Fischer et al., 2015) and extrapolated year-to-year mass balance variability available for 20 glaciers (Bauder et al., 2020). Furthermore, this approach also allows inferring a annual time series of Swiss glacier volume over the last decades.

The uncertainty was assessed on point level, as well as at the glacier-scale for the volume. The uncertainty of the ice thickness at points includes the individual contribution of the uncertainty in GPR measurements, the surface elevation and spatial interpolation. Since these individual contributors are independent from each other, they are assumed to be uncorrelated. Therefore, the uncertainty of the total ice volume is expected to be smaller than the sum of the uncertainty of the ice thickness at points, as individual errors cancel out when averaged over the entire glacier or all glaciers.

A total ice volume of $58.7 \pm 2.5\,\mathrm{km}^3$ was determined for 2016 (see Figure 8.4). The 251 glaciers with ice thickness measurements sum up to a volume of $54\,\mathrm{km}^3$ or 93% of the total volume.

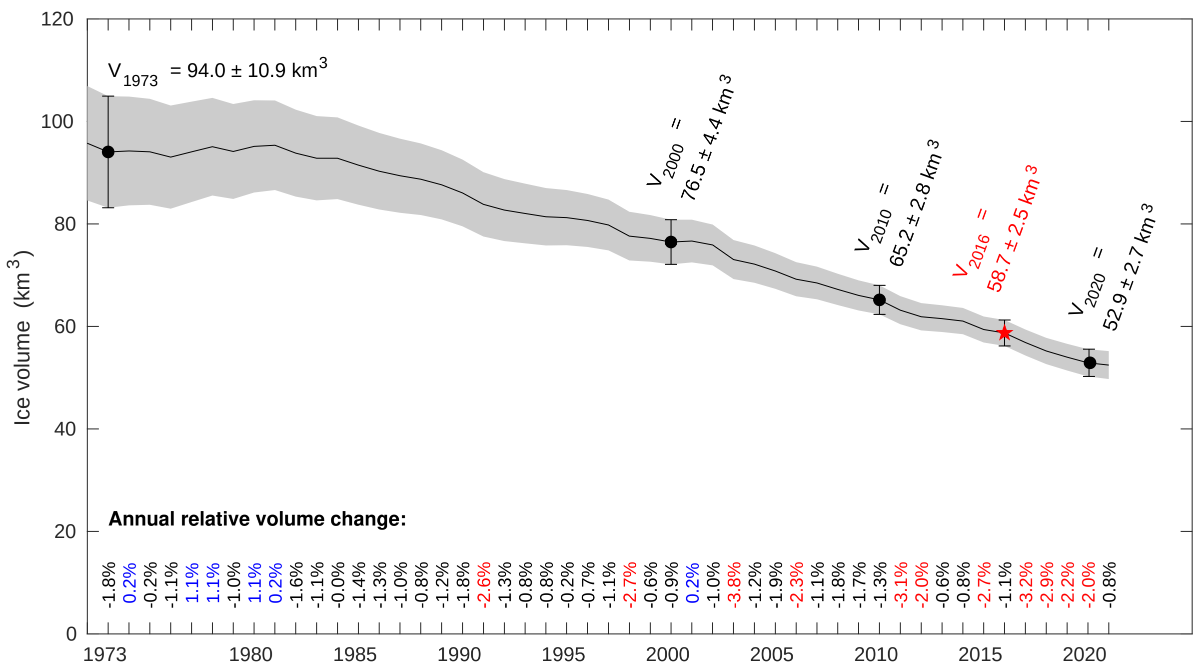

Figure 8.4: Temporal extrapolation of the total ice volume stored in Swiss glaciers for the period 1973-2021 based on the overall volume in 2016 (red asterisk). Total ice volume (black) with an uncertainty range (grey) and relative annual volume change is shown. Selected years correspond to available SGIs (see Section 8.2).

Grosser Aletschgletscher alone contains a volume of 11.7 km^3 of ice (2016), i.e. 20% of the total ice volume in the Swiss Alps. The uncertainty of $\pm 2.5\,km^3$ is 4.3% of the total volume and includes uncertainty contributions of 0.14 km^3 from glaciers with GPR measurements, 2.44 km^3 from glaciers where no GPR measurements have been acquired so far, uncertainty of 0.54 km^3 from surface elevation, 0.30 km^3 from area and 0.24 km^3 from the spatial interpolation. So the predominant contribution to the overall volume uncertainty stems from glaciers without direct measurements. These glaciers have an average ice thickness of less than 50 m and only contribute with 7% to the total volume. For glaciers with measurements, the uncertainty related to surface elevation is the most important contribution.

Data availability

The entire data set is available on the repository http://doi.org/10.3929/ethz-b-000434697. The data set covers all ice thickness measurements and a corresponding estimate of measurement uncertainty. For each glacier in the entire Swiss Alp maps of the ice thickness and the glacier bed topography are included. In addition, meta information regarding evaluation years of the ice thickness map and ice thickness uncertainty for each glacier are provided. This data base serves as an essential basis for various applications in research as well as assessments by public authorities or the general public.

Table 8.2: Area, mean (h_{mean}) and maximum (h_{max}) thickness and volume of the 100 largest glaciers in Switzerland sorted by decreasing volume, numbers refer to Table 3.1 and Appendix B

Glacier	No.	Area (km^2)	Volume km^3)	h_{mean} (m)	h_{max} (m)
Grosser Aletschgletscher	5	78.49	11.720	147.2	793.9
Gornergletscher	14	41.24	3.706	90.6	385.0
Fieschergletscher	4	29.75	3.532	116.9	436.7
Unteraargletscher	51	22.70	2.852	125.7	377.3
Rhonegletscher	1	14.64	1.456	99.4	418.9
Hüfifirn	73	12.63	1.227	104.2	304.7
Glacier de Corbassière	38	14.95	1.221	81.6	246.6
Oberaletschgletscher	6	17.05	1.201	68.1	225.3
Zmuttgletscher	15	14.82	1.022	69.7	265.4
Kanderfirn	109	11.97	1.015	90.9	227.8
Findelgletscher	16	13.87	1.012	73.5	206.2
Vadret da Morteratsch	94	14.93	0.899	61.4	280.7
Triftgletscher	55	14.56	0.802	55.1	324.1
Glacier d'Otemma	34	12.60	0.783	62.2	256.1
Glacier de Zinal	22	13.46	0.776	57.7	207.8
Turtmanngletscher	19	10.71	0.655	61.2	210.4
Glacier de la Plaine Morte	65	7.32	0.639	87.3	207.9
Unterer Grindelwaldgletscher	58	9.17	0.593	68.4	196.8
Allalingletscher	11	9.09	0.579	64.1	242.2
Gauligletscher	52	10.83	0.569	52.5	253.0
Feegletscher	13	13.83	0.562	41.2	161.2
Riedgletscher	17	7.23	0.551	76.4	194.8
Unterer Theodulgletscher		9.63	0.544	57.7	184.1
Glacier du Mont Miné	26	10.05	0.540	54.3	155.2
Vadrec del Forno	102	6.00	0.519	88.3	299.6
Glacier de Ferpècle	25	9.08	0.502	55.9	148.4
Langgletscher	18	8.01	0.487	59.1	203.6
Obers Ischmeer		7.34	0.477	67.7	273.2
Glacier de Saleinaz	42	6.69	0.455	68.1	203.0
Glacier du Trient	43	5.76	0.411	71.3	188.3
Glacier du Giétro	37	5.12	0.383	74.9	223.7
Glacier du Brenay	36	7.07	0.376	53.1	211.8
Rosenlauigletscher	56	5.38	0.340	63.2	219.9
Oberer Grindelwaldgletscher	57	8.33	0.335	43.6	179.7
Bas Glacier d'Arolla	27	5.07	0.300	59.8	192.6
Claridenfirn	141	4.71	0.296	68.1	216.2
Glacier du Mont Durand	35	6.21	0.270	43.4	154.3
Vadret da Tschierva	93	5.63	0.269	48.9	157.4
Griesgletscher	3	4.60	0.265	55.0	209.3
Glacier de Moiry	24	5.00	0.255	50.9	178.0
Tschingelgletscher	60	5.05	0.248	56.3	136.9

Glacier de Moming	23	5.43	0.244	44.9	189.4
Tellingletscher	193	5.13	0.225	50.4	138.9
Rottalgletscher (Lauterbrunnen)	243	3.62	0.225	67.5	213.7
Schwarzberggletscher	10	5.14	0.225	44.4	123.9
Mittelaletschgletscher	106	6.61	0.223	31.7	142.6
Vadret da Roseg	92	6.58	0.222	35.1	96.8
Glacier de Cheilon	29	3.51	0.209	59.5	193.6
Glacier de Tsanfleuron	33	2.44	0.206	84.3	175.2
Glacier de Tsijiore Nouve	28	2.82	0.195	69.3	180.4
Hobärggletscher	189	2.98	0.194	64.9	164.0
Hohlichtgletscher	186	4.54	0.189	42.2	193.9
Steingletscher	53	5.56	0.188	33.8	103.2
Bisgletscher	107	4.18	0.184	44.3	152.6
Mellichgletscher	184	3.08	0.170	55.5	113.2
Haut Glacier d'Arolla	205	3.62	0.161	45.6	137.2
Triftgletscher (Zermatt)	182	2.09	0.143	68.3	212.0
Vadret da Palü	100	5.37	0.142	29.1	84.0
Silvrettagletscher	90	2.67	0.141	55.1	119.8
Oberaargletscher	50	3.95	0.138	40.2	126.7
Vadrec da l'Albigna	116	2.40	0.135	57.7	151.5
Glatt Firn	139	2.80	0.129	46.2	95.8
Dammagletscher	70	3.77	0.124	32.8	63.9
Brunnifirn	72	2.19	0.115	52.5	152.3
Breithorngletscher (Lauterbrunnen)	241	2.53	0.114	52.4	189.1
Hohlaubgletscher	174	2.18	0.109	50.8	127.3
Hohwänggletscher	124	2.19	0.106	48.8	119.2
Bifertengletscher	77	2.60	0.104	46.9	109.5
Furgggletscher	181	3.82	0.102	27.8	91.7
Adlergletscher	383	2.10	0.095	46.0	133.4
Glacier d'Orny	108	1.31	0.093	70.7	133.6
Triftgletscher (Fieschertal)		1.94	0.091	45.3	101.6
Üssre Baltschiedergletscher	190	3.56	0.089	23.1	81.0
Glacier de Valsorey	39	2.03	0.088	43.4	88.0
Gabelhorngletscher	125	1.80	0.083	46.2	197.6
Weissmiesgletscher		1.92	0.082	41.4	116.8
Glacier de la Tsessette	215	2.06	0.081	39.2	74.7
Festigletscher	188	1.81	0.079	44.1	121.9
Wildstrubelgletscher	63	2.34	0.079	33.6	85.5
Hengsterengletscher NE		1.71	0.076	47.0	116.9
Vadret Tiatscha	96	1.87	0.076	43.2	92.2
Griessgletscher	74	2.08	0.075	41.3	104.3
Innre Baltschiedergletscher		1.68	0.075	42.5	109.3
Oberer Theodulgletscher	180	2.42	0.075	31.9	105.0
Minstigergletscher	164	2.19	0.075	32.0	96.3
Vadrec da Fedoz		1.90	0.073	40.0	111.7
Alpjergletscher		2.09	0.072	32.4	83.6
Mellichgletscher		1.53	0.072	47.3	125.2
Breithorngletscher (Zermatt)		1.95	0.069	35.9	64.0

Wendengletscher	369	1.66	0.068	41.2	145.8
Bidergletscher	177	1.25	0.068	54.4	112.3
Blüemlisalpgletscher	64	2.23	0.067	35.9	80.5
Blüemlisalpfirn		2.16	0.066	36.2	67.5
Flachensteinfirn	137	2.27	0.064	28.3	54.6
Giessengletscher	240	1.66	0.063	42.7	119.8
Kingletscher	361	1.17	0.062	53.3	144.2
Glatscher da Medel	280	1.78	0.062	34.9	74.0
Glacier de l'A Neuve	129	1.94	0.062	31.9	116.9
Driestgletscher	171	1.80	0.062	32.2	62.7
Vadret dal Tremoggia		1.83	0.061	34.5	85.3

8.4 Conclusion

The new Swiss Glacier Inventory SGI2016 that has been acquired based on high-resolution aerial imagery and digital elevation models (swissALTI3D, with 2 m resolution) in cooperation with swisstopo and GLAMOS brings together topographical and glaciological knowledge. Thereby the process, workflow and required glaciological adaptations to compile a highly detailed glacier inventory based on the swissTLM3D has been defined. This is the first step towards a consistent and high-quality data product of repeated glacier inventories in six-year time steps providing a high comparability for individual glaciers and glacier samples. The SGI2016 provides glacier outlines (area), supraglacial debris cover, ice divides, center lines and location points of all glaciers in Switzerland referring to the years 2013-2018. The data set contains 1'400 individual glacier entities with a total glacier surface area of $961 \pm 22\,\mathrm{km}^2$ (whereof 11%, or $104\,\mathrm{km}^2$ are debris-covered) and constitutes the so far most detailed cartographic representation of the glacier extent in Switzerland. The resulting high-resolution glacier inventory will support process studies and model validation/calibration for glaciers in the Swiss Alps. Since 2008 the Swiss glaciers were systematically surveyed for ice thickness using helicopter-borne GPR measurements. In the meantime, 2450 km of measurements exist for 251 glaciers that sum up to 81% of the glacierized area in the Swiss Alps. All available ice thickness measurements have been consistently compiled and harmonized with glacier surface elevation of the same datum allowing the glacier bed elevation to be calculated. This step was necessary to evaluate the spatial thickness distribution and to calculate the corresponding ice volume. A total volume of $58.7 \pm 2.5\,\mathrm{km}^3$ was obtained for the year 2016 and the corresponding extent of SGI2016. With regard to the ongoing mass loss, in 2021 a volume of $52.5 \pm 2.7\,\mathrm{km}^3$ was left.

References

Alean, J., Haeberli, W., and Schädler, B. (1983). Snow accumulation, firn temperature and solar radiation in the area of the Colle Gnifetti core drilling site (Monte Rosa, Swiss Alps): distribution patterns and interrelationships. *Zeitschrift für Gletscherkunde und Glazialgeologie*, 19(2):131–147.

Amt für Forst und Jagd (2019). Ausbruch Griesseeli, Spiringen-Urnerboden – Ereignisbericht. Technical report, Amt für Forst und Jagd, Abteilung Naturgefahren, Kanton Uri. pp. 28.

Antoni, C. (2005). Langjährige Messreihen in den Schweizer Alpen. Praktikumsararbeit ausgeführt an der VAW, ETH Zürich, unter Anleitung von A. Bauder (unveröffentlicht).

Bauder, A., Funk, M., and Bösch, H. (2002). Glaziologische Untersuchungen am Glacier de Giétro im Zusammenhang mit der Sicherheit der Stauanlage Mauvoisin. In *Moderne Methoden und Konzepte im Wasserbau*, volume 175, (Band 2), pages 419–431. Mitteilung der Versuchsanstalt für Wasserbau, Hydrologie und Glaziologie, ETH Zürich. Internationales Symposium 7.-9. Oktober 2002 in Zürich.

Bauder, A., Funk, M., and Huss, M. (2007). Ice volume changes of selected glaciers in the Swiss Alps since the end of the 19th century. *Annals of Glaciology*, 46:145–149.

Bauder, A., Huss, M., and Linsbauer, A., editors (2020). *The Swiss Glaciers 2017/18 and 2018/19*, volume 139/140 of *Glaciological Report*. Cryospheric Commission (EKK) of the Swiss Academy of Sciences (SCNAT).

Begert, M. and Frei, C. (2018). Long-term area-mean temperature series for Switzerland – Combining homogenized station data and high resolution grid data. *International Journal of Climatology*, 38(6):2792–2807.

Begert, M., Schlegel, T., and Kirchhofer, W. (2005). Homogeneous temperature and precipitation series of switzerland from 1864 to 2000. *International Journal of Climatology*, 25(1):65–80.

Blatter, H. and Hutter, K. (1991). Polythermal conditions in Arctic glaciers. *Journal of Glaciology*, 37(126):261–269.

Brun, F., Wagnon, P., Berthier, E., Jomelli, V., Maharjan, S. B., Shrestha, F., and Kraaijenbrink, P. D. A. (2019). Heterogeneous influence of glacier morphology on the mass balance variability in High Mountain Asia. *Journal of Geophysical Research*, 124(6):1331–1345.

Cuffey, K. M. and Paterson, W. S. B. (2010). *The Physics of Glaciers*. Elsevier B.V., New York, forth edition. pp. 480.

Faillettaz, J., Pralong, A., Funk, M., and Deichmann, N. (2008). Evidence of log-periodic oscillations and increasing icequake activity during the breaking-off of large ice masses. *Journal of Glaciology*, 54(187):725–737.

Firnberichte (1914–1978). *Der Firnzuwachs 1913/14–1976/77 in einigen schweizerischen Firngebieten*, number 1-64 in Vierteljahrsschrift der Naturforschenden Gesellschaft in Zürich. Jahresberichte herausgegeben von der Gletscher-Kommission der Physikalischen Gesellschaft Zürich, später Schweizerische Meteorologische Zentralanstalt und ab 1973 durch A. Lemans.

Fischer, M., Huss, M., Barboux, C., and Hoelzle, M. (2014). The new swiss glacier inventory SGI2010: Relevance of using high-resolution source data in areas dominated by very small glaciers. *Arctic, Antarctic, and Alpine Research*, 46(4):933–945.

Fischer, M., Huss, M., and Hoelzle, M. (2015). Surface elevation and mass changes of all Swiss glaciers 1980–2010. *The Cryosphere*, 9(2):525–540.

Gabbi, J., Huss, M., Bauder, A., Cao, F., and Schwikowski, M. (2015). The impact of Saharan dust and black carbon on albedo and long-term mass balance of an Alpine glacier. *The Cryosphere*, 9(4):1385–1400.

Geibel, L., Huss, M., Kurzböck, C., Hodel, E., Bauder, A., and Farinotti, D. (2022). Rescue and homogenisation of 140 years of glacier mass balance data in Switzerland. *Earth System and Science Data*, 14(7):3293–3312.

Geoplan AG (2020). Diskussion Auslösemechanismus Hochwasserereignis Triftbach Zermatt 24. Juli 2019. Technical Report VS 500013, Geoplan AG, 3940 Steg VS. pp. 12.

GLAMOS (1881–2020). The Swiss Glaciers, 1880–2018/19. Yearbooks 1-140, Cryospheric Commission of the Swiss Academy of Sciences (SCNAT). published since 1964 by Laboratory of Hydraulics, Hydrology and Glaciology (VAW) of ETH Zürich, www.glamos.ch.

GLAMOS (2020a). Computation of glacier-wide mass balance: evaluating the potential of the linear mass balance model. Internal Report 3, Glacier Monitoring Switzerland.

GLAMOS (2020b). Revised strategy for monitoring glacier length variation. Internal Report 4, Glacier Monitoring Switzerland.

Grab, M., Mattea, E., Bauder, A., Huss, M., Rabenstein, L., Hodel, E., Linsbauer, A., Langhammer, L., Schmid, L., Church, G., Hellmann, S., Déèze, K., Schaer, P., Lathion, P., Farinotti, D., and Maurer, H. (2021). Ice thickness distribution of all Swiss glaciers based on extended ground-penetrating radar data and glaciological modeling. *Journal of Glaciology*, 67(266):1074–1092.

Gugerli, R., Guidicelli, M., Gabella, M., Huss, M., and Salzmann, N. (2021). Multi-sensor analysis of monthly gridded snow precipitation on alpine glaciers. *Advances in Research and Science*, 18:7–20.

Gugerli, R., Salzmann, N., Huss, M., and Desilets, D. (2019). Continuous and autonomous snow water equivalent measurements by a cosmic ray sensor on an alpine glacier. *The Cryosphere*, 13(12):3413–3434.

Haeberli, W. and Funk, M. (1991). Borehole temperatures at the Colle Gnifetti core drilling site (Monte Rosa, Swiss Alps). *Journal of Glaciology*, 37(125):37–46.

Herreid, S. and Pellicciotti, F. (2020). The state of rock debris covering earth's glaciers. *Nature Geoscience*, 13(9):621–627.

Hoelzle, M., Darms, G., Lüthi, M. P., and Suter, S. (2011). Evidence of accelerated englacial warming in the Monte Rosa area, Switzerland/Italy. *The Cryosphere*, 5(1):231–243.

Hoelzle, M., Haeberli, W., Dischl, M., and Peschke, W. (2003). Secular glacier mass balances derived from cumulative glacier length changes. *Global and Planetary Change*, 36(4):295–306.

Huss, M. (2010). Mass balance of Pizolgletscher. *Geographica Helvetica*, 65(2):80–91.

Huss, M. and Bauder, A. (2009). 20th-century climate change inferred from four long-term point observations of seasonal mass balance. *Annals of Glaciology*, 50(50):207–214.

Huss, M., Bauder, A., and Funk, M. (2009). Homogenization of long-term mass-balance time series. *Annals of Glaciology*, 50(50):198–206.

Huss, M., Dhulst, L., and Bauder, A. (2015). New long-term mass balance series for the Swiss Alps. *Journal of Glaciology*, 61(227):551–562.

Huss, M., Schwyn, U., Bauder, A., and Farinotti, D. (2021). Quantifying the overall effect of artificial glacier melt reduction in Switzerland, 2005-2019. *Cold Regions Science and Technology*, 184(4):103237.

Huss, M., Voinesco, A., and Hoelzle, M. (2013). Implications of climate change on Glacier de la Plaine Morte, Switzerland. *Geographica Helvetica*, 68(4):227–237.

Kasser, P., Aellen, M., and Siegenthaler, H. (1986). Clariden. In *Die Gletscher der Schweizer Alpen, 1977/78 und 1978/79*, volume 99/100 of *Glaziologisches Jahrbuch der Gletscherkommission SNG*, pages 142–148. Versuchsanstalt für Wasserbau, Hydrologie und Glaziologie der ETH Zürich.

Landmann, J. M., Künsch, H. R., Huss, M., Ogier, C., Kalisch, M., and Farinotti, D. (2021). Assimilating near-real-time mass balance stake readings into a model ensemble using a particle filter. *The Cryosphere*, 15(11):5017–5040.

Langhammer, L., Rabenstein, L., Schmid, L., Bauder, A., Grab, M., Schaer, P., and Maurer, H. (2019). Glacier bed surveying with helicopter-borne dual-polarization ground-penetrating radar. *Journal of Glaciology*, 65(249):123–135.

Laternser, M. (1992). Firntemperaturmessungen in den Schweizer Alpen. Diploma thesis (unpublished), ETH Zürich. pp. 99.

Linsbauer, A., Huss, M., Hodel, E., Bauder, A., Fischer, M., Weidmann, Y., Bärtschi, H., and Schmassmann, E. (2021). The New Swiss Glacier Inventory SGI2016: From a Topographical to a Glaciological Dataset. *Frontiers in Earth Science*, 9:774.

Lüthi, M. (2000). Rheology of cold firn and dynamics of a polythermal ice stream: Studies on Colle Gnifetti and Jakobshavns Isbræ. Mitteilung 165, Versuchsanstalt für Wasserbau, Hydrologie und Glaziologie der ETH Zürich. pp. 212.

Maisch, M., Wipf, A., Denneler, B., Battaglia, J., and Benz, C. (2000). *Die Gletscher der Schweizer Alpen*. vdf, Hochschulverlag AG an der ETH Zürich, Zürich, 2. edition. Schlussbericht NFP31, 373 pp., ISBN 3 7281 2733 7.

Mattea, E. (2020). Measuring and modelling changes in the firn at Colle Gnifetti, 4400 m a.s.l., Swiss Alps. Msc thesis, Faculty of sciences and medicine, Department of Geosciences. University of Fribourg. pp. 128.

Müller, F., Caflisch, T., and Müller, G. (1976). Firn und Eis der Schweizer Alpen: Gletscherinventar. Publ. Nr. 57, Geographisches Institut der ETH Zürich, Zürich.

Müller, H. and Kappenberger, G. (1991). Claridenfirn-Messungen 1914-1984. Heft 40, Zürcher Geographische Schriften, Geographisches Institut der ETH Zürich. pp. 79.

Naegeli, K., Damm, A., Huss, M., Schaepman, M., and Hoelzle, M. (2015). Imaging spectroscopy to assess the composition of ice surface materials and their impact on glacier mass balance. *Remote Sensing of Environment*, 168:388–402.

Ogier, C., Werder, M. A., Huss, M., Kull, I., Hodel, D., and Farinotti, D. (2021). Drainage of an ice-dammed lake through a supraglacial stream: hydraulics and thermodynamics. *The Cryosphere*, 15(11):5133–5150.

Ohmura, A., Bauder, A., Müller, H., and Kappenberger, G. (2007). Long-term change of mass balance and the role of radiation. *Annals of Glaciology*, 46:367–374.

Østrem, G. and Brugman, M. (1991). Glacier mass-balance measurements – a manual for field and office work. Technical report, National Hydrology Research Institute. NHRI Science Report No. 4.

Paul, F. (2003). *The New Swiss Glacier Inventory 2000. Application of Remote Sensing and GIS*. PhD thesis, University of Zürich. 192 pp.

Paul, F., Frey, H., and Bris, R. L. (2011). A new glacier inventory for the European Alps from Landsat TM scenes of 2003: challenges and results. *Annals of Glaciology*, 52(59):144–152.

Paul, F., Rastner, P., Azzoni, R. S., Diolaiuti, G., Fugazza, D., Bris, R. L., Nemec, J., Rabatel, A., Ramusovic, M., Schwaizer, G., and Smiraglia, C. (2020). Glacier shrinkage in the alps continues unabated as revealed by a new glacier inventory from Sentinel-2. *Earth System and Science Data Discussions*, 12(3):1805–1821.

Raymond, M., Wegmann, M., and Funk, M. (2003). Inventar gefährlicher Gletscher in der Schweiz. Mitteilungen 182, Versuchsanstalt für Wasserbau, Hydrologie und Glaziologie der ETH Zürich, Gloriastrasse 37-39, CH-8092 Zürich. pp. 368.

Reijmer, C. H., van den Broeke, M. R., Fettweis, X., Ettema, J., and Stap, L. B. (2012). Refreezing on the Greenland ice sheet: a comparison of parameterizations. *The Cryosphere*, 6(4):743–762.

Rutishauser, A., Maurer, H., and Bauder, A. (2016). Helicopter-borne ground-penetrating radar investigations on temperate alpine glaciers: A comparison of different systems and their abilities for bedrock mapping. *GEOPHYSICS*, 81(1):WA119–WA129.

Scherler, D., Wulf, H., and Gorelick, N. (2018). Global assessment of supraglacial debris-cover extents. *Geophysical Research Letters*, 45(21):11798–11805.

Suter, S. (2002). Cold firn and ice in the Monte Rosa and Mont Blanc areas: spatial occurrence, surface energy balance and climatic evidence. Mitteilung 172, Versuchsanstalt für Wasserbau, Hydrologie und Glaziologie der ETH Zürich. pp. 188.

Suter, S. and Hoelzle, M. (2002). Cold firn in the Mont Blanc and Monte Rosa areas, European Alps: spatial distribution and statistical models. *Annals of Glaciology*, 35(1):9–18.

Suter, S., Laternser, M., Haeberli, W., Frauenfelder, R., and Hoelzle, M. (2001). Cold firn and ice of high-altitude glaciers in the Alps: measurements and distribution modelling. *Journal of Glaciology*, 47(156):85–96.

Van Tricht, L., Huybrechts, P., Van Breedam, J., Vanhulle, A., Van Oost, K., and Zekollari, H. (2021). Estimating surface mass balance patterns from unoccupied aerial vehicle measurements in the ablation area of the Morteratsch-Pers glacier complex (Switzerland). *The Cryosphere*, 15(9):4445–4464.

VAW (1997). Gletscherveränderungen im Val de Bagnes 1966 – 1996. Untersuchungen im Zusammenhang mit den Anlagen der Kraftwerke Mauvoisin AG. Zusammenfassend dargestellte Hauptergebnisse der jährlichen Messungen. Bericht Nr. 7903.55.04 (M. Aellen, unveröffentlicht). Im Auftrag der Kraftwerke Mauvoisin AG.

VAW (1998). Mauvoisin – Giétrogletscher – Corbassièregletscher. Glaziologische Studien im Zusammenhang mit den Stauanlagen Mauvoisin. Bericht Nr. 55.05.7903 (M. Funk, unveröffentlicht). Im Auftrag der Elektrizitätsgesellschaft Lauffenburg AG.

VAW (1999). Mattmark – Zusammenfassender Bericht über die hydrologischen und glaziologischen Messungen im Mattmarkgebiet. Bericht Nr. 7902.52.45 (H. Bösch und M. Funk, unveröffentlicht), Versuchsanstalt für Wasserbau, Hydrologie und Glaziologie der ETH Zürich. Im Auftrag der Kraftwerke Mattmark AG.

VAW (2022). Allalin-Gletscher – Bericht über die hydrologischen und glaziologischen Verhältnisse im Mattmarkgebiet 2020/2021. Bericht Nr. 7902-VAW-2022-03 (A. Bauder, unveröffentlicht), Versuchsanstalt für Wasserbau, Hydrologie und Glaziologie der ETH Zürich. Im Auftrag der Kraftwerke Mattmark AG.

Vincent, C., Gilbert, A., Jourdain, B., Piard, L., Ginot, P., Mikhalenko, V., Possenti, P., Meur, E. L., Laarman, O., and Six, D. (2020). Strong changes in englacial temperatures despite insignificant changes in ice thickness at Dôme du Goûter glacier (Mont Blanc area). *The Cryosphere*, 14(3):925–934.

WGMS (2020). Global Glacier Change Bulletin No. 3 (2016–2017). ICSU(WDS)-IUGG(IACS)-UNEP-UNESCO/WMO, World Glacier Monitoring Service, Zurich, Switzerland.

w/s/l (2014). Sicherheitskonzept Bisgletscher, Mess- und Alarmsystem Bisbachlawine. Technical report, wasser/schnee/lawinen - Ingenieurbüro André Burkard AG, Brig. pp. 16.

Zekollari, H., Huss, M., and Farinotti, D. (2020). On the imbalance and response time of glaciers in the european alps. *Geophysical Research Letters*, 47(2):e2019GL085578.

Zekollari, H. and Huybrechts, P. (2018). Statistical modelling of the surface mass-balance variability of the Morteratsch glacier, Switzerland: strong control of early melting season meteorological conditions. *Journal of Glaciology*, 64(244):275–288.

Zoller, N. (2010). Fliessbewegung des Grossen Aletschgletschers. Bachelorarbeit, Departement Erdwissenschaften / Versuchsanstalt für Wasserbau, Hydrologie und Glaziologie (VAW), ETH Zürich. pp. 45.

Acknowledgements

The Cryospheric Commission through its GLAMOS programme acknowledges long-term funding by the Federal Office for the Environment (BAFU), MeteoSwiss within GCOS Switzerland, the Swiss Academy of Sciences (SCNAT), and the support by the Federal Office of Topography swisstopo. GLAMOS again received solid support in this 141st/142nd measuring period from its reliable team of observers. Sincere thanks for their cooperation are extended to: the forestry services from the cantons of Berne, Glarus, Grisons, Obwalden, St. Gallen, Uri, Ticino, Vaud and Wallis, the staff of the hydro-power stations Aegina, Mattmark, Mauvoisin and, Oberhasli, all the individual helpers and the Aerial Photography Flying and Coordination Service (CCAP) of the Swiss Federal Office of Topography swisstopo. Colleagues from VAW / ETH Zürich and the Geographical Institutes of the University of Fribourg and Zürich provided valuable contributions to the publication of this glaciological report. Barbara Bauder is acknowledged for typewriting the many remarks on the individual glaciers.

A Remote Sensing

A.1 Aerial photographs

Aerial photographs are taken at periodic intervals by Swiss Federal Office of Topography swisstopo in order to provide a baseline documentation for various applications (mapping, glacier change, natural hazards, etc). In addition to the periodical surveys, high resolution aerial photographs have been acquired which are designed in particular for glaciological applications. These are listed in the following tables (A.1 and A.2). Not listed are the routinely aerial photos by swisstopo for updating their standard products (National Maps, orthophoto or DEM). In the year 2020, pictures were taken for the areal of the Cantons VD and VS, and in 2021 of the Cantons BE, OW, TI and UR, respectively. More detailed information is available on swisstopo's webviewer http://www.luftbildindex.ch.

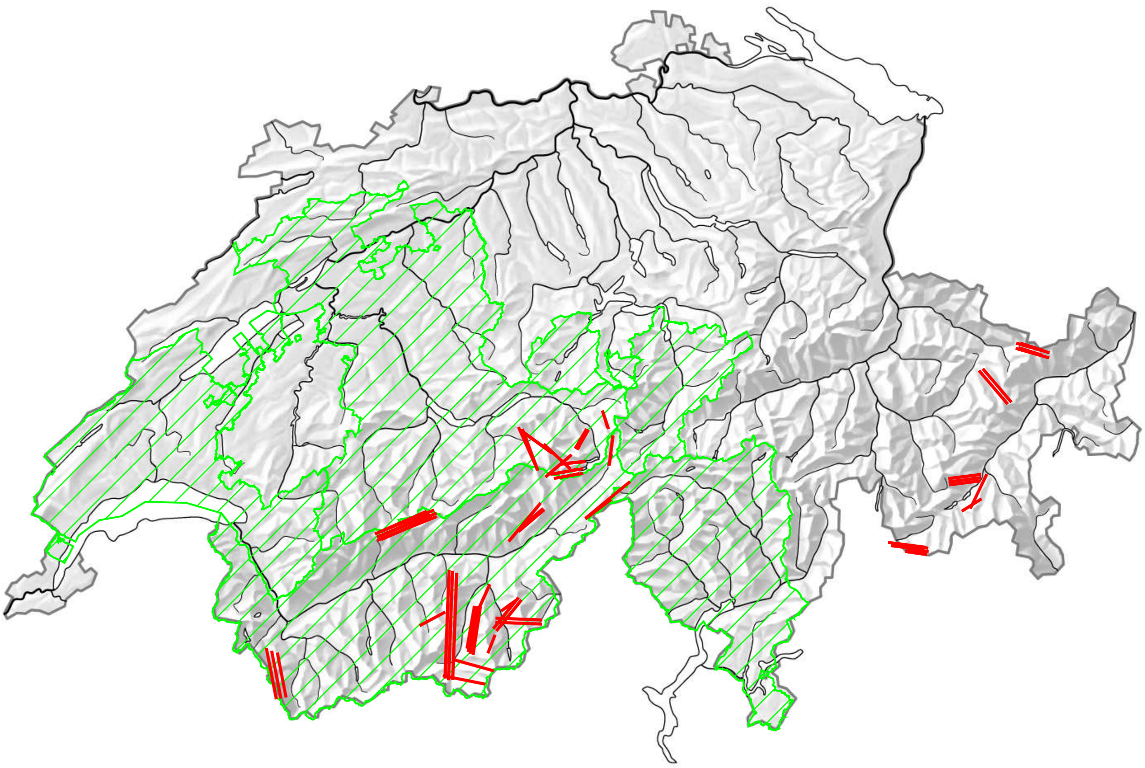

Figure A.1: Aerial photographs from the years 2020 and 2021 with specific surveys on glaciers (red) and coverage of swisstopo's periodic survey (green)

Table A.1: Aerial photographs taken in 2020.

Glaciers	Ct.	Date	Line No.	GSD
Ärlen c, Wiisenbach c, Golegg c, Grueben p	BE	09.09.20	12501202009090829	0.12
Bis p, Schali p, Hohlicht p, Brunegg p, Abberg c, Schölli c, Stelli c	VS	09.09.20	12501202009091028	0.2
Bis p, Schali p, Hohlicht p, Brunegg p, Piipji c, Abberg c, Schölli c, Stelli c, Jung c	VS	09.09.20	12501202009091046	0.2
Bis p, Schali p, Hohlicht p, Turtmann p, Brunegg p, Schölli c, Piipji c	VS	09.09.20	12501202009091056	0.2
Cengal c, Bondasca c, Trubinasca c	GR	09.09.20	12501202009090904	0.12
Cengal c, Bondasca p, Trubinasca p, Albigna p	GR	09.09.20	12501202009090911	0.12
Cengal p, Bondasca p	GR	09.09.20	12501202009090916	0.12
Corvatsch p	GR	09.09.20	12501202009090921	0.1
Gries c, Corno p, Chüeboden c, Sulz c, Blinnen p	VS	09.09.20	12501202009090750	0.2
Grosser Aletsch p	VS	14.09.20	12501202009141033	0.12
Gruebu p, Gamsa p, Mattwald c, Griessernu c, Rossbode p	VS	14.09.20	12501202009141002	0.12
Grüebu p, Fletschhorn c, Rossbode c	VS	14.09.20	12501202009141012	0.12
Grüebu p, Mattwald c	VS	14.09.20	12501202009140948	0.1
Ob. Grindelwald p, Wächselberg p	BE	13.09.20	12501202009131046	0.2
Oberaar c, Fiescher p	BE	09.09.20	12501202009090811	0.12
Oberaar p, Unteraar p, Fiescher p	BE	09.09.20	12501202009090805	0.12
Plaine Morte p, Lämmern c, Schwarz p	BE, VS	13.09.20	12501202009131004	0.12
Plaine Morte p, Tierberg c, Wildstrubel p, Steghorn c, Tälli c, Schwarz p, Altels c	BE, VS	13.09.20	12501202009131021	0.12
Plaine Morte p, Wildstrubel p, Lämmern p, Schwarz p	BE, VS	13.09.20	12501202009131013	0.12
Radönt c, Schwarzhorn c	GR	09.09.20	12501202009090945	0.12
Radönt p, Schwarzhorn c	GR	09.09.20	12501202009090939	0.12
Rhone p	VS	13.09.20	12501202009131054	0.12
Ried p	VS	14.09.20	12501202009141027	0.12
Silvretta c, Verstancla p, Tiatscha p, Plan Rai p	GR	13.09.20	12501202009130839	0.12
Silvretta p, Verstancla c, Vernela c, Maisas p, Tiatscha c, Plan Rai c	GR	13.09.20	12501202009130845	0.12
Trift p	BE	13.09.20	12501202009131116	0.12
Unt. Grindelwald p	BE	13.09.20	12501202009131038	0.2
Unteraar p	BE	13.09.20	12501202009131059	0.12
Unteraar p	BE	13.09.20	12501202009131105	0.12
Unteraar p, Ob. Grindelwald p	BE	09.09.20	12501202009090837	0.12

c Glacier shown completely
p Glacier shown partially

GSD: Ground sampling distance in (m)

Table A.2: Aerial photographs taken in 2021.

Glaciers	Ct.	Date	Line No.	GSD
A Neuve ^{p}, Orny ^{p}, Saleina ^{p}, Evole ^{c}, Planeureuse ^{c}, Tretsebo ^{c}, Dolent ^{p}		14.08.21	12501202108141802	0.2
A Neuve ^{p}, Trient ^{p}, Grands ^{p}, Saleina ^{p}, Dolent ^{p}		14.08.21	12501202108141644	0.15
A Neuve ^{p}, Trient ^{p}, Orny ^{p}, Saleina ^{p}, Planeureuse ^{p}, Tretsebo ^{c}, Dolent ^{c}		14.08.21	12501202108141654	0.2
Ärlen ^{c}, Wiisenbach ^{c}, Golegg ^{p}	BE	24.09.21	12504202109241041	0.1
Ärlen ^{p}, Wiisenbach ^{c}, Golegg ^{c}, Grueben ^{p}	BE	24.09.21	12504202109241034	0.1
Bis ^{p}, Schali ^{p}, Hohlicht ^{p}, Brunegg ^{p}, Abberg ^{c}, Schölli ^{c}, Stelli ^{c}	VS	14.08.21	12501202108141027	0.2
Bis ^{p}, Schali ^{p}, Hohlicht ^{p}, Brunegg ^{p}, Piipji ^{c}, Abberg ^{c}, Schölli ^{c}, Stelli ^{c}, Jung ^{c}, Unterer Theodul ^{p}	VS	14.08.21	12501202108141016	0.15
Bis ^{p}, Schali ^{p}, Hohlicht ^{p}, Turtmann ^{p}, Brunegg ^{p}, Schölli ^{c}, Piipji ^{c}, Oberer Theodul ^{p}	VS	14.08.21	12501202108141005	0.15
Cengal ^{c}, Bondasca ^{c}, Trubinasca ^{c}, Albigna ^{p}	GR	01.09.21	12501202109011825	0.12
Cengal ^{p}, Bondasca ^{p}, Albigna ^{p}	GR	01.09.21	12501202109011841	0.12
Cengal ^{p}, Bondasca ^{p}, Trubinasca ^{p}, Albigna ^{p}	GR	01.09.21	12501202109011833	0.12
Corvatsch ^{c}, Rosatsch ^{c}	GR	01.09.21	12501202109011035	0.1
Diablons ^{c}, Turtmann ^{p}, Brunegg ^{p}	VS	14.08.21	12501202108141039	0.15
Fee ^{p}, Hohlaub ^{p}, Chessjen ^{p}	VS	14.08.21	12501202108141856	0.15
Findelen ^{p}	VS	14.08.21	12501202108141027	0.2
Gorner ^{p}		14.08.21	12501202108141049	0.15
Gries ^{c}, Sulz ^{c}, Blinnen ^{c}, Rappen ^{c}, Fäldbach ^{c}	VS	24.09.21	12504202109241055	0.1
Grosser Aletsch ^{p}	VS	29.07.21	12504202107291020	0.12
Grosser Aletsch ^{p}	VS	29.07.21	12504202107291042	0.08
Grosser Aletsch ^{p}	VS	29.07.21	12504202107291035	0.08
Gruebu ^{p}, Gamsa ^{p}, Mattwald ^{c}, Griessernu ^{c}, Rossbode ^{p}	VS	14.08.21	12501202108141205	0.15
Grüebu ^{p}, Fletschhorn ^{c}, Rossbode ^{c}	VS	14.08.21	12501202108141211	0.15
Grüebu ^{p}, Mattwald ^{c}	VS	14.08.21	12501202108141247	0.1
Güglia ^{c}	GR	01.09.21	12501202109011012	0.12
Güglia ^{p}	GR	01.09.21	12501202109011019	0.12
Hohlaub ^{p}, Trift ^{c}, Mälliga ^{c}, Rottal ^{c}, Laggin ^{p}, Weissmies ^{p}, Tälli ^{c}, Zwischbergen ^{p}	VS	14.08.21	12501202108141845	0.15
Lagginhorn ^{p}, Hohlaub ^{c}, Trift ^{c}, Mälliga ^{p}, Laggin ^{p}, Weissmies ^{c}, Tälli ^{c}	VS	14.08.21	12501202108141838	0.15
Ob. Grindelwald ^{p}, Wächselberg ^{p}	BE	20.08.21	12501202108201009	0.25

Glaciers	Ct.	Date	Line No.	GSD
Oberaar ^{c}, Fiescher ^{p}	BE	26.08.21	12501202108261831	0.12
Oberaar ^{p}, Unteraar ^{p}, Fiescher ^{p}	BE	26.08.21	12501202108261837	0.12
Plaine Morte ^{p}, Lämmern ^{c}, Schwarz ^{p}	BE, VS	21.08.21	12501202108211852	0.12
Plaine Morte ^{p}, Tierberg ^{c}, Wildstrubel ^{p}, Steghorn ^{c}, Tälli ^{c}, Schwarz ^{p}, Altels ^{c}	BE, VS	21.08.21	12501202108211837	0.12
Plaine Morte ^{p}, Wildstrubel ^{p}, Lämmern ^{p}, Schwarz ^{p}	BE, VS	21.08.21	12501202108211845	0.12
Rhone ^{p}	VS	20.08.21	12501202108201021	0.15
Ried ^{p}	VS	14.08.21	12501202108141833	0.15
Ried ^{p}, Hohbärg ^{p}, Festi ^{p}, Kin ^{p}	VS	14.08.21	12501202108141801	0.15
Ried ^{p}, Hohbärg ^{p}, Festi ^{p}, Kin ^{p}	VS	14.08.21	12501202108141809	0.15
Ried ^{p}, Hohbärg ^{p}, Festi ^{p}, Kin ^{p}, Weingarten ^{p}	VS	14.08.21	12501202108141647	0.12
Ried ^{p}, Hohbärg ^{p}, Festi ^{p}, Kin ^{p}, Weingarten ^{p}	VS	14.08.21	12501202108141654	0.15
Silvretta ^{c}, Verstancla ^{p}, Tiatscha ^{p}, Plan Rai ^{p}	GR	01.09.21	12501202109011227	0.12
Silvretta ^{p}, Verstancla ^{c}, Vernela ^{c}, Maisas ^{p}, Tiatscha ^{c}, Plan Rai ^{c}	GR	01.09.21	12501202109011232	0.12
Traunter Ovas ^{c}	GR	01.09.21	12501202109011005	0.1
Trift ^{p}	BE	20.08.21	12501202108201055	0.1
Unt. Grindelwald ^{p}	BE	20.08.21	12501202108201002	0.2
Unteraar ^{p}	BE	20.08.21	12501202108201009	0.2
Unteraar ^{p}	BE	26.08.21	12501202108261825	0.12
Unteraar ^{p}, Ob. Grindelwald ^{p}	BE	21.08.21	12501202108211625	0.12

c Glacier shown completely
p Glacier shown partially

GSD: Ground sampling distance in (m)

B Remarks on Individual Glaciers

1 Rhone

2020: Luftbildaufnahmen am 13.9.2020 und photogrammetrische Bearbeitung durch swisstopo, glaziologische Interpretation und Analyse durch VAW/ETHZ. (VAW/ETHZ – A. Bauder)

2021: Luftbildaufnahmen am 20.8.2021 und photogrammetrische Bearbeitung durch swisstopo, glaziologische Interpretation und Analyse durch VAW/ETHZ. (VAW/ETHZ – A. Bauder)

3 Gries

2020: Luftbildaufnahmen am 9.9.2020 und photogrammetrische Bearbeitung durch swisstopo, glaziologische Interpretation und Analyse durch VAW/ETHZ. (VAW/ETHZ – A. Bauder)

2021: Luftbildaufnahmen am 24.9.2021 und photogrammetrische Bearbeitung durch swisstopo, glaziologische Interpretation und Analyse durch VAW/ETHZ. (VAW/ETHZ – A. Bauder)

5 Grosser Aletsch

2020: Luftbildaufnahmen am 14.9.2020 und photogrammetrische Bearbeitung durch swisstopo, glaziologische Interpretation und Analyse durch VAW/ETHZ. (VAW/ETHZ – A. Bauder)

2021: Luftbildaufnahmen am 29.7.2021 und photogrammetrische Bearbeitung durch swisstopo, glaziologische Interpretation und Analyse durch VAW/ETHZ. (VAW/ETHZ – A. Bauder)

7 Kaltwasser

2021: Erstmals Gletscherrand mit GPS aufgenommen. Der Gletscher ist allgemein sehr dünn und weist viele kleine Zungenlappen auf. (Ch. Kuonen)

10 Schwarzberg

2020: Luftbildaufnahmen am 27.8.2020 und photogrammetrische Bearbeitung durch swisstopo, glaziologische Interpretation und Analyse durch VAW/ETHZ im Auftrag der Kraftwerke Mattmark AG. (VAW/ETHZ – A. Bauder)

11 Allalin

2020: Luftbildaufnahmen am 27.8.2020 und photogrammetrische Bearbeitung durch swisstopo, glaziologische Interpretation und Analyse durch VAW/ETHZ im Auftrag der Kraftwerke Mattmark AG. (VAW/ETHZ – A. Bauder)

12 Chessjen

2020: Luftbildaufnahmen am 27.8.2020 und photogrammetrische Bearbeitung durch swisstopo-po, glaziologische Interpretation und Analyse durch VAW/ETHZ im Auftrag der Kraftwerke Mattmark AG. (VAW/ETHZ – A. Bauder)

14 Gorner

2020: Luftbildaufnahmen am 21.8.2020 und photogrammetrische Bearbeitung durch swisstopo, glaziologische Interpretation und Analyse durch VAW/ETHZ. (VAW/ETHZ – A. Bauder)

2021: Luftbildaufnahmen am 14.8..2021 und photogrammetrische Bearbeitung durch swisstopo, glaziologische Interpretation und Analyse durch VAW/ETHZ. (VAW/ETHZ – A. Bauder)

16 Findelen

2020: Luftbildaufnahmen am 21.8.2020 und photogrammetrische Bearbeitung durch swisstopo, glaziologische Interpretation und Analyse durch VAW/ETHZ. (VAW/ETHZ – A. Bauder)

2021: Luftbildaufnahmen am 14.8.2021 und photogrammetrische Bearbeitung durch swisstopo, glaziologische Interpretation und Analyse durch VAW/ETHZ. (VAW/ETHZ – A. Bauder)

17 Ried

2020: Koordinaten von Referenzpunkt FP75 neu bestimmt mit Swiss Grid App auf iPhone: 630'931 / 111'062 (P. Rovina) Am 26.09.2020 ereignete sich ein Eisabbruch von 3000 bis 4000 m^3 bei der Felsinsel oberhalb 3000 m.ü.M. (H. Werlen)

2021: Koordinaten von Referenzpunkt FP75 neu bestimmt mit Swiss Grid App auf iPhone: 630'930 / 111'061 (P. Rovina)

18 Lang

2021: Die Gletscherzunge ist nur noch sehr schmal und stark mit Schutt bedeckt. (H. Henzen)

19 Turtmann

2020: Ein grösserer Teil der Zunge brach am 6.8.2020 ab. Die Lawine mit der Abbruchmasse blieb auf der vorgelagerten Toteismasse liegen. Geschätztes Abbruchvolumen in der Grössenordnung von 100'000 m^3 Eis. (VAW/ETHZ – A. Bauder)

2021: Neuer Eisrand ist zu Fuss nicht zugänglich. Deshalb grobe Einmessung aus grösserer Distanz. Eisrand im linken Teil nicht erfasst. (A.Brigger)

22 Zinal

2020: Hauteur du front $\approx$40 m (F. Fellay)

25 Ferpècle

2020: Il y a rupture entre la langue glaciaire morte, qu'on a mesurée et la partie sommitale du glacier. L'accès à la nouvelle langue glaciaire est très délicat. (F. Fellay)

28 Tsidjiore Nouve

2021: Un noveau point de référence (4) a été ajouté. L'azimut des mesures a été modifié de 205° à 235°. (F. Fellay)

32 Mont Fort (Tortin)

2021: Le front glaciaire aux points 1-2-3-B est couvert de rochers et de matériel terreux. Il est donc difficile de le situer précisément. (F. Bourban)

33 Tsanfleuron

2021: formation d'un petit lac à la sortie d'eau (F. Fellay)

40 Tseudet

2021: Le glacier est désormais au-dessus d'une barre rocheuse difficile d'accès. Les éboulis présents sur une partie de la langue rendent difficile la détermination du front. (P. Stoebener)

42 Saleina

2021: Les éboulis recouvrent une partie de la langue, rendant la détermination de l'extrémité difficile (P. Stoebener)

43 Trient

2020: Visite du dimanche 18 octobre 2020: Buts: Evaluer visuellement l'état du glacier. Prendre des photos, en particulier depuis le point älpha", pour continuer la série commencée en 1969 par Monsieur Pierre Mercier. Mesurer la position du front du glacier. Lever le plus grand nombre possible de points en bordure de la langue glaciaire. Le ciel était bien dégagé durant toute la journée. Par contre, la lumière rasante de cette période de l'année générait un effet de contre-jour qui compliquait un peu les prises de vue. La surface du glacier était couverte d'une fine couche de neige fraîche, mais on distinguait bien la langue glaciaire et la surface rocheuse. La fonte durant l'année 2020 a été importante, comme les années précédentes. Le débit du torrent émissaire a été élevé durant l'été, mais ce n'était plus le cas lors de notre passage. Comme exprimé dans les rapports précédents, la fonte du glacier, initiée en 1987, se poursuit avec une intensité accrue depuis une dizaine d'années. 2020 fait partie des cinq années les plus chaudes enregistrées depuis 1864. L'amincissement de la langue glaciaire se poursuit inexorablement. La langue occupe maintenant une surface qui domine une forte pente. La ligne de rupture de pente est presque entièrement dégagée de la glace, pour la première fois. La pointe de la langue se trouve en haut du sillon rocheux dans lequel la masse principale de glace était engagée depuis 2004-2005. L'amincissement général de la langue glaciaire s'est poursuivi en 2020, de manière très importante. On remarque cette année aussi une augmentation de l'ouverture et de la profondeur des crevasses, allant parfois jusqu'à la roche. Sur la photo P1070164, on remarque, à droite, le point de référence pour le retrait 2020, dans l'axe du sillon rocheux. Ses coordonnées sont les suivantes: 2'567'773.054 / 1'096'288.134, à l'altitude de 2170 mètres environ. On observe un détail de la pointe gauche de la langue, encore engagée dans un autre sillon rocheux. La glace est crevassée et en partie éboulée, ce qui illustre bien la fonte de la langue. Année après année, on remarque la forte croissance des arbres autour du point älpha", qui cachent de plus en plus la langue glaciaire. Les températures croissantes favorisent l'essor de la végétation. Le relevé du périmètre de la langue glaciaire a été réalisé à l'aide de jumelle laser LEICA, sans couplage GPS, à partir du point de mesure Ï". Coordonnées du point Ï", en usage depuis 2004: 2'567'889 / 1'097'100 / 1994 m. Azimut principal du point Ï"vers le front: 180° (le nord est à 0° ou 360°). Les coordonnées de 32 points ont été relevées, en tout. Dans l'extrémité la plus basse de la langue, qui domine maintenant un sillon rocheux d'orientation approximative SW-NE. Le front se trouve à environ 2170 mètres d'altitude. Il s'agit de la base de la glace, au contact du rocher. (J. Ehinger)

2021: Visite du samedi 18 septembre 2021 Buts: Evaluer visuellement l'état du glacier. Prendre des photos, en particulier depuis le point älpha", pour continuer la série commencée en 1969 par Monsieur Pierre Mercier. La journée était très ensoleillée, avec quelques cumulus sur les reliefs. Les jumelles LEICA-Locator n'étaient malheureusement pas disponibles. J'ai donc dû me contenter de prendre des photos du glacier du Trient, à partir du point älpha"(2'567'313 / 1'097'365 / 1727 m) et à partir du point Ï"(2'567'889 / 1'097'100 / 1994 m). Au point älpha", on constate que la végétation a beaucoup poussé depuis 20 ans. Le glacier n'est presque plus visible, alors qu'une série de photos, commencée en 1969 par Monsieur Pierre Mercier, montrait bien les mouvements d'avance et de retrait de la langue glaciaire. Sur la photo prise du point Ï", on a une vue d'ensemble de la vallée, de la langue glaciaire, ainsi que de la rupture de pente qui sépare le plateau du Trient de la langue, à l'altitude de 2850 mètres environ. On distingue bien une série de sillons rocheux, autrefois couverts de glace. Visite du samedi 25 septembre 2021 Buts: Evaluer visuellement l'état du glacier. Prendre des photos. Mesurer la position du front du glacier. Lever le plus grand nombre possible de points en bordure de la langue glaciaire. Le ciel était dégagé durant toute la journée, avec des passages nuageux en altitude. Comme toujours à cette époque de l'année, la lumière rasante générait un effet de contre-jour qui compliquait un peu les prises de vue. Une fine couche de neige fraîche était tombée les jours précédents, mais fondait rapidement. La partie inférieure de la langue n'était déjà plus couverte ce jour-là, n'apportant plus aucune protection à la glace contre la fonte. La fonte durant l'année 2021 a été importante, comme les années précédentes, malgré des conditions météorologiques relativement favorables, avec un hiver neigeux et un été frais. Mais la pluie est tombée à des altitudes élevées, ce qui a même pu localement accélérer la fonte. Le débit du torrent émissaire a été élevé durant la fin de l'été, mais ce n'était plus le cas lors de mon passage. L'amincissement de la langue glaciaire se poursuit inexorablement. La langue occupe maintenant un épaulement qui domine une forte pente, tracée de sillons parfois assez profonds. La ligne de rupture de pente est presque entièrement hors de la glace. On remarque, au front, une zone de glace récemment éboulée, dégageant une surface bleue qui contraste avec la couleur grise de cette partie de la langue. De la glace éboulée occupe l'aval du front et s'engage dans le sillon autrefois occupé par l'axe principal de la langue. On observe bien de la glace morte encore présente dans un sillon secondaire parallèle. La glace est très crevassée, ce qui augmente encore considérablement la surface exposée à la fonte et accentue l'amincissement de ce qui reste de la langue. La surface bleue était perpendiculaire au faisceau laser des jumelles, ce qui rendait les mesures fiables. J'ai pu estimer également la hauteur de la paroi bleue à 30 mètres environ. Cela donne une idée de l'épaisseur de la langue glaciaire, au moins jusqu'à 2500 mètres d'altitude. Les photos montrent la rupture de pente entre le plateau du Trient et la langue glaciaire, qui coule vers le NNE. On remarque une légère couverture neigeuse sur la partie supérieure et de gros séracs en partie écroulés. Plusieurs traces d'éboulements glaciaires sont bien visibles , libérant des surfaces bleues. Un affaissement général est observable sur toute la largeur de la langue, dans ce secteur, témoignant du travail de sape des torrents sous-glaciaires. La pointe de la langue se trouve en haut du sillon rocheux dans lequel la masse principale de glace était engagée depuis 2004-2005. L'amincissement général de la langue glaciaire s'est poursuivi en 2021, de manière très importante et ne montre aucun signe de reprise. On observe bien la forme arrondie du front, avec de la glace morte, ou presque, qui occupe un sillon secondaire. Le profil du front est encore très vertical, malgré la fonte, mais de très nombreuses crevasses dissèquent la surface en des entailles profondes qui accélèrent les éboulements. Plus haut, on observe un affaissement très crevassé qui pourrait peut-être, à terme, séparer la langue en deux parties, coupant le front actuel d'une alimentation régulière en glace. Le relevé du périmètre de la langue glaciaire a été réalisé à l'aide de jumelle laser LEICA-Locator, sans couplage GPS, à partir du point de mesure Ï". Coordonnées du point Ï", en usage depuis 2004: 2'567'889 / 1'097'100 / 1994 m. Azimut principal du point Ï"vers le front: 180° (le nord est à 0° ou 360°). Les coordonnées de 22 points ont été relevées, en tout, ce qui est inférieur aux années passées. En effet, la bordure de la langue comporte moins de digitations depuis qu'elle s'est retirée sur l'épaulement. (J. Ehinger)

44 Paneyrosse

2020: Points 53 et 54 à refaire en 2021. Un guide de montagne a pu passer sous le glacier et en ressortir par les hauts. (J. Desarzens)

2021: Peu de neige fraiche (J. Desarzens)

45 Grand Plan Névé

2021: Points 1 et 11 pas retrouvé et mesuré (J. Desarzens)

47 Sex Rouge

2020: (1) Le glacier n'est plus apparent de P1 à 4 (mort ou reliquats enfouis sous les éboulis). (2) P3 (recouvert par les remblais de la nouvelle piste de ski) n'a pas été rétabli. (3) Implantation d'un nouveau point de mesure P400 (coord App-REGA) 2'582'693 / 1'130'900 / 2749, azimut 165° (4) P5, 500 et 51, agrandissement du plan d'eau résultant de la fonte du glacier (bordure du glacier = niveau du plan d'eau ou glace immergée, à vérifier plus précisément). (5) Outre le recul en situation mesuré, l'apparence générale du glacier laisse présager une perte de masse significative (J. Binggeli)

48 Prapio

2020: Relevé depuis l'antecime Sex Rouge (Peak Walk 2972 m): altération et contraction marquées conduisant à la séparation du glacier en deux parties distinctes. (J. Binggeli)

53 Stein

2020: Der Gletscher ist mit Geröll und Blöcken zugedeckt. (D. Rohrer)

2021: Die Mächtigkeit des Gletschers ist im vordersten Teil nur noch sehr gering. (D. Rohrer)

55 Trift (Gadmen)

2020: Luftbildaufnahmen am 13.9.2020 und photogrammetrische Bearbeitung durch swisstopo, glaziologische Interpretation und Analyse durch VAW/ETHZ. (VAW/ETHZ – A. Bauder)

2021: Luftbildaufnahmen am 20.8.2021 und photogrammetrische Bearbeitung durch swisstopo, glaziologische Interpretation und Analyse durch VAW/ETHZ. (VAW/ETHZ – A. Bauder)

57 Oberer Grindelwald

2020: Luftbildaufnahmen am 13.9.2020 und photogrammetrische Bearbeitung durch swisstopo, glaziologische Interpretation und Analyse durch VAW/ETHZ. (VAW/ETHZ – A. Bauder)

2021: Luftbildaufnahmen am 20.8.2021 und photogrammetrische Bearbeitung durch swisstopo, glaziologische Interpretation und Analyse durch VAW/ETHZ. (VAW/ETHZ – A. Bauder)

58 Unterer Grindelwald

2020: Luftbildaufnahmen am 13.9.2020 und photogrammetrische Bearbeitung durch swisstopo, glaziologische Interpretation und Analyse durch VAW/ETHZ. (VAW/ETHZ – A. Bauder)

2021: Luftbildaufnahmen am 20.8.2021 und photogrammetrische Bearbeitung durch swisstopo, glaziologische Interpretation und Analyse durch VAW/ETHZ. (VAW/ETHZ – A. Bauder)

59 Eiger

2020: Der Gletscher wird immer dünner. Kein Gletschertor vorhanden. Wegen den langen Distanzen am Limit der Instrumente wird die Messung immer schwieriger. (R. Schai)

60 Tschingel

2021: Viel Moränenmaterial; orographisch links ist es sehr schwierig den Gletscher unter dem Moränenmaterial zu finden. Es fällt auch viel Material von oben in diesen Trichter. Das Gletschervorfeld ist sehr matschig und mit Wasser durchtränkt. (R. Schai)

61 Gamchi

2020: Gletschervorfeld erodiert stark. Massenverlust auf besonnter Ost-Seite sehr auffällig. (M. Schenk)

2021: Neue Basislinie B (2’627’571.74 / 1’151’058.12 / 2120.44) - C (2’627’907.98 / 1’151’218.18 / 2114.25) eingerichtet

63 Lämmern

2021: Gletscherrand zu Fuss nicht gefahrlos erreichbar, deshalb Distanz ab Punkt h geschätzt. Koordinaten der Referenzpunkte ermittelt mit der RegaApp: Punkt g: 2’608’532 / 1’138’805, Punkt h: 2’608’475 / 1’138’840 (A. Meier-Glaser)

64 Blümlisalp

2020: Fotostandort am Gegenhang bei 2’624’213 / 1’150’931 (U. Burgener)

65 Plaine Morte (Rätzli)

2020: Luftbildaufnahmen am 13.9.2020 und photogrammetrische Bearbeitung durch swisstopo, glaziologische Interpretation und Analyse durch VAW/ETHZ. (VAW/ETHZ – A. Bauder)

2021: Luftbildaufnahmen am 21.8.2021 und photogrammetrische Bearbeitung durch swisstopo, glaziologische Interpretation und Analyse durch VAW/ETHZ. (VAW/ETHZ – A. Bauder)
Lac des Faverges on Plaine Morte has drained 29.7. until 2.8.2021. The lake drained at a much earlier stage than in the previous years. (VAW/ETHZ – M. Huss)

66 Tiefen

2020: Im rechten (nördlichen) Teil viel grösserer Rückgang als im linken Teil, der mit viel Schutt bedeckt ist. (L. Eggimann)

2021: Im rechten (nördlichen) Teil ist der Rückgang wiederum grösser als im linken Teil. Der linke Teil ist mit viel Schutt bedeckt. Im Vergleich gegenüber dem Vorjahr hat die Zunge leicht an Dicke eingebüsst. (L. Eggimann)

67 St. Anna

2020: Die sehr dünne Gletscherzunge vom letzten Jahr ist durchgeschmolzen. Der Gletscher hat sich vom praktisch flachen Vorfeld in das etwas steilere Gelände zurückgezogen. (L. Eggimann)

68 Chelen

2021: Im Randbereich deutlicher Volumenverlust. Es wurden 3 neue Referenzpunkte näher am Gletscher eingerichtet. (R. Planzer)

68 Rotfirn (Nord)

2021: Wie schon in den vergangenen Jahren konnte der Rotfirn wegen Steinschlaggefahr nicht mehr vermessen werden. (R. Planzer)

70 Damma

2021: Beim Dammagletscher werden momentan noch zwei Zungenlappen gemessen. Der restliche Gletscher hat sich bereits über eine Steilstufe zurückgezogen und ist ca. 170 m weiter oben. Der Eisrand oberhalb der Referenzpunkte 2017/2018 liegt in einer Mulde und ist mit viel Schutt bedeckt. Vielleicht schmilzt er dort deswegen etwas langsamer als in der näheren Umgebung. Da die Distanz zum Gletscher zu gross wurde beim Punkt 2018B ein neuer Referenzpunkt 2021 näher beim Gletscher erstellt. (M. Planzer)

71 Wallenbur

2020: Der nördliche Gletscherteil ist noch kompakt. Südlich der Mittelmoräne zerfällt der Gletscher langsam. Neuer Referenzpunkt auf der Messlinie FB63 eingerichtet. (P. Kläger)

2021: Der nördliche Gletscherteil ist noch kompakt. Südlich der Mittelmoräne zerfällt der Gletscher schnell. Die mit viel Schutt bedeckte Gletscherzunge im Talboden ist nun nicht mehr mit dem Seitenarm unterhalb des Sustenhorns verbunden. 2 Referenzpunkte näher zum Eisrand verschoben (P. Kläger)

72 Brunni

2020: Der Gletscher verliert vor allem an Mächtigkeit und der Gletschersee wird grösser. Zwischen Gletscher und Fels beim Referenzpunkt 9 fliesst viel Schmelzwasser und höhlt den Glescher zusätzlich von unten aus. (M. Planzer)

2021: Da bereits etwas Schnee lag, konnte der Gletscherrand nicht immer eindeutig bestimmt werden. Die Randbereiche werden immer flacher. (M. Planzer)

74 Griess

2021: Ein grosser Teil des Gletschers ist mit Schutt bedeckt. Am Zungenrand herrschte am Tag der Messung aktiver Steinschlag. (B. Annen)

77 Biferten

2020: Mit der treuen Seele Namens Hansruedi Hösli, alt Metzgermeister aus Ennenda, ziehe ich los, um den Zustand unseres Gletschers zu erfassen. Wunderbares Wetter begleitet unser Unternehmen. So fahren wir einmal mehr bis Hintersand um dort den Vermesser Bus zu parkieren und von dort zum Gletscher aufzusteigen. (Spektakuläre Taxifahrt Bericht Südostschweiz als PDF, schildert dies eindrücklich; als Beilage) Diesmal klappt auch der Stativwechsel von der Fridolinshütte hinunter zur Unterkunftshütte der KLL wunderbar. Marco Baggio hat sich in der neuen Rolle als Bauchef der KLL eingelebt und auch diese tolle Geste beibehalten, mir das Stativ durch seine Mitarbeiter an den SStart"verschieben zu lassen. So können wir etwas weniger schwer beladen, den Anstieg zum Gletscher beginnen, dies auf dem Hüttenweg zur Fridolinshütte. Wir kommen wie gewohnt zügig voran, kurze Halte um zu Fotografieren gehören trotzdem dazu, um das Umfeld und die Begebenheiten eben an diesem Tag, auch so festzuhalten. Eindrücklich ist dabei der Standort vorne am Tentiwang: dort wird einem bewusst, wie gewaltig der Gletscher einmal gewesen sein muss, wenn man sich dieses Tal aufgefüllt mit Eis vorstellt. Eben an dieser Stelle verlassen wir den Original-Hüttenweg und folgen den Wegspuren der KLL Arbeiter, die hinauf zu ihrer Unterkunftshütte unterhalb des Felsbandes am Bifertenfirn führen. Schweisstreibend und steil ist es allemal, doch dies gehört nun einmal zur Gletschermessung. Bei der Unterkunft angekommen, fasseïch noch zusätzlich das Stativ, um dann über die Schlüsselstelle, über schmierige Felsplatten und Geröll, die Station 12003 zu erreichen. Die Temperatur ist bereits beim Start eigentlich viel zu warm: +10°C zeigt das Thermometer an. Kurz retablieren": trockene Kleider, Znüni Kaffee aus der Thermosflasche und ein kleiner Energiespender in Form eines Riegels und los geht die Messung. Hansruedi muss ich auch nicht mehr gross instruieren, er ist bereits ein grosser Routinier in Sachen Gletschervermessung. So läuft er nach der Messung zur Orientierung auf dem Punkt E, zielstrebig zum ersten Punkt an der Gletscherzunge, der auch der Tiefste am Gletscher ist. Dieser liegt nur gerade 2.5 m höher als vor einem Jahr auf 1966.0 m.ü.M. Dies ist aber mit dem flachen Vorgelände gut erklärbar. Mit 7 weiteren Punkten ist schliesslich der erste Teil des Gletschers abgedeckt und für mich von der ersten Station nicht mehr weiter einsehbar. Das einstmals riesige Tor am Gletscherbach 1 ist kaum mehr auszumachen es liegt auf der Höhe von 1979.9 m.ü.M und hat sich um weitere 8 m gegen Süden davon gemacht. Der Abstand zur Fassung beträgt nun bereits beachtliche 240 m. Alle diese beschriebenen Vorkommnisse am Gletscher dokumentiere ich natürlich auch mit Bildern, die in diesem Bereich recht trist und grau ausfallen, Geröll und Steine bedecken das Eis und so ist es immer schwieriger, hier noch den Verlauf festzuhalten. Der Wechsel vom Standort 12003 zum Standort und Fixpunkt 20101 braucht so seine Zeit und da der Gletscherbach 2 immer noch immense Wassermengen führt muss ich wiederum wie bereits in den Vorjahren, den Umweg über den Gletscher nehmen. Dabei kann ich mit meinem Gehilfen noch kurz fachsimpeln und beraten. Hansruedi ist beeindruckt was sich da während seiner Abwesenheit in Sachen Messung bereits wieder verändert hat: die gewaltigen Gletscherbrüche am See und beim Gletschertor 2 sind in sich zusammengesackt und der Gletscher flacht mehr und mehr ab. Was aber auch ihn erschreckt, ist die dünne Nabelschnur"die den Gletscher im Bereich der unteren Brüche und am Fusse des Grünhorns noch am Leben erhält. Passiert da bereits im nächsten Jahr das Unabwendbare, dass die Gletscherzunge um 1.2 km! kürzer wird und der Gletscher so einen der grössten Schwunde in der Messreihe verzeichnen muss, da das restliche Eis nur mehr als Toteis behandelt wird! Während meiner Umgehung über das Eis, kann ich weitere eindrückliche Fotos schiessen. Auf der Station 20101 angelangt stationiere ich den Theodoliten, örientiere"das Instrument am Giebel der Grünhornhütte und so bin ich für die weiteren Messungen bereit. Die Temperatur auf dieser Station bei +25°C, dies ist mit Sicherheit keine gute Voraussetzung für die Eisbildung! Hansruedi fordere ich per Funk auf, mir, die noch nötigen Punkte bis zum Anfang des Gletschersees anzugeben. Danach kann auch er sich über den Gletscher zum westlichen Gletscherbereich verschieben. Ich nehme während dieser Zeit die Punkte am Gletscher auf, die nicht begehbar sind. So kann ich einige Punkte im Bereich, Anfang Gletschersee bis hin zum Gletschertor 2, Reflektor los aufnehmen, dies bei Horizontaldistanzen von 200m bis 250m. Eine gute Einrichtung am Theodolit, denn ansonsten müsste man dies wohl mit Schnitten bewerkstelligen. Sobald Hansruedi das Eisfeld überquert hat und am äussersten Ecken der Zunge im Westen angelangt ist, gibt er mir noch die restlichen Eckpunkte bis hin zum Gletschertor 2, an das er aber nicht mehr ganz hinzukommt, weil das Wasser des Gletscherbaches zu tief und auch zu ziehend ist. Gut habe ich diesen Bereich bereits Reflektor los bestimmt. So kann ich Hansruedi durchgeben, dass wir die Messung 2020 abschliessen können und er zu mir aufsteigen kann, so dass wir dann weiter über die Seitenmoräne Streiff- Becker aussteigen können, um so zur Fridolinshütte zu gelangen. Mit 21 Punkten ist der Gletscher kartiert, dies scheint wenig, doch die langen Strecken zwischen den Eckpunkten erfordern viel Zeit. Die Höhen beim Gletschertor 2 haben sich wie bereits angedeutet stark verändert. Im 2019 war die Tor Höhe noch 17.2m, im 2020 noch ganze 7.3 m, somit ist da der Schwund auch in der Masseäuszumachen. 10 m sind eine beachtliche Verminderung, bei gleichbleibender Gletscherbachhöhe von 2006 m.ü.M. Der Ausstieg über die Moräne fordert uns noch einmal alles ab, aber mit der Gewissheit, dass in der Fridolinshütte Kuchen und Kaffee wartet, beflügelt uns und so schaffen wir auch diese Herausforderung. Noch das Stativ in der alten Fridolinshütte deponieren und dann haben wir eine "bäumigeSStärkung verdient. Wenn der Gletschermesser auftaucht, dann sind auch die Fragen nicht weit: wieviel ist er zurückgegangen, wie dick ist das Eis und vieles mehr. Da muss ich die Alpinisten jeweils vertrösten und ihnen wenigstens die Resultate des Vorjahres präsentieren und meine heutigen Eindrücke einfach schildern, natürlich mit den Sorgen um die gesagte Nabelschnur. So könnte man noch lange vor der Hütte sitzen, sich's gut gehen lassen und all die Erlebnisse um die Gletschermessung schildern. Doch alles hat einmal ein Ende und so ziehe ich mit meinem Gehilfen ins Tal, um viele Eindrücke reicher und vor allem mit den Gedanken, wie denn wohl die Messung 2021 aussehen kann, wenn... Doch jetzt ist für dieses Jahr die Messung registriert und wir kommen wohlbehalten und gesund wieder ins Tal. Als Abschluss knipse ich noch mehrere Silberdisteln, die wie Sterne funkelnd in der Wiese blühen, einfach wunderbar! Ein grosses Dankeschön an Hansruedi Hösli, der liebend gerne mit mir die Zunge am Bifertengletscher vermisst und dies auch im hohen Pensionsalter! Es ist jedes Mal ein tolles Erlebnis mit ihm unterwegs zu sein. Die Auswertung im Büro ergibt schliesslich einen weiteren recht massiven Verlust im Mittelwert von 15.3 m Eis in der Länge des Gletschers. Dabei sind die 7.1 m2 Plusfläche gegenüber den totalen Schwundflächen von 12467.8 m2 wahrlich ein Tropfen auf den heissen Stein. Geteilt durch die gemessene Breite von 809.6 m ergibt dies dann oben erwähnten Mittelwert als Schwund! Es schmerzt, das Eis in so rasanter Geschwindigkeit abschmelzen zu sehen, doch solange ich gesund und fit bin, begleite ich meinen Gletscher durch dick und dünn. Die Hoffnung stirbt zuletzt und vielleicht ist ja der Virus der momentan die Menschheit geisselt, die Wende in Sachen Klimaerwärmung. Die Menschen merken allmählich, dass wir die Natur brauchen und nicht umgekehrt. So sehe ich der neuen Messung im 2021 gespannt entgegen und beende diesen Bericht. (H. Klauser)

78 Limmern

2020: Punkte 1 bis 4 sind stark schuttbedeckt. Gletscherzunge aper, etwas Neuschnee in hohen Lagen. (U. Steinegger)

79 Sulz

2020: Am 31.7.2020 kam es unterhalb der Ruchi zu einem Felssturz von ca. 25'000 m^3 (Schätzung). Das Material lagerte sich auf dem Gletscher ab. Das Gletschervorfeld wurde mit 2-4 m Felssturzmaterial aufgefüllt. (N. Philippi)

2021: Vor der Gletscherzunge liegt Felsmaterial, welches vermutlich von der orographisch rechten Gletscherflanke abgerutscht ist. Letztes Jahr lag weniger Felsmaterial dort. (N. Philippi)

80 Glärnisch

2020: Ich ziehe mit Noël Dobler dem Lernenden unseres Vermessungsbüro und sämtlichen Utensilien die das Vermessen des Gletschers braucht, los. Die Messung am Bifertenfirn 2020 liegt nur eine Woche zurück und ist mir noch in bester Erinnerung und lässt mich die beiden Messungen gut vergleichen. Das Wetter ist strahlend schön, als ich am Morgen aus dem Küchenfenster blicke um mich zu vergewissern, dass die abgemachte Messung am Glärnischfirn auch wirklich ausgeführt werden kann. Nach dem ausgiebigem Frühstück und der kurzen Radfahrt ins Büro um den Vermesserbus abzuholen und gleichzeitig Noël äufzuladen" geht es los Richtung Klöntal, Rossmattertal und schliesslich nach Wärben. Einmal mehr klappt es auch mit der kostenlosen Bewilligung durch die Gemeinde für die Fahrt ins Rossmattertal. Die Fahrt bis Wärben ist allemal eine Reise wert, eindrücklich schlängelt sich die Strasse durch das schmale Tal hinauf. Am Parkplatz in Wärben weitet sich das Tal erstmals und man erblickt das erste Zwischenziel zum Gletscher, die Glärnischhütte. Doch bis diese erreicht ist, fliessen bereits einige Schweisstropfen. Für Noël ist dieses Gebiet Neuweltrund um das Glärnischmassiv und er kommt aus dem Staunen kaum mehr heraus. Wir beladen unsere Rucksäcke mit Instrument, Stativ, Reflektor und Stab sowie eine Verlängerung, die uns hilft, bei stark überhöhten Punkten. So ziehen wir von dannen gen die Glärnischhütte: bei der Fixseilstelle oberhalb der Serpentinen über dem Parkplatz werden die Kletterkünste fotografisch festgehalten, um der Nachwelt zu zeigen, dass eine Gletschermessung kein Sonntagsspaziergang ist. Zügig kommen wir voran und schon bald ist auch der botanische Wunderplatz erreicht und somit ein kurzer Halt angesagt. Die blühenden Edelweisse am Wegesrand müssen einmal mehr fotografiert werden. Nach dieser Fotosession geht es nicht minder steil bergan bis zur Glärnischhütte. "Äs Chacheli Kaffiünd ein kurzer Schwatz mit dem Hüttenwart Team lassen wir uns auch in diesem Jahr nicht nehmen, da ich da doch bereits die ersten Impulse auffangen kann, um mir ein Bild zu machen, was mich erwartet. Da ich ja mehrheitlich das ganze Jahr draussen bin und auch in unsere Bergwelt schaue und zwischendurch auch ziehe, vermute ich, dass auch das 2020 nicht neue Erkenntnisse in Sachen Gletscher bringen wird. Doch die endgültige Gewissheit bringt erst die Messung und dessen Auswertung. Die Konsumation in der Hütte übernimmt der Hüttenwart, dies als Obolus an die jeweilige Dokumentation die ich im nach der Auswertung zukommen lasse. Herzlichen Dank! Gestärkt und für Noël in voller Erwartung auf das ewige Eis, ziehen wir weiter: überwinden mit kraxeln das zweite Felsband und gelangen über den Steinmann auf 2259 Meereshöhe langsam in die Nähe des Gletschers. Auf gut 2300 m.ü.M dann endlich; das Ëismeerliegt endlich vor uns. Für jemanden der dies das erste Mal sieht, immer äusserst beeindruckend, und für mich natürlich nicht weniger interessant, da ich ja die Messung vom letzten Jahr in etwa noch vor Auge habe und mir da bereits die ersten Schlüsse ziehen kann; ja es geht weiter mit der Schmelze und wie! Immer mehr Felsrippen stehen aus dem ewigen Eis und der Gletscher flacht mehr und mehr ab. Unsere endgültige Messstation ist aber immer noch eine halbe Stunde Fussmarsch entfernt. Dabei passieren wir die Stationen 12 und 13 im nördlichen Teil der "Gletscherrückstände": Seitenmoränen, Gletscherschliffe, kleine und grössere Seen, die sich im Vorgelände bilden. Für Noël sind diese zwei Stationen dann die letzten Kontrollmessungen, bevor die Messung abgeschlossen ist. Auf der Station 16 angelangt, nachdem auch da noch etwas Kraxeln und wegloses Gelände passiert werden muss, mache ich mich einerseits daran den Theodoliten über dem Fixpunkt zu stationieren, während sich Noël ein Bild macht, wie er mir schliesslich die Gletscherzunge kartieren kann. Ein kurzer Znüni, trockenes Gewand für den Operateur oder Gletschermesser und dann zieht mein Gehilfe los, Richtung südlicher Zipfel des Gletschers und zugleich Anfang der Messung. Klar, dass er in Sachen Handhabung der Messuntensilien keine Erklärungen braucht, da dies ja zu seinem täglichen Arbeitsablauf gehört. Ich orientiere das Instrument auf den bekannten Fernzielen Forst- und Druesberg. Bald ist der Messgehilfe am Start der Gletscherzunge (dies wirklich am äussersten Zipfel, der noch ohne Eisausrüstung erreicht werden kann) und die Messung beginnt. Behände und zielsicher zieht er von Eckpunkt zu Eckpunkt am Gletscher. Dabei zückt er auch seine eigene Kamera und hält seine immensen Eindrücke fest. Sein Arbeitsgewand ist nebst der warmen Oberkleidung aber immer noch die kurze Hose, was die warmen Temperaturen eindrücklich dokumentiert. Der ganze südliche Teil nehme ich von der Station 16 auf. Einige Punkte nahe am Felsenriff müssen mit der Verlängerung und je nachdem auch mit Exzentrischen Stellungen kartiert werden, damit nicht noch weitere Stationierungen von Nöten werden. Beim Erreichen des Felsenriffes auf dem das Instrument stationiert ist, kann sich der Messgehilfe kurz ausruhen und sich verpflegen, denn ich muss das Instrument auf die Station 14 umstellen und mich dort wiederum neu orientieren. Die Fernziele bleiben die gleichen und die Station 16 nehmen wir mit in die Orientierung, das heisst, dass Noël dies Station noch kurz ßignalisierenmuss, bevor seine Tour der Gletscherzunge entlang weiter geht. Die Punkte nach dem Fels Riff auf der nördlichen Seite, mit den Instrumentenstandorten 14 bis 16, muss er dabei umgehen, da sich in diesem Bereich der Gletscher nahe an die steilen Gletscherschliffe schmiegt und auch das stehen auf dem Eis ohne Steigeisen nicht möglich ist. Die Umgehung ist aber schnell bewältigt und bald ist Noël bereit, was er mir wie gewohnt per Funk mitteilt. So geht es rassig weiter und er erreicht den tiefsten Punkt am Gletscher, der im nördlichen Teil liegt, um sogleich wieder der Zunge entlang aufzusteigen Richtung nördliches Ende der Gletscherzunge. Und schon bald kann ich Noël zum Aufhören und Beenden der Messung der Zunge auffordern, ansonsten wäre er kaum zu bremsen und schliesslich am Schwandergrat zu finden (nein Spass beiseite: für ihn ist die Messung leider bereits fertig, ausser den 2 Kontrollfixpunkten. Noël hat gute Arbeit geleistet und dabei einen äusserst erlebnisreichen Tag in seiner Lehre verbringen dürfen.) Vom nördlichen Ende bis zur Station 13 und anschliessend 12, kann mein Gehilfe den Wegspuren der "Gärtlibesteigerfolgen und so sind die zwei Kontrollmessungen schnell im "Kastenünd registriert. Für Noël; Pause, für mich Export der Daten, Instrument einpacken und bereit machen für den Abstieg ins Tal. Eine weitere Messung kann ich abhacken. Dies bei ausgezeichneten Wetterverhältnissen: für den Gletscher zu warmen Temperaturen und einem mehrheitlich stahlblauen Himmel, die kurzen Wolkenintermezzo haben die Messung überhaupt nicht getrübt. Eines ist gewiss, der Gletscher wir wieder Schwundwerte ausweisen, die Frage wieviel, wird sich in der Auswertung im Büro zeigen. Viele Fotos zeigen das Gletschereis am Glärnischfirn und dokumentieren so den

Zustand im Jahr 2020, dabei sind natürlich die Vergleichsfoto von den Vorjahren ab denselben Standorten immer eindrücklich und von grosser Beweiskraft, dass die Gletscher bald einmal verschwinden. Der Abstieg zu Noël, der bei der Station 12 auf mich wartet nutze ich um noch einige Bilder zu knipsen, da ich die Zunge ein Stück weit noch verfolge, um dann über die Station 13 auf den erwähnten Weg der "Gärtlibesteigerßtosse und von dort weiter absteige zur Station 12. Noch einmal diskutieren wir das Erlebte und sind uns einig, dass das ewige Eis stark bröselt und uns zu immer länger andauernden Anmarschwegen zwingt, da wir immer weiter in die Höhe steigen müssen um dies zu erfassen. Dass wir wieder kommen ist aber gewiss, solange noch Eis zum Vermessen vorhanden ist. So nehmen wir den Abstieg hinunter ins Tal etwas zwei gespalten in Angriff: einerseits zufrieden und froh, die Messungen meiner beiden Gletscher bereits abgeschlossen zu haben und andererseits mit dem Bewusstsein, dass wir wiederum von einem Verlust der Eisdecke berichten müssen. Auch beim Zwischenhalt in der Glärnischhütte mit einem Stück Wähe und Getränk zur Stärkung, lässt uns unsere Mission nicht einfach los, hat es doch viele Alpinisten die zur Besteigung des Vrenelisgärtli hier nächtigen und daher ihr Tageswerk bereits erledigt haben und uns mit diversen Fragen um den Glärnischfirn beschäftigen. Diverse Gespräche zeigen aber immer mehr, dass doch bereits viele Menschen aufmerksam werden und das Thema Klimaerwärmung und Gletscherschwund ernst nehmen. Schliesslich steigen wir, mit all den Eindrücken ab ins Tal, immer noch konzentriert und aufmerksam, so dass wir unsere Messung unfallfrei beenden können. Mit dem Bus "holpern"wir schliesslich durchs Rossmattertal hinunter ins Klöntal. Am See entlang nehmen wir noch einen Alpinisten auf, den wir bereits bei der Glärnischhütte kurz angetroffen haben, er ist über Guppen aufs Vreneli geklettert und über die Glärnischhütte ins Tal gestiegen. Schliesslich wollte er zurück nach Schwändi um sein Auto abzuholen, dies notabene zu Fuss!! Diesen wohl zweistündigen Marsch haben wir ihm dann abgenommen. (keine Busverbindungen mehr im Klöntal!) So haben wir nebst der Messung für den Glärnischfirn eine zusätzliche gute Tat vollbracht. Noël hat diesen erlebnisreichen Tag schliesslich müde aber zufrieden mit der Taxifahrt seines Onkels nach Reichenburg an seinen Wohnort abschliessen dürfen. Toll, dass auch heutige Lehrlinge noch zu solchen Unternehmungen zu begeistern sind!! Die Auswertung der Messung vom Samstag 12.09.2020 verglichen mit der Messung vom 31.08.2019 bringt einen Schwund im Mittel von -23.3 m zu Tage. Dabei habe ich wie immer die beiden Zungenverläufe verglichen. Die dazwischenliegenden Flächen; Vorstoss und Schwund, sowie die gemessene Breite ergeben das obenstehende Resultat. Die zwei kleinen Vorstossflächen in der südlichen Region der Zunge von Total 1179.6 m2 sind gegenüber den beiden riesigen Schwundflächen von Total 13798.2 m2 nur einen Tropfen auf einen heissen Stein für die mittlere Schwundberechnung, die sich dann aus der Division durch die gemessene Breite von 542.38m ergibt. Die Vorstossflächen sind wohl eher Interpretationen der verschiedenen Messgehilfen zuzuschreiben, da in dieser Region die Zunge schlecht ausmachbar ist. Das Geröll verwehrt auch da die genaue Position der Zunge. Auch die Ausweisung des tiefsten Punkt bestätigt den Rückzug: die Zunge liegt nämlich um 13.6 Meter höher als noch im Jahr 2019 auf 2359.7 m.ü.M. Alles in allem sind dies eindrückliche Zahlen, was da alles innert einem Jahr so dahinschmilzt. Was der ganze Glärnischfirn dann noch an Masse verliert, dies wäre dann noch ein weiteres Kapitel in der Gletschermessung am Glärnisch, was jedoch der Grösse dieses Gletscherstromes wegen, nicht erfasst wird. Das Resultat ist einer der grösseren Schwunde in meiner Messreihe. In der Hoffnung, dass ein schneereicher und kalter Winter dieser Tendenz etwas Einhalt gebietet, freue ich mich bereits auf die nächste Messung um die weiteren Verläufe zu dokumentieren. (H. Klauser)

81 Pizol

2020: Eisrand teilweise stark mit Schutt bedeckt. (Th. Brandes)

2021: Die teilweise starke Schuttbedeckung behindert die Bestimmung des Eisrandes. (Th. Brandes)

82 Lavaz

2020: Der Gletscherrand konnte nicht vollständig aufgenommen werden, da auf der östlichen Seite des Gletschers die Gefahr von Steinschlag bestand. Die Seitenmoräne ist von Blockschutt und Altschnee überlagert. So war es schwierig den Gletscherrand zu eruieren. Hingegen ist klar ersichtlich, dass sich der Gletscher auf der östlichen Seite stark zurückgezogen hat. (L. Brunner)

2021: Der Gletscherrand war extrem schwierig zu erkennen, da er stark mit Schutt überdeckt ist. (R. Lutz)

83 Punteglias

2020: Situation am neuen Zungenrand lässt momentan keine Messung mehr zu, da kein Zugang möglich ist und auch kein geeigneter Referenzpunkt für eine Distanzmessung gefunden werden konnte. (L. Brunner)

84 Länta

2021: Zugang zum Gletscherrand zurzeit weiterehin wegen Steinschlag zu gefährlich. Die orographisch rechte Hälfte des Gletschers weist aufgrund der geringen Eisdicke einen raschen Rückgang auf. In der linken Hälfte verläuft der Rückzug deutlich langsamer, da die Eisdicke viel mächtiger ist. (L. Brunner)

85 Vorab

2021: Die einzelnen Ausläufer (gefüllte Rinnen) im nordöstlichen Teil des Gletschers sind bis auf eine Zunge alle geschmolzen. Die Bildung einzelner grösseren Seen ist gut sichtbar. (R. Deflorin)

86 Paradies

2021: Abnahme der Mächtigkeit offensichtlich. (C. Fisler)

87 Suretta

2021: Zwei Stellen waren unzugänglich und wurden deshalb mit Distanzmesser und Azimut bestimmt. Der restliche Polygonzug gelang wurde direkt mit GPS eingemessen. Bei der letzten Messung im 2019 behinderte Neuschnee die Bestimmung vom Eisrand. Die ermittelte Zunahme der Länge könnte darauf zurückzuführen sein. Der Fotovergleich zeigt tatsächlich, dass die Veränderungen gering sind. Die aktuelle Zunge ist durch zerklüftete Eisblöcke im westlichen Teil sowie durch tiefere Gletscherspalten geprägt. (C. Fisler)

88 Porchabella

2020: Der Gletscherrand war sehr gut erkennbar und konnte eindeutig vom Gletschervorfeld abgegrenzt werden. Am westlichen Rand des Messsektors verdecken Felssturzablagerungen den Eisrand. (I. Castelberg)

2021: Der Gletscherrand konnte bei guten äusseren Bedingungen gemessen werden, er war erkennbar und konnte optisch gut vom Gletschervorfeld getrennt erkannt werden. Am westlichen Rand verdecken Felssturzablagerungen von 2014 den Gletscherrand, in diesem Bereich wird der Rand nicht vermessen. Im Herbst 2021 war nur wenig Wasser in den Seelein auf dem Gletschervorfeld. Die Markierungen mit dem Messjahr an einigen Felsen am seitlichen Rand zeigen die Abnahme der Mächtigkeit der Eissschicht eindrücklich auf. (C. Bieler)

89 Verstancla

2021: Der Gletscherrand ist teilweise stark mit Material überdeckt. Durch den vorausgegangenen Schneefall konnte der Rand grösstenteils gut bestimmt werden. (J. Jakob)

90 Silvretta

2020: Luftbildaufnahmen am 13.9.2020 und photogrammetrische Bearbeitung durch swisstopo, glaziologische Interpretation und Analyse durch VAW/ETHZ. (VAW/ETHZ – A. Bauder)

2021: Luftbildaufnahmen am 1.9.2021 und photogrammetrische Bearbeitung durch swisstopo, glaziologische Interpretation und Analyse durch VAW/ETHZ. (VAW/ETHZ – A. Bauder)

91 Sardona

2020: Gletschervorfeld: eher flacher werdend, Ausnahme Linie 2. Im vergangenen Jahr wurde der Eisrand unterschätzt den dieses Jahr zeigte sich mit Altschnee überdecktes Eis. (Th. Brandes)

2021: Gletscherrand mit Ausnahme von Linie 2 eindeutig bestimmbar. (Th. Brandes)

94 Morteratsch

2020: Seitliche Bereiche konnten aufgrund von hoher Steinschlagaktivität nicht gemessen werden. DIes betrifft auch den tiefsten Punkt und das Gletschertor. (G.-A. Godly)

95 Calderas

2021: Am Gletschertor hat sich ein kleiner See gebildet. (G.-A. Godly)

96 Tiatscha

2020: Luftbildaufnahmen am 13.9.2020 und photogrammetrische Bearbeitung durch swisstopo, glaziologische Interpretation und Analyse durch VAW/ETHZ. (VAW/ETHZ – A. Bauder)

2021: Luftbildaufnahmen am 1.9.2021 und photogrammetrische Bearbeitung durch swisstopo, glaziologische Interpretation und Analyse durch VAW/ETHZ. (VAW/ETHZ – A. Bauder)

97 Sesvenna

2020: Das frühere Zungenende am vorgelagerten Toteis hat stark abgenommen. (G. Renz)

2021: Am rechten, unteren Zungenrand hat man einen inselartigen Vorsatz. Die Grenze in diesem Bereich zwischen Eis und Toteis (teilweise Schnee) war nicht immer klar definierbar. Das übriggebliebene Toteis im Vorfeld hat stark abgenommen. (G. Renz)

98 Lischana

2020: Schuttüberdeckung noch stärker als im 2017. Es wurden beide durch einen Felsriegel getrennte Gletscherteile vermessen. Am Rand des Gletschers liegt viel erodiertes Material und Geröll, deshalb ist der Gletscherrand nicht immer einfach zu eruieren. (G. Renz)

2021: Starke Altschneeüberdeckung erschwert das Auffinden vom Gletscherrand. Eindruck: Reduktion der Mächtigkeit und Reduktion der Zunge (G. Renz)

99 Cambrena

2020: Messung des Gletscherrandes ohne Gefahr, aber schwierig (viele Spalten auf der Gletscherzunge, steile Felsbänder am Rand; somit konnte nur ein kleiner Teil der Zunge gemessen werden. Gletscherzunge sehr steil (40°) (im mittleren Bereich), am Gletscherrand ca. 25°. (G. Berchier)

100 Palü

2020: Punto più basso: livello del laghetto (G. Berchier)

2021: Punto più basso: livello del laghetto (G. Berchier)

101 Paradisino

2020: Der Gletscherrand konnte nur beim Gletschertor eindeutig bestimmt werden, da der Gletscher bereits mit 40-60cm Neuschnee bedeckt ist. (G. Berchier)

103 Bresciana

2020: Fronte rilevato solo parzialmente. Ghiacciaio coperto da circa 30 cm di neve fresca. I punti rilevati sono però chiari e evidenti. Lungo il fronte sono presenti delle caverne di ghiaccio di recente formazione. (M. Soldati)

2021: Fronte libero da neve. Ghaicciaio ancora ricoperto dalla neve a partire da circa 3100 metri.In compenso si è notato una forte perdita di spessore nella parte frontale. (M. Soldati)

104 Basòdino

2020: Purtroppo a causa di un guasto tecnico al GPS è stato possibile unicamente il rilievo di pochi punti. Inoltre la neve che copriva il ghiacciaio ha reso difficile stabilire con precisione la presenza di ghiaccio. Per avere delle informazioni più corrette sull'arretramento del fronte occorrerà aspettare l'anno prossimo. (M. Soldati)

2021: Fronte privo di neve. (M. Soldati)

109 Alpetli (Kanderfirn)

2020: Zusätzlichen Referenzpunkt D (2'625'621 / 1'146'184) eingerichtet. (U. Burgener)

2021: Zusätzlichen Referenzpunkt E (2'625'464 / 1'146'225) eingerichtet. (U. Burgener)

111 Ammerten

2020: Die Flucht von P1 liegt nicht mehr am Gletschertor, sondern seitlich am Felswulst. Darum ist der Rückgang dort markanter. (W. Hodel)

2021: Auffallend ist der noch liegengebliebene Winterschnee, wie in den letzten Jahren nicht mehr vorgekommen. Die Nordflanke des Wildstrubel ist aber auch dieses Jahr nahezu schneefrei. (W. Hodel)

114 Plattalva

2020: Gletscher aper; bei Punkt 5 ist der Gletscherrand ausserhalb Messrichtung. (U. Steinegger)

115 Scaletta

2020: Ausdünnung am Zungenrand auffallend, Gletscher am Zerfallen, Messungen vor Ort wenig sinnvoll. (B. Teufen)

116 Albigna

2020: Im Zungenbereich Aufteilung des Gletschers in zentralen Teil (Gletschertor) mit stärkstem Rückzug und moränenüberdeckte Randbereiche. Insbesondere der orographisch rechte Teil mit der Steilwand (schwarze Wand) dürfte noch aus Toteis des Vadrec dal Castel Nord bestehen. (R. Kühne)

117 Valleggia

2020: Una piccola parte del ghiacciaio è ancora ricoperta dalla neve dell'inverno. Il lago postglaciale che si è formato assume dimensioni sempre maggiori. (M. Soldati)

2021: Una parte del ghiacciaio è ancora ricoperta dalla neve dell'inverno. Molto detrito presente sul ghiacciaio. Il lago postglaciale che si è formato assume dimensioni sempre maggiori. (M. Soldati)

119 Cavagnoli

2020: A causa del cattivo segnale GPS non è possibile determinare con precisione la perdita di spessore, che corrisponde a circa 1.5 metri. Ghiacciaio coperto da neve, spessore neve circa 15 cm. (M. Soldati)

2021: Forti perdite di ghiaccio nella parte centrae del piccolo ghiacciaio. Un pezzo laterale rimane solo una placca di ghiaccio destinata a scomparire a breve. Affiorano rocce sempre più frequenti. (M. Soldati)

120 Corno

2020: Nonostante la neve fresca fronte ben visibile. Rilevato punti lungo il profilo che serviranno da confronto durante il prossimo rilievo. (M. Soldati)

2021: Parte alta (ca 1/2 - 1/3 superiore) ancora ricoperta dalla neve. (M. Soldati)

173 Seewjinen

2020: Luftbildaufnahmen am 11.9.2020, photogrammetrische Auswertung und Analysen durch VAW/ETHZ im Auftrag der Kraftwerke Mattmark AG. (VAW/ETHZ – A. Bauder)

2021: Luftbildaufnahmen am 21.9.2021, photogrammetrische Auswertung und Analysen durch VAW/ETHZ im Auftrag der Kraftwerke Mattmark AG. (VAW/ETHZ – A. Bauder)

174 Hohlaub

2020: Luftbildaufnahmen am 11.9.2020, photogrammetrische Auswertung und Analysen durch VAW/ETHZ im Auftrag der Kraftwerke Mattmark AG. (VAW/ETHZ – A. Bauder)

2021: Luftbildaufnahmen am 21.9.2021, photogrammetrische Auswertung und Analysen durch VAW/ETHZ im Auftrag der Kraftwerke Mattmark AG. (VAW/ETHZ – A. Bauder)

C Investigators

C.1 Length Variation (2021)

Glacier	No.	Investigator
Albigna	116	AWN/GR, Natalie Soder
Allalin	11	VAW/ETHZ, Andreas Bauder
Alpetli (Kanderfirn)	109	KAWA/BE, Ueli Burgener
Ammerten	111	Walter Hodel
Arolla (Mont Collon)	27	DWFL/VS, François Fellay
Basòdino	104	SF/TI, Mattia Soldati
Bella Tola	21	no observeation during report period
Biferten	77	Hanspeter Klauser
Blüemlisalp	64	VAW/ETHZ, A. Bauder & E. Hodel
Boveyre	41	DWFL/VS, Pascal Stoebener
Breney	36	VAW/ETHZ, Andreas Bauder
Bresciana	103	SF/TI, Mattia Soldati
Brunegg (Turtmann)	20	DWFL/VS, Alban Brigger
Brunni	72	AFJ/UR, Michael Planzer
Calderas	95	AWN/GR, Gian Andri Godly
Cambrena	99	AWN/GR, Gilbert Berchier
Cavagnoli	119	SF/TI, Mattia Soldati
Cheillon	29	DWFL/VS, Olivier Bourdin
Chessjen	12	VAW/ETHZ, Andreas Bauder
Corbassière	38	VAW/ETHZ, Andreas Bauder
Corno	120	SF/TI, Mattia Soldati
Croslina	352	no observeation during report period
Damma	70	AFJ/UR, René Planzer
Dungel	112	VAW/ETHZ, A. Bauder & E. Hodel
Eiger	59	VAW/ETHZ, A. Bauder & E. Hodel
En Darrey	30	DWFL/VS, Olivier Bourdin
Fee	13	VAW/ETHZ, A. Bauder & E. Hodel
Ferpècle	25	DWFL/VS, François Fellay
Fiescher	4	VAW/ETHZ, A. Bauder & E. Hodel
Findelen	16	VAW/ETHZ, A. Bauder & E. Hodel
Firnalpeli (Ost)	75	VAW/ETHZ, A. Bauder & E. Hodel
Forno	102	AWN/GR, Renata Nyfeler
Gamchi	61	KAWA/BE, Martin Schenk
Gauli	52	KAWA/BE, Martin Haider

Glacier	No.	Investigator
Gelten	113	VAW/ETHZ, A. Bauder & E. Hodel
Giétro	37	VAW/ETHZ, Andreas Bauder
Glärnisch	80	Hanspeter Klauser
Gorner	14	VAW/ETHZ, A. Bauder & E. Hodel
Grand Désert	31	DWFL/VS, Frédéric Bourban
Grand Plan Névé	45	FFN/VD, Julien Desarzens
Gries	3	VAW/ETHZ, A. Bauder & E. Hodel
Griess	74	AFJ/UR, Beat Annen
Griessen	76	VAW/ETHZ, A. Bauder & E. Hodel
Grosser Aletsch	5	VAW/ETHZ, A. Bauder & E. Hodel
Hohlaub	174	VAW/ETHZ, Andreas Bauder
Hüfi	73	VAW/ETHZ, Andreas Bauder
Kaltwasser	7	DWFL/VS, Christian Kuonen
Kehlen	68	AFJ/UR, René Planzer
Lang	18	DWFL/VS, Hans Henzen
Lavaz	82	AWN/GR, Laura Brunner
Lenta	84	AWN/GR, Laura Brunner
Limmern	78	Urs Steinegger
Lischana	98	AWN/GR, Giorgio Renz
Lämmern	63	KAWA/BE, Adrian Meier-Glaser
Mittelaletsch	106	VAW/ETHZ, Andreas Bauder
Moiry	24	DWFL/VS, François Fellay
Moming	23	no observeation during report period
Mont Durand	35	VAW/ETHZ, Andreas Bauder
Mont Fort (Tortin)	32	DWFL/VS, Frédéric Bourban
Mont Miné	26	no observeation during report period
Morteratsch	94	AWN/GR, Gian Andri Godly
Mutt	2	VAW/ETHZ, Andreas Bauder
Oberaar	50	VAW/ETHZ, A. Bauder & E. Hodel
Oberaletsch	6	DWFL/VS, Christian Theler
Oberer Grindelwald	57	VAW/ETHZ, A. Bauder & E. Hodel
Otemma	34	VAW/ETHZ, Andreas Bauder
Palü	100	AWN/GR, Gilbert Berchier
Paneyrosse	44	FFN/VD, Julien Desarzens
Paradies	86	AWN/GR, Cristina Fisler
Paradisino (Campo)	101	AWN/GR, Gilbert Berchier
Pizol	81	KFA/SG, Thomas Brandes
Plattalva	114	Urs Steinegger
Porchabella	88	AWN/GR, Claudia Bieler
Prapio	48	no observeation during report period
Punteglias	83	AWN/GR, Laura Brunner
Rhone	1	VAW/ETHZ, A. Bauder & E. Hodel
Ried	17	DWFL/VS, Peter Rovina
Roseg	92	no observeation during report period
Rossboden	105	VAW/ETHZ, Andreas Bauder
Rotfirn (Nord)	69	VAW/ETHZ, Andreas Bauder

Glacier	No.	Investigator
Rätzli	65	VAW/ETHZ, A. Bauder & E. Hodel
Saleina	42	DWFL/VS, Pascal Stoebener
Sankt Anna	67	AFJ/UR, Lukas Eggimann
Sardona	91	KFA/SG, Thomas Brandes
Scaletta	115	Bernardo Teufen
Schwarz	62	no observeation during report period
Schwarzberg	10	VAW/ETHZ, Andreas Bauder
Seewjinen	173	VAW/ETHZ, Andreas Bauder
Sesvenna	97	AWN/GR, Giorgio Renz
Sex Rouge	47	Jacques Binggeli
Silvretta	90	VAW/ETHZ, A. Bauder & E. Hodel
Stein	53	KAWA/BE, Daniel Rohrer
Steinlimi	54	VAW/ETHZ, A. Bauder & E. Hodel
Sulz	79	WN/GL, Nadine Philippi
Suretta	87	AWN/GR, Cristina Fisler
Tiatscha	96	VAW/ETHZ, A. Bauder & E. Hodel
Tiefen	66	AFJ/UR, Lukas Eggimann
Trient	43	Jacques Ehinger
Trift (Gadmen)	55	VAW/ETHZ, A. Bauder & E. Hodel
Tsanfleuron	33	DWFL/VS, François Fellay
Tschierva	93	AWN/GR, Gian Andri Godly
Tschingel	60	KAWA/BE, Ralf Schai
Tseudet	40	DWFL/VS, Pascal Stoebener
Tsidjiore Nouve	28	DWFL/VS, François Fellay
Turtmann	19	DWFL/VS, Alban Brigger
Unteraar	51	VAW/ETHZ, A. Bauder & E. Hodel
Unterer Grindelwald	58	VAW/ETHZ, A. Bauder & E. Hodel
Val Torta	118	VAW/ETHZ, Andreas Bauder
Valleggia	117	SF/TI, Mattia Soldati
Valsorey	39	DWFL/VS, Pascal Stoebener
Verstankla	89	AWN/GR, Johannes Jakob
Vorab	85	AWN/GR, Renato Deflorin
Wallenbur	71	AFJ/UR, Pius Kläger
Zinal	22	DWL/VS, Gabriel Chevalier
Zmutt	15	VAW/ETHZ, Andreas Bauder

AFJ/UR	Amt für Forst und Jagd, Uri
AWN/GR	Amt für Wald und Naturgefahren, Graubünden
WN/GL	Wald und Naturgefahren, Glarus
AWL/OW	Amt für Wald und Landschaft, Obwalden
DWFL/VS	Dienststelle für Wald, Flussbau und Landschaft/Service des forêts des cours d'eau et du paysage, Wallis/Valais
FFN/VD	Service des forêts, de la faune et de la nature, Vaud
KAWA/BE	Amt für Wald, Bern
KFA/SG	Waldregion 3 Sargans, St. Gallen
SF/TI	Sezione forestale, Ticino
VAW/ETHZ	Versuchsanstalt für Wasserbau, Hydrologie und Glaziologie, ETH Zürich

C.2 Mass Balance and Velocity

Glacier	No.	Investigator
Allalin	11	VAW/ETHZ, Andreas Bauder
Basòdino	104	VAW/ETHZ, Giovanni Kappenberger
Clariden	141	VAW/ETHZ, Urs Steinegger
Corbassière	38	VAW/ETHZ, Andreas Bauder
Findelen	16	DGUF / GIUZ, Matthias Huss, Andreas Linsbauer
Giétro	37	VAW/ETHZ, Andreas Bauder
Gries	3	VAW/ETHZ, Matthias Huss
Grosser Aletsch	5	VAW/ETHZ, Andreas Bauder, Matthias Huss
Hohlaub	174	VAW/ETHZ, Andreas Bauder
Murtèl	377	DGUF, Matthias Huss
Pers	317	Philippe Hybrechts (VUB) DGUF, Matthias Huss, Andreas Linsbauer
Pizol	81	VAW/ETHZ / DGUF, Matthias Huss
Plaine Morte	65	DGUF, Matthias Huss
Rhone	1	VAW/ETHZ, Andreas Bauder
Sankt Anna	67	DGUF, Matthias Huss
Schwarzberg	10	VAW/ETHZ, Andreas Bauder
Silvretta	90	VAW/ETHZ, Andreas Bauder
Tsanfleuron	33	DGUF, Mauro Fischer

C.3 Englacial Temperature

Site (Glacier)	No.	Investigator
Colle Gnifetti (Gorner)	14	DGUF, Martin Hoelzle, Enrico Mattea, Horst Machguth

DGUF	Département des Géosciences, Université de Fribourg
GIUZ	Geographisches Institut, Universität Zürich
VUB	Vrije Universiteit Brussel
VAW/ETHZ	Versuchsanstalt für Wasserbau, Hydrologie und Glaziologie, ETH Zürich